ALFRED-WEGENER-INSTITUT
HELMHOLTZ-ZENTRUM FÜR POLAR- UND MEERESFORSCHUNG

What drives species into extinction?

Biochemical and molecular mechanisms involved in temperature-related stress responses in two marine bivalves

Dissertation

Zur Erlangung des akademischen Grades

Dr. rer. nat.

Sandra Götze

Master of Marine Sciences

Bremerhaven

Vorgelegt dem Fachbereich 2, der Universität Bremen

Datum des Prüfungskolloquiums: 10.2.2020

Universität Bremen

Gutachter: Prof. Dr. Hans-Otto Pörtner

Alfred-Wegener-Institut Helmholtz-Zentrum für Polar-und Meeresforschung

Head of section Integrative Ecophysiology

Am Handelshafen 12

27570 Bremerhaven, Germany

Gutachter: Prof. Dr. Inna Sokolova

University of Rostock

Institute for Biological Sciences Department of Marine Biology

Albert-Einstein-Straße 3

18059 Rostock, Germany

Prüfer: Prof. Dr. Wilhelm Hagen

University of Bremen

Marine Zoology, Department of Biology and Chemistry

Postfach 330 440

28334 Bremen

e-mail whagen@uni-bremen.de

Prüfer: Prof. Dr. Hans-Otto Pörtner

Alfred-Wegener-Institut Helmholtz-Zentrum für Polar-und Meeresforschung

Head of section Integrative Ecophysiology

Am Handelshafen 12

27570 Bremerhaven, Germany

e-mail: hans.poertner@awi.de

Prüfer: Dr. Reinhard Saborowski

Alfred-Wegener-Institut Helmholtz-Zentrum für Polar-und Meeresforschung

Function Ecology

27570 Bremerhaven, Germany

e-mail: Reinhard.saborowski@awi.de

Prüfer: Prof. Dr. Kai Bischof

University of Bremen

Marine Botany, Department of Biology and Chemistry

Postfach 330 440

28334 Bremen

e-mail: kbischof@uni-bremen.de

Universität Bremen

Ort, Datum: Bremerhaven, den

Versicherung an Eides Statt

Ich, Sandra Götze wohnhaft in der Borriesstr. 18, 27570 Bremerhaven

versichere an Eides Statt durch meine Unterschrift, dass ich die vorstehende Arbeit selbständig und ohne fremde Hilfe angefertigt und alle Stellen, die ich wörtlich dem Sinne nach aus Veröffentlichungen entnommen habe, als solche kenntlich gemacht habe, mich auch keiner anderen als der angegebenen Literatur oder sonstiger Hilfsmittel bedient habe.

Ich versichere an Eides Statt, dass ich die vorgenannten Angaben nach bestem Wissen und Gewissen gemacht habe und dass die Angaben der Wahrheit entsprechen und ich nichts verschwiegen habe.

Ich versichere an Eides Statt, dass die zu Prüfungszwecken beigelegte elektronische Version der Dissertation identisch ist mit der abgegebenen gedruckten Version.

Ich erkläre mich einverstanden, dass mittels geeigneter elektronischer Software die vorliegende Dissertation auf Plagiatsvorwürfe untersucht werden darf.

Die Strafbarkeit einer falschen eidesstattlichen Versicherung ist mir bekannt, namentlich die Strafandrohung gemäß § 156 StGB bis zu drei Jahren Freiheitsstrafe oder Geldstrafe bei vorsätzlicher Begehung der Tat bzw. gemäß § 161 Abs. 1 StGB bis zu einem Jahr Freiheitsstrafe oder Geldstrafe bei fahrlässiger Begehung.

_____

Ort, Datum Unterschrift

TABLE OF CONTENT

TABLE OF CONTENT

FIGURES AND TABLES

ABBREVIATIONS

%	Percentage
µg	Microgram
µl	Microliter
^{1}H-NMR	^{1}H- nuclear magnetic resonance
ABT	Arrhenius-breakpoint-temperature
ADP	Adenosine diphosphate
AMP	Adenosine monophosphate
ANOVA	Analysis of variance
ATP	Adenosine triphosphate
AWI	Alfred-Wegener-Institute
BCAA	Branched chain amino acids
BSA	Bovine serum albumin
CI	Condition index
CO_2	Carbon dioxide
CPMG	Call-Purcell-Meiboom-Gill (sequence)
D_2O	Deuterized water
DIC	Dissolved inorganic carbon
DT	Deadly Trio, Warming plus both stressors
DW	Dry weight
FR	Filtration rate (L/h*g dry weight) – C. Eymann
FW	Fresh weight
g	Units of gravity
glog	Generalized logarithm
HR	Heart rate (expressed as beats per minutes) – C. Eymann
HSF	Heat shock family
HSP	Heat shock protein
HSR	Heat shock response
IB	Immuno-blotting
KCl	Potassium chloride
kDa	Kilo Dalton (molecular weight of proteins)
kPa	Kilo Pascale (unit of pressure)
LAU	Arbitrary units
LC_{50}	Temperature at which 50 % of bivalves died
Ma	Million years ago
MDA	Malondialdehyde
ME	Mass extinction
$MgCl_2$	Magnesium chloride
MilliQ	Ultrapure water, deionized
mM	Millimoles per liter
MO_2	Oxygen consumption (µmol/h*g dry weight) – C. Eymann
Na_3VO_4	Sodium orthovanadate
O_2	Oxygen
OCLTT	Oxygen and capacity-limited thermal tolerance
OA	Ocean acidification
PCA	Principal component analysis
pH_E	Extracellular pH

pH_I	Intracellular pH
PLS-DA	Partial least square-discriminant analysis
PLA	Phospho-L-arginine
PMSF	Phenylmethylsulfonyl fluoride
PO_2	Partial pressure of oxygen
PSU	Practical salinity unit
PT	Permian-Triassic
PT-ME	Permian-Triassic mass extinction
Ppmv	Parts per million volume
PVDF	Polyvinylidendifluorid
ROS	Reactive oxygen species
RU	Research unit
Q10	measure of the rate of change driven by a temperature change of 10 °C
SD	Standard deviation
SDS-PAGE	Sodium dodecyl sulfate polyacrylamide gel electrophoresis
SMR	Standard metabolic rate
SST	Sea surface temperature
RT	Room temperature
RTA	Respiratory time activity – C. Eymann
SW	Seawater
TBST	Tris-buffered saline *plus* Tween 20 buffer
TERSANE	Temperature-related stresses as unifying principle in ancient mass extinctions
TMAO	Tri-methyl-amine-oxide
Tris-HCL	Tris-(hydroxymethyl)-aminomethane hydrochloride
TRS	Temperature-related-stresses
TSR	Temperature-size-rule
TSP	3-(trimethylsilyl) propionic-2,2,3,3-d4 acid, sodium salt
T_c	Temperature in the critical range
T_{Opt}	Temperature in the optimum range
T_p	Temperature in the pejus range
T_D	Lethal temperature
W	Warming
WB	Western-blotting
WHo	Warming *plus* hypoxia
WHc	Warming plus hypercapnia

SUMMARY

The industrial release of carbon dioxide (CO_2) interferes with the atmosphere altering the global climate and endangering terrestrial and marine fauna. Marine ecosystems are mainly affected by changes in seawater chemistry (ocean acidification) and temperature (warming) accompanied by a progressive loss of oxygen. It is expected that under unabated climate change, species will shift in distribution from the tropics to the poles, with consequences for ecosystem diversity and productivity. Similar to current projections of near-future ecosystem changes, paleontological research can tell us about past ecosystem crises and their outcome by investigating fossil records and geological proxies. Back then, profound changes in climate were often caused by massive volcanism leading to excessive greenhouse gas release. One of such past ecosystem crises was the transition between the Permian-Triassic around 252 Ma ago, which erased more than 80 percent of marine taxa. Specie's fate during past, current and future global climate change scenarios will depend on the magnitude and duration of such challenges but also on species' capacities to acclimate and adapt. Therefore, the main rationale of this study was to identify thermal turning points indicated by changes in metabolism and cellular stress parameters in response to temperature-related stresses. Two marine bivalves with rich fossil records, *Ostrea edulis* and *Pecten maximus*, were chosen a.o. due to differences in lifestyle, habitat, and anticipated tolerance to environmental stresses. Bivalves were subjected to acute exposures starting at their lower environmental thermal range (14°C) to either warming (W), warming *plus* hypoxia (WHo), warming *plus* hypercapnia (WHc) or the combined exposure of all three stresses (Deadly Trio, DT) until all bivalves died (*O. edulis* at 36°C and *P. maximus* at 28°C). Main investigations comprised an in-depth analysis of gill and phasic muscle metabolism and analysis of branchial stress parameters marked cellular damage and protection. Thermal turning points of the thermal windows were defined based on the mechanistic framework of the "oxygen and capacity-limited thermal tolerance" model (OCLTT) established by Pörtner and coworkers.

Data of *O. edulis* impressively underline the capacity of oysters to tolerate a wide margin of environmental conditions, at least short-term. Warming exposures were run during winter and during summer, revealing a season (and acclimation) dependent shift in performance. While winter acclimated oysters performed best between 18°C - 24°C, summer acclimated oysters did so between 22°C - 26°C. However, the upper thermal limits remained the same (34°C). Metabolic analysis of summer-acclimated oysters showed that for both W and DT exposed oysters, a critical temperature was reached at 34°C (onset of anaerobiosis). Preliminary analyses of branchial levels of HSP70 indicated that a heat shock response was not induced below 30°C.

Accordingly, the acute thermal window was not narrowed under DT. Contrary, data obtained for *P. maximus* revealed that king scallops only have low capacities to tolerate temperatures beyond their optimum (22°C) as they surpassed a critical temperature at 26°C and all scallops died at 28°C. The thermal window was narrowed when scallops were exposed to combined stress (WHo and WHc) and performed worst when challenged to DT. Scallops had higher rates of mortality, which decreased the half-maximal lethal temperatures (25°C in W *vs*. 22.5°C in DT) and lowered break-point temperatures of organismic parameters (see the thesis of C. Eymann). Gill metabolism was most tolerant to WHc, while alterations in branchial energy metabolism (onset of anaerobic metabolism) occurred immediately after exposure to WHo or DT symbolizing an imbalance between energy demand and supply. Scallops were fully able to maintain protein homeostasis when exposed to either W, WHo, or WHc even when sampled at 26°C. At this temperature (26°C), gills had upregulated levels of HSP70 that facilitate thermotolerance and protection of proteins. However, maintenance of cellular homeostasis in parallel to the temperature-driven high cellular processes (*Q10*) presumably further contributed to an energetic crisis (deriving from a mismatch between oxygen demand and supply). Scallops exposed to DT showed clear signs of protein damage (18°C - 22°C) followed by peaking levels of free branched chain amino acids at 26°C, indicating the degradation of proteins. Strikingly, this pronounced protein damage did not induce the upregulation of HSP70, but instead, at 26°C the structure of the gills was disrupted most likely because of ongoing apoptosis.

Biochemical and molecular findings presented in the current project provide first insights on how underlying mechanisms become operative in response to temperature-related stress. Pectinida and Ostreoida developed different strategies to inhabit subtidal or intertidal habitats. Sessile oysters show a “passive endurance” strategy with a high phenotypic plasticity enabling highly flexible cellular adjustments to maintain homeostasis and integrity under non-optimal warm and hypoxic conditions. Moreover, they possess high capacities to downregulate ATP-generating and ATP-consuming processes. Scallops follow a “be alert and active” strategy, which allows active swimming but results in lower capacities to endure unfavorable conditions via metabolic depression and limits the tolerance to hypoxia. Altogether, modern organismic and biochemical data support fossil records, which suggested that evolution might have favored oysters (being more tolerant toward warming and low oxygen concentration) during the Permian-Triassic mass extinction rather than scallops.

ZUSAMMENFASSUNG

Die industrielle Freisetzung von Kohlendioxid verändert maßgeblich das globale Klima und gefährdet so marine Ökosysteme. Diese werden vor allem durch die Erwärmung der Ozeane, Veränderungen der Meerwasserchemie sowie fortschreitende Sauerstoffmangelzonen bedroht. Es wird prognostiziert, dass sich die Artenvielfalt durch temperaturbedingte Abwanderung von Arten von den Tropen zu den Polen verlagern wird, mit negativen Auswirkungen auf Ökosysteme und deren Produktivität. Die paläontologische Forschung untersucht vergangene Ökosystemkrisen mittels fossiler Funde und geologischen Parametern. Vulkanismus, der massiv Treibhausgase freisetzte, war ein Auslöser für erdzeitgeschichtliche Klimaveränderungen und anschließende Massensterben. Eines der größten marinen Massensterben ereignete sich beim Übergang des Perm-Trias vor etwa 252 Millionen Jahren, bei dem mehr als 80 % der Meerestaxa ausgelöscht wurde. Das Schicksal mariner Arten während solcher klimatischer Krisen hängt von der Größe und Dauer dieser Veränderungen ab sowie von der Fähigkeit der Arten sich anzupassen. Der Lebensraum von marinen ektothermen Arten kann über ihr thermisches Fenster, also die Temperaturbereiche in denen die Art nachhaltig oder kurzfristig überleben kann, beschrieben werden.

Schwerpunkt der vorliegenden Arbeit war die Frage, wie sich das thermische Fenster zweier rezenter mariner Muschelarten in Reaktion auf temperaturbedingte Stressfaktoren verändert. Als Modellorganismen wurden die Europäische Auster (*Ostrea edulis*) und die große Pilgermuschel (*Pecten maximus*) aufgrund Fossilnachweisen, ihrer unterschiedlichen Lebensweise, Lebensräume und Toleranz gegenüber Klimaveränderungen ausgewählt. Beide Arten wurden akuten Stress-Versuchen ausgesetzt. In Gruppe „W“ wurde nur die Temperatur erhöht. In zwei anderen Gruppen wurden die Tiere neben dem Temperaturstress zusätzlich entweder Sauerstoffmangelstress (WHo) oder pH-Stress (WHc) ausgesetzt. Eine vierte Gruppe wurde allen Stressfaktoren ausgesetzt (DT). Die Temperatur wurde um 2°C alle 48 h bis zum Tod der Tiere erhöht (bei *O. edulis* T_D=36°C und *P. maximus* T_D=28°C). Die wichtigsten Analysen der vorliegenden Arbeit umfassen Untersuchungen des Stoffwechsels im Kiemen- und phasischen Muskel sowie des zellulären Stress-Status (Zellschädigung und Schutzmechanismen). Thermische Wendepunkte des thermischen Fensters basieren auf dem Konzept der "Sauerstoff und Kapazitäts-begrenzten thermischen Toleranz" (OCLTT). Die Daten von *O. edulis* unterstreichen die Fähigkeit von Austern, zumindest kurzfristig, auch drastische Veränderungen ihrer Umweltbedingungen zu tolerieren. Zudem zeigte sich eine saisonale Abhängigkeit des thermischen Fensters. Der Optimumbereich verschob sich von 18°C - 24°C (Winter) zu 22°C - 26°C (Sommer). Die oberen Temperaturgrenzen blieben

unverändert (T_C = 34°C). In Kiemen von W- als auch DT- exponierten Austern erfolgte eine Hitzeschutzantwort durch die Erhöhung von HSP70 ab 30°C. Bei 34°C akkumulierten in beiden Gruppen Metabolite anaerober Stoffwechselwege. Im Gegensatz dazu zeigten die von *P. maximus* erhobenen Daten, dass diese Art nur geringfügig Temperaturen oberhalb ihres Optimums (22°C) toleriert. Bei 26°C begann die Akkumulation von anaeroben Endprodukten, die mit dem Versterben der Tiere bei 28°C endete. Muscheln, die dem „Deadly Trio“ ausgesetzt waren, zeigten eine verminderte Toleranz gegenüber hohen Temperaturen, was sich in einer erhöhten Mortalität während der Versuche zeigte. Während sich der Kiemenstoffwechsel unter WHc nur geringfügig gegenüber der W Gruppe veränderte, kam es bereits zu Beginn unter Who und DT zu Störungen in branchialen Stoffwechselwegen und der Akkumulation von anaeroben Metaboliten. Dies deutet auf ein Ungleichgewicht zwischen Sauerstoffversorgung und Sauerstoffbedarf bereits bei moderaten Temperaturen hin. Allerdings waren alle Tiere bis auf die DT Gruppe selbst bei 26°C in der Lage, ihre Proteinhomöostase aufrechtzuerhalten, was durch den Aufbau von HSP70 in den Kiemen gewährleistet wurde. Die Aufrechterhaltung dieser zellulären Homöostase parallel zu den beschleunigten zellulären Prozessen (*Q10*) trug vermutlich weiter zu einem energetischen Defizit bei. Pilgermuscheln der DT Gruppe, zeigten deutliche Anzeichen von Proteinschädigung (18°C - 22°C), sowie erhöhten Konzentrationen an freien proteinogenen Aminosäuren (26°C). Überraschenderweise konnte trotz der Proteinschädigung in dieser Gruppe keine Hitzeschutzantwort nachgewiesen werden. Stattdessen waren in Tieren, die bei 26°C beprobt wurden, deutliche Veränderungen an den Kiemenstrukturen sichtbar, die auf apoptotische Prozesse hindeuten. Die biochemischen und molekularen Erkenntnisse der vorliegenden Arbeit geben weitere Hinweise auf die zugrundeliegenden Mechanismen in marinen Muscheln auf klimabedingte Stressfaktoren. Dabei zeigten beide Arten unterschiedliche Strategien vermutlich in Zusammenhang ihrer Lebensräume (subtidal *vs.* intertidal). Austern verfolgen eine "Überdauern und Ausharren"-Strategie, verbunden mit einer hohen phänotypischen Plastizität, welche hochflexibel die zelluläre Homöostase und Integrität unter nicht optimalen Bedingungen anpasst. Darüber hinaus haben Austern die Fähigkeit, über eine metabolische Depression ATP-generierende und ATP-verbrauchende Prozesse herunterzufahren. Im Gegensatz dazu zeigen Pilgermuschen eine "Reaktion- und Flucht“- Strategie, die niedrigen Kapazitäten der metabolischen Depression bedingt, woraus sich die niedrige Toleranz gegenüber Hypoxie ableitet. Die erhobenen organismischen und biochemischen Daten rezenter Arten unterstützen fossile Funde, die darauf hindeuten, dass Austern gegenüber Jakobsmuscheln während des Perm-Trias-Massensterbens einen Vorteil hatten.

INTRODUCTION

The industrial release of carbon dioxide (**CO_2**) interferes with the atmosphere altering the global climate. In consequence, marine habitats are a.o., affected by changes in seawater chemistry, temperature, currents, nutrient fluxes, and altered ecosystem communities if the anticipated degree and speed of change exceeds the speed of species adaption. However, the global climate does not change for the first time in earth history. In deep-times, ecological crises caused by, e.g. volcanic gas release have fundamentally altered marine ecosystems. The current PhD project is embedded in the project "Dynamics of thermal tolerance limits in marine bivalves: temperature related stressors in extant fauna and palaeo-analogues (BIV-TRS)", which is part of the interdisciplinary research unit (**RU**) "Temperature-related stressors as a unifying principle in ancient extinctions" (TERSANE) funded by the "Deutsche Forschungs-gemeinschaft." The following introduction outlines past and current climate crises and their effects on marine ectotherms. Furthermore, it is outlined how paleontology research and modern ecophysiology research can benefit from each other and how "BIV-TRS" plays a part.

1.1 Ecological background

1.1.1 Climate crises and mass extinctions during earth history

Various minor and major marine mass extinctions (**MEs**) occurred during earth history. Paleontological research investigates the causes and consequences of ME by analyzing geological proxies (e.g., oxygen isotopes) and fossil records to reconstruct changes in the paleoclimate (e.g., Clarkson et al., 2015; Veizer and Prokoph, 2015). At least two major ecological crises were initiated by rapid changes of temperature-related stresses (**TRS**; namely warming, hypoxia and hypercapnia; Joachimski et al., 2012; Stanley, 2016; Knoll et al., 2007). Massive volcanism and basalt eruption frequently caused past greenhouse gas release and climate warming (Bambach et al., 2004; Grant et al., 2017; Burgess et al., 2017). The synergistic interaction of the three big environmental drivers, warming, hypoxia and hypercapnia is, due to their devastating impacts on flora and fauna, often denoted as "Deadly Trio" (**DT**; e.g., Bijma et al., 2013; Foster et al., 2019). TERSANE investigates two MEs that caused TRS: one at the Permian-Triassic (**PT**) transition (~ 252 Ma) and one at the Pliensbachian-Toarchian transition (~ 190 Ma). Subsequently, I will focus on the PT transition that was one of the most severe marine crises (Bambach et al., 2004; Clarkson et al., 2015). Outgassing of Siberian traps critically increased atmospheric CO_2 - mounting a cascade of climate changes and ultimately leading to a warm, anoxic and CO_2 rich ocean (Knoll et al., 1996; Wignall and Twitchett, 1996).

A study published in 2018 substantiated this hypothesis establishing a Community Earth System model which simulated climate changes at the PT transition by subjecting an initial climate state to the anticipated immediate increase in CO_2 during that time (~5500 parts per million volumes (**ppmv**) CO_2, Penn et al., 2018). Modeled changes were consistent to geological proxies obtained from stable isotopes suggesting that sea surface temperatures rose about 11 °C simultaneously to a drop in seawater pH of up to 0.7 pH units (Joachimski et al., 2012; Sun et al., 2012; Clarkson et al., 2015). Furthermore, the meridional circulation slowed-down about 80 % contributing to stratification and depletion of global marine oxygen (Lau et al., 2016; Penn et al., 2018). The sum of all changes led to a phenomenon known as "big dying," erasing ~ 80 % to 95 % of marine taxa (Benton and Twitchett, 2003; Song et al., 2013). From past events such as the PT-ME, we learned much about the deadly outcome of rapid climate changes for modern marine biota. Crucial for the survival of a respective species in a certain habitat is its capacity to sustain, resist and/or adapt to changes and to stay within its realized thermal window based on the OCLTT concept. Although ultimate triggers and time scales are not the same as in the past, today's anthropogenic climate change is hypothesized to be analogous with an anticipated speed and degree of change exceeding the speed of adaption of many taxa.

1.1.2 Climate change in the Holocene

Since the beginning of the industrial revolution and resulting extensive combustion of fossil fuels, atmospheric CO_2 concentrations increased from ~280 ppmv to ~410 ppmv (2019; https://www.esrl.noaa.gov/gmd/ccgg/trends/). Under humankind's "business-as-usual" behavior, atmospheric CO_2 may rise as high as 1370 ppmv by the end of the century causing global warming (Rhein et al., 2013, RCP 8.5 IPCC). The sea surface temperature of, e.g. the Atlantic Ocean has already increased about 0.41°C from 1950 to 2009 and is expected to increase up to 4°C by the end of the century (Hoegh-Guldberg et al., 2014). In addition to warming, atmospheric CO_2 reacts with seawater (**SW**) leading to partial absorption of CO_2 from the atmosphere (Sabine et al., 2005) and hence, decreases the oceans pH and alters the SW carbonate chemistry as explained by the following equation:

$$CO_{2\,(atmos)} \leftrightarrow CO_{2\,(aq)} + H_2O \leftrightarrow H_2CO_3 \leftrightarrow H^+ + HCO_3^- \leftrightarrow 2H^+ + CO_3^{2-} \quad \text{(Doney et al., 2009, equation 1)}$$

The pH of seawater dropped from preindustrial ~8.179 to ~8.069 (today), and marine habitats will have to face a further drop of 0.3 – 0.4 pH units by 2100 (Orr et al., 2005; Doney et al.,

2009). pH is expressed on a logarithmic scale. Hence, the decrease of only 0.1 pH units already represents an increase in H^+ ions of ~ 30 %. As the ocean becomes more acidic (due to H^+ ions), the process was denoted as ocean acidification (**OA**; e.g., Orr et al., 2005). The present study uses the term hypercapnia instead, which refers to the elevated seawater CO_2 concentrations. In hypercapnic seawater, lower concentrations of calcium carbonate ions are dissolved than in normcapnic SW. This is potentially harmful for shell-forming marine organisms such as corals, molluscs and echinoderms as the formation of biogenic calcium carbonate [$CaCO_3$] come with higher energetic costs possibly decreasing shell formation (Orr et al., 2005; Ries et al., 2009; Thomsen et al., 2015). Various studies have shown that (at least some) calcifying species have reduced rates of calcification and growth rates under high-CO_2 conditions (e.g., Doney et al., 2009; Kroeker et al., 2010; Pandolfi et al., 2011). Similar to past climate changes, the expansion of anoxic areas will accompany warming and hypercapnia also in the near future. Oxygen-solubility will decrease with increasing temperatures, and oxygen may become fully depleted in stratified water layers (Diaz and Rosenberg, 2008; Keeling et al., 2010; Breitburg et al., 2018). Predicted consequences for marine biota are manifold and depend on the stressors, their magnitude and duration, climate zonation, species, life stage, and community structure (Guinotte and Fabry, 2008; Wittmann and Pörtner, 2013; Parker et al., 2013; Gattuso et al., 2015).

1.2 Impact of temperature on marine ecosystems

1.2.1 Species geographical distribution and composition of ecosystems

Temperature is the major driver determining the distribution of marine ectotherm species as organismic performance is fundamentally linked to respective temperatures of the environment (Hochachka and Somero, 2002; Somero, 2005). Accordingly, temperature affects these species in a strict dependency on all levels of organismic organization (Kassahn et al., 2009). Fundamental and realized thermal niches of a species follow the shape of a performance curve which can be described and explained by the concept of oxygen and capacity-limited thermal tolerance (short **OCLTT**) established by Pörtner and co-workers (2001; 2002; Pörtner et al. 2010; Pörtner et al., 2017; See section **2.2** for further details). Only within a thermal optimum marine ectotherm species can sustain at population level. Although thermal adaption is possible, recent research indicates that the degree of global warming is likely to exceed the speed of adaption (e.g., Hoegh-Guldberg and Bruno, 2010; Burrows et al., 2011). Life stages can differ in their thermal sensitivity with juveniles and reproducing adults being the most vulnerable

("bottleneck effect," Pörtner and Farrell, 2008; Byrne and Przeslawski, 2013). To stay within their optimal thermal range species already have or will shift in latitudinal distribution as well as depth distribution leading to changes in food-web structure, productivity, and therefore, altered marine communities (Perry et al., 2005; Beukema et al., 2009; Hoegh-Guldberg and Bruno, 2010; Koenigstein et al., 2016; Calosi et al., 2016). Species populating habitats today at their upper thermal optimum at present are at high risk to become locally extinct in the near future as their performance will decrease with few degrees of warming (see below). Cold-adapted species are predicted to shift their distribution towards the poles (Perry et al., 2005; Beukema et al., 2009). Negative changes in marine benthic and fish communities have been observed within the past 50 years, e.g., in communities of the Ligurian Sea (Cattaneo-Vietti, 2018).

1.2.2 The oxygen and capacity-limited thermal tolerance (OCLTT)

The OCLTT describes the range of thermal performance in marine ectotherms in relation to their aerobic scope (2001; 2002; Pörtner et al. 2010; Pörtner et al., 2017, **Fig. 1,** from IPCC AR5 WGII Figure 6.5). Traditional parameters investigating the OCLTT are ventilation rates, oxygen consumption ($\mathbf{MO_2}$), and blood oxygen content ($\boldsymbol{PO_2}$). The underlying concept builds on the assumption that the routine performance of an organism (maintenance, growth, reproduction, etc.) has to be fully powered by aerobic metabolism/energy gain for long-term survival. Within a species-specific thermal optimum ($\mathbf{T_{Opt}}$), this holds true as oxygen demand and supply to tissues is balanced. The remaining aerobic power budget (excess of aerobic energy available) leaves the organism sufficient energy to invest in growth, storage, or reproduction (**Fig. 2,** from Sokolova et al., 2012). Within the thermal optimum, the cellular homeostasis is balanced. Temperatures below or above (the thermal optimum) progressively decrease the aerobic power budget due to an ongoing mismatch between oxygen demand and supply ($\mathbf{T_p}$ range). Organisms react a.o. with enhanced ventilation or circulation to meet the new requirements for maintenance (Frederich and Pörtner, 2000; Braby and Somero, 2006; Xing et al., 2016). In turn, possible expenditures for growth or reproduction will cease as maintenance costs rise and decrease the aerobic power budget (**Fig. 2**). Declining concentrations of PO_2 disturb cellular metabolism altering e.g. gene expression or metabolic pathways (Heise et al., 2006; Tomanek et al., 2011). Long term survival is still possible if the duration (or magnitude) of the thermal stress is time-limited (e.g., in the case of intertidal habitats or seasonal seawater changes), but less competitive species may decrease in abundance as they might be outcompeted by more competitive species. The thermal window may also shift

in T_{Opt} through acclimation limited by the species capacity to acclimate (Pörtner et al., 2010). Further warming relates to higher costs of maintenance deriving from an increased oxygen demand due to a temperature-dependent acceleration of cellular processes (***Q*10**). In addition, cellular components may get heat-damaged, also depleting energy reserves when counterbalanced (e.g., Hertz, 2012). High temperatures enhance proton leakage at the inner mitochondrial membrane limiting mitochondrial oxidative respiration (Pörtner et al., 1999; Abele et al., 2002). The release of reactive oxygen species (**ROS**) induces oxidative stress, which, together with heat-stress, induces the cellular heat-shock response (**HSR**; e.g., Lesser, 2006; Richter et al., 2010).

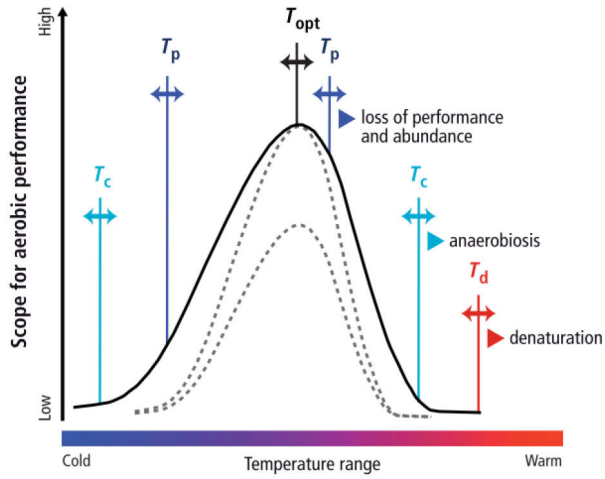

Fig. 1
Temperature-dependent aerobic performance curve of a marine ectotherm species from cold to warm temperatures based on the OCLTT concept (Pörtner, et al. 2017). The figure highlights thermal optimum (T_{Opt}), pejus (T_p), and critical ranges (T_c) with onset of anaerobiosis and finally lethal temperature (T_d) and denaturation of cellular proteins at T_d. Dashed lines indicate how thermal tolerance is affected in response to additional stressors such as e.g. hypoxia or hypercapnia.

From: IPCC AR5 WGII Figure 6.5

The HSR mediates a transient resistance against thermal stress by enhanced expression of heat shock proteins (**HSP**s), securing proper protein folding and mediate repair of damaged proteins (Lindquist, 1986; Tomanek, 2008). Maintenance of protein homeostasis has high energetic costs as all processes from protein biosynthesis over heat shock response to degradation by the proteasome consume adenosine triphosphate (**ATP**; Carter and Houlihan, 2001; Cherkasov et al., 2006; Goldberg, 2003). Organismic responses to increasing the aerobic energy gain (e.g., heart rate or ventilation) reach a limit when the performance is maximal. At the Arrhenius breakpoint temperature (**ABT**), organismic performance cannot be sustained and decreases (e.g., Pörtner, 2001; Xing et al., 2016). An insufficient aerobic energy gain to fully meet the energy demand is compensated by the onset of anaerobiosis. The transition from aerobic to anaerobic energy gain is denoted as a critical temperature ($\mathbf{T_c}$). Anaerobic energy production depletes energy storage and leads to the accumulation of acidic metabolites such as lactate, succinate, or acetic acid. Acidic end products of anaerobiosis decrease the extracellular pH ($\mathbf{pH_E}$) and the intracellular pH ($\mathbf{pH_I}$) if not eliminated (Ellington, 1983; Walsh et al., 1984).

Furthermore, at high concentrations, anaerobic end products become toxic and may induce metabolic rate depression (Storey and Storey, 1990; Reipschläger and Pörtner, 1996). Survival becomes strictly time limited at T_c and longer endurance or even higher temperatures will finally lead to the death of the organism ($\mathbf{T_D}$).

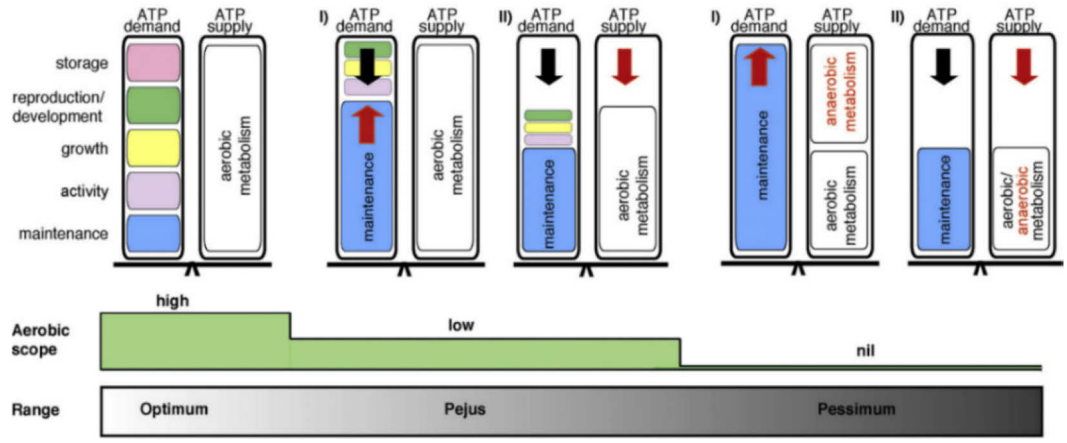

Fig. 2 Equilibrium between energy demand that is needed for organismic function (maintenance, activity, growth, reproduction/development and storage) and supply by either aerobic or anaerobic metabolism in connection to the aerobic scope defined by the OCLTT.

Figure from Sokolova et al., 2012

1.2.3 The OCLTT and temperature-related stresses

Various studies have shown that the thermal window and hence, species' performance and fitness is narrowed if organisms are challenged in addition to warming to hypoxia and/or hypercapnia (See **Fig 1;** Pörtner and Farrell, 2008; Pörtner, 2010). Both stressors reduce the aerobic scope by inducing hypoxaemia and disruption of physiological processes (Metzger et al., 2007; Pörtner, 2010; Wittmann and Pörtner, 2013). Both stresses affect organisms, especially at both edges of the thermal window (cold and warm extremes) as the already impaired performance is further reduced and hence cause more easily the death of the organism (Metzger et al., 2007).

As outlined above, oxygen ($\mathbf{O_2}$) per se defines organismic performance as underpinning principle: sufficient oxygen supply is mandatory for any aerobic organism, and its decline below critical levels is deadly (Diaz and Rosenberg, 2008). Oxygen availability in seawater is about 30 fold lower than in the atmosphere, and hence water-breathing organisms have to invest more effort to warrant sufficient O_2 supply to tissues (e.g., Verberk et al., 2011 and 2015). Solubility of O_2 in SW depends on temperature, salinity, and pressure, with values ranging between 11.2 mg $\cdot$ L^{-1} (0°C at 35 Practical Salinity Units, **PSU**) and 5.6 mg $\cdot$ L^{-1} (35°C at 35

PSU) at the sea surface (Benson and Krause, 1984). Marine organisms respond differently to declining O_2 values (e.g., Grieshaber et al., 1994). Oxyregulating species (e.g., fish) regulate their oxygen consumption and keep oxygen concentrations in their blood or hemolymph stable. Once oxygen availability falls below a critical minimum ($\mathbf{P_{Crit}}$), these organisms become oxyconformers where the ambient oxygen tension is limited and organisms shift to anaerobic energy metabolism (e.g., Grieshaber et al., 1988; Pörtner and Grieshaber, 1993). Oxyconformers, among them many bivalves, have only limited capacities to maintain hemolymph oxygen concentration by compensatory adjustments in ventilation and circulation when SW oxygen decreases. Many marine mollusks are well adapted to tolerate hypoxia and even anoxia, which they frequently experience for variable durations (e.g., intertidal or burrowing habitats). Tolerance to hypoxia can be achieved, for example, by metabolic rate depression (a trait especially oysters and mussels master perfectly), optimized anaerobic pathways to gain maximum energy, a more inactive lifestyle (and hence a slower metabolism), or by subsequently reducing body size (e.g., Stickle et al., 1989; Grieshaber et al., 1994; Clark et al., 2013).

Hypercapnia (besides affecting calcification rates) affects the acid-base metabolism of marine species (Pörtner et al., 2004; Pörtner, 2008; Wittmann and Pörtner, 2013). For species' homeostasis, it is crucial to keep the levels of their extracellular pH ($\mathbf{pH_E}$) and intracellular pH ($\mathbf{pH_I}$) in narrow borders as otherwise enzymatic reactions or mitochondrial ATP synthesis might be impaired (Heisler, 1988; Pörtner and Bock, 2000). Excessive levels of H^+ ions can be eliminated, for example, by binding to bicarbonates (passive buffering) or by active ion exchange across cell membranes through ion transport proteins such as the Na+/K+ ATPase (Pörtner et al., 2004; Melzner et al., 2009). Marine invertebrates, such as bivalves with low capacities for acid-base regulation, are expected to be more vulnerable to hypercapnia than species with high capacities for acid-base regulation (Michaelidis et al., 2005; Melzner et al., 2009; Wittmann and Pörtner, 2013).

1.3 Model organisms

From a retrospective view, bivalve mollusks appear to be ideal model organisms to understand past and future climate changes scenarios as their shells keep well preserved with fossil records covering more than 500 Ma of earth history. This taxon did not change drastically in morphology, lifestyle, or presumably physiology, thus allowing a comparison between palaeo and extant bivalves.

1.3.1 Evolution of bivalves

The appearance of bivalve mollusks is associated with the Cambrian (~ 540 Ma; Runnegar and Pojeta, 1974). The earliest fossil documentation of Pectinidae is dated back to the late Devonian (~ 372 Ma), with four genera surviving the PT-ME (Waller, 2006). Brachiopod taxa dominated the Permian fauna, but populations collapsed during the PT transition. Back then, early bivalves were initially less dominant. As they were one of the less affected groups during this ME, early bivalves could recover fast with extensive rates of adaptive radiation leading to a huge macroevolutionary turnover with bivalves then becoming diverse and dominating members of the palaeofauna (Sepkoski, 1981; Fraiser and Bottjer, 2007; Ros and Echevarría, 2011). Fossil records from the PT-ME implicate that the orders of Ostreida, Trigoniida, and Mytilida were less affected than Pectinida, Myalinida, and Pholadomyida (Tu et al., 2016).

1.3.2 Extant bivalves

In the present study, two economically and ecologically important extant marine bivalve species were chosen: one from the order Ostreoida, the European oyster *Ostrea edulis,* and one from the order of Pectinida, the King scallop, *Pecten maximus*. Both orders have experienced various marine mass extinctions with a rich fossil record available for integration to scientific studies in the field of paleontology. First, the appearance of true oysters occurred within the PT transition, and it seems likely that both families belonging to the Ostreoidae derived from a common ancestor in the Permian (Lopha-like oysters, Nakazawa and Newell, 1968).

Today, bivalves are dominant members of the modern benthic fauna with high ecological and economic values. Bivalves are among the largest classes contributing to estuarine and coastal benthic invertebrate communities. Many bivalves, especially oysters and mussels, are considered to be keystone species as they are particularly relevant for marine biodiversity (e.g., Smith et al., 2014). They provide habitat (e.g., oyster or mussel beds) for other benthic organisms and positively influence seawater quality (Asmus and Asmus, 1991; Gutiérrez et al., 2003; Kreeger et al., 2018). Furthermore, bivalve adaptation to highly variable environments promoted the evolution of a high genetic and phenotypic plasticity enabling these species to endure broad ranges in salinity, oxygen, and temperature (Hedgecock 2005; Dame, 2016). As hypoxia-tolerant organisms, bivalves possess extensive anaerobic metabolic pathways (e.g., review by De Zwaan and Wijsman, 1976; Müller et al., 2012). Oysters (and other intertidal or infaunal bivalves) can shut close under unfavorable conditions or low tides outliving these conditions by reduction of the standard metabolic rate (**SMR**). This trait enables them to be

exceptionally tolerant to fluctuations in O_2 - surviving even weeks of anoxia by switching to metabolic depression and anaerobiosis (Brinkhoff et al., 1983; Seaman, 1991; Grieshaber et al., 1994; Michaelidis et al., 2005). Scallops inhabit coastal and offshore subtidal seafloor habitats and are adapted to a more stable environment. They differ from other bivalves, firstly by their anatomy, as they cannot tightly close their valves as other bivalves (Tremblay and Guderley, 2013), and secondly, by their active lifestyle with swimming by jet propulsion via rapid valve clapping (Wilkens, 2006). The unique trait of pectinids being capable of swimming (serving as escape behavior) developed in the Early Triassic (Waller, 2006; Hautmann, 2010). The active lifestyle demands more energy, and hence, scallops have been shown to maintain higher levels of mantle cavity PO_2 correlated to higher standard metabolic rates (SMR) than e. g. mud clams (Abele et al., 2010). Swimming actions are mainly fueled by adenosine triphosphate deriving from the consumption of arginine phosphate (**PLA**; Grieshaber and Gäde, 1977; Wilkens, 2006; Guderley and Pörtner, 2010).

1.3.3 The European oyster (*Ostrea edulis*)

The European flat oyster *Ostrea edulis* (Linnaeus 1758, Fig **3**) is a bivalve mollusk of the order Ostreoida (family Ostreoidae). Oysters commonly reach ~ 11 cm in size and have a lifespan of 10-15 years (www.fao.org). As filter feeders, they nourish on algae. *O. edulis* reach maturity after ~3 years with frequent changes in sex (hermaphrodite). They inhabit hard substrates in high densities within the intertidal to subtidal zone of estuarine or coastal areas, mainly at depths between 0-6 m, but some individuals have been found as deep as 50 m offshore. Native distribution extends from the Norwegian Sea, the North Sea to the Iberian Peninsula, the Atlantic coast of Morocco, as well as the Mediterranean Sea with extensions to the Black Sea (www.fao.org, see Fig. **4**). *O. edulis* has been introduced to North America, Australia and Japan.

Fig. 3 Adult *O.edulis* used in the present study. Oyster has a size of about 7 cm. **Photo credit S. Götze**

While being very abundant in the past, natural populations became scarce in the last century. Reasons were over-fishing, the introduction of *Crassostrea gigas* (a habitat competing oyster species) and the weakening of *Ostrea* populations by bacterial and virus diseases (Da Silva et al., 2005; Culloty and Mulcahy, 2007; Beck et al., 2011). *O. edulis* was incorporated into the list of endangered and/or decreasing species and habitats by the Convention for the Protection

of the Marine Environment of the North-East Atlantic (**OSPAR agreement 2008-6**) and various European countries started protection and renaturation programs (e.g., "**Restore,**" 2016). Due to their endangered status, the production for the human food market derives solely from aquaculture with 2 t global production for 2016 (www.fao.org).

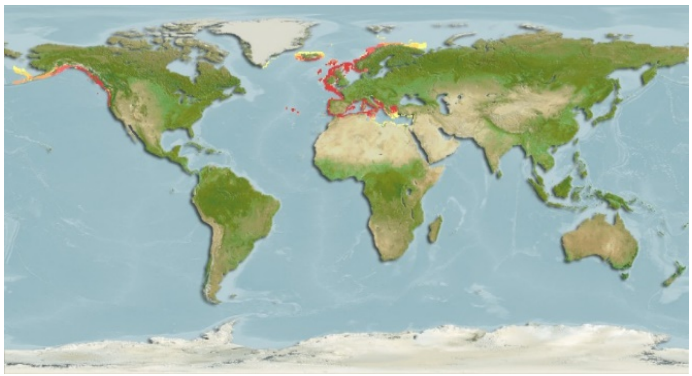

Fig. 4 Geographical map showing native distribution of *O.edulis*. Red areas indicate best suitable habitats with high occurrences (in the past), Orange to yellow indicate habitats were populations occurred but not with highest populations. The native range comprised coastal areas Northeast Pacific, Northeast Atlantic and Mediterranean Sea. The map was generated with www.aquamaps.org.

1.3.4 The King scallop (*Pecten maximus*)

The King scallop, *Pecten maximus* (Linnaeus 1758, Fig. **5**) is a subtidal bivalve belonging to the order of Pectinida (family Pectinidae). King scallops commonly reach sizes of ~ 15 cm with a similar lifespan as *O. edulis*. They are permanent hermaphrodites, reproducing between April and September. The habitat comprises coastal and offshore areas, and scallops occur in depths of up to 250 m preferentially residing on sand, gravel bottom, or muddy substrates.

Fig. 5 Adult *P.maximus* used in the present study (size 11 cm). **Photo credit S. Götze**

Native populations of *P. maximus* extend from northern Norway, the North Sea, the Iberian Peninsula, the Mediterranean Sea and the most southern distribution in West Africa (See Fig. **6**). Furthermore, King scallops are found around the Azores, Madeira and the Canaries. *Pecten maximus* is extensively fished in the UK, France and Spain (Brand et al., 2006), and they are one of the most intensively captured and produced bivalves with nearly ~108 t in 2016 (~ 60 000 t global capture plus 48 t global aquaculture, www.fao.org).

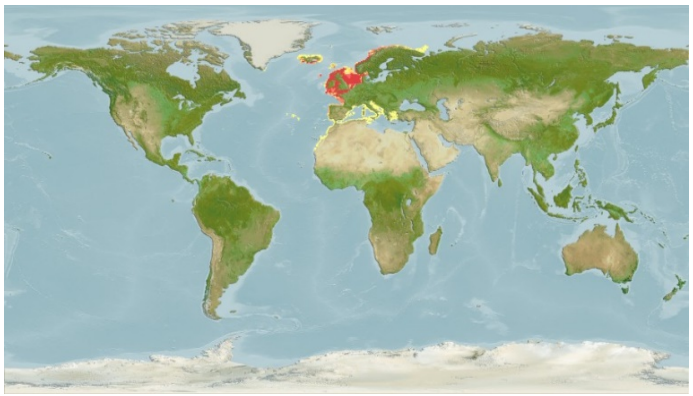

Fig. 6 Geographical map showing native distribution of P. *maximus.* Red areas indicate best suitable habitats with high occurrences (in the past), Orange to yellow indicate habitats were populations occurred but not with highest populations. The native range comprised coastal areas of Eastern Atlantic and the Mediterranean Sea. The Map was computer generated with www.aquamaps.org. (version of Aug. 2016.

1.4 Rationale

Oxygen demand and supply to tissues in extant facultative aerobe marine invertebrates today follow the same physiological principles as in the past. This enables us to understand the fundamental mechanisms which drive species into extinction in recent taxa and to help understanding palaeo-findings as the outcome of past climate crises, which was the main aim of BIV-TRS. *O. edulis* and *P. maximus*, were chosen due to rich fossil records of the respective orders, and their high ecological and economic value. For the integration of the findings to the PT-ME, we subjected both species to acute temperature-related stresses. The pH was reduced in our experiments by about 0.6 pH Units (to ~7.5, within the range of pH reduction during the PT-ME Clarkson et al., 2015). Estimates for the PT-ME regarding oxygen go as low as full oxygen depletion developing over a few millions of years (anoxia, e.g., Wignall and Twitchett, 1996; Weidlich et al. 2003). However, we did not want to kill the bivalves by instantly subjecting them to anoxia but rather investigate mechanisms that are activated in response and hence, we chose a reduction to ~55% O_2 saturation staying above the critical PO_2 value. For a widespread and integrative assessment, BIV-TRS was subdivided into two PhD projects, which were closely interlinked, with common hypotheses, but approaching the objectives from different organismic viewpoints. As organismic responses are manifold and reflect the responses of various processes, approaches integrating macrophysiology and molecular biology must be designed to understand a species' fate more comprehensively (e.g., Clark et al., 2016). The current project focused on biochemical and molecular mechanisms involved in TRS responses with the following specific research aims:

1.4.1 Research aims

1. The fundamental aim was to determine the acute thermal window of both bivalves and to define T_o, T_p, T_c and T_d along a thermal gradient starting at the lower annual habitat temperature (14 °C) until the lethal temperature was reached. Turning point temperatures of organismic performance such as heart rate, oxygen consumption and filtration rate (see section **1.2**) were determined in the thesis of C. Eymann. Cellular markers (current thesis) aimed to identify changes in energy metabolism as, for example, the onset of anaerobiosis (for T_c) and to determine the status of cellular homeostasis (cellular damage and defense) along the thermal window. Damage was investigated on the level of proteins and lipids. As heat-protective measure an important member of the heat-shock response, the heat-inducible isoform of HSP70 was investigated. We proposed that both thermal windows reflect the adaption of *O. edulis* and *P. maximus* to their habitat (intertidal *vs.* subtidal) and lifestyle (sessile *vs.* swimming), as explained in section **1.3.2**. We expected that *O. edulis* possess high capacities to endure temperatures beyond T_p possibly by switching to metabolic depression as they do, for example, during low-tide. Active *P. maximus* were expected to be less tolerant toward temperatures past T_{Opt} as it was anticipated that their high metabolism exacerbates the mismatch between oxygen demand and supply and hence causes a faster decrease in performance.

2. Single and combined exposures to hypercapnia and hypoxia narrow the thermal window and decrease the aerobic scope of performance visible by an earlier onset of anaerobiosis and impairments in cellular homeostasis (see section **1.2.3**). Based on findings obtained in part 1, the second aim was to understand the effects of additional, single and combined stressors on the above mentioned biochemical and molecular parameters. Of special interest was the question of how and to which extent scallops and oysters were capable of maintaining homeostasis. *P. maximus* was anticipated to be more sensitive, especially to hypoxia, than *O. edulis* due to its active lifestyle and higher metabolic rates. To test this, *P. maximus* was exposed to the same acute exposures as described in **1**, but this time in the presence of either hypoxia (WHo), hypercapnia (WHc), or the combination of all stresses (denoted as "Deadly Trio"; DT). *O. edulis* was exposed only to acute warming and DT. The same organismic and cellular markers were investigated as for **1** to determine shifts in thermal performance**.**

3. Experimental findings were evaluated in the context of extinction patterns of both orders during the PT-ME to approach the lead question "What drives species into extinction?" In addition to findings from **1** and **2,** a small meta-analysis underlined differences in the vulnerability of both orders now and then.

MATERIAL AND METHODS

2.1 Exposures

2.1.1 Animal origin and maintenance

The Biological Station of Toralla (ECIMAT, University of Vigo, Spain) provided all bivalves. Adult European oysters (*Ostrea edulis*) were taken from raft cultured populations grew in the estuary of Ferrol (**CF-139;** 43º 27.86 N, 8º 11.84W) and the estuary of Ares (**CF-168;** 43º 24.82, N 8º 09.70W) and experienced the same environmental parameters and fluctuations as wild oysters. Adult King scallops (*Pecten maximus*) living in the estuary of Vigo (~42°14'46.6"N 8°44'18.5"W) were caught by SCUBA divers of the Biological Station. The distance between the locations is ~180 km (**Fig. 7**).

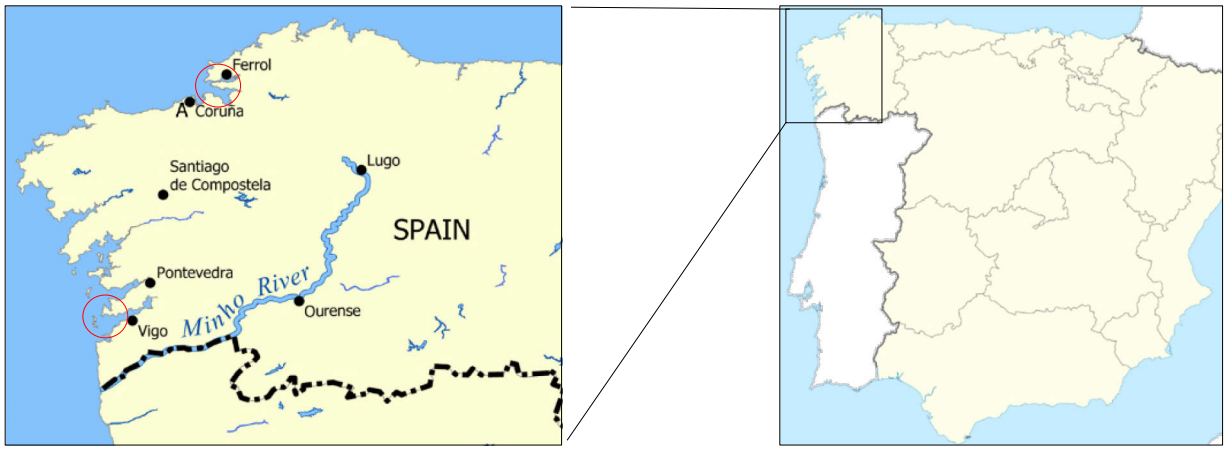

Fig. 7 Geographical map of the region of Galicia where both species originated. A "zoom-in" is made for the estuary of Ferrol and the estuary of Vigo. The red circle indicates the origin of animals.

Bivalves were transported to the Alfred-Wegener Institute Helmholtz Center for Polar and Marine Research (AWI, Bremerhaven) within 24 hours. The environmental conditions at the time of collection were as follows: seawater temperature 12-14°C (for oysters and scallops obtained in early spring) and ~18°C (for scallops obtained in autumn 2017) at full salinity of ~33 PSU. The average size and weight of both species used in the exposures is depicted in **Tab 1**.

All bivalves were acclimated for at least four weeks at ambient SW temperature and full salinity. Feeding took place three times per week using either a mixture of commercial algal blend (Nyos, PhytoMaxx) or a self-cultivated algal mixture including *Rhodomonas spec*., *Phaeodactylum tricornutum, Chaetocerus spec*., and *Isochrysis galbana.* Epibionts were carefully removed from each bivalve, and individual length, width and weight were recorded.

Tab. 1 Mean size (in cm) and weight (in g) of the different batches of bivalves obtained between 2017 and 2019.

Species	Season obtained	Year	Experiment	Mean size		
				length (cm)	width (cm)	weight (g)
O.edulis	Spring	2017	Warming	6.7 ± 0.5	6.5 ± 0.75	63 ± 12
	Spring	2019	Warming	7.4 ± 0.6	7.2 ± 0.6	87 ± 15
	Spring	2019	Deadly Trio	7.4 ± 0.5	7.4 ± 0.7	89 ± 16
P.maximus	Authumn	2017	Warming	11.2 ± 0.8	9.6 ± 0.5	167 ± 32
	Authumn	2017	Warming + Hypercapnia	9.6 ± 0.5	10.9 ± 0.7	172 ± 42
	Spring	2018	Warming + Hypoxia	10.2 ± 1.1	11.7 ± 1.3	190 ± 41
	Spring	2018	Deadly Trio	10.7 ± 1.1	12.3 ± 1.2	194 ± 42

2.1.2 Experimental design

All exposures were performed together with C. Eymann. The full experimental design comprised four groups: acute warming (**W**), acute warming *plus* hypoxia (**WHo**), acute warming *plus* hypercapnia (**WHc**), and the combination of all three stressors (**DT**; **Fig. 8**). Gas concentrations were held at >90 % O_2 air saturation (PO_2 = 19.2 to 20.6 kPa depending on temperature)in the normoxic exposures (W and WHc), and at 55-60 % O_2 air saturation (PO_2 = 10.7 to 13.5 kPa depending on temperature) in the hypoxic exposures (Who and DT). Levels of carbon dioxide were held at ~550 ppm CO_2 in the normocapnic exposures (W and WHo) and at 1800 ppm CO_2 in the hypercapnic exposures (WHc and DT). The levels of both gases were mixed by a gas-mixing device (HTK, Hamburg). The exposures were carried out in temperature constant rooms using recirculating systems equipped with a thermostat for temperature control. Oysters and scallops were introduced at ambient density.

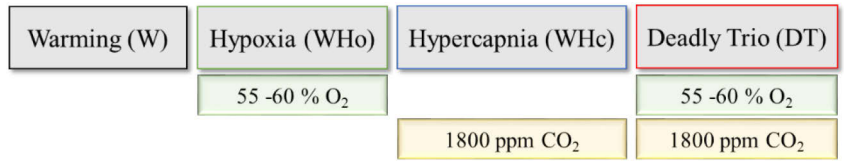

Fig. 8 Illustration of the four different exposures including the chosen SW parameters for oxygen (O_2) and carbon dioxide (CO_2).

Due to technical issues with the gas mixing device, *O. edulis* was initially only exposed to warming (spring 2017, data are presented as joint work with C. Eymann in **publication 1**). In spring 2018, the full experimental approach was performed for *P. maximus* (data presented in **manuscript 2 and 3**). Subsequently, the full experimental approach for *O. edulis* should have been run in autumn 2018, but the batch of oysters died. After acclimation of a new batch, the HTK system broke and could not be repaired before spring 2019. Resulting time constraints made it impossible to run the full experimental approach, so only warming and DT were run (preliminary data are presented in supplementary). Exposures started at 14°C (lower annual habitat temperature) except for the run in 2019, which started at 18°C (within the optimal

temperature range, **publication 1**). The temperature was increased once by 2°C every 48 hours and kept constant for 43 hours before sampling. Exposures ended at the acute lethal temperature, which was reached at 36°C for *O. edulis* and at 28°C for *P. maximus*. Bivalves were fed at least twice a day with algal mixtures containing a minimum of 3,000 cell/ml (as indicated earlier) to prevent starvation. Tanks were cleaned when necessary to hold the levels of nitrite, nitrate and ammonium below critical concentrations. Dead bivalves were removed at sight.

2.1.3 Analysis of seawater chemistry

Throughout all experiments, seawater parameters were tightly regulated and temperature (± 0.5°C borders), salinity (± 0.5 PSU borders), partial pressures of oxygen (P_{O_2}) and carbon dioxide (P_{CO_2}) were held in closest possible borders. Temperature and salinity were measured with a conductometer (WTW, LF-197). P_{O_2} was measured with calibrated O_2-optodes (PreSens, Germany). P_{CO_2} was measured by a Vaisala device (Vaisala, Finland). At each temperature, pH was measured with a pH electrode (InLab® Routine Pt1000, Mettler Toledo), calibrated at the respective temperature (pH buffer solutions by National Bureau of Standards, NBS standards, Fisher Scientific) and then converted to $pH_{Freescale}$ (Riebesell et al. 2010; Waters and Millero, 2013). Further SW chemistry (nitrite, nitrate and ammonia) was determined by the institutional training laboratory for lab assistants (**Head** Timo Hirse). Annette Tillmann determined the concentration of dissolved inorganic carbon (**DIC**) using a continuous flow analysis (CFA; QuAAtro, Seal Analytical; based on Stoll et al., 2001). Carbonate chemistry parameters (total alkalinity, saturation state (Ω) for calcite and aragonite) were calculated using CO2SYS software (Lewis and Wallace, 1998) using barometric pressure values, as well as DIC, pH, temperature and salinity values determined for the respective day and temperature step. For calculations, we used K1 and K2 from Millero (2010), the KSO_4 dissociation constant from Dickson (1990), freescale for seawater pH, and the $[B]_I$ value from Uppström (1974).

2.1.4 Survival and mortality

Bivalve survival was calculated based on excess animals which were not used for tissue analyses (at start n >20). Dead specimens were subtracted from the number of residual animals and the survival per temperature step was expressed in percentages (**%**). The half-maximal lethal temperature ($\mathbf{LC_{50}}$) was calculated for each exposure.

2.1.5 Tissue sampling

At each respective sampling temperature (4°C interval) between 4 and 8 bivalves were sampled (**Fig. 9**). In the case of oysters, only those being open for at least 30 to 60 min prior to sampling were taken to prevent sampling of oysters, which were metabolically inactive. Bivalves were dissected on ice. The hemolymph was drawn from the beating heart with a syringe for analysis of PO_2 (for the project of C. Eymann). Thereafter, gill, mantle, muscle, and hepatopancreas were removed and shock-frozen in liquid nitrogen. Tissues were stored at - 80°C until further analyses.

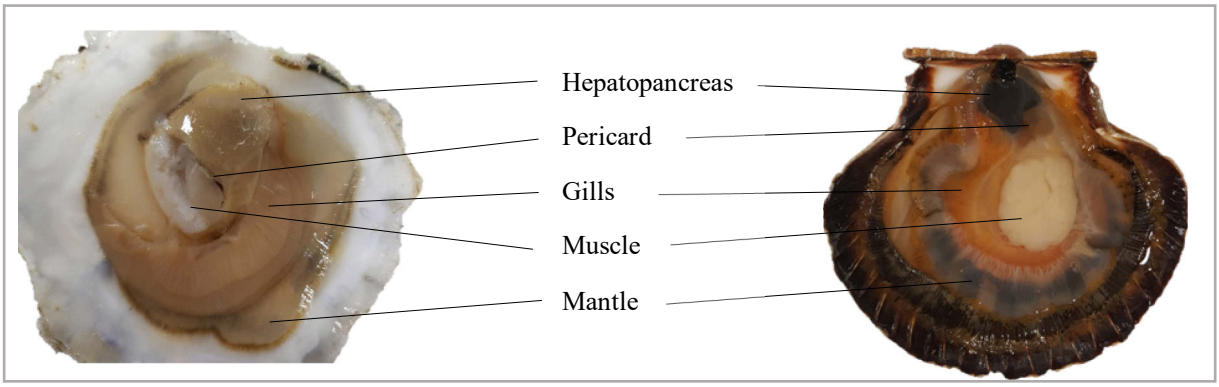

Fig 9 Illustration of oyster (left) and scallop (right) anatomy showing location of the hepatopancreas, pericard, gills, mantle and muscle.

2.2 NMR spectroscopy

Untargeted metabolic profiling by ^{1}H-Proton-NMR spectroscopy was performed to identify changes in metabolites and associated metabolic pathways. Laboratory work comprised metabolite extraction, NMR-spectroscopy, evaluation of spectra, including identification of metabolites, as well as statistical analysis by the online platform www.metaboanalyst.ca. Additionally, for *P. maximus* in-depth pathway analyses of gill and phasic muscle were carried out.

Data source for publications:

O. edulis gill tissue run in 2017 contributed to **publication 1**

P. maximus gill tissue of full exposure set contributed to **manuscript 2**

(*O. edulis gill tissue run in 2019 will contribute to manuscript 4*)

2.2.1 Extraction of metabolites

Tissue metabolites were extracted with methanol-chloroform (Tripp et al., 2017). In the case of oysters, only gills were analyzed, whereas in the case of scallops, both gill and phasic muscle were analyzed. Extracts were prepared using 40 - 50 mg of tissue (fresh weight, **FW**), homogenized in ice-cold methanol (8 mL g^{-1} tissue) and MilliQ water (2.5 mL g^{-1} tissue). Homogenization was done by Precellys 24 (Bertin Technologies, France) for 20 s at 6,000 rpm and 4°C. Thereafter, chloroform (8 mL g^{-1} tissue) and MilliQ (4 mL g^{-1} tissue) were added, vortexed, and incubated for ten minutes. Homogenates were centrifuged for ten minutes at 3,000 rpm at 4°C and the upper layer (containing the polar metabolites) was dried overnight via a Vacufuge® (Concentrator Plus, Eppendorf). The pellets were stored at 4°C until further analysis and resuspended in the 2-fold volume of the FW in deuterized water (**D_2O**). Three-(trimethylsilyl) propionic-2,2,3,3-d4 acid sodium salt (**TSP**; 0.05 %; Sigma Aldrich, St. Louis, USA) was included in D_2O as an internal standard.

2.2.2 Untargeted ^{1}H-NMR spectroscopy

One dimensional ^{1}H-NMR spectroscopy was carried out in an ultra-shielded vertical 9.4 T NMR spectrometer (Advance III HD 400 WB, Bruker-BioSpin GmbH, Germany) equipped with a triple tuned ^{1}H-^{13}C-^{31}P-HRMAS NMR probe. All samples were run with the Call-Purcell-Meiboom-Gill (**CPMG**) sequence using the software TOPSPIN 3.2 (TopSpin 3.2, Bruker-BioSpin GmbH, Germany). Each spectrum was baseline, shim, and phase-corrected and calibrated to the TSP signal using the software Chenomx NMR suite 8.1 (Chenomx Inc., Canada). The assignment of peak signals to the respective metabolite was carried out using the internal database of Chenomx and literature data available for bivalves (e.g., Tikunov et al. 2010; Tikunov et al. 2014; Capello et al. 2018). A detailed list of assigned metabolites for both species is shown in supplementary ST 2-4, and an exemplary 1D-^{1}H-NMR spectra *P. maximus* is shown in **S8**.

2.2.3 Statistical analysis

Metabolite concentrations from gills of both species were generalized log transformed and metabolite concentrations from phasic muscle tissue of *P. maximus* were cube root transformed to obtain a normalized data distribution (Purohit et al., 2004). Data sets of scallops were further normalized against the sum of adenylates (AMP, ADP, and ATP). For statistical analysis, the online platform *Metaboanalyst* was used (www.metaanalyst.ca; Xia and Wishart 2016). An unsupervised principle component analysis (**PCA**) was used to determine statistical outliers

within data sets. These values were then deleted for the subsequent analysis. In-depth analysis by one-way ANOVA was followed by a post-hoc test (either Tukey or Fisher's LSD; p-value ≤ 0.05) for the factors "temperature" and "exposure." Cluster analysis of metabolite profiles was performed by a supervised partial least–square discriminant analysis (**PSL-DA**). Metabolites significantly altered as provided by MetaboAnalyst (4.0) were plotted as mean concentrations (**mM**) ± the standard deviation (**SD**) using Sigma Plot (12.0, Systat Software, Inc.).

2.2.4 Pathway analysis

Data sets were further analyzed for changes in metabolic pathways at elevated temperatures and/or additional stressors. All data sets were normalized as described above. A two-group comparison was performed with *Metaboanalyst* using the following settings as recommended by Xia and Wishart (2010):

Pathway library: zebrafish (*Danio rerio*)
Pathway enrichment analysis: "global test" - based on a Bayesian generalized linear model
Pathway topological analysis: 'relative betweenness centrality'

Identified pathways suggested by metaboanalyst were controlled for plausibility and, e.g., pathways associated with bacterial metabolism were excluded. Pathways with significant changes in metabolites (determined in ANOVA) and a p-value < 0.0033 which equals a [-LOG(p)] change > 2.5 were considered to be relevant and the results integrated into a cell model showing metabolic pathways (Schemes 1-2 in **manuscript 2** for gills of *P. maximus*).

2.3 Heat shock response

Protein levels of the heat-inducible isoform of heat-shock protein 70 (**HSP70**) as a measure of the cellular stress response were determined in scallops and oysters (2019). Laboratory work comprised homogenization of gill tissue, soluble protein determination after Bradford (1976), SDS-PAGE, and detection via a specific antibody.

Data sources for publications:

Gill tissue of *P. maximus* (full exposure set) contributed to **manuscript 3**
(Gill tissue analysis of O. edulis will contribute to manuscript 4 once available)

2.3.1 Preparation of extracts and protein determination

Tissues (~ 50 mg) were extracted in a 5-fold volume of ice-cold homogenization buffer (10 mM Tris-HCL, 10 mM KCL, 1.5 mM $MgCl_2$, 0.5 mM PMSF, 1 mM Na_3VO_4, and 5 µg/ml full protease inhibitor mix (Sigma, P8340)). A reference sample contained subsamples (n = 15) taken across treatments for standardization between blots. Homogenization was done by Precellys 24 (Bertin Technologies, France) for 20 s at 6,000 rpm at 4°C. Samples were centrifuged for 15 minutes at 13,000 g and 4°C to remove cell debris. The soluble protein concentration in the supernatant was determined after Bradford (1976). Bovine serum albumin (BSA) was used as a protein standard in concentrations between 0 µg to 5 µg of protein. The reaction was started with the addition of 250 µl of dye reagent (Applichem, A6932) and the plate was incubated for ten minutes to allow a full-color response. The optical density was measured at 600 nm with a microplate reader (BioTek Power wave HT). The protein concentration was calculated according to the equation of the calibration straight of the BSA (µg/µl protein). All samples were heat-denatured (10 min, 95°C) in SDS-loading buffer containing 2.5 % ß-mercaptoethanol (Laemmli, 1970) to a final protein concentration of 1 µg protein per µl solution and stored at -80°C.

2.3.2 SDS-PAGE and Western blotting (WB)

Electrophoresis was carried out in BioRad Mini-Protean chambers using ten percent (weight per volume) acrylamide gels, according to Laemmli (1970). Samples containing 10 µg protein were randomized and applied to the gels. Furthermore, each gel contained a protein marker (BioRad, Precision plus Protein Standards) and the reference sample. The electrophoresis was carried out at 200 Volt for 45 min at room temperature. Proteins were transferred on polyvinylidene difluoride (**PVDF**) membranes using Mini Trans-Blot® Cell systems (BioRad) in ice-cold transfer buffer (192 mM Glycine, 25 mM Tris, 0.037% SDS (weight/vol), 20% Methanol (vol/vol)) for two hours at 200 milliamperes per chamber.

2.3.3 Immunodetection

After WB, membranes were incubated for 1 hour at RT in five percent (weight /vol) nonfat milk in Tris-buffered saline plus Tween 20 buffer (**TBST**, 20 mM Tris, 150 mM sodium chloride, 0.1 % Tween 20**)** to block unspecific binding sites. The primary antibody HSP70 (MA3-006; Thermo Fisher Scientific) was used at a 1:5000 dilution in five percent nonfat milk in TBST overnight at 4°C. The membranes were then washed, incubated in an anti-mouse secondary antibody in five percent nonfat milk in TBST (1:40000, GE Healthcare, Munich, Germany) for

2 hours, and washed again to remove non-bound secondary antibody. Membranes were incubating for 3 min in enhanced chemiluminescence solution (ECL; GE Healthcare, Munich, Germany). Signals were detected using a cooled charge-coupled image reader (Fujifilm Intelligent dark box LAS 1000). The signal intensity (given as luminescence arbitrary units = **LAU**) was quantified using AIDA Image Analyzer v. 3.52 (Raytest, Straubenhardt, Germany) software. The intensity of each sample was normalized against the signal of the reference sample.

2.4 Cellular damage

The status of cellular damage was analyzed by quantification of polyubiquitin-conjugates and malondialdehyde. The content of polyubiquitin-conjugates was analyzed with a specific antibody. Malondialdehyde was measured after Uchiyama and Mihara (1978) modified after Abele et al. (2002)**.**

Data source for publications:

P. maximus gill tissue (full exposure set) contributed to **manuscript 3**

2.4.1 Polyubiquitin-conjugates

Levels of polyubiquitin-conjugates were detected in gill extracts prepared for HSP70, and IB was carried out as described in **section 2.2**. Electrophoresis was carried out using eight percent (w/Vol) acrylamide gels, and the primary anti-ubiquitin antibody was used at a dilution of 1:2000 (P4D1, Enzo Life Sciences). This antibody detects ubiquitin-conjugates of any size, revealing a binding smear on the blot and the intensity of the whole smear was used for quantification. The intensity of each sample was normalized against the signal of the reference sample.

2.4.2 Malondialdehyde (MDA)

Gills were grounded with mortar and pestle in the presence of liquid nitrogen. About 75 mg of the tissue powder was transferred to a Precellys 24 tube containing ice-cold 0.2% phosphoric acid in a 1:5 tissue to acid ratio. Homogenization was carried out with a Precellys 24 device for 2x 15 s at 5,000 rpm at 4°C (Bertin Technologies, France). Then, two percent of phosphoric acid was added to yield a final concentration of 1.1% phosphoric acid. Each sample was divided

into two (samples of 200 µl each); to one subsample the identical volume of thiobarbituric acid (TBA; 1% TBA in 50 mM NaOH) was added; to the other subsample (blank sample) 200 µl of an HCL solution (3 mM) was added. Samples were adjusted with pH-paper to a pH of 1.6 and incubated at 100°C for 60 minutes in a water bath. After transferring the solutions to new tubes, 1 ml of butanol (100%) was added and vortexed (40 sec). Samples were centrifuged for five minutes, 1000 g at RT. The upper phase was taken, transferred to a new tube and centrifuged again for five minutes at 14,000 g (RT). The supernatant was measured at 530 nm in a microplate reader (Berthold), and the absorbance was quantified by a standard series using Malondialdehyde-bis-acetate ranging from 0 - 40 mM.

PUBLICATIONS

Publication I

"Thermal performance of the European oyster *Ostrea edulis* (Linnaeus, 1758) explaining ecological findings under climate change"

Accepted for publication in ***Marine Biology*** (05.11.2019)

Manuscript 2

"Single and combined effects of the "Deadly trio" hypoxia, hypercapnia and warming on the cellular metabolism of the great scallop *Pecten maximus*"

Submitted for publication in ***Comparative Biochemistry and Physiology - Part B: Biochemistry & Molecular Biology***

Manuscript 3

"Effects of climate drivers on cellular damage and stress response of the great scallop *Pecten maximus"*

To be submitted to *Journal of Experimental Marine Biology and Ecology*

PUBLICATIONS

Publication I

"Thermal performance of the European oyster *Ostrea edulis* (Linnaeus, 1758) explaining ecological findings under climate change"

Accepted for publication in Marine Biology (in press)

Shared first authorship with Charlotte Eymann

Contribution of the candidate in % of the total workload

Experimental concept and design	45 % *
Experimental work and data acquisition	40 % *
Experimental work and data acquisition for my part	90 %
Data analysis and interpretation	50 % *
Preparation of figures and tables	35 % *
Drafting the manuscript	65 %

* Shared experiments with C. Eymann

Thermal performance of the European Flat Oyster, *Ostrea edulis* (Linnaeus, 1758) – explaining ecological findings under climate change

Charlotte Eymann[1*], Sandra Götze[1*], Christian Bock[1], Helga Guderley[2], Andrew H. Knoll[3], Gisela Lannig[1], Inna M. Sokolova[4], Martin Aberhan[5], Hans-O. Pörtner[1]

[1] Alfred Wegener Institute Helmholtz Centre for Polar and Marine Research. Am Handelshafen 12, 27515 Bremerhaven, Germany

[2] Department of Biology, Institut de Biologie Integrative et des Systemes, 1030 Avenue de la Medecine Universite Laval, Quebec City, Quebec Canada G1V 0A6,

[3] Department of Organismic and Evolutionary Biology, Harvard University, Cambridge, MA 02138, USA;

[4]Marine Biology, Faculty of Mathematics and Natural Sciences, University of Rostock, Rostock, Germany

[5] Museum für Naturkunde, Leibniz Institute for Evolution and Biodiversity Science, 10115 Berlin, Germany

[*] Lead authors contributing equally to this paper

Corresponding author:

Prof. Dr. Hans-O. Pörtner

Alfred Wegener Institute Helmholtz Centre for Polar and Marine Research

Am Handelshafen 12

27515 Bremerhaven, Germany

T: +49 471 4831 2015

e-mail: Hans.Poertner@awi.de

Abstract

Climate change challenges marine organisms by constraining their temperature-dependent scope for performance, fitness and survival. According to the concept of Oxygen and Capacity Limited Thermal Tolerance (OCLTT) the overall thermal performance curve relates to an organism's aerobic power budget, its overall aerobic scope for growth, exercise, reproduction and other performances. We hypothesize that physiological principles shaping tolerance in extant ecosystems have also been operative during climatic changes in the distant past. To compare response patterns in extant fauna and their palaeo-relatives, we started here by studying the metabolic background of performance in the European flat oyster *Ostrea edulis* at organismic and cellular levels, focusing on the acute thermal window and the metabolic changes towards upper lethal temperatures. We investigated the response of the oysters (pre-acclimated at 12 °C) to a short-term warming protocol (by 2 °C every 48 h) from 14 to 36 °C which we identified as the lethal temperature. At the organismic level, heart and filtration rates were recorded. Gill metabolites were studied by ^{1}H NMR spectroscopy to address thermal responses at the cellular level. Feeding activity by *O. edulis* (assessed by the filtration rates) was highest between 18 °C - 24 °C when overall energy expenditure (indicated by heart rate as a proxy for routine metabolic rate) is moderate. We conclude that this range reflects the thermal optimum of this species. Beyond 26 °C the gill tissue of *O. edulis* became partly anaerobic, and cardiac dysfunction (arrhythmia) developed at 28 °C followed by an Arrhenius break point (30 °C). This mirrors performance constraints and a wide temperature range of passive tolerance which may be a long-standing characteristic of ostreids and support survival in extreme environments and during climate oscillations, in their present habitat as well as the past.

Keywords: performance, untargeted ^{1}H-NMR based metabolic profiling, ocean warming, thermal window, OCLTT, anaerobiosis, palaeo-perspective

Introduction

Marine ecosystems are currently challenged by increasing atmospheric CO_2 concentrations and associated climate change, which cause ocean warming, acidification and progressive hypoxia, the latter as a result of reduced oxygen solubility and increased water column stratification (Sabine et al. 2004; Hoegh-Guldberg and Bruno 2010; Pörtner et al. 2014). Temperature is a key driver of ongoing global change. Under unabated warming the global mean ocean surface temperature is expected to increase by 1.8 – 4 °C by the end of the 21st century (Rhein et al. 2013). This will drive shifts in the geographical and depth distribution of species (Beukema et al. 2009; Calosi et al. 2016; Koenigstein et al. 2016), leading to shifts in the composition of marine communities, reduced complexity of benthic habitat and loss of some species (e.g. Garrabou et al. 2009; Bertolino et al. 2015; Cattaneo-Vietti 2018). The impact of warming on marine organisms is likely to depend on their fundamental thermal niche relative to the realized niche occupied in their current habitats, so that species living near their thermal tolerance limits will be harmed by warming, while those living at temperatures below their thermal optimum may benefit from warming, e.g. through increased growth, reproduction or recruitment (Shepard et al. 2010).

The changes in the ocean projected for this century and beyond may reach extreme values depending on emissions scenarios and extreme events such as marine heat waves. Similar to projections of ecosystem changes caused by ongoing climate change, past ocean changes of the three drivers of marine global change even larger than those anticipated for the 21st century, caused ecological crises characterized by species losses and distributional changes (Bambach et al. 2004; Knoll et al. 2007; Joachimski et al. 2012). During the end-Permian mass extinction 252 million years ago over 80 % of the marine fauna went extinct, as sea surface temperatures increased by up to 11 °C (Wignall and Twitchett 1996; Stanley 2016; Penn et al. 2018). Experimental studies of extant fauna simulating different climate futures support a basic understanding of how climate change will impact marine fauna and how it may have done so in the distant past, assuming similar physiological mechanisms in place. As the capacities of individual species and functional groups to cope with environmental changes may differ, comparative studies of extant relatives of species and groups may provide explanations of ongoing ecological change as well as patterns of extinction as observed in the palaeo-record of past evolutionary crises.

Temperature is an abiotic factor with a pervasive effect on all levels of an animal's physiology and aerobic performance (Hochachka and Somero 2002; Pörtner et al. 2014). The

relationship between temperature and organism performance has been described by the oxygen- and capacity limited thermal tolerance (OCLTT) concept established by Pörtner (2001; Pörtner et al. 2009; 2017). According to OCLTT, the range of active thermal tolerance is the thermal range of survival at individual to population levels since maintenance costs and additional functions such as growth, reproduction and species interactions are fully covered by aerobic metabolism. The more temperature exceeds the optimum range, the more aerobic power budget decreases beyond pejus limits (conditions are getting worse) due to an over-proportional rise in energetic costs which demand an increasing fraction of oxygen supply, finally resulting in the onset of anaerobiosis (beyond a critical temperature), and ultimately, death of the organism. Accordingly, the OCLTT concept helps to understand physiological capacities of a species in relation to their environmental niches (Pörtner et al. 2017). Key parameters required to understand the effects of temperature on aerobic power scope include measures of energy demand [such as the oxygen uptake rate (MO_2)], as well as the traits related to oxygen uptake and distribution (including ventilation rates, cardiac function, and blood oxygen content), ideally combined with whole animal performance indicators such as growth, activity or reproduction. Further drivers such as ocean acidification or hypoxia may influence these basic responses to temperature as well as the respective OCLTT indicators.

Previous studies have shown a strong positive correlation between MO_2 and heart rate in marine invertebrates (HR, Marshall and McQuaid 1992; Schiffer et al. 2014; Bakhmet 2017), and HR measurements have been used to determine thermal tolerance windows in mollusks (Zittier et al. 2015; Xing et al. 2016). Heart rate (HR) was shown to increase exponentially with increasing temperature until reaching a species-specific break point beyond which HR dropped in mollusks and crustaceans (Widdows 1973; Frederich and Pörtner 2000; Braby and Somero 2006; Xing et al. 2016). The cardiograms of stressed molluscs also displayed arrhythmic and asystolic heart beats (Nicholson 2002; Domnik et al. 2016).

Filtration rate is another important performance indicator in bivalves. Temperature-dependent filtration rate is a major contributor to the aerobic power budget of bivalve mollusks, because filtration is essential for both oxygen uptake at the gills and nutrient delivery. In bivalves, filtration rates are strongly affected by temperature (Møhlenberg and Riisgård 1978; Jørgensen et al. 1990), reflecting altered water viscosity (Petersen et al. 2003) and metabolic capacity (Specht and Fuchs 2018), with consequences for an organism's energy budget. Therefore, the temperature window where cardiac function and filtration rates can be optimally or at least adequately maintained is linked with the thermal tolerance limit where long-term

energy homeostasis and positive aerobic power scope can be sustained. While the overall metabolic balance involving optimal cardiac performance and oxygen and food uptake (e.g. through filtration) ensures long-term survival and fitness of an organism, the ability to withstand extreme warming (such as can occur during prolonged heat waves) is important in determining the thermal tolerance limits.

During warming, the transition to partial anaerobiosis occurs well before the lethal temperature is reached. In parallel, metabolic depression may reduce energy demand extending survival. Transition to partial anaerobiosis might be related to a critical decrease in the oxygen content of the mantle cavity as also seen in the body fluids of other invertebrates (Taylor 1976; Brinkhoff et al. 1983; review by De Zwaan and Wijsman 1976), reflecting a mismatch between oxygen supply and demand (e.g. Frederich and Pörtner 2000; Melzner et al. 2007; Giomi et al. 2013).

As part of a larger effort to systematically compare the vulnerability of various bivalve groups to climate change (ongoing and during the geological past, DFG-funded Research Group Tersane) we study the development of thermal constraints in the European flat oyster *Ostrea edulis* (*O. edulis*, Linnaeus, 1758), a molluscan keystone species that occurs naturally in the North-Eastern Atlantic, from the Norwegian coast down to Morocco, and in the entire Mediterranean Basin (FAO). When measuring survival, filtration rate, heart rate, and cellular biomarkers for anaerobiosis we follow the hypothesis that physiological principles identified in extant fauna have also shaped the survival, performance, geographical distribution and demise of related marine fauna in the distant past (Pörtner et al. 2005; Knoll et al. 2007). Responses to climate-induced changes in ambient drivers such as temperature, CO_2 and oxygen (Penn et al. 2018) can in fact constrain geographical distribution. However, associated extinction risks are not sufficiently considered (Finnegan et al. 2015). As a first step we aim to link the observed temperature-induced changes at different functional levels and define the oyster's fundamental thermal niche for later comparison to other bivalve species and groups in extant fauna and palaeo-analogues. We chose oysters as a model organism because fossils suggest that this clade shows relatively high tolerance to environmental perturbation as well as strong competitiveness against other molluscan species (Guo et al. 2018).

Material and Methods:

Animal origin and maintenance

Adult, raft cultured *Ostrea edulis* grown in the estuary of Vigo (Spain, **CF-139**: Ría de Ferrol 43º 27.86 N, 8º 11.84W; **CF-168;** Ria de Ares 43º 24.82, N 8º 09.70W; and **CF-095** Ria de Ares 43º 24.55, N 8º 10.16W) and exposed to the full range of natural environmental conditions, were obtained from the Biological Station of Toralla (ECIMAT, University of Vigo) in spring 2017. Environmental conditions at the time of collection were as follows: water temperature ~14 °C and a salinity of ~33 PSU. Oysters had an average size of 6.7 ± 0.5 cm in length, and 6.5 ± 0.7 cm in width. The mean total weight was 63 ± 12 g. Oysters were wrapped in wet tissues and transported to the Alfred-Wegener Institute Helmholtz Center for Polar and Marine Research (AWI, Bremerhaven) by air within 24h after collection. Upon arrival, the animals were immediately transferred to the institutional aquarium system filled with North Sea water (SW, 12 °C, 32 PSU) and pre-acclimated for at least 2 weeks. They were fed every other day either with a commercial algal blend (Nyos, PhytoMaxx) or a self-cultivated algal mixture containing *Rhodomonas sp., Phaeodactylum tricornutum*, *Chaetocerus sp.*, and *Isochrysis galbana*. Prior to the experiments epibionts were carefully removed and each oyster was measured, weighed and individually labelled.

Experimental setup and water chemistry

Randomized groups of labelled oysters were transferred to constant temperature rooms and incubated at 12 °C in recirculating aquarium systems as described in Schalkhausser et al. (2013). Briefly, the system consisted of header, receiver and reservoir tanks and several experimental tanks, that were either populated with individual oysters (animals used for simultaneous recordings of heart rate, see below) or several oysters (15-20 oysters per 27 L tanks) later used for tissue sampling. Oxygenation in all flow-through tanks was kept > 90 % by continuous aeration (see Table 1). Throughout all experiments, oysters were fed by regular addition of a self-cultivated algal mixture. Algal concentrations were maintained at a minimum of 3000 cells mL^{-1} SW. Every day the experimental tanks were checked for mortality and faeces, and cleaned if necessary. After a 3 day pre-acclimation period to allow for recovery from handling, temperature was increased within 5 h overnight by 2 °C once every 48 h and kept at the targeted value ± 0.5 °C (see Table 1) for 40 - 43 h. Measurements were performed and samples taken at 14 °C, 18 °C, 22 °C, 26 °C, 30 °C, 32 °C, and 34 °C, respectively. Heart rate

was monitored online throughout exposure and analyzed for each 2 °C temperature step. After warming to 36 °C all remaining oysters died within 18 h. This protocol was run in triplicate.

Water temperature, salinity, partial pressures of oxygen (PO_2) and carbon dioxide PCO_2) were monitored daily. PO_2 was determined using O_2-optodes (PreSens, Germany), and PCO_2 was measured with a Vaisala device (Vaisala, Finland). The pH was measured using a pH electrode (InLab® Routine Pt1000, Mettler Toledo) calibrated with National Institute of Standards and Technology standard pH buffer solutions (National Bureau of Standards, NBS standards, Fisher Scientific). pH was converted to $pH_{Freescale}$ (Waters and Millero 2013) as recommended in the guide for best practice in ocean acidification research (Riebesell et al. 2010). All devices were calibrated at the respective temperatures. The concentration of dissolved inorganic carbon (DIC) was determined using continuous flow analysis (CFA; QuAAtro, Seal Analytical) according to Stoll et al. (2001). Seawater carbonate chemistry parameters (total alkalinity, saturation state (Ω) for calcite and aragonite) were calculated using CO2SYS software (Lewis and Wallace 1998) using barometric pressure values, as well as DIC, pH, temperature and salinity values determined for the respective day and temperature step. For calculations, we used K1 and K2 from Millero (2010), the KSO_4 dissociation constant from Dickson (1990), freescale for seawater pH, and the $[B]_I$ value from Uppström (1974). Levels of nitrite, nitrate and ammonium were monitored and held below critical concentrations by regular SW exchanges, approximately twice a week. Detailed seawater physiochemical conditions at each temperature step are shown in Table1.

Filtration rate

Since oysters retained the algae with 100% efficiency, filtration rates (FR) were calculated as the decrease of *Rhodomonas sp.* concentration over time standardized to soft body dry weight (DW) (Møhlenberg and Riisgård 1978; Nielsen et al. 2017). At each temperature step the same individuals were placed in separate, temperature-controlled cylindrical 1 L tanks, and allowed to recover from handling stress for 1 h prior to the start of FR determination. Then, *Rhodomonas sp.* was added (final concentration 20.000 cells mL^{-1} to ensure sufficient algae provision for maximal FR) and samples were taken after 0, 15 and 30 min. Gentle bubbling during the experiment prevented the sedimentation of algal cells. Algal concentration was measured with a MultisizerTM 3 Coulter Counter (Beckman; USA) fitted with a 100 µm aperture tube. Separate 1 L tanks fitted with shells only, served as controls for algal sedimentation, which was

negligible. Directly after each animals' death, soft body mass was taken and dried for 48 hours at 80 °C.

The filtration rate (FR) was calculated according to Coughlan (1969) and is expressed as DW-specific rates (L h^{-1} gDW^{-1}):

$$FR = \frac{V}{(t * n)} * ln\frac{C_0}{C_t} : DW$$

where V is the water volume of the experimental tank (L), t is the time (h), n is the number of individuals per tank (here, n = 1). C_0 and C_t are the algal concentrations (cells mL^{-1}) at time 0 and t, DW is the dry weight of the soft body mass (g).

Heart rate

Cardiac activity was measured using photo-plethysmography (Depledge and Andersen 1990; Zittier et al. 2015). The shell above the pericardium was sanded down carefully, and the plethysmograph (iSiTEC, Germany) was fixed (Pattex Ultra superglue, Germany). The signal was amplified (Type HBA-100; iSiTEC, Germany) and recorded with the software LabChart (ADInstruments, Australia). HRs of eight oysters in total were monitored throughout exposure, during 36 h per temperature step. HR data (beats per min, bpm) were analyzed manually, excluding periods immediately after disturbances, such as the presence of researchers close to the experimental setup as well as low signal to noise ratios. This resulted in an analysis of 45 min recordings per temperature step using LabChart 8 Reader (ADInstruments, Australia). The whole plethysmograms of the 36 h recording were checked for pauses in the heart rate (≥ 15 min), which we defined as cardiac arrest (**Fig. 1**). Periods of cardiac arrest were expressed in % fractions of time in the total 36 h measurement period.

Tissue sampling and metabolite extraction

For tissue analyses, only open and ventilating oysters were randomly selected, weighed, and dissected on ice (n = 6-8). Oysters were checked regularly throughout the sampling day and only oysters that were open for at least 30 min prior to sampling were sacrificed. Tissues (gills, mantle, hepatopancreas and muscle) were removed quickly, shock-frozen in liquid nitrogen, and stored at -80 °C for further analyses. Gill metabolites were extracted using the methanol-chloroform extraction technique for small samples as described in Tripp et al. (2017). Gill tissue (40 - 50 mg) were homogenized in ice-cold methanol (8 mL g^{-1} tissue) and ice-cold MilliQ water (2.5 mL g^{-1} tissue) with Precellys 24 (Bertin Technologies, France) for 20 s at 6,000 rpm

at 4 °C. Thereafter, chloroform (8 mL g^{-1} tissue) and MilliQ (4 mLg^{-1} tissue) were added. The homogenate was vortexed, incubated on ice for 10 min, and centrifuged for 10 min at 3,000 rpm and 4 °C. The upper methanol layer, containing polar metabolites, was used und dried using a SpeedVac at RT (RVC 2–33 IR, Christ GmbH, Germany) overnight. Dried pellets were stored at 4 °C until further analysis. Prior to analysis each pellet was re-suspended in a defined volume of deuterized water (D_2O), 2-fold of the initial tissue weight. D_2O contained 0.05 wt % of 3-(trimethylsilyl) propionic-2,2,3,3-d4 acid, sodium salt (TSP) (Sigma Aldrich, St. Louis, USA) as an internal standard and chemical shift reference. Final TSP concentration in each sample was 3.2 mM.

Untargeted ^{1}H NMR based metabolic profiling

One dimensional ^{1}H-NMR spectroscopy was conducted in an ultra-shielded vertical 9.4 T NMR spectrometer (Advance III HD 400 WB, Bruker-BioSpin GmbH, Germany) using a high-resolution magic angle (HRMAS) probe for small volumes . The suspension was transferred into a standard 50 µl zirconia on rotor of a triple tuneable ^{1}H-^{31}P-^{31}C HRMAS probe. Sample spinning rate was 3000 Hz at 20°C. TOPSPIN 3.2 software (TopSpin 3.2, Bruker-BioSpin GmbH, Germany) was used for acquisition. The NMR protocol comprised four different techniques as described in detail by Schmidt et al. (2017). The Call-Purcell-Meiboom-Gill (CPMG) sequence was used for metabolite analysis and quantification. Each spectrum was baseline, shim, and phase corrected and calibrated to the TSP signal with the software Chenomx NMR suite 8.1 (Chenomx Inc., Canada). Thereafter, the ^{1}H-NMR signals within each spectrum were assigned to metabolites by their chemical shifts using the Chenomx database. After assignment, the integration routine within Chenomx was used for metabolite quantification based on the TSP standard concentration. The concentrations of the proteinogenic branched chain amino acids valine, leucine, and isoleucine were summed for analysis.

Statistical analysis

The statistical analysis for temperature impacts on heart rate (HR) and filtration rate (FR) was performed with SigmaPlot 3.5 (Systat software Inc.). The temperature-induced changes in HR and FR were detected by one-way repeated ANOVA followed by a pairwise post hoc Holm-Sidak test. An Arrhenius plot was used to detect discontinuities in the temperature dependent slopes of HR and the Arrhenius break temperatures (ABTs) were calculated from intersections of linear regressions (Nickerson et al. 1989; Yaeger and Ultsch 1989).

The temperature-dependent performance curve of FR_F was fitted according to Schmalenbach et al. (2009):

$$FR_F(T) = Ae^{-0.5(\frac{\ln(\frac{x}{x_0})}{B})^2})$$

where A, B and x_0 are coefficients of variation and x are FRs at ambient temperature.

The temperature-dependent performance curve of HR_F was fitted according to Pörtner and Knust (2007):

$$HR_F(T) = F_1(T) + F_2(T) = (A_1e^{B_1T} + C_1) + (A_2e^{B_2T} + C_2)$$

F_1 (T) describes the temperature-dependent increase of HR until maximum. F_2 (T) represents the declining course in HR.

Gill metabolic profiles were analyzed for changes using *Metaboanalyst* (Metaboanalyst 3.6; Xia and Wishart 2016). Compound concentrations were normalized by generalized log-transformation for stabilizing the variance across metabolites as described by Purohit et al. (2004). Thereafter, a univariate one-way ANOVA followed by a Tukey's HSD was performed. The multivariate analysis comprised an unsupervised principle component analysis (PCA) aiming to find the directions that best explained the variance in the data set. Furthermore, we performed a supervised partial least–square discriminant analysis (PSL-DA) for class separation taking the weighted sum of squares of the PSL loadings (=Variable Importance in Projection; VIP) into account. The significance threshold was set to $P < 0.05$.

Results

Mortality

Mortality of the oysters throughout exposure was negligible (< 7 %) until 36 °C was reached. The remaining oysters died during the first 18 h after reaching 36 °C.

Filtration rate

Filtration rates (FR) of *O. edulis* had an optimum between 18-26 °C (**Fig. 2;** repeated 1-way ANOVA, $F = 8.10$, $DF = 6$, $P < 0.001$). Individuals varied more in absolute FR values at 26 °C compared to other temperatures. Mean FR increased from 3.0 ± 2.0 L h^{-1} gDW^{-1} at 14 °C to a maximum of 7.7 ± 4.5 L h^{-1} g DW^{-1} at 22 °C followed by a progressive decrease resulting in a minimal FR of 0.3 ± 0.3 L h^{-1} g DW^{-1} at 34 °C.

Heart rate

Heart rate (HR, **Fig.3**) increased from 11.98 ± 1.88 bpm at 14 °C and reached 41.54 ± 4.34 bpm at 30 °C, with a mean linear increase of 1.85 ± 0.70 bpm $°C^{-1}$. Further warming from 30 °C to 36 °C decreased HR at a rate of 1.81 ± 1.66 bpm $°C^{-1}$ leading to a HR of 30.69 ± 7.53 bpm at 36 °C. The calculated Arrhenius break temperature was 30.33 °C (**Fig. 4**). From 14 °C to 26 °C HR showed a regular heart beat rhythm with increasing frequency and amplitude at increasing temperatures (**Fig. 5 a-b**). At 28 °C animals started to show temporary cardiac arrhythmia which was counterbalanced by high cardiac activity up to 30 °C (**Fig. 5c**). The frequency of arrhythmia increased with rising temperatures, combined with a significantly reduced HR at 36 °C (repeated 1-way ANOVA, $F = 96.86$, $DF = 6$, $P < 0.001$).

O. edulis showed temperature dependent periods of cardiac arrest (**Fig. 5d**), which could be divided in three phases: From 14 to 22 °C the occurrence of cardiac arrests increased slightly from 0.2 ± 0.1 % to 1.3 ± 0.3 % of the recording time. At 24 °C and 26 °C, cardiac arrests reached a maximum at 3.8 ± 0.7 % of total measurement time (1-way ANOVA, $F = 16.154$, $DF = 11$, $P < 0.001$). Above 26 °C cardiac arrest was rare and only observed at 32 °C (0.15 ± 0.06 %) and 36 °C (0.53 ± 0.15 %).

Metabolites

We identified 25 metabolites in the gill extracts of *O. edulis* (typical ^{1}H-NMR spectrum shown in **Fig. 6**). Main compounds were osmolytes and amino acids. Organic osmolytes were taurine, betaine, trimethyl-N-oxide (TMAO) and homarine, with taurine and betaine exhibiting the highest concentrations in all spectra. Free amino acids were alanine, ß-alanine, glutamine, glutamate, glycine, valine, isoleucine, leucine, lysine, arginine, homocysteine, and aspartate. Furthermore, we found signals of the adenylates such as ATP and ADP that were, however, not clearly distinguishable and three intermediates of the Krebs cycle: succinate, malate and fumarate, which are biomarkers for anaerobic metabolism. We further identified three membrane related intermediates sn-glycero-3-phosphocholine, choline, and o-phosphocholine. UDP-glucose was the only sugar and key metabolite of the carbohydrate pathway identified. The singlet of acetate was assigned despite overlapping with arginine, lysine, and 4-aminobutyrate.

Metabolite profiles under acute warming

Principal component analysis did not indicate any specific outliers in the sample classes (data not shown). The class membership prediction by PLS-DA revealed that the gill metabolome of *O. edulis* was homogeneous in bivalves within the temperature range between 14 °C and 26 °C (**Fig. 7a**). The largest variance across the two principal components was found in the 26 °C group indicating high heterogeneity between samples. Some individual profiles clustered closer to the profiles of samples taken at temperatures below 26 °C, while others were closer to the cluster of samples taken at 34 °C. The metabolome of *O. edulis* started to shift at 30 °C with a complete separation from all other clusters at 34 °C. The main metabolites explaining the PLS-DA projection (Fig. **7b**) show the highest scores for the intermediates related to anaerobiosis such as fumarate, succinate and malate. The univariate analysis complements the PLS-DA results. Alanine, as a marker for early anaerobiosis, increased significantly from the initial value of 0.46 ± 0.11 mM at 14 °C to 0.84 ± 0.23 mM at 26 °C but showed no further increase with further warming (**Fig 8**). The metabolites of late anaerobiosis (succinate, malate, and fumarate) remained at baseline levels (0.02 ± 0.01 mM for succinate and fumarate, and 0.1 ± 0.03 mM for malate) until 22 °C was reached. At 26 °C all three metabolites increased significantly and reached their maximum concentration at 34 °C with 0.083 ± 0.04 mM (succinate), 0.36 ± 0.27 mM (malate) and 0.06 ± 0.02 mM (fumarate, $P \leq 0.001$).

Discussion

Filtration and heart rates. We investigated the response of the European flat oyster, *O. edulis*, to acute warming. Following the OCLTT concept, we aimed to depict the acute thermal tolerance window of *O. edulis* by linking performance indicators, filtration rate (FR), heart rate (HR) and hence, indirectly, oxygen supply, while identifying the thermal constraints to aerobic metabolic performance, as determined from cellular markers for anaerobiosis. In combination with an in-depth-analysis of cardiac online recordings, the present data suggest not only a physiological, but also a behavioral change of *O. edulis* exposed to warming.

For comparison to literature data, it is important to be sure that FR is determined under optimal conditions, considering methodological, abiotic, and biotic aspects which ensure that bivalves are fully open, and thus, display maximal filtration (Riisgård 2001). FR increased linearly with warming as long as the animals were within their window of thermal tolerance as identified in literature studies (Kittner and Riisgard 2005; Riisgard et al. 2003). Beyond such limits, FR dropped in association with a progressive reduction in valve gape (Jørgensen et al.

1990; Kittner and Riisgard 2005). Overall, the FR of *O. edulis* followed a temperature-dependent bell shaped curve between 14 and 36°C. Similar curves were described by Widdows (1976) for *Mytilus edulis* between 10 and 28°C and by Petersen et al. (2003) for Arctic clams, *Hiatella arctica* and *Mya sp.* between -1 and 11 °C. *O. edulis* filtered at maximum rates between 18 and 26 °C reaching on average 7.7 ± 4.5 L h^{-1} gDW^{-1}, which is comparable to the 7.3 ± 1.7 L h^{-1} gDW^{-1} at 22 °C when using *Rhodomonas* cultures (Nielsen et al. 2017). Notably, three out of seven individuals showed impaired FR at 26 °C suggesting a constraining temperature (see discussion below).

Temperature dependent changes in the HR of *O. edulis* revealed a warming induced limitation at higher temperatures than those observed for FR. An Arrhenius break point temperature (ABT) of HR was reached at 30 °C. Close to the ABT, we observed onset of cardiac arrhythmia occurring from 28 °C onwards. Warming-induced loss of rhythmic HR has previously been shown for other bivalves (Trueman and Lowe 1971; Babry and Somero 2006; Xing et al. 2016). While monitoring HR we observed infrequent periods of cardiac arrest. Nearly complete suppression of HR occurs with some delay upon valve closure in bivalves (Trueman and Lowe 1971; Lannig et al. 2008).

Notably, at the lower exposure temperatures (14 to 22 °C), we observed cardiac arrest periods in *O. edulis* that may reflect the natural, rhythmic opening/closure behavior of bivalves. For example, Ortmann and Grieshaber (2003) monitored valve movements of the Asian clam, *Corbicula fluminea*, over a period of two years, and showed that valve opening/closure followed a circadian rhythm during summer.

Progressive warming of *O. edulis* led to extended periods of cardiac arrest at 24 °C and 26 ° C, possibly reflecting a behavioral response to less favorable conditions by extended valve closure. During winter season, when temperature (< 5 °C) and food availability were very low, Asian clams also showed extended closure periods of several days (Ortmann and Grieshaber 2003). *Mytilus galloprovincialis* remained open for approximately 90 % of the time under favorable conditions and closed its valves for up to 50 % of the time when temperatures became unfavorable (Anestis et al. 2007). Benefits for immersed bivalves to remain closed during intervals of poor algal supply or hypoxia are mainly interpreted as energy saving strategies since upon closure metabolic rate (SMR) is reduced (Jørgensen et al. 1986; Ortmann and Grieshaber 2003; Sokolova et al. 2012; Riisgard and Larsen 2015). However, further warming will cause energy demand to rise with oxygen consumption increasing steadily without leveling off (Newell et al. 1977; Shumway and Koehn 1982; Haure et al. 1998). Accordingly, periods of

cardiac arrests ceased in *O. edulis* above 26 °C, paralleled by an opening of the shell (personal observations) that enables aerobic metabolism to fuel most if not all of the rising energy demand. Previous studies have shown that increasing acclimation temperature elevated the respiratory time activity (RTA, fractional time that animals spend open, ventilating actively) in the Eastern oyster, *Crassostrea virginica* (Lannig et al. 2006). Similarly, periods of cardiac arrest became scarce at temperatures of 28 °C and beyond in *O. edulis* indicating a disruption of the normal valve closing pattern in response to warming for increased oxygen uptake to cover high cellular energy demand.

Mode of metabolism

The main cellular response to warming beyond 26 °C was an increase in the levels of anaerobic metabolites indicating an onset of anaerobiosis with levels peaking shortly before death of the organisms at 34 °C. Anaerobic end product concentrations (e.g. succinate, acetate, or propionate) are highly variable depending on preferred anaerobic pathways; they may also depend on tissue (anaerobic pathways of bivalves reviewed by De Zwaan and Wijsman 1976; Livingstone 1991; Müller et al 2012). In gill tissues of *O. edulis,* succinate was the predominant anaerobic end product. We observed a significant rise of anaerobic end products at 26 °C, 10 °C below the lethal temperature. Interestingly, oysters sampled at this temperature were most diverse in their branchial metabolomic profiles as indicated by the PLS-DA model. Here, the individuals clustered either closer to profiles of lower temperature groups (= performing better) while two samples were closer to the metabolomic pattern found at 34 °C (= performing worse).

The onset of anaerobiosis at 26 °C paralleled the increased cardiac arrest times and may be a response to valve closure and associated oxygen deficiency, as part of the energy saving strategy. In contrast to alanine levels (early anaerobiosis) which remained stable beyond 26 °C, those of succinate (fumarate and malate) showed a second, more drastic rise at 34 °C, thereby indicating severe oxygen deficiency, due to an increase in branchial energy demand, cutting back on time for survival. Indeed, further warming to 36 °C resulted in death of all animals.

The average annual SW temperatures in NW Spain (Galicia) where the oysters were collected ranges between 11 °C and 21 °C with temperatures above 16 °C between May to November (Pazos et al. 1997; www.seatemperature.org). Aquaculture oysters are raft cultured in the estuary and experience the same environmental parameters as wild oysters. Our data indicate an optimal temperature range for the Spanish oyster population between 18 to 24 °C suggested by moderate, rhythmic HR and maximal filtration (**Fig.9**) consistent with the

prevailing summer temperatures in oyster' habitat. Similarly, a study of the brown mussel *Perna perna* from the Gulf of Mexico, revealed a long-term upper tolerance limit at around 30 °C, congruent with the ambient seasonal SW temperature (Hicks and McMahon 2002).

Notably, European oysters displayed a broad temperature span of 10 °C between T_{crit} and the lethal temperature, while other studies showed this range to be much narrower. For example, the temperate sublittoral king scallop, *Pecten maximus* displayed an upper limit to its thermal optimum at around 25 °C (Artigaud et al. 2014), and reached the lethal temperature at 26 -28 °C (Götze et al. in prep.). One reason might be, that oysters, being adapted to a highly variable environment, have a broad passive tolerance range to endure abiotic challenges beyond the optimum (Pörtner et al. 2017). This is in agreement with studies showing that the upper thermal tolerance limit of bivalves correlates significantly with habitat (littoral vs. sublittoral) and tidal height distribution (e.g. Wilson 1981; Wilson and Elkaim 1991).

While temperature induced changes in oxygen consumption and heart rates are positively correlated in marine invertebrates (Marshall and McQuaid 1992; Schiffer et al. 2014; Bakhmet 2017) our data suggest moderate metabolic costs for *O. edulis* within its thermal optimum. Hence, the thermal limit to HR is not yet reached, leaving some room for an increase in aerobic metabolism, a conclusion supported by an ABT at around 30 °C. According to Guderley and Pörtner (2010), maintenance costs (measured as standard metabolic rate = SMR) are moderate within the optimum range and fully covered by aerobic metabolism; this is paralleled by a maximum scope for growth, with sufficient energy being provided by the aerobic power budget. Furthermore, in NW Spain the predominant phytoplankton blooms occur from May to September (Bode et al. 2005). During these months with ample food supply and favorable ambient temperatures, *O. edulis* should have a high net gain in body weight. Indeed, earlier studies showed that the scope for growth was maximal at around 15 °C (Newell et al. 1977; Buxton et al. 1981). Accordingly, *O. edulis* spends most of the year at temperatures within its active thermal tolerance range (Pörtner et al. 2017).

The progressive rise in HR above 22 °C when FR starts to level off indicates a rise in baseline aerobic energy demand which increasingly constrains aerobic performance. This is in line with the study of Buxton et al. (1981) showing that between 20 and 25 °C filtration efficiency declined while oxygen demand still rose, resulting in a shrinking scope for growth. Consequently, a reduction in valve gape might be a behavioral response to limit food intake and thus digestion costs as maintenance costs rise. This might indicate that *O. edulis* has reached the upper pejus temperature range of OCLTT (conditions getting worse; Pörtner et al. 2017).

Further warming (≥ 26 °C) emphasized performance limitations as indicated by a significantly reduced FR, the onset of cardiac dysfunction (e.g. arrhythmia) and paralleled by the accumulation of anaerobic end products. According to OCLTT, the onset of anaerobiosis indicates that an organism surpasses the critical temperature (T_{crit}), where survival becomes strictly time-limited due to the mismatch between aerobic energy demand and supply (Pörtner et al. 2017). Gill metabolism indicates T_{crit} being surpassed from 26 °C onwards, several degrees below the temperature threshold for cardiac dysfunction. Accordingly, gill functioning seems to be a more sensitive thermal stress indicator than HR. This can be explained by the high metabolic activity and energy demand of gills (see discussion above). In its natural environment, *O. edulis* might undergo partial anaerobiosis at this temperature (26 °C); at the same time the species can survive in a time-dependent manner as indicated by the rhythmic and not yet fully maximized heart rate. This response and associated metabolic depression may support extended passive survival of *O. edulis*. Finally, arrhythmia and an ABT setting in at around 28 -30 °C indicate diminished O_2 distribution to tissues associated with limited circulatory performance, and accordingly, cardiac failure corroborating that the upper thermal limit has been reached (Somero 2002). While in other species T_{crit} and cardiac ABT are similar cardiac ABT of the oyster is shifted to higher temperatures within the passive tolerance range. Furthermore, anaerobiosis as an alternative energy supply also supports passive survival (Pörtner 2001; Han et al. 2017) until finally a lethal temperature is reached at 36 °C.

Outlook

Our results indicate that *O.edulis* in NW Spain lives currently largely within its thermal optimum range. This population, however, might be negatively affected in the course of projected ocean warming. SW temperatures exceeding 26 °C may constrain oyster performance unless acclimatization occurs. Elevated temperatures may also make oysters susceptible to bacterial and viral infection (Zannella et al. 2017), leading to altered species composition of communities that may contribute to weaken the European oyster populations (Poloczanska et al. 2013). Further research is needed to understand the long-term effects of thermal stress on this species, and to what extent and how *O. edulis* is able to resist the warming trend. One crucial factor of resilience is set by the cellular capacity to maintain cellular homeostasis and integrity. Temperature stress induces cellular protective responses such as upregulation of e.g. heat shock proteins, or antioxidant pathways, which demand energy and diminish growth or reproduction. The sum of cellular protection mechanisms is defined as the capacity of passive

tolerance, which is strictly time-limited (Pörtner 2010). Therefore, one crucial aspect of further research will be to understand the passive capacity of *O. edulis* and how it is influenced as well as exploited during combined exposures to warming, oxygen deficiency and increased CO_2 levels. The combined capacities of both active and passive tolerance mechanisms may influence the selective survival of species under climate change and associated extreme conditions and may thereby shape related changes in community composition (see introduction). If such principles hold for ongoing climate change they may also have been operative during climate driven evolutionary crises in Earth history.

Acknowledgments:

This study was funded by the Deutsche Forschungsgemeinschaft (DFG Po278/16-1) and is embedded in the Research Unit TERSANE (FOR 2332: Temperature-related stressors as a unifying principle in ancient extinctions). We thank I. Ketelsen, F. Feliz Moraleda, and R. Gorniak for technical support and assistance during the exposures and animal care. Furthermore, we want to thank the section Marine BioGeoScience, in particular S. Trimborn, A. Terbrüggen and T. Brenneis for providing access to the Coulter Counter and the Observer microscope. We thank the Biological station of Toralla (ECIMAT, Spain), in particular A. Villanueva and D. Costas for support in animal supply.

Compliance with Ethical Standards:

This study was funded by the Deutsche Forschungsgemeinschaft (DFG Po278/16-1).

Conflict of Interest: Authors declare that they have no conflict of interest.

Ethical approval: All applicable international, national, and/or institutional guidelines for the care and use of animals were followed.

References:

Anestis A, Lazou A, Pörtner H-O, Michaelidis B (2007) Behavioral, metabolic, and molecular stress response of marine bivalve *Mytilus galloprovincialis* during long-term acclimation at increasing ambient temperature. Am J Physiol Regul Integr Comp Physiol 293:911-921. https://doi.org/10.1152/ajpregu.00124.2007.

Artigaud S, Lacroic C, Pichereau V, Flye-Sainte-Marie J (2014) Respiratory response to combined heat and hypoxia in the marine bivalves *Pecten maximus* and *Mytilis spp.* Comp Biochem Physiol A Mol Integr Physiol 175:135-140. https://doi.org/10.1016/j.cbpa.2014.06.005.

Bakhmet IN (2017) Cardiac activity and oxygen consumption of the blue mussel (*Mytilus edulis*) from the White Sea in relation to body mass, ambient temperature and food availability. Polar Biol 40:1959-1964. https://doi.org/10.1007/s00300-017-2111-6.

Bambach RK, Knoll AH, Wang SC (2004) Origination, extinction, and mass depletions of marine diversity. Paleobiology 30:522-542. https://doi.org/10.1666/0094-8373(2004)030<0522:OEAMDO>2.0.CO;2.

Bertolino M, Betti F, Bo M, Cattaneo-Vietti R, Pansini M, Romero J, Bavestrello G (2015) Changes and stability of a Mediterranean hard bottom benthic community over 25 years. J Mar Biol Assoc UK 96:341–350. DOI: https://doi.org/10.1017/S0025315415001186.

Beukema JJ, Dekker R, Jansen JM (2009) Some like it cold: populations of the tellinid bivalve *Macoma balthica* (L.) suffer in various ways from a warming climate. Mar Ecol Prog Ser 384:135-145. https://doi.org/10.3354/meps07952.

Bode A, Álvarez-Ossorio T, González N, Lorenzo J, Rodríguez C, Varela M, Varela MM (2005) Seasonal variability of plankton blooms in the Ria de Ferrol (NW Spain): II. Plankton abundance, composition and biomass. Estuar Coast Shelf Sci 63:285-300. https://doi.org/10.1016/j.ecss.2004.11.021.

Braby CE and Somero GN (2006) Following the heart: temperature and salinity effects on heart rate in native and invasive species of blue mussels (genus *Mytilus*). J Exp Biol 209:2554-2566. https://doi.org/10.1242/jeb.02259.

Brinkhoff W, Stöckmann K, Grieshaber M (1983) Natural occurence of anaerobiosis in molluscs from intertidal habitats. Oecol 57:151-155. https://doi.org/10.1007/BF00379573.

Buxton CD, Newell RC, Field JG (1981) Response-surface analysis of the combined effects of exposure and acclimation temperatures on filtration, oxygen consumption and scope for growth in the oyster *Ostrea edulis*. Mar Ecol Prog Ser 6:73-82. https://doi.org/10.3354/meps006073.

Calosi P, De Witt P, Thor P, Dupont S (2016) Will life find a way? Evolution of marine species under global change. Evol Appl 9:1035-1042. https://doi.org/10.1111/eva.12418.

Cattaneo-Vietti R (2018) Structural changes in Mediterranean marine communities: lessons from the Ligurian Sea. Rend Fis Acc Lincei 29:515–524. https://doi.org/10.1007/s12210-018-0670-2.

De Zwaan A and Wijsmann TCM (1976) Anaerobic metabolism in bivalvia (mollusca) - Characteristics of anaerobic metabolism. Comp Biochem Physiol B 54:313-324. https://doi.org/10.1016/0305-0491(76)90247-9.

Depledge M and Andersen B (1990) A computer-aided physiological monitoring system for continuous, long-term recording of cardiac activity in selected invertebrates. Comp Biochem Physiol A Mol Integr Physiol 96:473-477. https://doi.org/10.1016/0300-9629(90)90664-E.

Dickson AG (1990) Standard potential of the (AgCl(s)+1/2H2(g) = Ag(s)+HCl(aq))cell and the dissociation constant of bisulfate ion in synthetic sea water from 273.15 to 318.15K. J Chem Thermodyn 22.113–127.

Domnik NJ, Polymeropoulos ET, Elliott NG, Frappell PB, Fisher JT (2016) Automated non-invasive video-miscroscopy of oyster spat heart rate during acute temperature change: Impact of acclimation temperature. Front Physiol 7:236. https://doi.org/10.3389/fphys.2016.00236.

Finnegan S, Anderson SC, Harnik PG, Simpson C, Tittensor DP, Byrnes JE, Finkel ZV, Lindberg DR, Liow LH, Lockwood R, Lotze HK, McClain CR, McGuire JL, O'Dea A, Pandolfi JM (2015) Paleontological baselines for evaluating extinction risk in the modern oceans. Science 348:567-570. https://doi.org/10.1126/science.aaa6635.

Frederich M and Pörtner H-O (2000) Oxygen limitation of thermal tolerance defined by cardiac and ventilatory performance in spider crab, *Maja squinado*. Am J Physiol Regul Integr Comp 279:R1531-R1538. https://doi.org/10.1152/ajpregu.2000.279.5.R1531.

Garrabeu J, Coma R, Bensoussan N, et al (2009) Mass mortality in Northwestern Mediterranean rocky benthic communities: effects of the 2003 heat wave. Global Change Biol 15:1090-1103. https://doi.org/10.1111/j.1365-2486.2008.01823.x.

Giomi F and Pörtner H-O (2013) A role for haemolymph oxygen capacity in heat tolerance of eurythermal crabs. Front Physiol 4:110. https://doi.org/10.3389/fphys.2013.00110.

Guderley H and Pörtner H-O (2010) Metabolic power budgeting and adaptive strategies in zoology: Examples from scallops and fish. Can J Zool 88:753–763. https://doi.org/10.1139/Z10-039.

Guo X, Li C, Wang H, Xu Z (2018) Diversity and evolution of oysters. J Shellfish Res 37:755-771. https://doi.org/10.2983/035.037.0407.

Han G, Zhang S, Dong Y (2017) Anaerobic metabolism and thermal tolerance: The importance of opine pathways on survival of a gastropod after cardiac dysfunction. Integr Zool 12:361–370. https://doi.org/10.1111/1749-4877.12229

Haure J, Penisson C, Bougrier S, Baud J (1998) Influence of temperature on clearance and oxygen consumption rates of the flat oyster *Ostrea edulis*: determination of allometric coefficients. Aquaculture 169:211-224. https://doi.org/10.1016/S0044-8486(98)00383-4.

Hicks DW and McMahon RF (2002) Respiratory responses to temperature and hypoxia in the nonindgenous Brown Mussel, *Perna perna* (Bivalvia. Mytilidae) from the Gulf of Mexico. J Exp Mar Biol Ecol 277:61-78. https://doi.org/10.1016/S0022-0981(02)00276-9.

Hochachka PW and Somero GN (2002) Biochemical adaptation: Mechanism and process in physiological evolution. Oxford University Press, New York. 480 pp. ISBN 0-195-11702-6.

Hoegh-Guldberg O and Bruno JF (2010) The impact of climate change on the world's marine ecosystems. Science 328:1524-1528. https://doi.org/10.1126/science.1189930.

Joachimski MM, Lai X, Shen S, Jiang H, Luo G, Chen B, Chen J, Sun Y (2012) Climate warming in the latest Permian and the Permian–Triassic mass extinction. Geology 40:195-198. https://doi.org/10.1130/G32707.1

Jørgensen CB, Møhlenberg F, Sten-Knudsen O (1986) Nature of relation between ventilation and oxygen consumption in filter feeders. Mar Ecol Prog Ser 29:73-88. http://dx.doi.org/10.3354/meps029073.

Jørgensen CB, Larsen PS, Riisgård HU (1990) Effects of temperature on the mussel pump. Mar Ecol Prog Ser 64: 89-97.

Kittner C and Riisgård HU (2005) Effect of temperature on filtration rate in the mussel *Mytilus edulis:* no evidence for temperature compensation. Mar Ecol Prog Ser 305:147-152. https://doi.org/10.3354/meps305147.

Knoll AH, Bambach RK, Payne JL, Pruss S, Fischer WW (2007) Paleophysiology and end-Permian mass extinction. EPSL 256:295-313. https://doi.org/10.1016/j.epsl.2007.02.018.

Koenigstein S, Mark FC, Gößling-Reisemann S, Reuter H, Pörtner H-O (2016) Modelling climate change impacts on marine fish populations: process-based integration of ocean warming, acidification and other environmental drivers. Fish Fish 17:972-1004. https://doi.org/10.1111/faf.12155.

Lannig G, Flores JF, Sokolova IM (2006) Temperature-dependent stress response in oysters, C*rassostrea virginica:* Pollution reduces temperature tolerance in oysters. Aquat Toxicol 79:278–287. https://doi.org/10.1016/j.aquatox.2006.06.017.

Lannig G, Cherkasov AS, Pörtner H-O, Bock C, Sokolova IM (2008) Cadmium-dependent oxygen limitation affects temperature tolerance in eastern oysters (*Crassostrea virginica* Gmelin). Am J Physiol Regul Integr Comp Physiol 294:R1338–R1346. https://doi.org/10.1152/ajpregu.00793.2007.

Lewis E and Wallace DWR (1998) Program Developed for CO_2 System Calculations. United States: N.p. Technical Report ORNL/CDIAC-105, Osti.Gov. DOI:10.2172/639712.

Livingstone DR (1991) Origins and Evolution of pathways an anaerobic metabolism in the animal kingdom. Amer Zool 31:522-534. https://doi.org/10.1093/icb/31.3.522.

Marshall DJ and McQuaid CD (1992) Relationship between heart rate and oxygen consumption in the intertidal limets *Patella granularis* and *Siphonaria oculus*. Comp Biochem Physiol A Mol Integr Physiol 102:297-300. https://doi.org/10.1016/0300-9629(92)90583-C.

Melzner F, Bock C, Pörtner H-O (2007) Allometry of thermal limitation in the cephalopod *Sepia officinalis*. Comp Biochem Physiol A Mol Integr Physiol 146:149–154. https://doi.org/10.1016/j.cbpa.2006.07.023.

Millero FJ and DiTrolio BR (2010) Use of thermodynamics in examining the effects of ocean acidification. Elements 6:299–303. https://doi.org/10.2113/gselements.6.5.299.

Møhlenberg F and Riisgård HU (1978) Efficiency of particle retention in 13 species of suspension feeding bivalves. Ophelia 17:239-246. https://doi.org/10.1080/00785326.1978.10425487.

Müller M, Mentel M, van Hellemond JJ, Henze K, Woehle C, Gould SB, Yu R-Y, van der Giezen M, Tielens AGM, Martin W (2012) Biochemistry and Evolution of Anaerobic Energy Metabolism in Eukaryotes. Microbiol Mol Biol Rev 76:444–495. https://doi.org/10.1128/MMBR.05024-11.

Newell RC, Johson LG, Kofoed LH (1977) Adjustment of the components of energy balance in response to temperature change in *Ostrea edulis*. Oecol 30:97-110. https://doi.org/10.1007/BF00345414.

Nicholson S (2002) Ecophysiological aspects of cardiac activity in the subtropical mussel *Perna viridis* (L.) (Bivalvia:Mytilidae). J Exp Mar Biol Ecol 267:207–222. https://doi.org/10.1016/S0022-0981(01)00362-8.

Nickerson DM, Facey DE, Grossman GD (1989) Estimating physiological thresholds with continous two-phase regression. Physiol Zool 62:866-887.

Nielsen M, Hansen BW, Vismann B (2017) Feeding traits of the European flat oyster, *Ostrea edulis*, and the invasive Pacific oyster, *Crassostrea gigas*. Mar Biol 164:6. https://doi.org/10.1007/s00227-016-3041-5.

Ortmann C and Grieshaber MK (2003) Energy metabolism and valve closure behaviour in the Asian Clam *Corbidula fluminea*. J Exp Biol 206:4167- 4178. https://doi.org/10.1242/jeb.00656.

Pazos AJ, Román G, Acosta CP, Abad M, Sánchez JL (1997) Seasonal changes in condition and biochemical composition of the scallop *Pecten maximus* L. from suspended culture in the Ria de Arousa (Galicia, N.W. Spain) in relation to environmental conditions. J Exp Mar Biol Ecol 211:169-193. https://doi.org/10.1016/S0022-0981(96)02724-4.

Penn JL, Deutsch C, Payne JL, Sperling EA (2018) Temperature-dependent hypoxia explains biogeography and severity of end-Permian marine mass extinction. Science 362:eaat1327. https://doi.org/10.1126/science.aat1327.

Petersen JK, Sejr MK, Larsen JEN (2003) Clearance rates in the Arctic bivalve *Hiatella arctica* and *Mya sp.* Polar Biol 26:334-341. https://doi.org/10.1007/s00300-003-0483-2.

Poloczanska E, Brown C, Sydeman W, Kiessling W, Schoeman D, Moore P, Brander K, Bruno JF, Buckley LB, Burrows MT, Duarte C, Halpern BS, Holding J, Kappel CV, O'Connor MI, Pandolfi JM, Parmesan C, Schwing F, Thompson SA, Richardson AJ (2013) Global imprint of climate change on marine life. Nat Clim Change 3:919-925. https://doi.org/10.1038/nclimate1958.

Pörtner H-O (2001) Climate change and temperature-dependent biogeography: oxygen limitation of thermal tolerance in animals. Naturwissenschaften, 88:137-146. https://doi.org/10.1007/s001140100216.

Pörtner H-O, Langenbuch M, Michaelidis B (2005) Synergistic effects of temperature extremes, hypoxia, and increases in CO_2 on marine animals: From earth history to global change. J Geophys Res C 110:C09S10. https://doi.org/10.1029/2004JC002561.

Pörtner H-O and Knust R (2007) Climate change affects marine fishes through the oxygen limitation of thermal tolerance. Science 315:95-97. https://doi.org/10.1126/science.1135471.

Pörtner H-O (2010) Oxygen-and capacity-limitation of thermal tolerance: a matrix for integrating climate-related stressor effects in marine ecosystems. J Exp Biol 213:881-893. https://doi.org/10.1242/jeb.037523.

Pörtner H-O (2014) How and how not to investigate the oxygen and capacity limitation of thermal tolerance (OCLTT) and aerobic scope–remarks on the article by Gräns et al. J Exp Biol 217:4432-4433.

Pörtner H-O, Bock C, Mark FC (2017) Oxygen-and capacity-limited thermal tolerance: bridging ecology and physiology. J Exp Biol 220:2685-2696. https://doi.org/10.1242/jeb.134585.

Purohit PV, Rocke DM, Viant MR, Woodruff DL (2004) Discrimination models using variance-stabilizing transformation of metabolomic NMR data. Omics 8:118-130. https://doi.org/10.1089/1536231041388348.

Riebesell U, Fabry VJ, Hansson L, Gattuso JP (2011) (Eds.) Guide to best practices for ocean acidification research and data reporting. Office for Official Publications of the European Communities, Luxembourg, 258 pp. DOI 10.2777/66906.

Riisgård HU (2001) Comment: Physiological regulation vs. autonomous filtration in filter-feeding bivalves: Starting points for progress. Ophelia 54:193-209. https://doi.org/10.1080/00785236.2001.10409465.

Riisgård HU, Kittner C, Seerup DF (2003) Regulation of opening state and filtration rate in filter-feeding bivalves (*Cardium edule, Mytilus edulis, Mya arenaria*) in response to low algal concentration. J Exp Mar Biol Ecol 284:105-127. https://doi.org/10.1016/S0022-0981(02)00496-3.

Riisgård HU and Larsen PS (2015) Research Note. Physiological regulated valve-closure makes mussels long-term starvation survivors: test of hypothesis. J Molluscan Stud 81:303-307.

Rhein M, Rintoul SR, Aoki S, et al (2013) Observations: Ocean. In Stocker TF, Qin D, Plattner G-K, Tignor M, Allen SK, Boschung J, Nauels A, Xia Y, Bex V, Midgley PM (eds.) Climate Change 2013: The Physical Science Basis. Contribution of Working Group I to the Fifth Assessment Report of the Intergovernmental Panel on Climate Change. Cambridge, GB. Cambridge University Press, pp. 255-316.

Sabine CL, Feely RA, Gruber N, Key RM, Lee K, Bullister JL, Wanninkhof R, Wong CS, Wallace DR, Tilbrook B, Millero FJ, Peng T-H, Kozyr A, Ono T, Rios AF (2004) The oceanic sink for anthropogenic CO_2. Science 305:367-371. https://doi.org/10.1126/science.1097403.

Schalkhausser B, Bock C, Stemmer K, Brey T, Pörtner H-O, Lannig G (2013) Impact of ocean acidification on escape performance of the king scallop, *Pecten maximus,* from Norway. Mar Biol 160:1995-2006. https://doi.org/10.1007/s00227-012-2057-8.

Schiffer M, Harms L, Lucassen M, Mark FC, Pörtner H-O (2014) Temperature tolerance of different larval stages of the spider crab *Hyas araneus* exposed to elevated seawater PCO_2. Front Zool 11:87. https://doi.org/10.1186/s12983-014-0087-4.

Schmalenbach I, Buchholz F, Franke HD, Saborowski R (2009) Improvement of rearing conditions for juvenile lobsters (*Homarus gammarus*) by co-culturing with juvenile isopods (*Idotea emarginata*). Aquaculture 289:297-303. https://doi.org/10.1016/j.aquaculture.2009.01.017.

Schmidt M, Windisch HS, Ludwichowski KU, Seegert SLL, Pörtner H-O, Storch D, Bock C (2017) Differences in neurochemical profiles of two gadid specied under ocean warming and acidification. Front zool 14:49. https://doi.org/10.1186/s12983-017-0238-5.

Shepard S, Beukers-Stewart B, Hiddink JG, Brand AR, Kaiser MJ (2010) Strengthening recruitment of exploited scallops *Pecten maximus* with ocean warming. Mar Biol 157:91-97. https://doi.org/10.1007/s00227-009-1298-7.

Shumway SE and Koehn RK (1982) Oxygen consumption in the american oyster *Crassostrea virginica.* Mar Ecol Prog Ser 9: 59-68. https://doi.org/10.3354/meps009059.

Stanley SM (2016) Estimates of the magnitudes of major marine mass extinctions in earth history. PNAS 113:E6325-E6334. https://doi.org/10.1073/pnas.1613094113.

Stoll MHC, Bakker K, Nobbe GH, Haesel RR (2001) Continuous-Flow analysis of dissolved inorganic carbon content in seawater. Anal Chem 73:4111–4116. https://doi.org/10.1021/ac010303r.

Specht JA and Fuchs HL (2018) Thermal and viscous effect of temperature on mercenaria mercenaria suspension feeding. Mar Ecol Prog Ser 589:129-140. https://doi.org/10.3354/meps12431.

Sokolova IM, Frederich M, Bagwe R, Lannig G, Sukhotin AA (2012) Energy homeostasis as an integrative tool for assessing limits of environmental stress tolerance in aquatic invertebrates. Mar Environ Res 79:1-15. https://doi.org/10.1016/j.marenvres.2012.04.003.

Somero GN (2002) Thermal physiology and vertical zonation of intertidal animals: Optima, limits and costs of living. Integr Comp Biol 42:780–789. https://doi.org/10.1093/icb/42.4.780.

Taylor AC (1976) The cardiac responses to shell opening and closure in the bivalve *Arctica islandica* (L.) J Exp Biol 64:751-759.

Tripp-Valdez MA, Bock C, Lucassen M, Lluch-Cota SE, Sicard MT, Lannig G, Pörtner H-O (2017) Metabolic response and thermal tolerance of green abalone juveniles (*Haliotis fulgens*: Gastropoda) under acute hypoxia and hypercapnia. J Exp Mar Biol Ecol 497:11-18. https://doi.org/10.1016/j.jembe.2017.09.002.

Trueman ER and Lowe GA (1971) The effect of temperature and littoral exposure on the heart rate of a bivalve mollusc, *Isognomum alatus*, in tropical condtions. Comp Biochem Physiol A Mol Integr Physiol 38:555-564. https://doi.org/10.1016/0300-9629(71)90122-8.

Uppström LR (1974) Boron/chlorinity ratio of deep-sea water from the Pacific Ocean. Deep-Sea Res Oceanogr Abstr 21:161–162. https://doi.org/10.1016/0011-7471(74)90074-6.

Waters JF and Millero FJ (2013) The free proton concentration scale for seawater pH. Mar Chem 149:8-22. https://doi.org/10.1016/j.marchem.2012.11.003.

Widdows J (1973) Effect of temperature and food on the heart beat, ventilation rate and oxygen uptake of *Mytilus edulis*. Mar Biol 20: 269-276. https://doi.org/10.1007/BF00354270.

Widdows J (1976) Physiological adaption of *Mytilus edulis* to cyclic temperatures. J Comp Physiol B 105:115-128. https://doi.org/10.1007/BF00691115.

Wignall PB and Twitchett RJ (1996) Oceanic anoxia and the end Permian mass extinction. Science 272:1155-1158. DOI:10.1126/science.272.5265.1155.

Wilson JG (1981) Temperature tolerance of circatidal bivalves in relation to their distribution. J Therm Biol 6:279-286. https://doi.org/10.1016/0306-4565(81)90016-4.

Wilson JG and Elkaim B (1991) Tolerances to high temperature of infaunal bivalves and the effect of geographical distribution, position on the shore and season. J Mar Biol Assoc UK 71:169 - 177. https://doi.org/10.1017/S0025315400037486.

Xia J and Wishart DS (2016) Using MetaboAnalyst 3.0 for Comprehensive Metabolomics Data Analysis. Curr Protoc Bioinformatics 55:14.10.1-14.10.91. https://doi.org/10.1002/cpbi.11.

Xing Q, Li Y, Guo H, Yu Q, Huang X, Wang S, Hu X, Zhang L, Bao Z (2016) Cardiac performance: a thermal tolerance indicator in scallops. Mar Biol 163:244. https://doi.org/10.1007/s00227-016-3021-9.

Yeager DP and Ultsch GR (1989) Phyiological regulation and conformation: A basic program for the determination of critical points. Physiol Zool 62:888-907.

Zannella C, Mosca F, Mariani F, Franci G, Folliero V, Galdiero M, Tiscar PG, Galdiero M (2017) Microbial diseases of bivalve mollusks: Infections, immunology and antimicrobial defense. Mar Drugs 15:E182. https://doi.org/10.3390/md15060182.

Zittier ZM, Bock C, Lannig G, Pörtner H-O (2015) Impact of ocean acidification on thermal tolerance and acid–base regulation of *Mytilus edulis* (L.) from the North Sea. J Exp Mar Biol Ecol 473:16-25. https://doi.org/10.1016/j.jembe.2015.08.001.

Tab. 1 Summary of water chemistry parameters during acute warming exposures

Temperature, salinity, $pH_{Freescale}$, PO_2, and PCO_2, were determined in water samples collected throughout the exposures. The total alkalinity (TA), ΩAragonite and ΩCalcite were calculated using co2sys software. Data are presented as means ± SD (n =18-27).

$T_{Nominal}$	T (°C)		Sal (SWU)		$pH_{Freescale}$		PO_2 (% air saturation)		PCO_2 (µatm)		TA (mmol/kg SW)		ΩAragonite		ΩCalcite	
(°C)	Mean	±SD	Mean	±SD	Mean	±SD	Mean	±SD	Mean	±SD	Mean	±SD	Mean	±SD	Mean	±SD
14	14.05	0.34	32.74	1.14	8.185	0.021	91.44	1.09	404	36	2683.99	141.31	3.02	0.17	4.73	0.26
18	18.38	0.19	32.63	0.76	8.105	0.051	96.28	4.48	511	66	2629.19	194.07	2.88	0.49	4.47	0.76
22	22.03	0.23	32.98	0.76	8.031	0.039	97.69	2.01	583	62	2390.51	10.83	2.51	0.19	3.85	0.30
26	26.02	0.48	32.87	0.21	8.048	0.110	95.93	2.10	672	198	2321.84	150.92	2.62	0.81	3.97	1.24
30	29.85	0.57	33.22	0.32	8.027	0.106	94.07	2.60	612	171	2342.06	228.72	3.20	0.80	4.79	1.21
32	32.10	0.47	33.43	0.21	7.99	0.10	91.60	3.24	718	177	2374.16	264.50	3.11	0.84	4.68	1.25
34	34.16	0.38	33.60	0.78	8.056	0.074	92.41	3.19	633	105	2517.92	179.30	3.95	0.74	5.83	1.09

Fig. 1

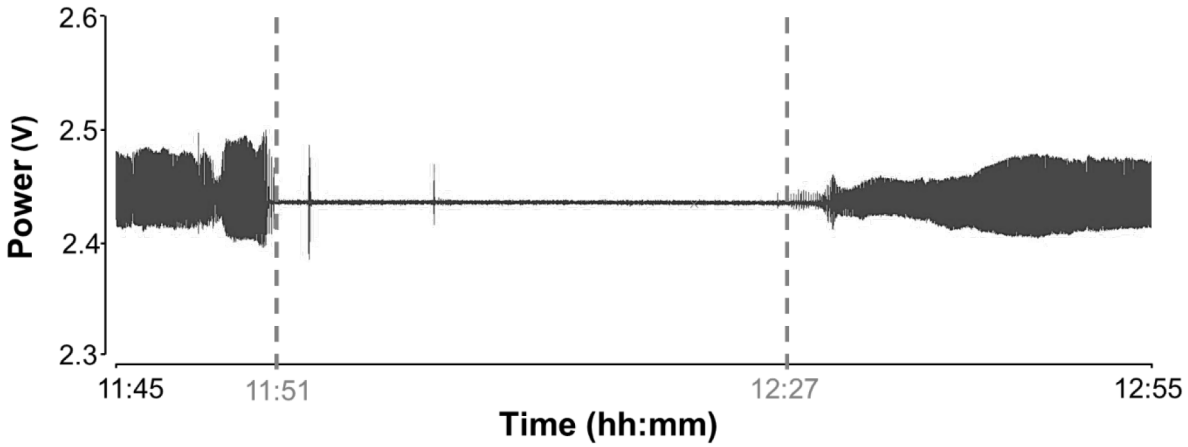

Fig.1: Cardiac arrest of *O. edulis*. Dashed lines symbolize the onset and end of a cardiac arrest period. Y-axis illustrates the cardiac amplitude in voltage oscillations (V). Single spikes during the cardiac arrest periods are due to technical errors.

Fig. 2

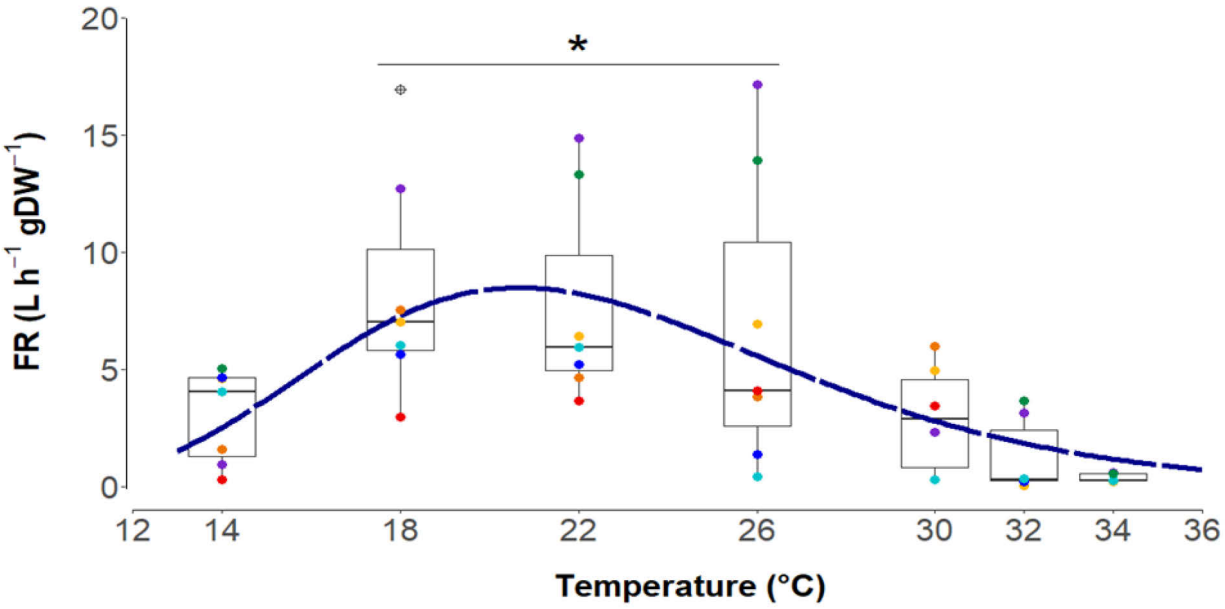

Fig. 2 Filtration rate (FR) of *O. edulis*. Each colored point indicates an individual. Boxplots show the variations of FR at the ambient temperature. Asterisk and horizontal line denote a significant difference of FRs at 18, 22 and 26°C from FRs at lower / higher temperatures (repeated 1-way ANOVA, Holm-Sidak Test, $F = 8.10$, $P < 0.001$). Nonlinear regressions (dashed line) show the modelled FR after Schmalenbach et al. (2009):

$FR_F(T) = 8.487e^{-0.5(\frac{\ln(\frac{x}{20.68})}{0.25})^2}$), r2 = 0.41. N = 6 - 7

Fig3

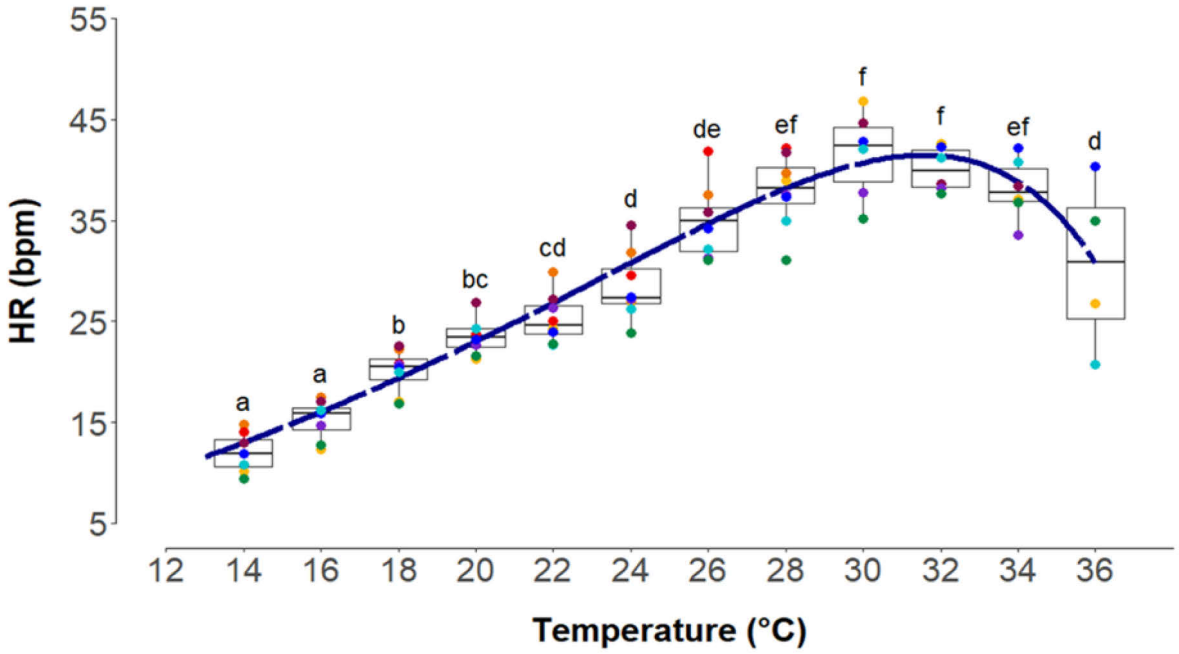

Fig. 3 Impact of acute warming on heart rate (HR) of. *O. edulis*. HRs of individuals are indicated by different colors. Different letters indicate significant changes between temperature steps (repeated 1-way ANOVA, Holm-Sidak Test, F = 96.86, P < 0.001). Non-linear regression after Pörtner & Knust (2007) is shown as dashed line:

$HR_F(T) = (10.83 * e^{0.06097*T} + 3.57e008) + (-0.0215 * e^{0.2177*T} - 3.57e008)$, r2 = 0.90. N= 4 - 8

Fig 4

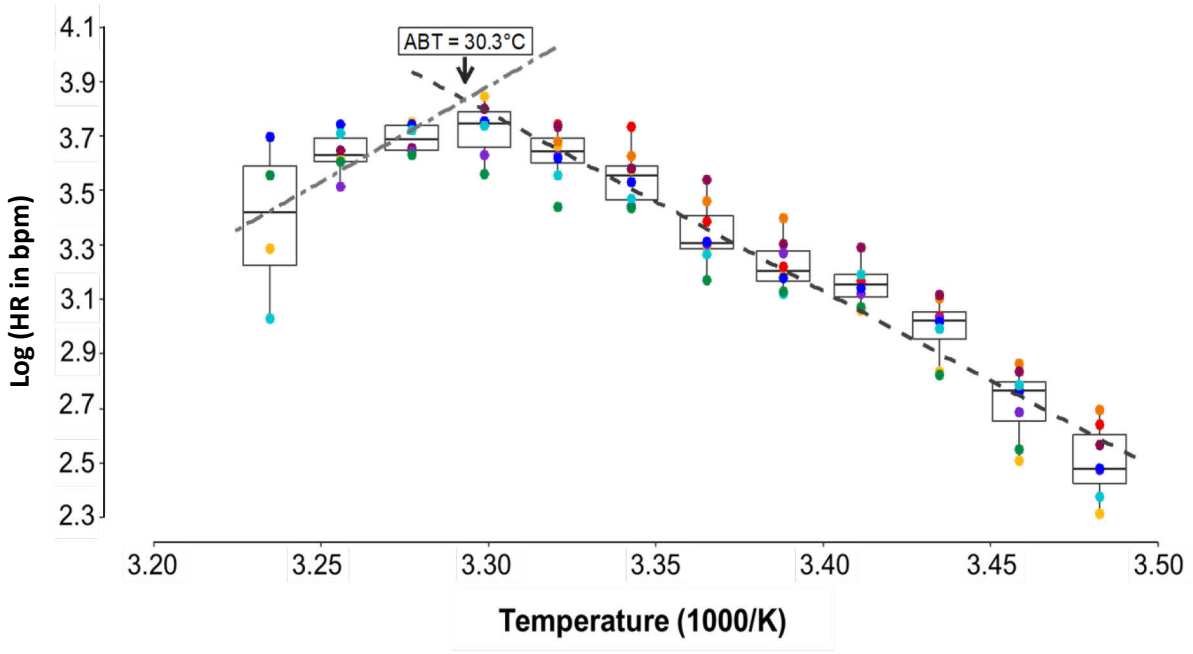

Fig. 4 Arrhenius plot showing an impact of acute warming on heart rate (HR) of *O. edulis*. Arrhenius Break Temperature (ABT) was analyzed from linear regression lines (dashed lines) intersecting at the respective breakpoint with f(log HR $_{14\text{-}30°C}$) = 11.0559 + (-2.8519 × Temp), r2 = 0.97, P < 0.001; and f(log HR $_{32\text{-}36°C}$) = -8.374 + (3.049 × Temp), r2 = 0.87, P = 0.2308. N = 4-8

Fig. 5 a-d

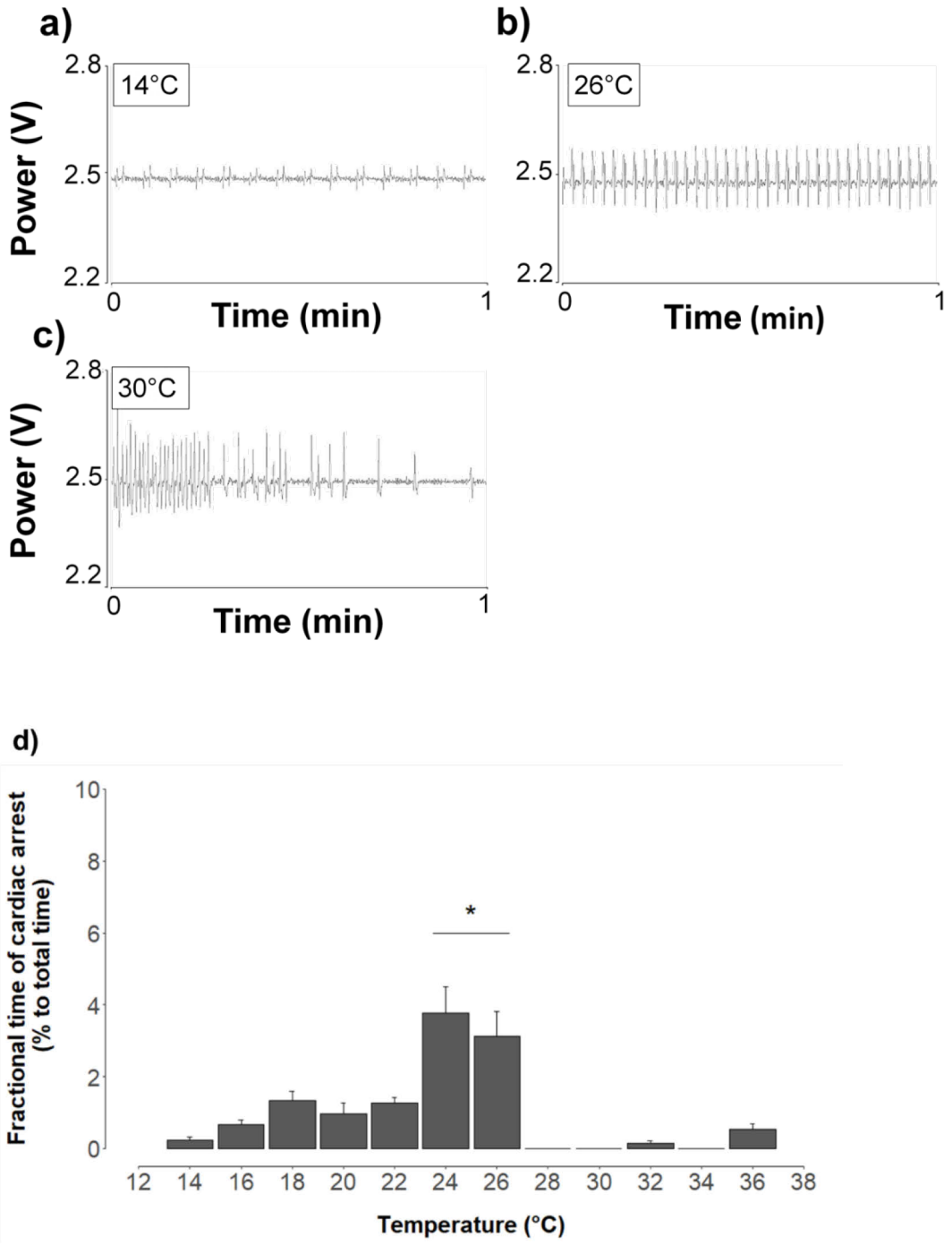

Fig. 5 Impact of acute warming on cardiac performance of *O.edulis* **a)** Rhythmic heartbeat at 14 °C and **b)** Rhythmic heartbeat at 26 °C **c)** Distinctly arrhythmic heartbeat at 30 °C **d)** Fractions of cardiac arrest periods in total measurement time (36 h) at each temperature step. HR pauses were defined as cardiac arrest periods of at least 15 min. * denotes significant differences among temperature steps (1-way ANOVA, Holm-Sidak Test, $F = 16.154$, $P < 0.001$). Data are mean +/- SE, N = 4-8.

Fig. 6

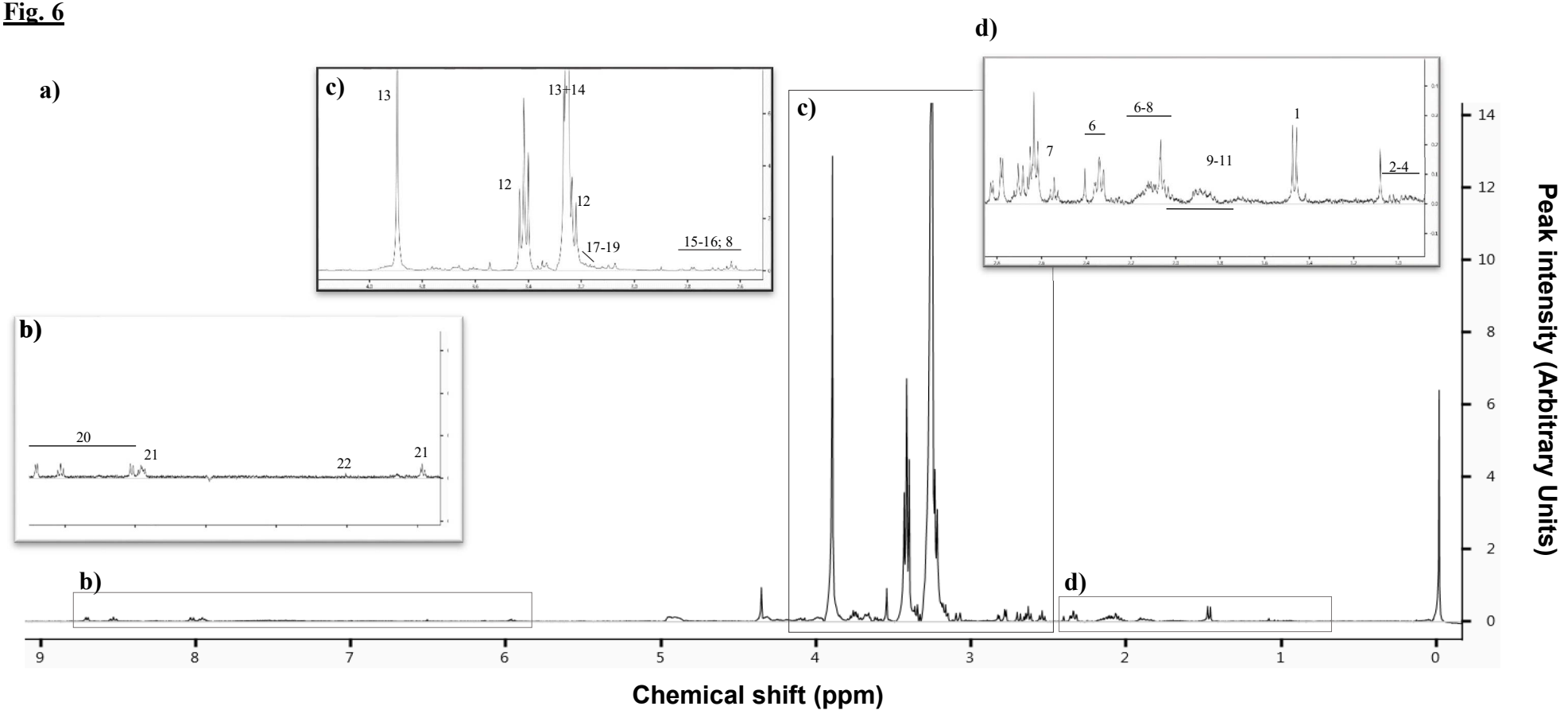

Fig. 6 Representative spectrum of gill metabolites depicted in a one-dimensional 400 MHz CPMG ^{1}H–NMR spectrum of a tissue extract from *O.edulis* sampled at 34°C. (a) Shown are the entire spectra and (b-d) enlarged areas of this spectrum with identified metabolites. Keys: Alanine (1); Valine (2); Isoleucine (3); Leucine (4); Succinate (5); Glutamate (6); Glutamine (7); Homocysteine (8); Arginine (9); Lysine (10); Acetate (11); Taurine (12); Betaine (13); Trimethylamide-N-oxide (TMAO; 14); Aspartate (15); Hypotaurine (16); Choline (17); O-Phosphocholine (18); Sn-Glycero-3phosphocholine (19); Homarine (20); UDP-Glucose (21); Triphosphate (22)

Fig. 7

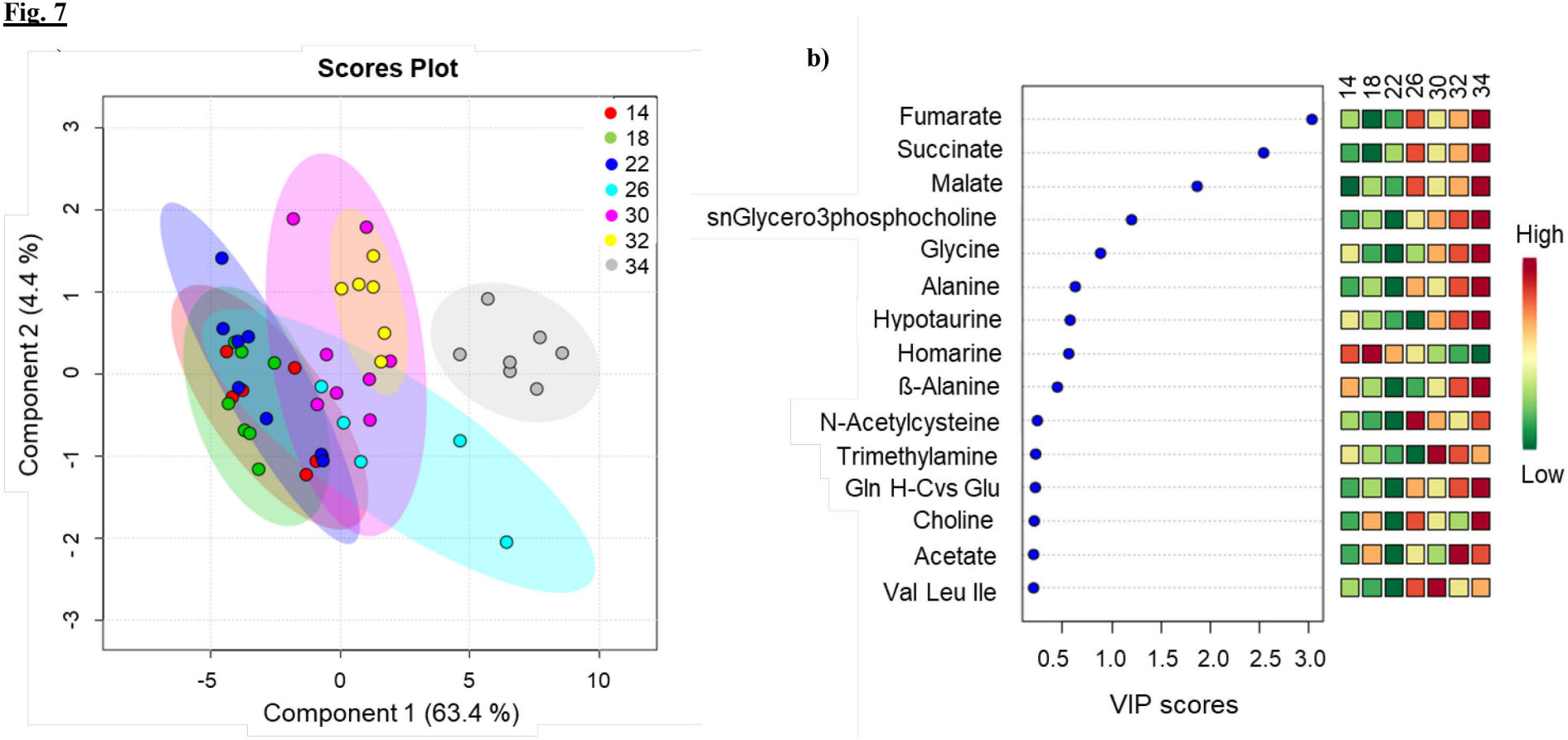

Fig. 7 Impact of acute warming on the metabolic profile of gill tissue from *O. edulis*. **a)** Score Plot of the PLS-DA model for the normalized concentrations of assigned gill tissue metabolites found in *O. edulis* sampled at 14 °C, 18 °C, 22 °C, 26 °C, 30 °C, 32 °C, and 34 °C. Ellipses correspond to a confidence interval of 95 %. **b)** Variable Importance in Projection (VIP) are the weighted sum of squares of the PLS loadings.

Fig.8

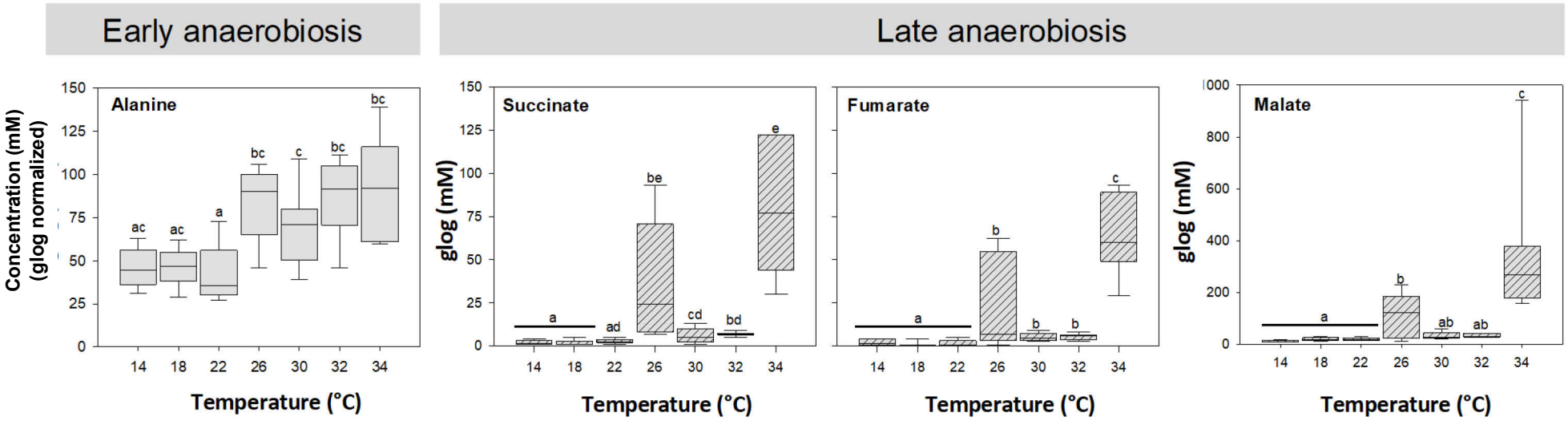

Fig. 8. Impact of acute warming on the levels of gill metabolites in *O. edulis.* Concentrations (mM) were glog transformed, normalized and analyzed by 1-way ANOVA, followed by a Post-Hoc test. Significant differences between data are indicated by different letters ($P<0.05$). Data are shown as box plots, N = 5-8

Fig. 9

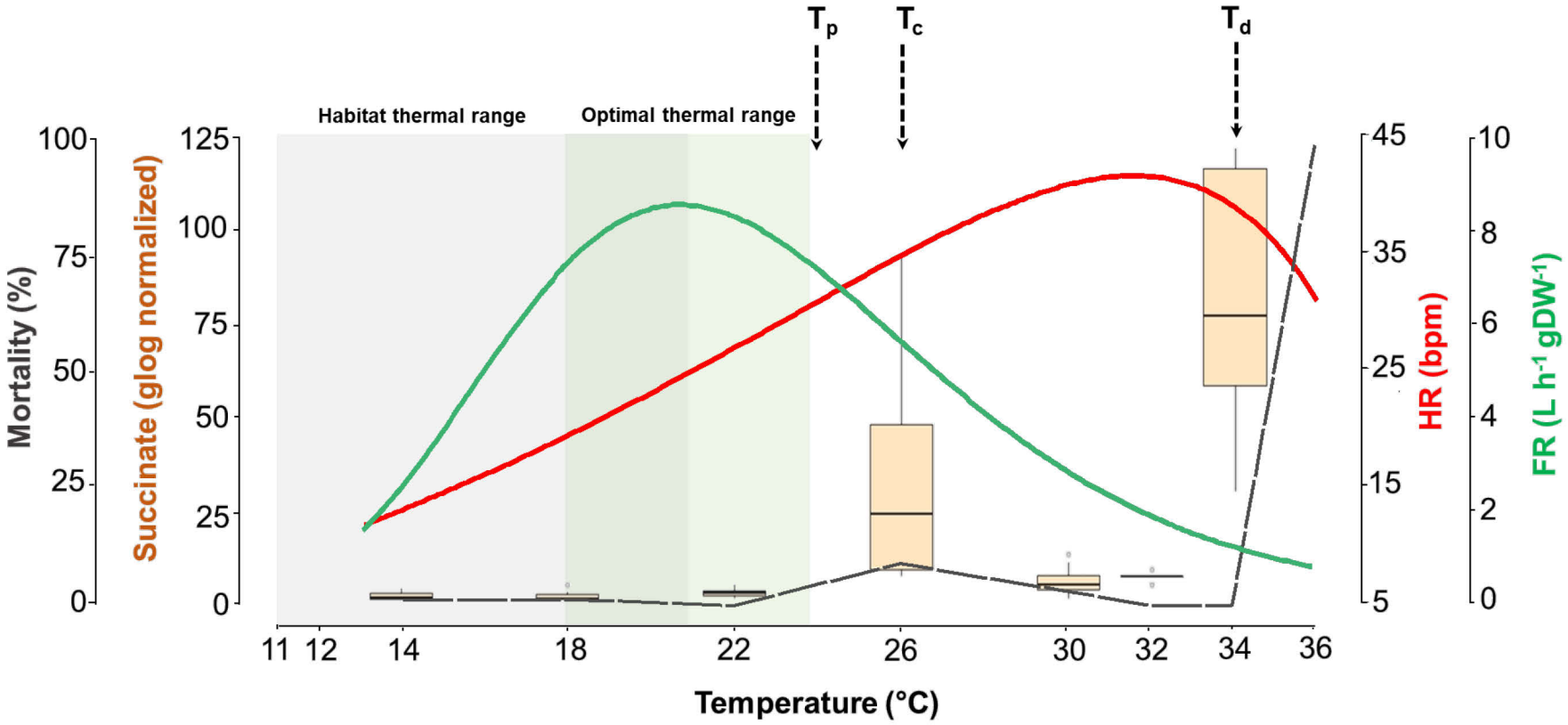

Fig. 9: Acute thermal window of *O.edulis* integrating temperature dependent mortality (black), temperature induced changes in filtration rate (FR, green), heart rate (HR, red) and succinate levels (mM, glog transformed) in gills as an anaerobic biomarker (boxplot). The annual habitat temperature range is highlighted in grey. The derived optimal temperature range is marked in green. Dashed black arrows indicate putative values of T_p (pejus temperature), T_c (critical temperature) and T_d (deadly temperature).

Manuscript II

"Single and combined effects of the "Deadly trio" hypoxia, hypercapnia and warming on the cellular metabolism of the great scallop *Pecten maximus*"

Submitted for publication in Comparative Biochemistry and Physiology - Part B: Biochemistry & Molecular Biology – *currently under review*

Contribution of the candidate in % of the total workload

Experimental concept and design	50 % *
Experimental work and data acquisition	80 % *
Data analysis and interpretation	95 %
Preparation of figures and tables	100 %
Drafting the manuscript	90 %

* Shared experiments with C. Eymann

Comparative Biochemistry and Physiology - Part B: Biochemistry & Molecular Biology

Single and combined effects of the "Deadly trio" hypoxia, hypercapnia and warming on the cellular metabolism of the great scallop *Pecten maximus*

Sandra Götze[1], Christian Bock[1], Charlotte Eymann[1], Gisela Lannig[1], Jennifer B. M. Steffen[2], Hans-O. Pörtner[1]

[1] Alfred Wegener Institute Helmholtz Centre for Polar and Marine Research. Am Handelshafen 12, 27515 Bremerhaven, Germany

[2] Marine Biology, Faculty of Mathematics and Natural Sciences, University of Rostock, Rostock, Germany

Corresponding author:

Sandra Goetze
Alfred Wegener Institute Helmholtz Centre for Polar and Marine Research
Am Handelshafen 12
27515 Bremerhaven, Germany
T: +49 471 4831
e-mail: Sandra.Goetze@awi.de

Declarations of interest: none

Abstract

In the ocean the main climate drivers affecting marine organisms are warming, hypercapnia, and hypoxia. We investigated the acute effects of warming (W), warming *plus* hypercapnia (WHc), warming *plus* hypoxia (WHo), and a combined exposure of all three stressors (Deadly Trio, DT) on king scallops (*Pecten maximus*). All exposures started at 14 °C and temperature was increased by 2 °C once every 48 h until the lethal temperature (28 °C) was reached. Gill samples were taken at 14 °C, 18 °C, 22 °C, and 26 °C and analyzed for their metabolic responses by ^{1}H-nuclear magnetic resonance (NMR) spectroscopy. Gill metabolism was affected by all treatments. Scallops were most tolerant to warming *plus* hypercapnia and were most susceptible to oxygen reduction (WHo and DT). Metabolic changes became most apparent at temperatures exceeding 20 °C with significant accumulations of glycogenic amino acids (e.g. glycine and valine) and anaerobic end-products (e.g. acetic acid and succinate). Accordingly, metabolic analysis revealed alterations in mitochondrial energy metabolism, which were most pronounced in scallops exposed to high temperatures and DT. In all exposures to combined drivers (WHo, WHc and DT) the upper thermal limit of *P. maximus* was lowered (and hence the thermal niche narrowed) as a consequence of an imbalance between energy demand and supply setting in at lower temperatures, indicated by the onset of anaerobic metabolism. This became also visible in higher rates of mortalities at lower temperatures which led to a lowered LT_{50} (from 26 °C in W to 22.5 °C in DT).

Keywords: ^{1}H NMR, metabolomics, metabolic pathways, palaeo-physiology, ocean climate change

Abbreviations:

^{1}H-NMR = proton nuclear magnetic resonance, W = warming exposure, WHo = warming *plus* hypoxia, WHc= warming *plus* hypercapnia, DT = deadly trio, ANOVA = analysis of variance, PLS-DA = partial least square-discriminant analysis, PCA = principal component analysis, PT = Permian-Triassic, PTME = Permian-Triassic Mass extinction, Ma = Million years ago, BCAA = branched chain amino acids; OCLTT = oxygen and capacity limited thermal tolerance, SMR = standard metabolic rate

Introduction:

The evolution of marine flora and fauna during Earth's history was shaped more than once by environmental disturbances. Some of the most severe marine mass extinctions were triggered by volcanism and the accompanying release of greenhouse gases, which among others, led to warming, ocean acidification, changes in ocean currents and stratification, and the consecutive development of anoxic zones (Aberhan and Baumiller, 2003; Bachan and Payne, 2015). Today's anthropogenic climate forcing is estimated to be analogous to past crises (Penn et al., 2018), affecting the oceans by the same drivers as in the past, however, present changes have not reached past extremes. Models predict an ocean surface temperature increase by 1.8 - 4 °C until the end of the 21th century, and a seawater (SW) pH drop of 0.3 – 0.4 pH units (equals ~ 800 ppmv CO_2) in a "business-as-usual" scenario (Feely et al., 2009; Rhein et al., 2013; RCP 8.5). Simulation of the Permian-Triassic (PT) transition using Community Earth System modeling (transition initiated by an instantaneous increase in pCO_2 to 5580 ppmv) revealed that outgassing of Siberian traps caused warming by 11 °C, ocean acidification due to the subsequent CO_2 uptake by the ocean, as well as the depletion of global marine oxygen by 75 % (Penn et al., 2018). The PT transition was one of the most severe marine crises erasing up to 95 % of marine taxa (Bambach et al., 2004; Song et al., 2013). Accordingly, the patterns of mass extinctions and how palaeo species were affected may harbor valuable knowledge for understanding the impacts of progressive extant climate change on marine biota when extrapolated into the future. Projected impacts on marine fauna are diverse depending on the type of stressor, it's magnitude, as well as duration of exposure, geographical location, species, life stage, and ecosystem interactions (Guinotte and Fabry, 2008; Pörtner, 2012; Wittmann and Pörtner, 2013; Parker et al., 2013).

Assuming that the mechanisms that have shaped the fate of fauna in the deep past are still in place in extant fauna, observed fossil patterns are likely related to the capacity of organisms to tolerate environmental changes such as low oxygen concentrations, temperature extremes or elevated CO_2 levels. For insights into paleophysiology, bivalve mollusks appear to be ideal model organisms as they keep well preserved due to their calcareous shell, and their fossil record covers more than 500 Ma of Earth history. Furthermore, this group did not change drastically in morphology, life style, or presumably physiology, allowing a comparison between palaeo-, and extant forms. Fossil records from the PTME indicate that orders of ostreida, trigoniida and mytilida performed better than pectinida, myalinida, and pholadomyida and that the latter ones had a higher rate of extinction (Tu et al., 2016). Subtidal pectinids have been

shown to be more sensitive to hypoxia or anoxia compared to other bivalves such as e.g. ostreoids or mytilids as the latter are as inhabitants of the intertidal extraordinary well adapted to low oxygen concentrations (Shumway and Koehn, 1982; Laing, 2000; Artigaud et al., 2014; Laudien et al., 2002). Furthermore, scallops are uniquely different from other bivalves by their anatomy as they cannot tightly shut close their valves compared e.g. to oysters, and are able to escape from predators by rapid valve clapping (Wilkens, 2006; Tremblay and Guderley, 2013). Valve clapping requires high-energy supply via anaerobic mechanisms, and is associated with accelerated heart rate, stroke volume and depletion of oxygen from the hemolymph (Thompson et al., 1980). Recovery from muscular fatigue relies on an oxygenated environment (Grieshaber, 1978). Accordingly, we hypothesize that scallops such as *P. maximus* are more vulnerable to environmental changes than other bivalve mollusks (see above).

Warming, hypercapnia or hypoxia affect marine organisms through impairments from the whole organism to molecular hierarchy of functions with consequences for organismal performance (e.g. reviewed by Kassahn et al., 2009). Full understanding of such impacts requires not only the study of the effects of individual but also of combined stressors. Available results obtained in marine invertebrates and fish imply disturbances of processes, such as acid-base homeostasis, respiration rates, and stress response pathways with fundamental effects on growth, reproduction and fitness (e.g. Pörtner et al., 2004; Artigaud et al., 2015a, 2015b; Ern et al., 2017; Stapp et al., 2017, 2018). One main underpinning principle shaping tolerance to environmental changes are disturbances in energy homeostasis, when aerobic energy supply becomes constrained, not or not fully meeting the animal's requirements (for more detail see Pörtner, 2002; Guderley and Pörtner, 2010; Sokolova et al., 2012; Pörtner et al., 2017). Under environmental extremes such as oxygen deficiency or temperature extremes a systemic disruption of oxygen metabolism (often characterized by the onset of anaerobiosis), and consequently, cellular damages and disturbance of homeostasis may occur (Heise et al., 2003; Heise et al., 2006). Intermediate or end-products of cellular pathways characterize such shift in energetics. Investigations of the metabolome and metabolic pathways provide valuable insight into underlying cellular mechanisms in response to environmental stressors (e.g. Viant et al., 2003; Lenz et al., 2005; Rebelein et al., 2018). Metabolic profiles are species and tissue specific and metabolite biomarkers can be used to assess environmental stress, toxicity and disease (Jones et al., 2008; Wu and Wang, 2010; Ellis et al., 2014; Palma et al., 2019). The accumulation of metabolites involved in anaerobic energy metabolism under environmental stressors such as temperature or ocean acidification, has been shown to be an important indicator for the loss in

aerobic scope with strictly time-limited survival (Lannig et al., 2010; Tripp-Valdez et al., 2017; Zittier et al., 2018). Similarly, we here focus on the contribution of various metabolic processes and report changes in gill metabolism identified by untargeted metabolic profiling using ^{1}H-NMR spectroscopy. We specify potential biomarkers of stress and explain organismic constraints through cellular metabolism in *P. maximus* under single and combined exposures to acute warming, hypoxia and hypercapnia.

Material and Methods:

Animal origin and maintenance

In autumn 2017 adult king scallops, *P. maximus*, were caught by scuba divers in the estuary of Vigo (Spain, ~42°14'46.6"N 8°44'18.5"W). Surface seawater (SW) temperature was ~ 18 °C with full salinity. Scallops were transported submerged under aerated water at 10 °C by car within 24 h to the Alfred Wegener Institute Helmholtz Centre for Polar and Marine Research (AWI, Bremerhaven). Upon arrival, scallops were immediately transferred to the institutional aquarium system filled with North Sea water (at 14 °C and full salinity) and acclimated for at least 4 weeks. Scallops were fed 3 times a week by a mixture of commercial algal blend (Nyos, PhytoMaxx) and a self-cultivated algal mixture including *Rhodomonas spec*., *Phaeodactylum tricornutum, Chaetocerus spec*., and *Isochrysis galbana* (minimum 3000 cells/ml SW). Epibionts were carefully removed prior to the experiments and each scallop was measured, weighed and labelled individually. Animals had an average size of 10.4 ± 1.1 cm length, 10.8 ± 1.3 cm width, and 163.4 ± 46.0 g weight.

Experimental setup and water chemistry

The experimental setup comprised four exposures running independently: acute warming (W), acute warming *plus* hypercapnia (WHc), acute warming *plus* hypoxia (WHo), and the combination of all three stressors (Deadly trio, DT). Oxygenation and carbon dioxide levels were controlled and mixed by a gas-mixing device (HTK, Hamburg). In W and WHc exposures P_{O_2} was kept above 90 %, and in WHo and DT exposures between 55-60 %. Under WHc and DT P_{CO_2} levels were set to around 1800 ppm and under WHo and DT to ~ 550 ppm. The SW was continuously bubbled with the respective gas mixture as indicated above.

P. maximus were randomly assigned to one of the exposures and acclimated for a minimum of 3 days. Exposures were carried out in closed-recirculating aquarium systems as described in Eymann, Götze et al. (in press). Briefly, the experimental system comprised a

header, a receiver (~ 100 l), a reservoir tank (~ 100 l) and four experimental tanks (52 l volume each). Each tank contained 15 scallops at the beginning. Throughout exposure scallops were fed twice a day to exclude effects of starvation (diet and concentration as indicated earlier) and the aquaria were cleaned regularly from faeces. All exposures started at 14 °C and temperature was increased by 2 °C every 48 h until 28 °C when the remaining scallops died (T_{Death}). The respective target temperature (± 0.5 °C) was reached within 5 h. Water parameters, i.e. temperature, salinity, concentration of oxygen (P_{O_2}) and carbon dioxide (P_{CO_2}) were monitored daily as described in Eymann, Götze et al. (in press). Detailed seawater physiochemical conditions at each temperature step are shown in Table 1. Levels of nitrite, nitrate and ammonium were monitored and held below critical concentrations by regular SW exchanges, performed approximately twice a week.

Survival

Animal survival was calculated based on scallops not used for tissue analyses (at start n = 34 scallops in W/WHc and 25 scallops in WHo/DT). Dead scallops were subtracted from the number of residual scallops and the survival per temperature step is expressed in percentage (%). For each exposure the half-maximal lethal temperature (LC_{50}) was determined.

Tissue sampling

Between six to eight scallops were sacrificed at 14 °C, 18 °C, 22 °C, and 26 °C each. In the WHo only four scallops survived until 26 °C ending the exposure after sampling. Scallops were opened on ice and different tissues (gills, mantle, hepatopancreas, phasic and tonic muscle) were removed quickly, snap-frozen in liquid nitrogen, and stored at -80 °C until further analyses.

Tissue extraction and metabolic profiling

We homogenized gill samples as described by Tripp-Valdez et al. (2017). Briefly, metabolites were extracted from 40 - 50 mg of tissue (fresh weight, FW) by methanol-chloroform extraction. The methanol fraction was dried overnight and the pellet was re-suspended in the 2-fold volume of FW in deuterized water (D_2O) comprising 3-(trimethylsilyl) propionic-2,2,3,3-d4 acid, sodium salt (TSP; 0.05 %; Sigma Aldrich, St. Louis, USA) as internal standard. Untargeted metabolic profiling based on one dimensional ^{1}H-NMR spectroscopy was carried out in an ultra-shielded vertical 9.4 T NMR spectrometer (Advance

III HD 400 WB, Bruker-BioSpin GmbH, Germany) using a triple tuned ^{1}H-^{13}C-^{31}P-HRMAS NMR probe. TOPSPIN 3.2 software (TopSpin 3.2, Bruker-BioSpin GmbH, Germany) was used for acquisition and a Call-Purcell-Meiboom-Gill (CPMG) sequence was chosen for metabolic profiling (described in detail in Schmidt et al., 2017). The spectra were baseline, shim, and phase corrected and calibrated to the TSP signal using the software Chenomx NMR suite 8.1 (Chenomx Inc., Canada). Thereafter, metabolites were assigned according to the chemical shift of their NMR signals using the internal database of Chenomx and literature data (e.g. Tikunov et al., 2010, 2014; Capello et al., 2018). Metabolite quantification was based on the integration routine within Chenomx calibrating the TSP signal integral to a concentration of 3.2 millimolar (mM).

Statistical analysis

Statistical analysis was carried out with the online platform *Metaboanalyst* (Metaboanalyst 4.0, Xia and Wishart, 2016). Data sets were normalized to the adenylate concentration (sum of AMP+ADP+ATP) and generalized log (g-log) transformed for normal data distribution (Purohit et al. 2004). Unsupervised principle component analysis (PCA) did not detect any outliers. For in depth analysis, temperature and exposure groups were analyzed by one-way ANOVA followed by a post-hoc test (Fisher's LSD; p-value ≤ 0.05). Significant differences between groups of altered metabolites were displayed as provided by MetaboAnalyst 4.0 using Sigma Plot (12.0, Systat Software, Inc.). Relevant metabolites are presented in the results as mM concentrations normalized to the total adenylate concentration. The distinction of metabolite profiles was identified by a supervised partial least–square discriminant analysis (PSL-DA) analysis. The two components accounting for the highest variance are illustrated as 2D score and the distance of the samples reflect the dissimilarity in metabolite patterns.

Pathway analysis

Metabolic pathways were analyzed as described in Xia and Wishart (MetaboAnalyst 4.0; Xia and Wishart, 2010; Xia and Wishart, 2016). Data sets were normalized as described above. Since this analysis is restricted to a two-group comparison the statistics were performed as follows: pathway changes within one exposure group were tested against metabolic status at 14 °C, whilst effects of additional stressors (hypoxia, hypercapnia and deadly trio) were tested against the warming exposure. The pathway library of the zebrafish (*Danio rerio*) was used for

pathway identification since most of the profiled metabolites could be assigned to a specific pathway from this library. Further specific statistical methods were 'global test' based on a Bayesian generalized linear model (Goeman et al., 2004) for the determination of global metabolite patterns that are related to specific pathways (pathway enrichment analysis). The importance of a compound/metabolite for a specific metabolic network/pathway (pathway topological analysis) was estimated by a centrality measurement (Aittokallio and Schwikowski, 2006). Identified pathways were checked for plausibility and those identified as being highly uncertain or of false origin were excluded (i.e. pathways with > 30 compounds but only one assigned compound, or pathways associated to specific plant or bacterial metabolism). Residual pathways where considered when associated metabolites displayed significant changes and the pathway was rated by the above mentioned statistical measures with a p-value < 0.0033 which equals a [-LOG(p)] change > 2.5.

Results:

Survival

The survival of *P. maximus* differed between exposures (**Fig.1**). Under warming 82 % of scallops were alive at 22 °C. Further warming to 25 °C reduced the number of scallops to 50 % indicating that 25 °C was the half-maximal lethal temperature (LC_{50}). All residual scallops died upon transition to 28 °C (T_{Death}). Warming *plus* hypercapnia decreased scallop survival as at 22 °C only 57 % of bivalves were still alive and numbers decreased to 50 % at 24 °C (LC_{50}). Similar to W, all scallops died upon transition to 28 °C. Warming *plus* hypoxia led to the same LC_{50} of 24 °C as under WHc. Further warming to 26 °C killed 13 out of 17 residual scallops, leaving four live scallops, which were sacrificed for tissue analysis. Under DT, one fifth of initially introduced scallops died within 48h after exposure started (14 °C). Further warming decreased the number of scallops further, so that at 22.5 °C only half of the scallops were still alive (LC_{50}) while the remaining scallops survived until at 28 °C.

Metabolites

We identified 34 metabolites in gills with amino acids, amino acid derivates and osmolytes as main compound classes. The metabolic profiles of gills varied with warming and additional treatment (**Fig 2 a/b**). On the left, each score plot displays the individual metabolic profiles sorted according to exposures. On the right, profiles are sorted according to sample temperatures, so differences between exposures are emphasized. Temperature alone altered

metabolite profiles above 20 °C with distinctly different profiles at 26 °C (**W**; **Fig. 2a)**. Additional hypoxia (WHo) diminished the metabolic variance seen under warming alone meaning that all scallops exhibited similar metabolic profiles at all temperatures. Additional hypercapnia (WHc) affected metabolite profiles only slightly as the patterns are very similar to those found under warming alone. Simultaneous exposure to all three stressors (DT) diminished the metabolic variance between scallops, but not to the degree observed under warming and hypoxia. Again, the metabolic profiles sampled at 26 °C were fully distinct from all others. Sampling at 14 °C after only 2 days of WHc, WHo, or DT exposure resulted in slight differences in metabolite profiles of individual scallops (**Fig 2b**). Profiles of scallops exposed to WHo or WHc overlapped and were mostly similar to profiles of the W group while scallops exposed to DT had distinctly shifted profiles. This picture remained constant until 26 °C was reached. Here, the individual variability was drastically diminished but, nevertheless, the metabolite profiles of scallops exposed to W, Who, and WHc clustered again indicating similar metabolic responses.

Significant changes in individual metabolite levels, which underpinned the changes in metabolite profiles outlined above, are depicted according to their metabolite class in **Fig 3a-c** and a summary of the statistics is shown in **Tab 2a.** Temperature alone affected the glycine derivate NN-dimethylglycine (amino acid, **a**), acetic acid (related to energy metabolism, **b**) and taurine (osmolyte, **c**). NN-dimethylglycine (0.2 ± 0.1 mM, 14 °C) and acetic acid (0.1 ± 0.03 mM, 14 °C) increased above 22 °C (0.4 ± 0.03 mM and 0.2 ± 0.03 mM at 26 °C, respectively), while taurine (64 ± 10.4 mM, 14 °C) decreased concomitantly (40.2 ± 8.5 mM, 26 °C). Additional hypoxia affected solely acetic acid, which increased significantly to its highest values at 18 °C (from 0.09 ± 0.02 mM at 14 °C to 0.37 ± 0.012 mM at 18 °C). Acetic acid levels were still elevated at 26 °C but levels were significantly lower than at 18 °C ($p < 0.05$). Exposure to warming *plus* hypercapnia (WHc) affected again NN-dimethylglycine and O-phospho-choline (the latter is only depicted in **Tab 2a**). NN-dimethylglycine concentrations were twice as high at 26 °C (0.6 ± 0.01 mM) than at 14 °C (0.3 ± 0.01 mM). Exposure to DT affected most metabolites. Glycine, NN-dimethylglycine, valine and threonine all accumulated at 26 °C. Acetic acid increased significantly between 18-22 °C and the concentration returned to baseline levels at 26 °C. Concomitantly, succinate accumulated at 26 °C (from 0.03 ± 0.01 mM at 14 °C to 0.11 ± 0.05 mM at 26 °C).

Comparing exposures revealed that additional drivers caused several metabolites to develop patterns different from warming alone with most changes occurring at 26 °C (**Tab.2b**).

At 14 °C, the levels of four metabolites were different from those levels found under warming alone (choline, o-phosphocholine, sn-3-glycerophosphocholine and glycine) and in all cases these metabolites differed between W and DT. At 18 °C only the levels of acetic acid determined in WHo and DT were found to be different from W. At 22 °C and 26 °C several metabolites were altered between exposures leading to the distinctly altered metabolite profiles indicated by the PLS-DA (**Fig 2B**). Metabolite levels changed significantly in response to warming *plus* hypoxia and in many cases similarly to the response to DT throughout all temperatures. The majority of significant changes in individual metabolite levels occurred in DT. Contrary, only three metabolites differed between W and WHc (at 14 °C o-phosphocholine; at 22 °C acetic acid; at 26 °C NN-dimethylglycine).

Pathway analysis of gills

Out of 36 putative pathways, seventeen met the selection criteria and 12 pathways changed with a [-LOG(p)] change > 2.5. **Tab 3** summarizes pathways affected at 26 °C during each exposure. Warming affected pathways contributing to carbohydrate metabolism, amino acid metabolism and metabolism of other amino acids. Warming *plus* hypercapnia (WHc) also affected amino acid metabolism (as in W) as well as lipid metabolism. Warming *plus* hypoxia (Who) affected only two pathways associated again in the metabolism of carbohydrates (as in W). Most branchial pathway changes were observed in scallops exposed to all three drivers (DT). Here, more than half of all pathways identified (3 out of 8) are involved in amino acid metabolism. Remaining pathways contributed to the conversion of carbohydrates as also seen for W and WHo exposures.

Discussion:

We applied untargeted metabolic profiling based on NMR spectroscopy and pathway analysis to identify metabolic and pathway changes in the king scallop, *P. maximus* during exposure to acute warming as well as additional hypoxia (WHo), hypercapnia (WHc) or the combination of all three drivers (Deadly Trio, DT). Overall, hypoxia had a stronger impact than hypercapnia, and effects were even more pronounced in scallops exposed to DT. Gill tissues had characteristic metabolic profiles and drivers affected this organ differently with only few alterations observed during warming and most pathways changing under the DT (as seen at 26 °C).

The baseline metabolic profile of gill tissue contained large fractions of free amino acids (e.g. glycine or alanine) and amino acid derivates (such as taurine). This is in line with literature describing the dominant presence of these metabolites in the metabolome of marine invertebrates (Tikunov et al., 2010; Tripp-Valdez et al., 2017; Capello et al., 2018), as all of these metabolites affect osmoregulation. Marine bivalves are mainly osmoconformers and regulate their cellular osmolality by modulating the content of compatible solutes rather than by inorganic ion transport (Somero and Yancey, 2011). Accordingly, the main share of metabolites found in *P. maximu*s are compatible solutes, but in addition to their osmotic function, they may have additional roles as they e.g. positively influence protein and membrane stability (Rudolph et al., 1986; Rishi et al., 1998; Yancey, 2005). The main share of energy production in well-oxygenated gill tissue comes from oxidative cellular respiration. A study by Hansen and coworkers (2010) emphasized that taurine concentrations are higher in oxidative than in glycolytic tissue. Indeed, at temperatures within the environmental thermal range (10 – 18 °C) gill tissue had significantly higher taurine concentrations than phasic muscle (14 and 18 °C, $p < 0.012$; data not shown here). At 22 °C and 26 °C this difference decreased as taurine levels fell in gills and remained stable in phasic muscle.

Tissue- as well as species-specific metabolic profiles were identified in various studies (e.g. Tikunov et al., 2010; Hurley-Sanders et al., 2015; Tripp-Valdez et al., 2017; Capello et al., 2018). Some stress assessment studies hypothesize that aerobic tissues such as gills tend to be more sensitive to stressors than other organs such as muscle (Lannig et al., 2010; Tripp-Valdez et al., 2017, 2019). Our analysis of phasic muscle tissue of *P. maximus* revealed only few and minor metabolic responses (data not shown), underpinning the particular responsiveness of invertebrate gill tissue to changes in environmental conditions.

Effects of warming (Scheme 1)

Acute warming affected metabolic pathways only at temperatures exceeding 20 °C (**Scheme 1**). At 22 °C and 26 °C, branchial levels of NN-dimethylglycine increased. This metabolite is a precursor of glycine and has been suggested to be a putative biomarker for starvation in abalone digestive gland tissue (Sheedy et al., 2016). We can exclude starvation as scallops were fed throughout exposures with maximal feeding and filtration efficiencies at 21 °C (Eymann personal comm.). Another metabolite affected was acetic acid which is considered to be an end-product of late anaerobiosis (Pörtner and Grieshaber, 1993). It accumulated at 26 °C shortly before the lethal temperature (28 °C) was reached, while succinate, another marker of

anaerobiosis (Müller et al., 2012), remained unchanged and was only seen to accumulate under DT (see below). Accumulation of acetic acid thus indicates a shift towards anaerobiosis and a disruption in energy homeostasis. This is in line with previous studies of temperate *P. maximus* which showed that scallops thrive below 23 °C (also long-term), and surpass an upper thermal limit in parallel with an onset of anaerobiosis at around 25 °C (Laing, 2000; Artigaud et al., 2014). Finally, warming led to decreasing taurine concentrations at 26 °C. For marine invertebrates, taurine is often discussed in the context of osmoregulation, but as only few and random osmolyte changes occurred, we propose that no osmoregulatory stress was induced in *P. maximus.* However, taurine may function as a pH buffer in the mitochondrial matrix as hypothesized for vertebrates (Hansen et al., 2006; Hansen et al., 2010). Taurine was found to activate mitochondrial respiration (Schaffer et al., 2016), also seen in Pacific oysters (Sokolov and Sokolova, 2019). With respect to its possible role as a mitochondrial buffer or substrate the depletion of taurine might indicate enhanced mitochondrial respiration or even dysfunction at 26°C. However, we did not analyze mitochondria in the context of this study so the consequences of taurine depletion, if any, remain speculative.

Effects of hypoxia

Our study revealed that gill tissue of *P. maximus* was particularly responsive to hypoxia although oxygen levels were kept above critical levels throughout exposures (O_2 between 8.0 – 6.5 mg O_2/L from 14 to 28 °C, considering a critical O_2 threshold of 1.42 ± 0.14 mg O2 identified by Vaquer-Sunyer and Duarte, 2008; **Scheme 2**). Hence, aerobic metabolism should remain undisturbed but immediately after the onset of exposure to hypoxia glycine accumulated and remained elevated during progressive warming, paralleled by an accumulation of acetic acid and acetoacetate (significantly higher at 26 °C than during W exposure). Glycogenic amino acids, such as glycine, have multiple cellular functions as they e.g. serve as osmolytes, promote protein synthesis, or are used for energy production via glycolysis (Ellis et al., 1985; Wang et al., 2013). It is known, that 'stressed cells' switch to pronounced protein catabolism and exploit a.o. glycogenic amino acids to fuel energy metabolism (e.g. Salway, 2004). Elevated levels of amino acids such as e.g. alanine, glycine, or arginine have also been found in abalone in response to environmental hypoxia (Tripp-Valdez et al., 2017; Venter et al., 2018). Together with the accumulation of acetic acid changes are indicative of alterations in branchial energy metabolism in *P. maximus*. This is further supported by the implied mobilization of lipid energy reserves via ß-oxidation of acetoacetate (**Tab 2B**). This metabolite did not alter with warming

but was significantly higher in scallops exposed to either WHo or DT at 26 °C indicating a pronounced energetic demand. Interestingly, increasing acetylcarnitine levels (which were solely found in phasic muscle but not in gills) in phasic muscle tissue indicates enhanced fatty acid transport into the mitochondria for ß-oxidation (0.019 ± 0.007 mM at 14 °C and 0.054 ± 0.018 mM at 22 °C, $p = 0.002$) in line with the enhanced energetic need as also indicated by the branchial data. Artigaud and coworkers investigated the molecular adaptation of *P. maximus* (mantle tissue) to heat stress (2015a, 2015b). They found that exposure to 25 °C for 56 days led to an upregulation of genes associated with lipid metabolism coinciding with a decrease in condition and explained their findings by the need of *P. maximus* to meet the increasing metabolic demand at this temperature.

Effects of hypercapnia

Acute hypercapnia on top of warming had the lowest impact on branchial metabolism of *P. maximus* (**Scheme 2**). NN-dimethylglycine and O-phosphocholine levels accumulated (Tab 2A) with unclear biological function of dimethylglycine (see discussion above). O-phosphocholine is an intermediate needed for the synthesis of phosphatidylcholine which by itself is an important component of cell membranes and associated to cell membrane integrity (Kraffe et al., 2004). It is known that both, warming and hypercapnia, can alter the lipid composition of cell membranes (Strobel et al., 2013; Valles-Regino et al., 2015), endanger cell membrane homeostasis by the oxidation of lipids, or affect acid-base homeostasis (Wittmann and Pörtner, 2013). Previous studies of temperate and boreal *P. maximus* (Schalkhauser et al., 2013; Schalkhauser et al., 2014) showed that temperate king scallops were better able to maintain acid-base homeostasis than boreal ones explaining why the temperate population was more tolerant towards hypercapnia. The low impact of WHc on gill metabolism and survival observed in the current study using temperate king scallops from Galicia (Spain) also suggests that this *P. maximus* population is tolerant to environmental hypercapnia.

Effects of Deadly Trio

Exposure to all three drivers combined affected branchial metabolism most severely. The use of metabolic pathways was consistent between individual scallops indicating that the DT constrains metabolic responses into a certain direction as observed already under WHo, which may be the key underlying driving force. Interestingly, the metabolic response was more uniform under WHo than under DT. This may be due to a stimulatory effect of hypercapnia

under DT, as observed earlier in mollusks (e.g. Lannig et al., 2010; Zittier et al., 2015; Tripp-Valdez et al., 2017). Immediately after the onset of exposure to DT the branchial levels of glycine increased indicating a cellular stress response similar to that during hypoxia (see discussion above). Most likely, glycine derived from protein degradation and was catabolized further for glycolytic energy production. Altered metabolite pattern of choline, phosphocholine and sn-glycero-3-phospholipid (compared to W, **Tab 2B**) indicates that cellular membrane integrity might be affected, as all three metabolites are involved in cell membrane homeostasis (as mentioned above; reviews by Ernst et al., 2016; Harayama and Riezman, 2018).

DT caused pronounced alterations in mitochondrial energy metabolism at temperatures ≥ 18 as can be concluded from gills switching from acetic acid accumulation at 18 °C and 22 °C to succinate accumulation at 26 °C. The contrasting changes in acetic acid and succinate concentrations indicate that Co-A may be transferred from succinyl-CoA to acetic acid by acetic acid: succinate CoA-transferase causing the accumulation of succinate (Müller et al., 2012).

Rates of oxygen consumption did not differ significantly between scallops during warming and DT exposures indicating that they did not save energy by metabolic depression. Limits in oxygen consumption were reached under DT at 20 °C (Eymann personal comm.). These observations support the conclusion that temperature-dependent limitations in oxygen supply paralleled by an acceleration of cellular metabolic rate lead to a severe mismatch between energy demand and supply according to the concept of oxygen and capacity limited thermal tolerance (OCLTT; Pörtner et al., 2017), as a potential mechanism decreasing the upper limit of thermal tolerance. This is in line with one of the few earlier studies on combined stress exposures in juvenile green abalone (*Haliotis fulgens*; + 3 °C per day; 50 % O_2; ~1000 µatm pCO_2, Tripp-Valdez et al., 2017). The authors stated that in green abalone exposure to combined stressors strongly perturbed energy metabolism at higher temperatures, indicated by an early onset of anaerobiosis (accumulation of anaerobic end products and glycogenic amino acids) and coinciding with a lowered upper thermal tolerance (T_c and CT_{max} were reached at lower temperatures).

Transfer to the field and outlook

Temperature has an overarching impact on an animal's physiology and aerobic performance and, thus, shapes the fundamental niche of a species (Somero, 2002; Pörtner et al., 2017), and building on that, its realized niche (Pörtner et al., 2017). Metabolic responses to acute warming are altered by additional exposures to hypoxia and / or hypercapnia as indicated

by shifts in mitochondrial energy metabolism at temperatures above 22 °C. These additional environmental stressors narrow the thermal niche of *P. maximus* by disturbing cellular energy metabolism at lower temperatures during DT (starting at 18 °C, see discussion above), and consequently lowering its upper thermal limit leading to enhanced mortality and lowered LC_{50} (from 25 °C to 22.5 °C in DT). In contrast to other bivalves such as mussels or oysters, the scallop's lifestyle likely reflects an evolutionary trade-off as the capacity to be alert and ready to swim does not select for a high capacity in metabolic depression (reduction of standard metabolic rate; SMR) or tolerance of oxygen depletion (shut close and outlive unfavorable conditions). Indeed, scallops have been shown to maintain higher levels of mantle cavity PO_2 correlated to a higher SMR than seen in e.g. sessile mud clams (Abele et al., 2010). However, not going into significant metabolic depression may indicate a higher vulnerability of scallops to environmental challenges compared to other molluscs. Accordingly, ongoing global warming combined with the expansion of oxygen-depleted hypercapnic water layers has negative consequences for the survival of *P. maximus* populations.

The above-described relationships may also have been decisive when pectinid ancestors were exposed to rapid and extreme changes of environmental conditions during past marine crises. In the PTME near surface temperature increased by about 11 °C accompanied by oxygen depletion of three quarters (Penn et al., 2018), eliminating the vast majority of marine biota. While ancient bivalves overall were one of the less affected groups with a fast recovery rate (Fraiser and Bottjer, 2007), the huge loss of oxygenated habitat in combination with warming likely had severe consequences for some of them, e.g. indicated by extinction patterns of ancient scallops. Tu and coworkers investigated extinction and recovery patterns from the Changhsingian (latest Permian) to Anisian (Middle Triassic) and reported that pectinida (together with myalinida and pholadomyida) were more negatively affected than ostreida or mytilida (2016). This is supported by the findings of Penn et al. (2018; see introduction) who stated that under simulated modern climate changes reaching the same dimensions as during the Permian-Triassic, modern *P. maximus* would lose up to 100 % of their present habitat. While some aspects explaining the special vulnerability of pectinids are emerging, further study is needed to fully understand the mechanisms involved in shaping vulnerability to environmental change.

Acknowledgments:

The study was funded by the Deutsche Forschungsgemeinschaft (Po278/16-1) and is part of the Research Unit TERSANE (FO 2332). We thank Anette Tillman, Lea Philipps, and Timo Hirse for the analysis of water quality and concentrations of dissolved inorganic carbon. Martin Aberhan for helpful discussion of the evolution of bivalves and mass extinction events and Inna Sokolova for the discussion of biochemical pathways. We thank the Biological station of Toralla (ECIMAT, Spain), in particular A. Villanueva and D. Costas for support in animal supply and F. Feliz Moraleda for transportation of scallops to the AWI.

References

Aberhan, M., Baumiller, T., 2003. Selective extinction among Early Jurassic bivalves: A consequence of anoxia. J. Geol. 31, 1077-1080. https://doi.org/10.1130/G19938.1.

Abele, D., Kruppe, M., Philipp, E.E.R., Brey, T., 2010. Mantle cavity water oxygen partial pressure (PO_2) in marine molluscs aligns with lifestyle. Can. J. Fish. Aquat. Sci. 67, 977-986. https://doi.org/10.1139/F10-035.

Aittokallio, T. and Schwikowski, B., 2006. Graph-based methods for analysing networks in cell biology. Brief Bioinform. 7, 243–255. https://doi.org/10.1093/bib/bbl022.

Artigaud, S., Lacroic, C., Pichereau, V., Flye-Sainte-Marie, J., 2014. Respiratory response to combined heat and hypoxia in the marine bivalves *Pecten maximus* and *Mytilus spp.* Comp. Biochem. Physiol. Part A 175, 135-140. https://doi.org/10.1016/j.cbpa.2014.06.005.

Artigaud, S., Richard, J., Thorne, M.AS., Lavaud, R., Flye-Sainte-Marie, J., Jean, F., Peck, L.S., Clark, M.S., Pichereau, V., 2015a. Deciphering the molecular adaption of the king scallop (*Pecten maximus*) to heat stress using transcriptomics and proteomics. BMC Genomics 16, 988. https://doi.org/10.1186/s12864-015-2132-x.

Artigaud, S., Lacroix, C.C.L., Richard, J.J.R., Flye-Sainte-Marie, J., Bargelloni, L.L.B., Pichereau, V., 2015b. Proteomic responses to hypoxia at different temperatures in the great scallop (*Pecten maximus*). PeerJ 3:e871 https://doi.org/10.7717/peerj.871.

Bachan, A., Payne, J.L., 2015. Modelling the impact of pulsed CAMP volcanism of PCO_2 and δ13C across the Triassic-Jurassic transition. Geol. Mag. 153, 252-270. https://doi.org/10.1017/S0016756815000126.

Capello, T., Giannetto, A., Parrino, V., Maisano, M., Olivia, S., De Marco, G., Guerriero, G., Mauceri, A., Fasulo, S., 2018. Baseline levels of metabolites in different tissues of mussel *Mytilus galloprovincialis* (Bivalvia: Mytilidae). Comp. Physiol. Part D 26, 32-39. https://doi.org/10.1016/j.cbd.2018.03.005.

Ellis, L.L., Burcham, J.M., Paynter, K.T., Bishop, S.H., 1985. Amino acid metabolism in euryhaline bivalves. Regulation of glycine accumulation in ribbed mussel gills. J. Exp. Zool. 233, 347-358. https://doi.org/10.1002/jez.1402330303.

Ellis, R.P., Spicer, J.I., Byrne, J.J., Sommer, U., Viant, M.R., White, D.A., Widdicombe, S., 2014. ^{1}H NMR Metabolomics Reveals Contrasting Response by Male and Female Mussels Exposed to Reduced Seawater pH, Increased Temperature, and a Pathogen. Environ. Sci. Technol. 48, 7044-7052. https://doi.org/10.1021/es501601w.

Ern, R., Johansen, J.L. Rummer, J.L. Esbaugh, A., 2017. Effects of hypoxia and ocean acidification on the upper thermal niche boundaries of coral reef fishes. Biol. Lett. 13, 20170135. https://doi.org/10.1098/rsbl.2017.0135.

Ernst, R., Ejsing, C.S., Antonny, B., 2016. Homeoviscous adaptation and the regulation of membrane lipids. J. Mol. Biol. 24, 4776-4791. https://doi.org/10.1016/j.jmb.2016.08.013.

Feely, R.A., Doney, S.C., Cooley, S.R., 2009. Ocean acidification: Present conditions and future changes in a high CO_2 world. Oceanography 22, 36-47.

Grieshaber, M., 1978. Breakdown and formation of high-energy phosphates and octopine in the adductor muscle of the scallops, *Chlamys opercularis* (L.), during escape swimming and recovery. J. Comp. Physiol. 126, 269–276. https://doi.org/10.1007/BF00688937.

Guinotte, J.M. and Fabry, V.J., 2008. Ocean acidification and its potential effects on marine ecosystems. Ann. N. Y. Acad. Sci. 1134, 320–342. https://doi.org/10.1196/annals.1439.013.

Guderley, H., and Pörtner, H.O., 2010. Metabolic power budgeting and adaptive strategies in zoology: Examples from scallops and fish. Can. J. Zool. 88, 753–763. https://doi.org/10.1139/Z10-039.

Goeman, J.J., Van de Geer, S.A., De Kort, F., Houwellingen, H.C., 2004. A global test for groups of genes: testing association with a clinical outcome. Bioinformatics 20, 93-99. https://doi.org/10.1093/bioinformatics/btg382

Hansen, S.H., Andersen, M.L., Birkedal, H., Cornett, C., Wibrand, F., 2006. The important role of taurine in oxidative metabolism. In: Oja S.S., Saransaari P. (Eds) Taurine 6. Advances in Experimental Medicine and Biology vol 583. Springer, Boston, MA. https://doi.org/10.1007/978-0-387-33504-9_13.

Hansen, S.H., Andersen, M.L., Cornett, C., Gradinaru, R., Grunnet, N., 2010. A role for taurine in mitochondrial function. J. Biomed. Sci. 17, https://doi.org/10.1186/1423-0127-17-S1-S23.

Harayama, T., and Riezman, H., 2018. Understanding the diversity of membrane lipid composition. Nature Reviews, Mol. Cell. Biol. 19, 281-296. https://doi.org/10.1038/nrm.2017.138.

Heise, K., Puntarulo, S., Pörtner, H.O., Abele, D., 2003. Production of reactive oxygen species by isolated mitochondria of the Antarctic bivalve *Laternula elliptica* (King and Broderip) under heat stress. Com. Biochem. Physiol. C 134, 79-90. https://doi.org/10.1016/S1532-0456(02)00212-0.

Heise, K., Puntarulo, S., Nikinmaa, M., Abele, D., Pörtner, H.O., 2006. Oxidative stress during stressful heat exposure and recovery in the North Sea eelpout *Zoarces viviparus* L. J. Exp. Biol. 209, 353-363. https://doi.org/10.1242/jeb.01977.

Hurley-Sanders, J.L.H., Levine, J.F., Nelson, S.A.C., Law, J.M., Showers, W.J., Stoskopf, M.K., 2015. Key metabolites in tissue extracts of *Elliptio complanata* identified using ^{1}H nuclear magnetic resonance spectroscopy. Conserv. Physiol. 3, cov023, https://doi.org/10.1093/conphys/cov023.

Jones, O.A., Dondero, F., Viarengo, A., Griffin, J.L., 2008. Metabolic profiling of *Mytilus galloprovincialis* and its potential applications for pollution assessment. Mar. Ecol. Prog. Ser. 369, 169-179. https://doi.org/10.3354/meps07654.

Kassahn, K.S., Crozier, R.H., Pörtner, H.O., Caley, M.J., 2009. Animal performance and stress: responses and tolerance limits at different levels of biological organization. Biol. Rev. 84, 277-292. https://doi.org/10.1111/j.1469-185X.2008.00073.x.

Kraffe, E., Soudant, P., Marty, Y., 2004. Fatty acids of serine, ethanoamine, and choline plasmogens in some marine bivalves. Lipids 39, 59-66. https://doi.org/10.1007/s11745-004-1202-x.

Lannig, G., Eilers, S., Pörtner, H.O., Sokolova, I., Bock, C., 2010. Impact of Ocean acidification on energy metabolism of oyster, *Crassostrea gigas* – Changes in metabolic pathways and thermal response. Mar. Drugs 8, 2318-2339. https://doi.org/10.3390/md8082318.

Laing, I., 2000. Effect of temperature and ration on growth and condition of king scallop (*Pecten maximus*) spat. Aquaculture 183, 325-334. https://doi.org/10.1016/S0044-8486(99)00262-8.

Laudien, J., Schiedek, D., Brey, T., Pörtner, H.O., Arntz, W.E., 2002. Survivorship of juvenile surf clams *Donax serra* (Bivalvia, Donacidae) exposed to severe hypoxia and hydrogen sulphide. J. Mar. Biol. Ecol. 1, 9-23. https://doi.org/10.1016/S0022-0981(02)00030-8.

Lenz, E.M., Weeks, J.M., Lindon, J.C., Osborn, D., Nicholson, J.K., 2005. Qualitative high field ^{1}H-NMR spectroscopy for the characterization of endogenous metabolites in earthworms with biochemical biomarker potential. Metabolomics 1, 123-136. https://doi.org/10.1007/s11306-005-4435-4.

Müller, M., Mentel, M., van Hellemond, J.J., Henze, K., Woehle, C., Gould, S.B., Yu, R.-Y., van der Giezen, M., Tielens, A.G.M., Martin, W.F., 2012. Biochemistry and Evolution of Anaerobic Energy Metabolism in Eukaryotes. Microbiology and Molecular Biology Reviews 76, 444–495. https://doi.org/10.1128/MMBR.05024-11

Palma, P.F.S., Bock, C., Silva, T.S., Guerreiro, P.M., Power, D.M., Pörtner, H.O., Canario, A.V.M., 2019. STC1 and PTHrP Modify Carbohydrate and Lipid Metabolism in Liver of a Teleost Fish. Sci. Rep. 9, https://doi.org/10.1038/s41598-018-36821-2.

Parker, L.M., Ross, R.M., O'Connor, W.A., Pörtner, H.O., Scanes, E., Wright, J.M., 2013. Predicting the response of Molluscs to the Impact of Ocean acidification. Biology 2, 651-692. https://doi.org/10.3390/biology2020651.

Penn, J.L., Deutsch, C., Payne, J.L. Sperling, E.A., 2018. Temperature-dependent hypoxia explains biogeography and severity of end-Permian marine mass extinction. Science 362 (6419). https://doi.org/10.1126/science.aat1327.

Purohit, P.V., Rocke, D.M., Viant, M.R., Woodruff, D.L., 2004. Discrimination models using variance-stabilizing transformation of metabolomic NMR data. Omics 8, 118-130. https://doi.org/10.1089/1536231041388348.

Pörtner, H.O. and Grieshaber, M.K., 1993. Characteristics of the critical PO 2 (s): gas exchange, metabolic rate and the mode of energy production. p. 330–357. In The Vertebrate Gas Transport Cascade: Adaptations to Environment and Mode of Life, ed. by J. E. P. W. Bicudo, CRC Press Inc., Boca Raton (FL), U.S.A.

Pörtner, H.O., 2002. Climate variations and the physiological basis of temperature dependent biogeography: systemic to molecular hierarchy of thermal tolerance in animals. Comp. Biochem. Physiol. Part A 132, 739-761. https://doi.org/10.1016/S1095-6433(02)00045-4.

Pörtner, H.O., Langenbuch, M., Reipschläger, A., 2004. Biological impact of elevated ocean CO_2 concentrations: Lessons from animal physiology and earth history. J. Oceanography 60, 705-718. https://doi.org/10.1007/s10872-004-5763-0

Pörtner, H.O., 2012. Integrating climate-related stressors effects on marine organisms: unifying principles linking molecule to ecosystem-level changes. Mar. Ecol. Prog. Ser. 470, 273-290. https://doi.org/10.3354/meps10123.

Pörtner, H.O., Bock, C., Mark, F.C., 2017. Oxygen-and capacity-limited thermal tolerance: bridging ecology and physiology. J. Exp. Biol. 220, 2685-2696. https://doi.org/10.1242/jeb.134585.

Rebelein, A., Pörtner, H.O., Bock, C., 2018. Untargeted metabolic profiling reveals distinct patterns of thermal sensitivity in two related notothenioids. Comp. Biochem. Physiol. Part A 217, 43-54. https://doi.org/10.1016/j.cbpa.2017.12.012.

Rishi, V., Anjum, F., Ahmad, F., Pfeil, W., 1998. Role of-compatible osmolytes in the stabilization of proteins during heat stress. Biochem. J. 329, 137-143. https://doi.org/10.1042/bj3290137.

Rhein, M., Rintoul, S.R., Aoki, S., et al., 2013. Observations: Ocean. In Stocker TF, Qin D, Plattner G-K, Tignor M, Allen SK, Boschung J, Nauels A, Xia Y, Bex V, Midgley PM (eds.) Climate Change 2013: The Physical Science Basis. Contribution of Working Group I to the Fifth Assessment Report of the Intergovernmental Panel on Climate Change. Cambridge, GB. Cambridge University Press, pp. 255-316.

Rudolph, A.S., Crowe, J.H., Crowe, L.M., 1986. Effects of three stabilizing Agents: Proline, Betaine, and Trehalose on membrane phospholipids. Arch. Biochem. Biophys. 245, 134-143. https://doi.org/10.1016/0003-9861(86)90197-9

Salway, J. G., 2004. Metabolism at a glance. Wiley. Blackwell Science, London.

Schalkhausser, B., Bock, C., Stemmer, K., Brey, T., Pörtner, H.O., Lannig, G., 2013. Impact of ocean acidification on escape performance of the king scallop; *Pecten maximus*, from Norway. Mar. Biol. 160, 1995-2006. https://doi.org/10.1007/s00227-012-2057-8.

Schalkhausser, B., Bock, C., Pörtner, H.-O., Lannig, G., 2014. Escape performance of temperate king scallop, *Pecten maximus* under ocean warming and acidification. Mar. Biol. 161, 2819-2829. https://doi.org/10.1007/s00227-014-2548-x.

Schaffer, S.W., Shimada-Takaura, K., Jong, C.J., Ito, T., Takahashi, K., 2016. Impaired energy metabolism of the taurine-deficient heart. Amino Acids 48, 549-58. https://doi.org/10.1007/s00726-015-2110-2.

Schmidt, M., Windisch, H.S., Ludwichowski, K.U., Seegert, S.L.L., Pörtner, H.O., Storch, D., Bock, C., 2017. Differences in neurochemical profiles of two gadid species under ocean warming and acidification. Front. Zool. 14, https://doi.org/10.1186/s12983-017-0238-5.

Sheedy, J.R., Lachambre, S., Gardner, D.K., Day, R.W., 2016. ^{1}H-NMR metabolic profiling of abalone digestive gland in response to short-term starvation. Aquacult. Int. 24, 503-521. https://doi.org/10.1007/s10499-015-9941-4.

Shumway, S.E., and Koehn, R.K., 1982. Oxygen consumption in the American oyster *Crassostrea virginica*. Mar. Ecol. Prog. Ser. 9, 59–68. https://doi.org/10.3354/meps009059.

Sokolova, I.M., Frederich, M., Bagwe, R., Lannig, G., Sukhotin, A.A., 2012. Energy homeostasis as an integrative tool for assessing limits of environmental stress tolerance in aquatic invertebrates. Mar. Environ. Res. 79, 1-15. https://doi.org/10.1016/j.marenvres.2012.04.003.

Sokolov, E.P. and Sokolova, I.M., 2019. Compatible osmolytes modulate mitochondrial function in a marine osmoconformers *Crassostrea gigas* (Thunberg, 1793). Mitochondrion 45, 29-37. https://doi.org/10.1016/j.mito.2018.02.002

Somero, G.N. 2002. Thermal physiology and vertical zonation of intertidal animals: optima, limits, and costs of living. Int. Comp. Biol. 42, 780–789. https://doi.org/10.1093/icb/42.4.780.

Somero, G.N. and Yancey, P.H., 2011. Osmolytes and cell-volume regulation: Physiological and Evolutionary Principles. In Comprehensive Physiology, R. Terjung (Ed.). https://doi.org/10.1002/cphy.cp140110.

Stapp, L., Thomsen, J., Schade, H., Bock, C., Melzner, F., Pörtner, H.O., Lannig, G., 2017. Intra-population variability of ocean acidification impacts on the physiology of Baltic blue mussels (*Mytilus edulis*): integrating tissue and organism response. J. Comp. Physiol. B – Biochem. Syst. Environ. Physiol. 187, 529-543. https://doi.org/10.1007/s00360-016-1053-6.

Stapp, L., Parker, L., O'Connor, W.A., Bock, C., Ross, P.M., Pörtner, H.O., Lannig, G., 2018. Sensitivity to ocean acidification differs between populations of the Sydney rock oyster: Role of filtration and ion-regulatory capacities. Mar. Environ. Res. 135, 103-113. https://doi.org/10.1016/j.marenvres.2017.12.017.

Strobel, A., Graeve, M., Pörtner, H.O., Mark, F.C., 2013. Mitochondrial Acclimation Capacities to Ocean Warming and Acidification Are Limited in the Antarctic Nototheniid Fish, *Notothenia rossii* and *Lepidonotothen squamifrons*. Plos One 8, e68865. https://doi.org/10.1371/journal.pone.0068865.

Thompson, R.J., Livingstone, D.R., De Zwaan, A., 1980. Physiological and biochemical aspects of the valve snap and valve closure responses in the giant scallop *Placopecten magellanicus.* J. Comp. Physiol. 137, 97-104. https://doi.org/10.1007/BF00689207.

Tikunov, A.P., Johnson, C.B., Lee, H., Stoskopf, M.K., Macdonald, J.M., 2010. Metabolomic investigations of American oysters using ^{1}H-NMR spectroscopy. Mar. Drugs 8, 2578-2596. https://doi.org/10.3390/md8102578.

Tikunov, A.P., Stoskopf, M.K., Macdonald, J.M., 2014. Fluxomics of the Eastern Oyster for environmental stress studies. Metabolomics 4, 53-70. https://doi.org/10.3390/metabo4010053.

Tremblay, I., and Guderley, H.E., 2013. Scallops show that muscle metabolic capacities reflect locomotor style and morphology. Physiol. Biochem. Zool. 87, 231–244. https://doi.org/10.1086/674107.

Tripp-Valdez, M. A., Bock, C., Lucassen, M. Lluch-Cota, S. E., Sicard, M. T., Lannig, G., & Pörtner, H. O., 2017. Metabolic response and thermal tolerance of green abalone juveniles (*Haliotis fulgens*: Gastropoda) under acute hypoxia and hypercapnia. J. Exp. Mar. Biol. Ecol. 497, 11-18. https://doi.org/10.1016/j.jembe.2017.09.002.

Tripp-Valdez, M.A., Bock, C., Lannig, G., Koschnick, N, Pörtner, H.O., Lucassen, M., 2019. Assessment of muscular energy metabolism and heat shock response of the green abalone *Haliotis fulgens* (Gastropoda: Philipi) at extreme temperatures combined with acute hypoxia and hypercapnia. Comp. Biochem. Physiol. Part B: Biochem. Mol. Biol. 227, 1-11. https://doi.org/10.1016/j.cbpb.2018.08.009.

Tu, C., Chen, Z.Q., Harper, D.A.T., 2016. Permian–Triassic evolution of the Bivalvia: Extinction-recovery patterns linked to ecologic and taxonomic selectivity. Palaeogeogr. Palaeoclimatol. Palaeoecol. 459, 53-62. https://doi.org/10.1016/j.palaeo.2016.06.042.

Valles-Regino, R., Tate, R., Kelaher, B., Savins, D., Dowell, A., Benkendorff, K., 2015. Ocean warming and CO_2-induced acidification impact the lipid content of a marine predatory gastropod. Mar. Drugs. 13, 6019-6037. https://doi.org/10.3390/md13106019.

Viant, M.R., Rosenblum, E.S., Tjeerdema, S., 2003. NMR-based metabolomics: A powerful approach for characterizing the effects of environmental stressors on organism health. Environ. Sci. Technol. 37, 4982-4989. https://doi.org/10.1021/es034281x.

Venter, L., Loots, D.T., Mienie, L.J., Jansen van Rensburg, P.J., Mason, S., Vosloo, A., Lindeque, J.Z., 2018. The cross-tissue metabolic response of abalone (*Haliotis midae*) to functional hypoxia. Biol. Open 7, https://doi.org/10.1242/bio.031070.

Wilkens, L.A., 2006. Neurobiology and behavior of the scallop. In: Shumway SE, Parson GJ (Eds) Scallops: biology, ecology and aquaculture, 1st edn. Elsevier, Amsterdam, pp 317–356.

Wittmann, A.C. and Pörtner, H.O., 2013. Sensitivities of extant animal taxa to ocean acidification. Nat. Clim. Change 3, 995-1001. https://doi.org/10.1038/nclimate1982.

Wang, W., Wu, Z., Dai, Z., Yang, Y., Wang, J., Wu, G., 2013. Glycine metabolism in animals and humans: implications for nutrition and health. Amino Acids 45, 463-477. https://doi.org/10.1007/s00726-013-1493-1.

Wu, H., and Wang, W.X., 2010. NMR-based metabolomic studies on the toxicological effects of cadmium and copper on green mussels *Perna viridis*. Aquat. Toxicol. 100, 339-345. https://doi.org/10.1016/j.aquatox.2010.08.005.

Xia, J., Wishart, D.S., 2010. MetPA: A web based metabolomics tool for pathway analysis and visualization. Syst. Biol. 26, 2342-2344. https://doi.org/10.1093/bioinformatics/btq418.

Xia, J., Wishart, D.S., 2016. Using MetaboAnalyst 3.0 for Comprehensive Metabolomics Data Analysis. Curr Prot. Bioinf. 55, 14.10.1-14.10.91. https://doi.org/10.1002/cpbi.11.

Yancey, P.H., 2005. Organic osmolytes as compatible, metabolic, and counteracting cytoprotectants in high osmolarity and other stresses. J. Exp. Biol. 208, 2819-2830. https://doi.org/10.1242/jeb.01730.

Zittier, Z., Bock, C., Lannig, G., Pörtner, H.O., 2015. Impact of ocean acidification on thermal tolerance and acid–base regulation of *Mytilus edulis* (L.) from the North Sea. J. Exp. Mar. Biol. Ecol. 473, 16-25. https://doi.org/10.1016/j.jembe.2015.08.001.

Zittier, Z., Bock, C., Sukhotin, A.A., Häfker, N.S., Pörtner, H.O., 2018. Impact of ocean acidification on thermal tolerance and acid–base regulation of Mytilus edulis from the White Sea. Polar Biol. 41**,** 2261–2273.

Tab 1: Summary of water chemistry parameters during acute warming exposures

Temperature (T_{nom} = target temperature and T_{meas} = measured temperature in systems; °C), salinity (PSU), $pH_{Freescale}$, PO_2, (% air saturation) and PCO_2, (µatm) were determined in water samples collected throughout W, WHo, WHc, and DT exposures. Data are presented as means ± SD (n =5-7 single measurements).

Warming

T_{nom} (°C)	T_{meas} ± SD (°C)	Sal ± SD (PSU)	$pH_{Freescale}$ ± SD	PO_2 (%) ± SD	PCO_2 (µatm) ± SD
14	14.4 ± 0.3	34.4 ± 0.3	8.011 ± 0.037	96.2 ± 0.8	705 ± 87
18	18.2 ± 0.2	34.0 ± 0.5	7.965 ± 0.042	91.1 ± 1.6	712 ± 93
22	22.0 ± 0.1	34.0 ± 0.3	8.035 ± 0.054	93.5 ± 3.8	633 ± 97
26	26.3 ± 0.7	33.3 ± 0.7	7.977 ± 0.035	95.2 ± 3.0	748 ± 66

Warming *plus* Hypoxia

T_{nom} (°C)	T_{meas} ± SD (°C)	Sal ± SD (PSU)	$pH_{Freescale}$ ± SD	PO_2 (%) ± SD	PCO_2 (µatm) ± SD
14	14.0 ± 0.1	33.5 ± 0.4	8.103 ± 0.008	58.1 ± 2.8	473 ± 39
18	18.1 ± 0.2	33.8 ± 0.2	8.118 ± 0.006	61.4 ± 1.8	449 ± 8
22	22.0 ± 0.3	34.0 ± 0.2	8.048± 0.013	58.8 ± 2.6	538 ± 18
26	26.2 ± 0.1	34.4 ± 0.4	8.011± 0.031	64.4 ± 2.6	597 ± 35

Warming *plus* Hypercapnia

T_{nom} (°C)	T_{meas} ± SD (°C)	Sal ± SD (PSU)	$pH_{Freescale}$ ± SD	PO_2 (%) ± SD	PCO_2 (µatm) ± SD
14	13.9 ± 0.1	33.5 ± 0.4	7.512 ± 0.021	96.2 ± 0.3	2050 ± 65
18	18.2 ± 0.1	33.8 ± 0.2	7.529 ± 0.009	95.4 ± 1.2	2062 ± 47
22	22.3 ± 0.0	34.0 ± 0.2	7.548 ± 0.012	93.3 ± 1.6	2054 ± 97
26	26.1 ± 0.2	34.4 ± 0.4	7.552 ± 0.018	91.2 ± 1.0	2124 ± 96

Deadly Trio

T_{nom} (°C)	T_{meas} ± SD (°C)	Sal ± SD (PSU)	$pH_{Freescale}$ ± SD	PO_2 (%) ± SD	PCO_2 (µatm) ± SD
14	14.4 ± 0.2	33.8 ± 0.9	7.619 ± 0.023	54.5 ± 2.1	1611 ± 78
18	17.8 ± 0.1	34.2 ± 0.4	7.665 ± 0.015	56.2 ± 2.6	1688 ± 280
22	22.2 ± 0.1	34.1 ± 0.2	7.583 ± 0.015	51.9± 3.0	1969 ± 192
26	26.3 ± 0.2	33.8 ± 0.0	7.538 ± 0.029	51.0± 4.1	2312 ± 78

Figure 1:

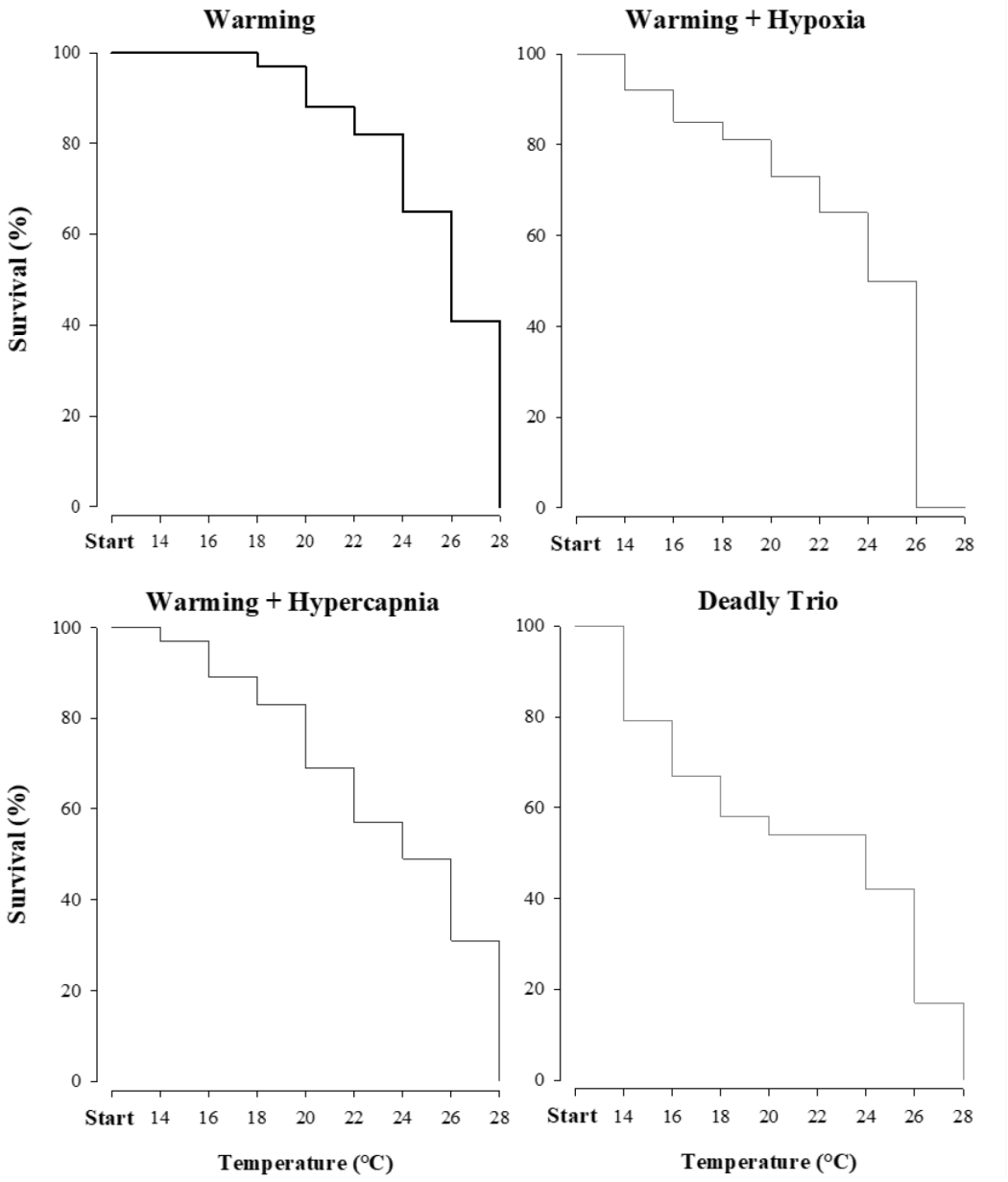

Fig. 1: Survival of *P. maximus* under warming, warming *plus* Hypoxia, warming *plus* Hypercapnia, and Deadly Trio (warming *plus* Hypoxia *plus* Hypercapnia). The temperature at which 50 % of scallops had died (LC_{50}) was reached at 25 °C (W), 24 °C (WHo), 24 °C (WHc), and 22.5 °C (DT). The percentage of surviving scallops is shown for every 2 °C temperature increase.

Figure 2: PLS-Da Score Plot of gill metabolite profiles from *P. maximus*

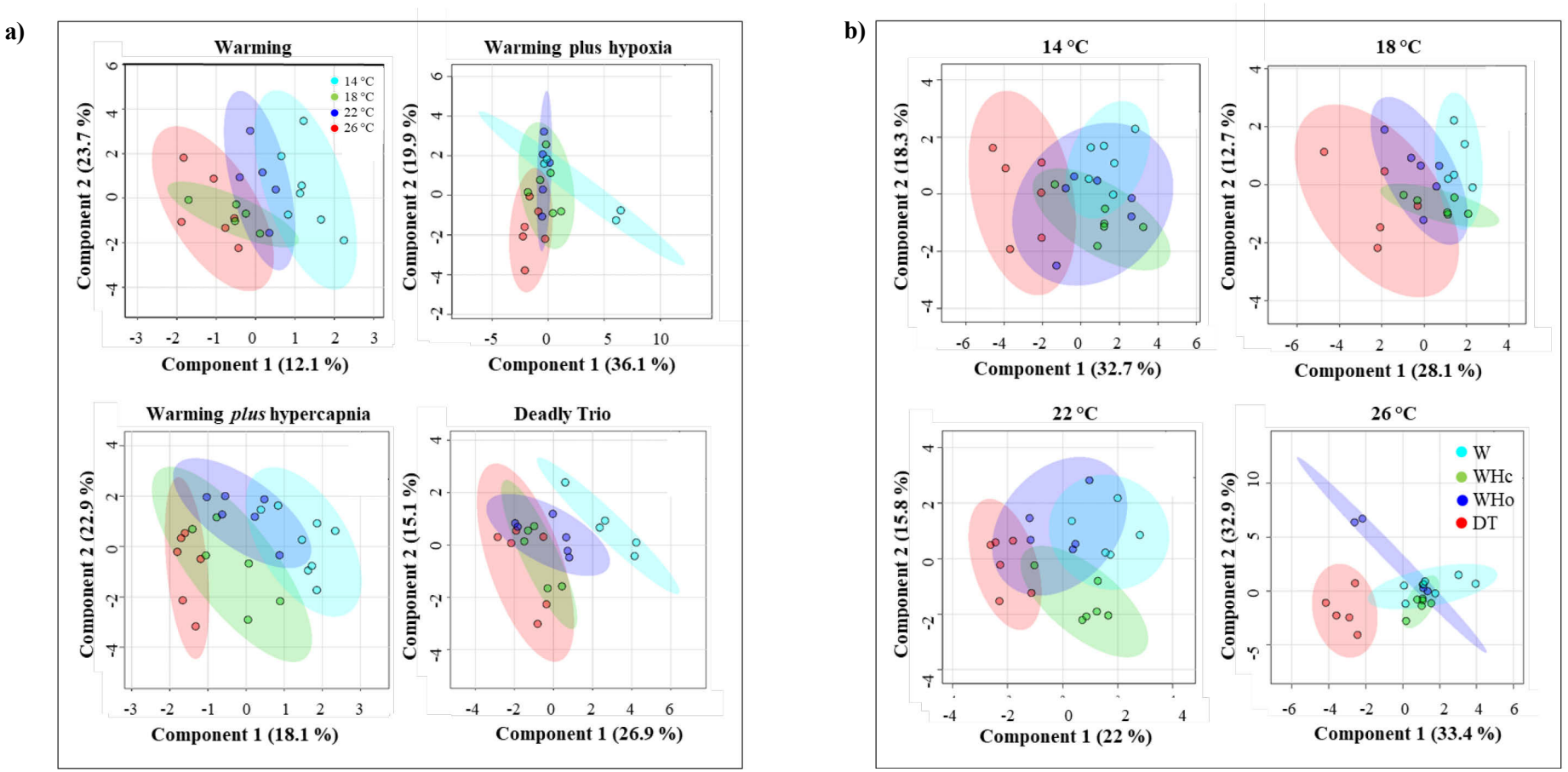

Fig. 2: Impact of the different stress exposures and sample temperature on the branchial metabolic profile of *P. maximus*. a) Score Plots of the PLS-DA model of assigned gill tissue metabolites sampled at 14 °C (red), 18 °C (green), 22 °C (dark blue), and 26 °C (light blue) in the respective exposures. **b)** Score Plots assembled according to the respective sample temperature show the differences between branchial metabolic profiles according to the respective exposure group. Warming (light blue), WHc (green), WHo (dark blue), DT (red). Ellipses correspond to a confidence interval of 95%.

Figure 3:

a) Amino Acids and derivates

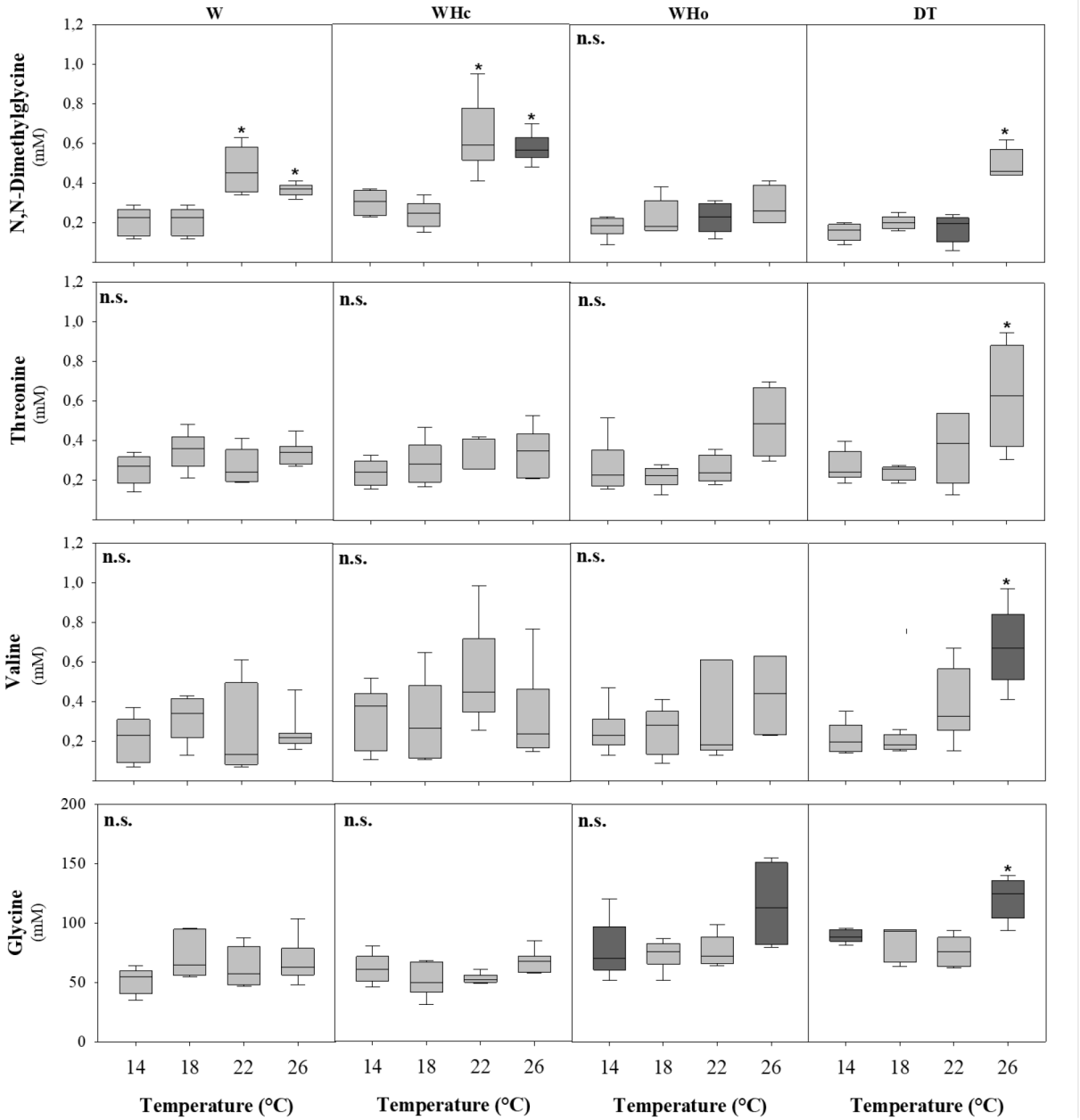

b) Related to energy metabolism

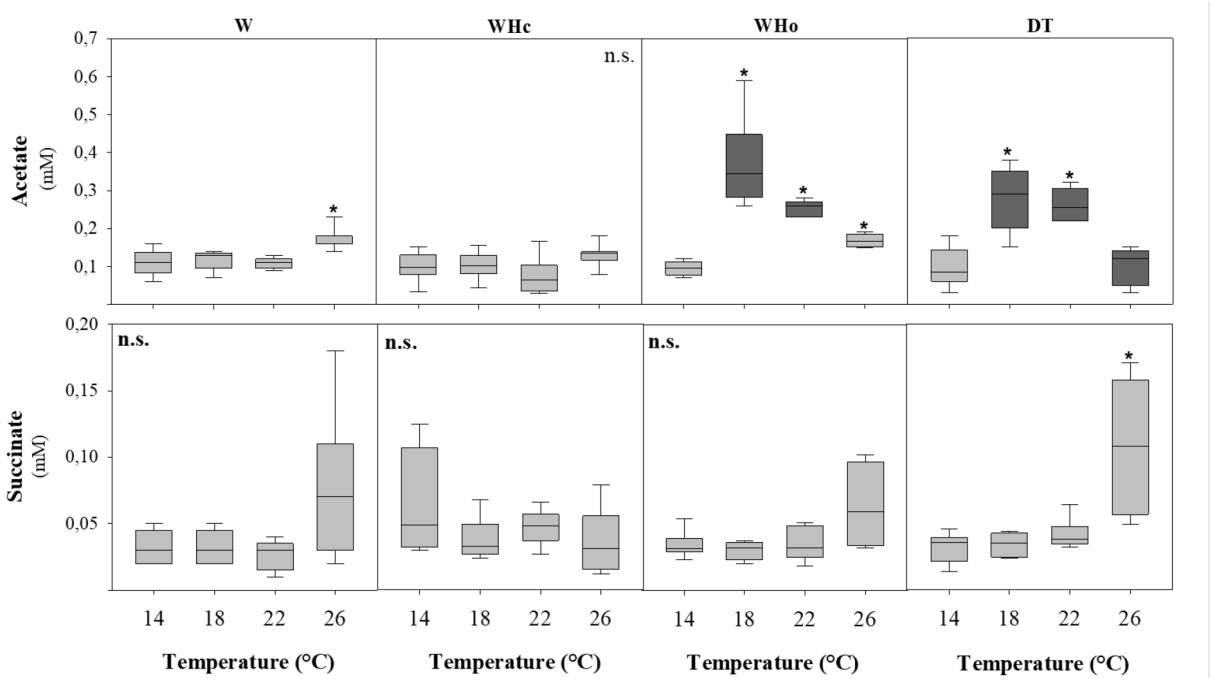

c) Osmolytes

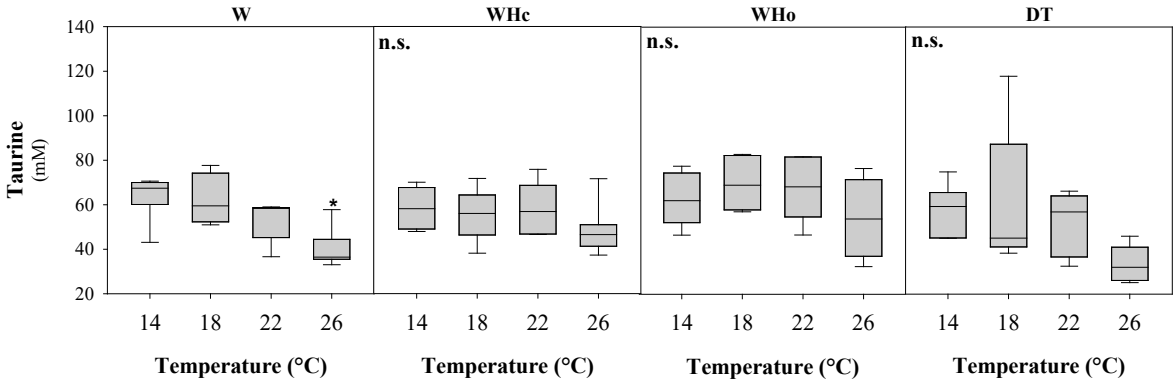

Fig. 3: Metabolite levels in gill tissue of *P. maximus*. **a)** Amino acids **b)** metabolites related to energy metabolism **c)** osmolytes. Data show mean, normalized concentration given as mM ± SD. Asterisks mark significant differences to concentrations at 14 °C. Dark grey bars indicate that the metabolite concentration was significantly different from the group sampled after warming to this temperature.

Tab. 2A

Results of one-way ANOVA for significant changes in gill metabolite levels tested against a) temperature. Shown is the compound, the f-value, p-value, [-LOG10(p)], and the resulted Fisher' LSD.

Warming

Compound	F-value	P-value	[-LOG10(p)]	Fisher's LSD
NN Dimethylglycine	15,0	3,0E-05	4,5	14, 18 < 22, 26
Taurine	8,5	8,7E-04	3,1	14, 18, 22 > 26
Acetic acid	6,9	2,5E-03	2,6	14 - 22 < 26

Hypercapnia

Compound	F-value	P-value	[-LOG10(p)]	Fisher's LSD
NN Dimethylglycine	17,0	6,2E-06	5,2	14, 18 < 22, 26
O-Phosphocholine	7,0	1,7E-03	2,8	14, 18, 22 < 26

Hypoxia

Compound	F-value	P-value	[-LOG10(p)]	Fisher's LSD
Acetic acid	35,2	1,6E-07	6,8	14 < 18 - 26; 18 > 26

Deadly Trio

Compound	F-value	P-value	[-LOG10(p)]	Fisher's LSD
NN Dimethylglycine	13,3	8,2E-05	4,1	14 - 22 < 26
Succinate	11,6	1,8E-04	3,7	14 - 22 < 26
Valine	11,5	1,9E-04	3,7	14, 18 < 22, 26; 22 < 26
Acetic acid	9,8	4,7E-04	3,3	14 < 18, 22 ; 18, 22 > 26
Glycine	9,6	5,2E-04	3,3	14 - 22 < 26
Threonine	5,2	9,0E-03	2,0	14 - 22 < 26

Tab. 2B

Results of one-way ANOVA for significant changes in gill metabolite levels tested against exposure. Shown is the compound, the f-value, p-value, [-LOG10(p)], and the resulted Fisher' LSD.

14 °C

Compound	F-value	P-value	[-LOG10(p)]	Fisher's LSD
Choline	15,1	2,3E-05	4,6	W - DT
O-Phosphocholine	13,7	4,3E-05	4,4	W - HO, HC, DT
sn-Glycero-3-phosphocholine	7,9	1,1E-03	2,9	W - DT
Glycine	6,4	3,3E-03	2,5	W - HO, DT

18°C

Compound	F-value	P-value	[-LOG10(p)]	Fisher's LSD
Acetic acid	20,1	5,7E-06	5,2	W - HO, DT

22°C

Compound	F-value	P-value	[-LOG10(p)]	Fisher's LSD
Acetic acid	23,3	2,0E-06	5,7	W - HO, HC, DT
Choline	13,6	7,0E-05	4,2	W - DT
NN Dimethylglycine	12,6	1,1E-04	3,9	W - HO, DT
O-Phosphocholine	9,3	6,2E-04	3,2	W - DT
Dimethysulfone	8,3	1,2E-03	2,9	W - HO

26°C

Compound	F-value	p.value	[-LOG10(p)]	Fisher's LSD
Acetoacetate	13,8	5,1E-05	4,3	W - HO; DT
Choline	12,8	8,1E-05	4,1	W - DT
Glycine	11,4	1,7E-04	3,8	W - HO, DT
Dimethysulfone	7,5	1,6E-03	2,8	W - HO, DT
Trigonelline	6,8	2,7E-03	2,6	W - HO, DT
NN Dimethylglycine	5,8	5,4E-03	2,3	W - HC
Acetic acid	5,6	6,1E-03	2,2	W - DT
Valine	5,4	7,3E-03	2,1	W - DT

Tab. 3

Significant changes in gill metabolic pathways with a [-LOG(p)] change of > 2.5. As a reference metabolic pathways of the zebrafish (*Danio rerio*) were chosen. Shown is the pathway including the total number of compounds, the number and names of the identified hits, the raw p-value, the [-LOG(p)] change, as well as Holm adjust, FDR, and IMP. Metabolites written in bold indicate a significant change determined in the ANOVA.

Warming

14 *vs.* 26 °C	Pathway	Incr/ Decr	Total Cmpd	Hits	Compounds identified in the pathway	Raw p	[-LOG(p)]	Holm adjust	FDR	IMP
Carbohydrate metabolism	Pyruvate metabolism	↑	22	1	**Acetic acid**	2E-03	6,1	0,1	0,0	0,1
	Glycolysis or Gluconeogenesis	↑	26	1	**Acetic acid**	2E-03	6,1	0,1	0,0	0,0
Amino acid metabolism	Glycine, serine and threonine metabolism	↑	31	6	Choline, Threonine - Glycine - Sarcosine, Betaine - **Dimethylglycine**	8E-03	4,8	0,3	0,1	0,3
Metabolism of other Amino acids	Taurine and hypotaurine metabolism	↓	7	2	**Taurine**, Hypotaurine	4E-02	3,1	1,0	0,2	0,5

Warming + Hypercapnia

14 *vs.* 26 °C	Pathway	Incr/ Decr	Total Cmpd	Hits	Compounds identified in the pathway	Raw p	[-LOG(p)]	Holm adjust	FDR	IMP
Amino acid metabolism	Glycine, serine and threonine metabolism	↑	31	6	Choline, Threonine - Glycine - Sarcosine, Betaine - **Dimethylglycine**	2E-02	4,0	0,6	0,0	0,3
Lipid metabolism	Glycerophospholipid metabolism	↑	27	3	Glycerophosphocholine, **Choline** - Phosphocholine	2E-02	3,9	0,6	0,0	0,1

Warming + Hypoxia

14 *vs.* 26 °C	Pathway	Incr/ Decr	Total Cmpd	Hits	Compounds identified in the pathway	Raw p	[-LOG(p)]	Holm adjust	FDR	IMP
Carbohydrate metabolism	Pyruvate metabolism	↑	22	1	**Acetic acid**	2E-03	6,2	0,1	0,03	0,08
	Glycolysis or Gluconeogenesis	↑	26	1	**Acetic acid**	2E-03	6,2	0,1	0,03	0,03

Deadly Trio

14 *vs.* 26 °C	Pathway	Incr/ Decr	Total Cmpd	Hits	Compounds identified in the pathway	Raw p	[-LOG(p)]	Holm adjust	FDR	IMP
Amino acid metabolism	Glycine, serine and threonine metabolism	↑	31	6	Choline**, Threonine - Glycine -** Sarcosine, Betaine **- Dimethylglycine**	7E-07	14,2	0,0	0,0	0,3
Carbohydrate metabolism	Butanoate metabolism	↑	22	3	Glutamate, **Succinate**, Acetoacetate	5E-04	7,6	0,0	0,0	0,1
Amino acid metabolism	Valine, leucine and isoleucine biosynthesis	↑	13	4	**Valine**, Leucine, Isoleucine, **Threonine**	8E-04	7,1	0,0	0,0	1,0
Carbohydrate metabolism	Propanoate metabolism	↑	20	2	**Succinate**, ß-Alanine	9E-04	7,0	0,0	0,0	0,0
Amino acid metabolism	Alanine, aspartate and glutamate metabolism	↑	24	5	Aspartate, Alanine, Glutamate - Glutamine, **Succinate**	1E-03	6,8	0,0	0,0	0,6
Carbohydrate metabolism	Citrate cycle (TCA cycle)	↑	20	1	**Succinate**	1E-03	6,7	0,0	0,0	0,0
Amino acid metabolism	Valine, leucine and isoleucine degradation	↑	38	4	**Valine**, Leucine, Isoleucine, Acetoacetate	2E-03	6,3	0,1	0,0	0,0
Metabolism of other Amino acids	Glutathione metabolism	↑	26	2	**Glycine**, Glutamate	5E-02	2,9	1,0	0,1	0,0

Scheme 1:

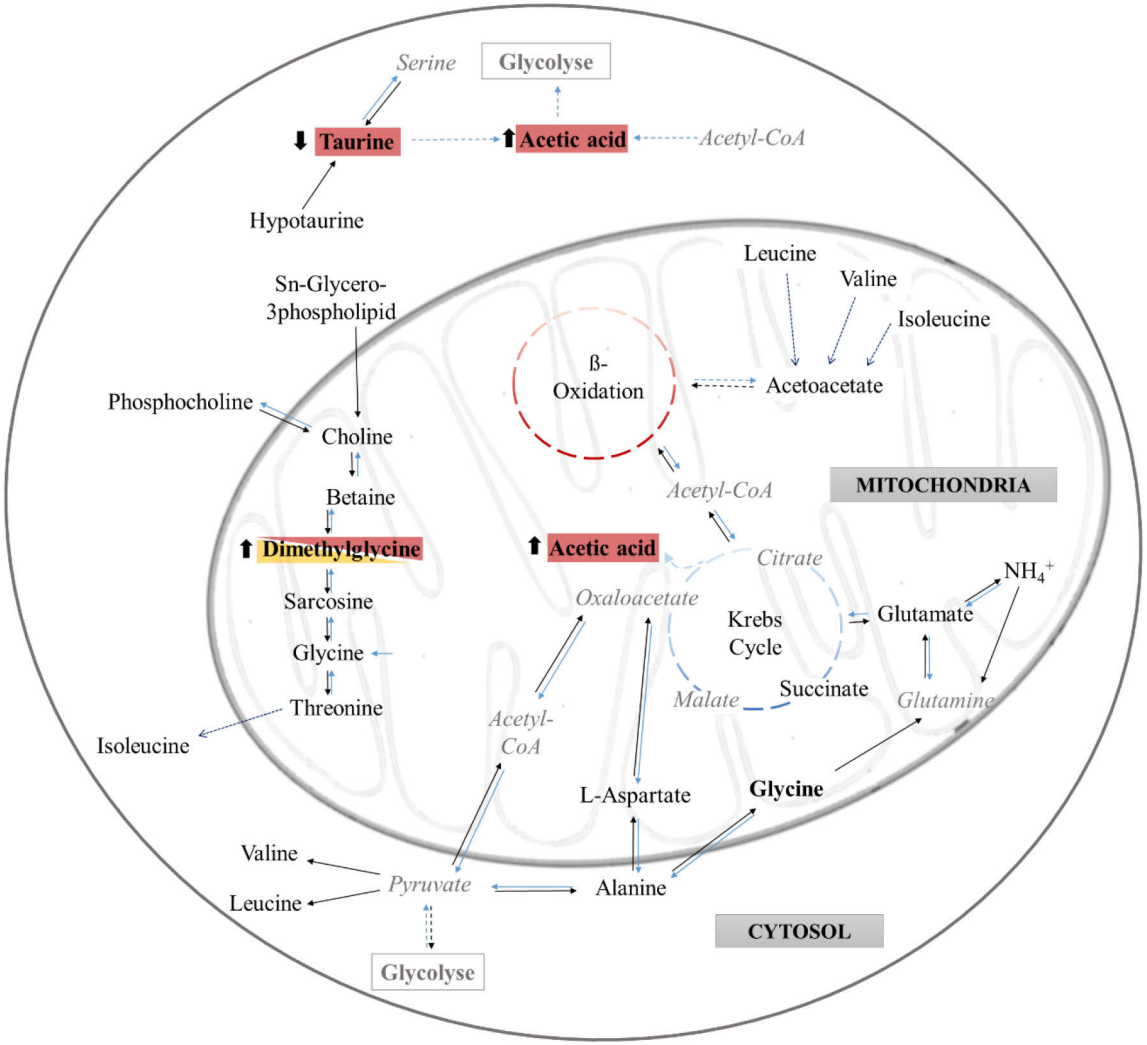

Scheme 1: Assigned metabolites found in gill of *P. maximus* exposed to acute warming. Metabolites in bold indicate significant changes in metabolite levels, while grey and italic metabolites are not assigned intermediates of the pathway. Metabolite names in colored boxes code for the sampling temperature (orange 22 °C and red 26 °C). Arrows indicate an increase (up) or decrease (down) of the respective metabolite concentration

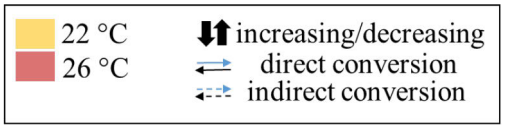

Scheme 2:

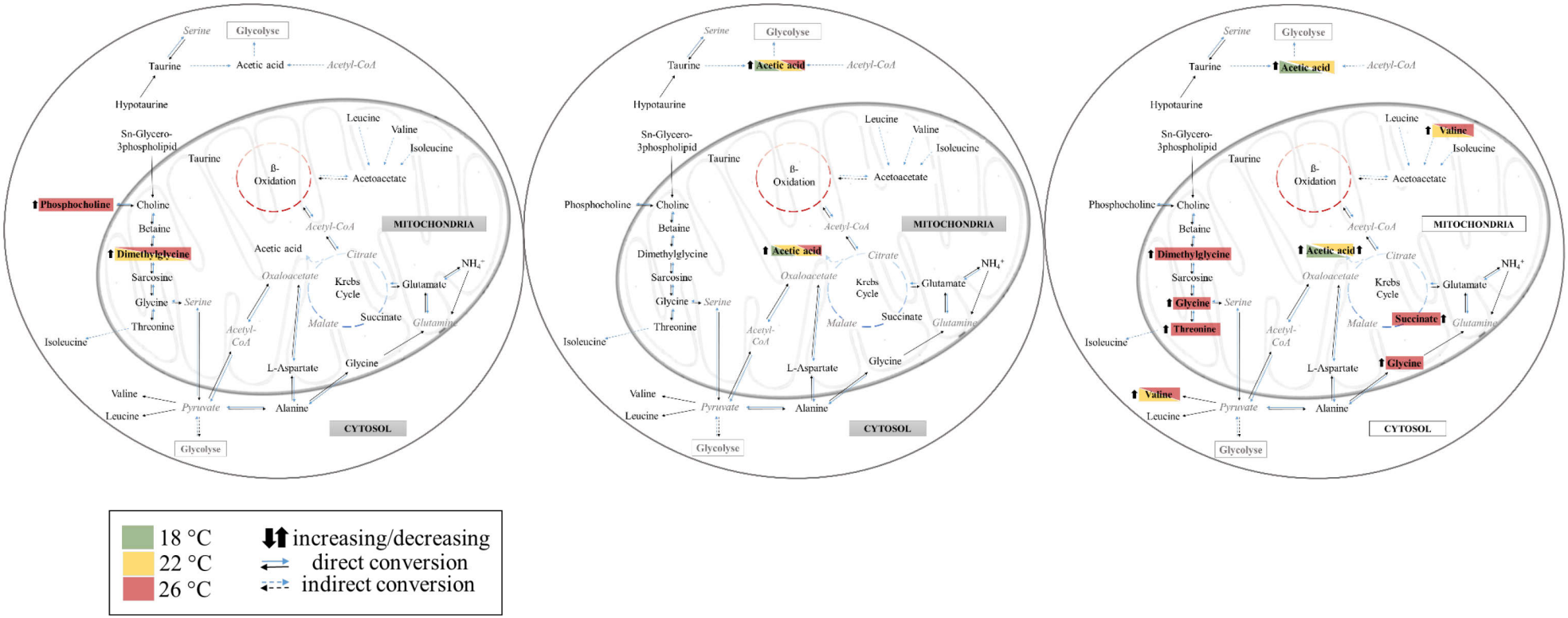

Scheme 2: Assigned branchial metabolites of *P. maximus* exposed to acute WHc (left), WHo (middle), and DT (right). Metabolites in bold indicate significant changes in metabolite levels, while grey and italic metabolites are not assigned intermediates of the pathway. Metabolite names in colored boxes code for the temperature (green 18 °C, orange 22 °C, red 26 °C). Arrows indicate an increase (up) or decrease (down) of the respective metabolite concentration.

Manuscript III

"Effects of climate drivers on cellular damage and stress response of the great scallop *Pecten maximus*"

To be submitted to the *Journal of Experimental Marine Biology and Ecology*

Contribution of the candidate in % of the total workload

Experimental concept and design	50 % *
Experimental work and data acquisition	50 % *
Experimental work and data acquisition for my part	85 %
Data analysis and interpretation	95 %
Preparation of figures and tables	100 %
Drafting the manuscript	95 %

* Shared experiments with C. Eymann

Proposed Journal: Journal of Experimental Marine Biology and Ecology

Effects of climate drivers on cellular damage and stress response of the great scallop *Pecten maximus*

Sandra Götze, Charlotte Eymann, Gisela Lannig, Christian Bock, Hans-Otto Pörtner

Alfred Wegener Institute Helmholtz Centre for Polar and Marine Research
Am Handelshafen 12, 27570 Bremerhaven, Germany

Corresponding author:

Sandra Götze
Alfred Wegener Institute Helmholtz Centre for Polar and Marine Research
Am Handelshafen 12
27515 Bremerhaven, Germany
e-mail: Sandra.goetze@awi.de

Abstract

The cellular stress response provides protection of cellular homeostasis under potentially harmful conditions. In the consensus of marine climate change we investigated the acute effects of warming (W), warming *plus* hypercapnia (WHc), warming *plus* hypoxia (WHo), and combined exposure of all stressors (Deadly Trio, DT) on the cellular stress response in King scallops (*Pecten maximus*). Exposures started at 14 °C and increased every other day until the lethal temperature was reached (28 °C). We analyzed contents of malondialdehyde via thiobarbituric acid as indication for damage of lipids, HSP70, ubiquitin-conjugates as indication for protein damage, and branched-chained amino acids as indication for protein degradation in gill tissue of *P. maximus* at four temperatures (14, 18, 22, and 26 °C). Irrespective of temperature or additional stress no damage of lipids occurred. HSP70 was elevated in gill tissue of scallops exposed to W, WHo, and WHc at 26 °C. Strikingly, HSP70 remained low in scallops exposed to DT throughout the exposure. Levels of ubiquitin-conjugates and branched chain amino acids remained low in scallops exposed to W, WHo, and WHc indicating that scallops were fully able to maintain protein homeostasis. Scallops exposed to DT showed clear signs of protein damage (18 °C and 22°C) followed by peaking levels of BCAAs at 26 °C marking degradation of proteins. The structure of gills was disrupted in scallops sampled under DT at 26 °C. Hence, combined exposure of climate drivers induced protein stress due to protein damage and protein catabolism in *P. maximus*. Parallel the observed failure of the heat-shock response might have led to a disruption (via apoptosis) of gill tissue.

Key Words: Heat shock, protein damage, apoptosis, cellular resilience, thermal tolerance, bivalve

Glossary:

BRAA = Branched chain amino acid; **DT** = Deadly Trio exposure; **ETC** = electron transport chain; **FW** = Fresh weight; **HSR** = Heat shock response; **HSP70** = Heat shock protein 70; **MDA** = Malondialdehyde; NMR = Nuclear magnetic resonance; **SW** = Seawater; **ROS** = reactive oxygen species; **W** = warming exposure; **WHo** = warming exposure *plus* hypoxia; **WHc** = warming exposure *plus* hypercapnia

1. Introduction:

With the industrial revolution that started nearly 200 years ago and the extensive combustion of fossil fuels, global climate is changing drastically and endangers marine and terrestrial ecosystems (Costello et al., 2010; Gattuso et al., 2015; Stanton et al., 2015). When humankind behavior remains unchanged ocean surface temperatures will increase up to 4 °C accompanied by a drop in seawater pH (up to 0.4 pH units) and enlarging occurrence of hypoxic zones until the end of the 21th century (Rhein et al., 2013, RCP 8.5). Species fate will depend on the magnitude and duration of such changes and on their capacity to acclimate. Accordingly, it emerges crucial to understand organisms' physiological responses to such changes. As marine ectotherms cannot regulate their body temperature, the same relies on the surrounding seawater and hence, performance is fundamentally linked to respective temperatures (Hochachka and Somero, 2002; Somero, 2005; Kassahn et al., 2009). Organismic responses to cooling or warming comprises changes in breathing, feeding, and circulation (Frederich and Pörtner, 2000; Braby and Somero, 2006; Xing et al., 2016). Furthermore, alterations in gene expression and metabolic pathways counterbalance cellular damage, provide protection, and ensure maintenance of cellular homeostasis (Hertz, 2012).

One important and intensively studied mechanism for cellular stress is the heat shock response (HSR; e.g. reviewed by Richter et al., 2010). Originally, it was described as cytoprotective measure facilitating protection and repair against heat stress (Lindquist, 1986; Kregel, 2002; Lenz et al., 2018). However, by now it is clear that many more stresses activate the HSR, a.o. exposure to oxidants, viral infections, or heavy metal pollution (e.g. Heckathorn et al., 1999; Piano et al., 2004; Padmini, 2010). Upon activation a transcriptional cascade of heat shock factors is initiated (e.g. HSF-1, Sarge et al., 1993) translocating from the cytoplasm to the nucleus activating HSF-dependent genes. These genes encode for proteins of the heat-shock (HSP) family, which include chaperones that refold misfolded proteins into their native confirmations or targeting their removal (Shi et al., 1998; Feder and Hofmann, 1999; Park et al., 2007). Hence, analysis of HSPs may serve as an indirect measure for protein damage and mark the onset a species becomes (thermally) stressed and has surpassed its thermal optimum range (according to the OCLTT; see Pörtner, 2002; Pörtner et al., 2017). The HSR has been intensively studied throughout all phyla. In marine ectotherms, the induction of HSR correlates with the recent thermal history of the individual (Chapple et al., 1998; Piano et al., 2002, 2004; Anestis et al., 2007; Brun et al., 2008; Fabbri et al., 2008). Season and ambient seawater (SW) temperatures were shown to shift thresholds of HSP induction in various bivalves (Roberts et

al., 1997; Buckley et al., 2001; Hamdoun et al., 2003). For example, in *Mytilus trossolus,* the threshold temperature of HSP induction shifted from 23 °C during winter to 28 °C during summer (Buckley et al., 2001). In the Pacific oyster, *Crassostrea gigas*, induction of HSP69 and HSC72 shifted from 37 °C (winter) to 40 °C (summer) with a positive impact on oysters' survival (shift of lethal temperature from 44 °C to 46 °C; Hamdoun et al., 2003). Furthermore, a study on the Peruvian scallop, *Argopecten purpuratus* reported that the degree of HSP70 expression upon heat stress decreased in mature and spawned individuals compared to immature ones (Brokordt et al., 2015). Both, hypoxia and hypercapnia have been associated to activate or modulate the HSR. While hypoxia has been mainly reported to activate HSP expression (David et al., 2005; Anestis et al., 2010; Brokordt et al., 2015), hypercapnic stress was related to cause opposing responses in dependence of the duration of the exposure and time of sampling (Thompson et al., 2015; Wang et al. 2016; Goncalves et al. 2017; Sokołowski and Brulinska, 2018). For example, Wang and coworkers (2016) exposed adult *C. gigas* for up to 28 days to either normocapnic or hypercapnic conditions (1000 µatm vs. 2000 µatm PCO_2). They found that HSP70 expression was highly upregulated after 7 days but ongoing exposure (14 and 28 days) resulted in a significant down-regulation of HSP70. Another study exposed the Baltic clam, *Limecola balthica*, to SW reduced to a pH of 6.3(Sokołowski and Brulinska, 2018). They stated that HSP70 first increased (after day 14) but then significantly decreased (day 56). Contrary, wild-type Sydney rock oysters (*Saccostrea glomerata*) responded to a four-week exposure to 846-µatm pCO_2 with constantly upregulated HSP70 levels (Thompson et al., 2015).

Among cellular compounds proteins are endangered by many environmental stressors as they can easily become misfolded or denatured (e.g. Davies, 2005). Damaged proteins beyond repair are removed by either lysosomal or proteasomal degradation (Goldberg and Dice, 1974; Ciechanover, 2005). About ~ 90 % of short living cellular proteins are degraded by the ATP/ubiquitin-dependent proteasome pathway, for which proteins must be first labeled with ubiquitin chains (Goldberg, 2003). Accumulation of ubiquitin-conjugated proteins can serve as direct measure for intracellular (irreversible) protein damage. However, protein turnover bears a considerable cost as synthesis and degradation demand a high share of energy (Hawkins, 1991; Carter and Houlihan, 2001). Some studies stated that protein damage in response to environmental stress affects an organisms' energetic balance and dimishs growth, reproduction and ultimately limits geographical distribution, as more energy has to be spent for maintaining protein homeostasis (Hofmann and Somero, 1995, 1996; Dutton and Hofmann, 2008, 2009).

Indeed, ubiquitination pattern in intertidal and subtidal mussels of the genus Mytilus were linked to season (as HSP70) and distribution (Hofmann and Somero, 1995). The study showed that ubiquitin-conjugates accumulated during summer while levels remained low during winter. Furthermore, during summer, levels of ubiquitin-conjugates were higher in intertidal mussels than in subtidal mussels. In a later study, the authors compared *M. trossolus* (cold adapted) from Bodega Bay (California) to the in this area invading mussel *M. galloprovincialis* (warm adapted; Dutton and Hofmann, 2008). Analysis revealed that *M. trossolus* experienced environmental stress during summer while *M. galloprovincialis* experienced stress only during winter. The authors stated that their findings mirror the distribution limits of both species as Bodega Bay is the southern edge of distribution for *M. trossolus* and the northern range edge of the distribution of *M. galloprovincialis*.

Furthermore, climate drivers can induce oxidative stress in marine invertebrates (Chandel et al., 2000; Dean, 2010; Tomanek et al., 2011). Elevated levels of CO_2 affect the mitochondrial electron transport chain (ETC) potentially leading to electron leakage releasing reactive oxygen species (ROS; Murphy, 2009; Tomanek et al., 2011). ROS randomly damage cellular components such as lipids, proteins, or DNA impairing the cellular homeostasis and may even lead to apoptosis if not counterbalanced by antioxidant defense (Hensley et al., 2000; Finkel and Holbrook, 2000; Strobel et al., 2013; Valles-Regino et al., 2015). Accordingly, it is not surprising that hypercapnic exposure (2 weeks to SW pH of 7.5) was shown to upregulate several proteins (such as peroxiredoxins) involved in antioxidant defense in *Crassostrea virginica* (Tomanek et al., 2011).

In the consensus of the bigger DFG-granted research project TERSANE (Temperature-related stresses as a unifying principle in ancient extinctions), we studied single and combined effects of climate stresses (warming, hypoxia, and hypercapnia) on the King scallop *Pecten maximus.* For an integrative approach, we performed parallel investigations of organismic, metabolic and cellular parameters that were divided to three studies with different emphases (Götze et al. submitted; Eymann et al. unpublished). In the present study, we assessed cellular stress by using in particular biomarkers for protein and lipid damage and heat shock response. Together with metabolic and organismic data, the results will help to understand better physiological and cellular constraints of King scallops in the course of future climate change. Furthermore, this knowledge will also help to understand why Pectinida suffered more (compared to other bivalve taxa) during some past marine extinction events such as during the Permian-Triassic transition ~252 million years ago (as suggested e.g. by Tu et al., 2016).

2. Material and Methods:

2.1 Animals

SCUBA divers of the Biological Station of Toralla (ECIMAT, University of Vigo) caught adult King scallops (Pecten maximus) in the estuary of Vigo (Spain, ~42°14'46.6"N 8°44'18.5"W) in autumn 2017. Water parameters at time of capture were ~18 °C at full salinity. Scallops were transported submerged (in aerated water at 10 °C) within 24 h to the Alfred Wegener Institute Helmholtz Centre for Polar and Marine Research (AWI, Bremerhaven, Germany). Upon arrival, scallops were introduced to the institutional aquarium systems and acclimated to 14 °C and full salinity for a minimum of 4 weeks. Scallops had an average size of 10.4 ±1.1cm in length, 10.8 ± 1.3 cm in width, and weighted 163.4 ± 46.0 g.

2.2 Experimental setup and tissue sampling

Gill tissue samples of *P. maximus* used in the present study derived from scallops sampled in experiments run and described in Götze et al. (submitted). Briefly, scallops were distributed to four experimental setups: warming under normoxia and normocapnia (control; W), warming *plus* hypoxia and normocapnia (WHo), warming *plus* hypercapnia and normoxia (WHc), and warming under a combined exposure of both stresses (deadly trio, DT). In normoxic exposure seawater was kept fully oxygenated (> 90 % P_{O_2}) and in the hypoxic exposures the oxygen content was reduced to 55-60 % P_{O_2}. In the normocapnic exposures CO_2 was held as low as possible (400 –600 ppm) and was increased in WHc and DT to 1800 ppm CO_2. Exposures started at 14 °C and the temperature was increased once 2 °C every 48 h until all scallops died. The lethal temperature was reached in W, WHc, and DT at 28 °C. Under WHo, 13 out of 17 residual scallops died at the transition of 24 °C to 26 °C leaving only four scallops alive which were then sampled. Tissue samples (gill, mantle, phasic and tonic muscle) were taken at 14 °C, 18 °C, 22 °C and 26 °C and shock frozen in liquid nitrogen (n per temperature = 6, except WHo at 26 °C where n = 4).

2.3 Lipid peroxidation

Malondialdehyde (MDA) was measured as marker for lipid peroxidation using a thiobarbituric acid test developed by Uchiyama and Mihara (1978) and modified after Abele et al. (2002). Briefly, ~ 75 mg of gill tissue was homogenized with Precellys 24 (Bertin Technologies, France; 2x 15 s at 5.000 rpm and 4 °C) in 0.2 % phosphoric acid (1:5 ratio, wet tissue to acid volume). After homogenization, phosphoric acid (2 %) was added to a final concentration of 1.1 %. Each sample was divided into two (200 µl each); one subsample was supplemented with

thiobarbituric acid (TBA; 1% TBA in 50 mM NaOH) and the other one with the equal volume of HCl (3 mM). All samples were adjusted to a pH of 1.6 using pH paper before the homogenates were incubated for 60 min at 100 °C using a water bath. Thereafter, 1 ml pure Butanol was added, vortexed (40 sec) and centrifuged for 5 min at 1000 g at room temperature (RT). The upper phase was collected and centrifuged again for another 5 min at 14 000 g. The supernatant was measured in triplicates at 530 nm in a microplate reader (Berthold). The absorbance was quantified by a standard series using Malondialdehyde-bis-acetate. Levels of MDA were expressed in nmol per g wet weight (ww) gill tissue.

2.4 SDS-PAGE and Western Blotting

Gill tissues were extracted in the 5-fold volume of ice-cold homogenization buffer (10 mM Tris-HCL, 10 mM KCL, 1.5 mM $MgCl_2$, 0.5 mM PMSF, 1 mM Na_3VO_4, and 5 µg/ml full protease inhibitor mix (Sigma, P8340)) with Precellys 24 (Bertin Technologies, France). Homogenization was performed for 20 s at 6000 rpm and 4 °C. Homogenates were centrifuged afterwards (15 min, 13000 g, 4 °C). The soluble protein concentration was determined after Bradford (1976) using bovine serum albumin (BSA) as standard. All samples were diluted with SDS-loading buffer containing 2.5 % ß-mercaptoethanol to a final concentration of one µg protein per µl. samples were heat-denatured for 10 min at 95 °C according to Laemmli (1970). Always, 10-µg protein per sample were randomly applied to 10 % (weight (w)/volume (vol) acrylamide gels and run at 200 V for ~ 45 min using Biorad Mini-Protean chambers. Furthermore, each gel contained a protein marker and a reference sample for quantification across gels. After electrophoresis proteins were transferred on polyvinylidene difluoride (PVDF) membranes using Mini Trans-Blot® Cell systems (BioRad) filled with ice-cold transfer buffer (25 mM Tris, 192 mM Glycine, 20 % pure Methanol) according to the manufacturer's guidelines (2h at 200 mA per system).

2.5 Immunodetection

Unspecific binding sites on the membranes were blocked for 1 h at RT using 5 % (w/vol)) nonfat milk in TBST (20 mM Tris-HCL (pH 7.5), 137 mM NaCl, 0.1 % Tween-20 (vol/vol)). Antibodies for HSP70 (1:5000, MA3-006; Thermo Fisher Scientific) and ubiquitin (1:2000, P4D1, Enzo Life Sciences) were used in 5 % nonfat milk in TBST and prepared freshly before use. Membranes were incubated overnight at 4 °C in the respective antibody solution. Membranes were washed thoroughly with TBST buffer and incubated for 2 h at RT in anti-mouse secondary antibody coupled to horseradish-peroxidase (1:40000, NA931V, GE

Healthcare, Munich, Germany). Chemiluminescence was detected by ECL solution (GE Healthcare, Munich, Germany) using a cooled charge-coupled image reader (Fujifilm Intelligent dark box LAS 1000). Calculation of the signal intensity (given as arbitrary units = LAU) was done using the AIDA Image Analyzer v. 3.52 (Raytest, Straubenhardt, Germany) software. The HSP70 antibody detects several members of the heat shock protein 70-kDa family. We detected two isoforms (~ 69-70 kDa range) in gill samples of *P. maximus* and hence intensities of both were taken together for quantification. The ubiquitin antibody detects ubiquitin-conjugates of any protein size resulting in a typical binding smear on the blot. In this case, the intensity of the whole lane was used. All intensities were normalized against the reference sample run on all gels.

2.6 Untargeted ^{1}H metabolic profiling

Soluble metabolites were extracted and analyzed as described in (Götze et al., submitted). Briefly, metabolites were gained from gill tissue using a chloroform-methanol extraction protocol for small quantities originally described by Wu and coworkers (2008). Dried metabolites were suspended in deuterized water including an internal standard (D_2O; 2fold volume related to applied fresh weight in mg). One dimensional ^{1}H-NMR spectroscopy was carried out in an ultra-shielded vertical 9.4 T NMR spectrometer (Advance III HD 400 WB, Bruker-BioSpin GmbH, Germany) connected to a triple tuned ^{1}H-^{13}C-^{31}P-HRMAS NMR probe. The Call-Purcell-Meiboom-Gill (CPMG) sequence was used for metabolic profiling (described in detail in Schmidt et al., 2017). Correction and normalization of each spectra was done using Chenomx NMR suite 8.1 (Chenomx Inc., Canada). Metabolites were assigned to their NMR signals and quantification by the integration routine within Chenomx. The concentrations of the branched chain amino acids (BRAA) valine, leucine and isoleucine were totaled up and normalized against the sum of adenylates as these signals were not clearly distinguishable (AMP, ADP, ATP).

2.7 Statistical Analysis

Data sets of MDA, HSP70, ubiquitin-conjugates and BRAAs were plotted as mean values ± SD and analyzed by Sigma Plot (12.0, Systat Software, Inc.) For temperature, and or stress related effects between the groups a two-way analysis of variance (ANOVA) followed by a post-hoc test (Tukey) was done. Significant differences between groups were considered to be true when the p-value was below 0.05. In the rare case that the Shapiro-Wilk test for

normality failed, ANOVA on ranks (Kruskal-Wallis) was performed followed by a post-hoc test (Dunn's method).

3. Results:

3.1 Malondialdehyde (MDA)

The mean branchial concentrations of MDA are illustrated in **Fig 1**. Scallops sampled in the warming group had on average 423 ± 103 nmol˙g^{-1} FW MDA at 14 °C. However, as concentrations were highest in scallops sampled at 18 °C (568 ± 140 nmol˙g^{-1} FW) these were statistical different from those measured at 26 °C (327 ± 57 nmol˙g^{-1} FW at 26 °C; $p = 0.006$) but not yet from levels measured at 14 °C and 22 °C (429 ± 90 nmol˙g^{-1} FW). In WHo, MDA remained constant until a temperature of 22 °C (364 ± 78 nmol˙g^{-1} FW). Levels at 26 °C were with 173 ± 50 nmol ˙g^{-1} FW significantly lower ($p < 0.041$). Under WHc, MDA remained constant until 18 °C (377 ± 80 nmol ˙g^{-1} FW) and decreased thereafter as well. MDA was significantly lower at 26 °C (252 ± 144 nmol ˙g^{-1} FW) compared to levels measured at 14 °C and 18 °C ($p < 0.016$). No temperature-induced changes in MDA levels were detected in gill tissue of scallops exposed to DT ($p = 0.052$).

Comparing exposures revealed that scallops exposed to WHo (331 ± 138 nmol˙g-1 FW), WHc (359 ± 119 nmol˙g-1 FW), or DT (414 ± 64 nmol˙g-1 FW) had similar levels of MDA as those measured under W alone (at 14 °C; $p = 0.451$). Exposure had no effect on MDA when scallops were sampled 18 °C ($p = 0.081$) but levels were significantly lower in scallops exposed to WHc than scallops exposed to W at 22 °C ($p = 0.016$). In gill tissue of scallops exposed to WHo, WHc and DT MDA was significantly lower than in scallops sampled at this temperature under warming alone (26 °C, $p < 0.035$).

3.2 HSP70

The normalized branchial levels of HSP70 are shown in **Fig 2**. In gills of scallops sampled at 14 °C (W) HSP70 accounted to 1131 ± 438 LAU. Warming to 18 °C did not alter HSP70 levels. Further warming increased HSP70 to 1839 ± 1296 LAU (at 22 °C) and levels reached highest values at 26 °C (2659 ± 1566 LAU; significant different from values determined at 14 °C and 18 °C with $p = 0.034$ and $p = 0.048$ respectively). In gill tissue of scallops exposed to either WHo (1719 ± 165 LAU) or WHc (1685 ±356 LAU) levels of HSP70 remained low until 22 °C and increased thereafter (3350 ± 850 LAU in WHo and 2866 ± 792 LAU in WHc at 26 °C, p for both < 0.001). In contrast, levels of HSP70 were not altered at any temperature when scallops were exposed to DT ($p = 0.260$). Exposure did not affect HSP70

when scallops were sampled at 14 °C ($p = 0.907$) and 22 °C ($p = 0.907$ and $p = 0.161$). At 18 °C, scallops exposed to WHc had significantly higher levels of HSP than scallops exposed to DT ($p = 0.008$). Scallops exposed to DT at 26 °C had significantly lower HSP70 values than those scallops exposed to WHo ($p = 0.037$) and WHc ($p = 0.033$) but not from those exposed to W ($p = 0.065$).

3.3 Ubiquitin-conjugates and AS backbone

The normalized levels of ubiquitin-conjugates are depicted in **Fig 3 panel A**. Levels accounted to 11325 ± 3145 LAU in scallops sampled at 14 °C (W). Further warming until 22 °C slightly lowered levels of ubiquitin-conjugates (9744 ± 1508 LAU at 22 °C, not yet statistical significant). Because of this, ubiquitin-conjugates from scallops sampled taken at 26 °C (14861 ± 1807 LAU) were significantly different to values of scallops sampled at 18 °C ($p = 0.014$) and 22 °C ($p = 0.008$), but not to values of scallops sampled at 14 °C ($p = 0.117$). WHo caused a slight but steady increase of ubiquitin-conjugates from 9069 ± 1796 LAU (14 °C) to 14503 ± 1686 LAU (26 °C, significant different from 14 °C, $p < 0.05$, ANOVA on ranks). A similar effect was found in scallops exposed to WHc. Ubiquitin conjugates increased from 9272 ± 1031 LAU at 14 °C to 13368 ± 2587 LAU at 26 °C (significant different from 14 °C, $p = 0.025$). In DT exposed scallops levels of ubiquitin-conjugated accounted to 14726 ± 2868 LAU (14 °C). A temperature increase to 18 °C caused a drastic increase of ubiquitinated proteins (34939 ± 10565 LAU, $p < 0.001$). With further warming levels decreased again reaching finally initial values at 26 °C (13336 ± 2710 LAU). At 14°C scallops exposed to WHo or WHc had significantly lower levels of ubiquitinated proteins compared to scallops exposed to warming alone or the deadly trio (p-value for WHo and WHc to DT below 0.016). At intermediate temperatures (18 °C and 22 °C), the amount of ubiquitin-conjugates was significantly higher in DT than W exposed scallops (p- value of all < 0.001). However, at 26 °C the groups were not significantly different from each other ($p = 0.559$).

Panel **B** illustrates the pool of free amino acids leucine (Leu), isoleucine (Ile) and valine (Val) measured by ^{1}H NMR spectroscopy. The amino acid backbone pool remained constant in scallops exposed to either W, WHo, or WHc at all temperatures ($p = 0.420$, $p = 0.347$, $p = 0.191$). In scallops exposed to DT, levels accounted to 0.484 ± 0.17 mM at 14 °C and remained the same when scallops were sampled at 18 °C. Thereafter, levels increased to 1.110 ± 0.29 mM at 26 °C (value significantly different from values measured at 14 °C and 18 °C with $p = 0.002$ for both).

4. Discussion:

We investigated effects of single and combined stresses (warming, hypoxia and hypercapnia) on cellular compounds associated to damage and stress in *P. maximus*.. None of the stresses caused damage of lipids. However, protein damage occurred in scallops challenged to DT (at 18 °C and 22 °C) finally resulting in an elevated pool of branched chained amino acids indicating protein degradation (at 26 °C). Our findings indicate that the heat stress response (HSR) is strictly driven by temperature, but not by additional (single) stress such as hypoxia or hypercapnia as the onset of HSP70 occurred in all three exposure groups (W, WHo, WHc) at the same temperature (26 °C). Strikingly, HSP70 remained constantly low throughout all temperatures in scallops exposed to DT. In the following section, we will discuss findings of the current study also referring to knowledge obtained in both parallel studies which focused on organismic and metabolic changes (Eymann personal comments; Götze et al., submitted).

4.1 Thermal stress

In marine ectotherms, induction of HSP70 is closely related to the organism's thermal history, and thus, depends on season and habitat (Roberts et al., 1997; Buckley et al., 2001; Hamdoun et al., 2003; Brun et al., 2008; Tomanek, 2008). Furthermore, the magnitude of induction is correlated to geographical distribution and life status of the respective species (Hofmann and Somero, 1996; Brun et al., 2008; Brokordt et al., 2015). For example, activation of HSR differed between *Mytilus trossolus* and *Mytilus galloprovincialis* in accordance with both species distribution (Hofmann and Somero, 1996). HSP was induced at lower temperatures (23 °C vs. 25 °C) and with a smaller magnitude in the northerly-distributed *M. trossolus* compared to the more southerly-distributed *M. galloprovincialis*. Furthermore, a comparative study on *Placopecten magellanicus* (adapted to colder and deeper waters) and *Argopecten irradians* (inhabits shallow subtidal areas with considerable fluctuations; Brun et al., 2008) showed that the magnitude of HSP70 expression was more rapid and pronounced in *A. irradians* than in *P. magellanicus.* These findings indicate that species adapted to more stressful (intertidal) or warmer habitats (tropic) tent to react with more pronounced HSR to protect themselves than species adapted to more stable and colder habitats. Indeed, Tomanek described that commonly subtidal bivalves induce HSPs only above temperatures they experience in their habitat while intertidal species, such as mussels or oysters, increase levels of HSPs already at temperatures within the thermal range they experience(2008). Intertidal bivalves are believed to meet exaggerated denaturation of proteins during low tide by enhanced induction of HSR (Hofmann, 2005).

King scallops used in the present study were caught in the estuary of Vigo (Spain) which is an area providing protected habitats due to its coastline characteristics and the islands near the estuary. Hence, this population of *Pecten maximus* experiences relatively stable environmental conditions throughout the year with SW surface temperatures between 16 °C - 21 °C during summer and minimum temperatures around 10-11 °C during winter (Pazos et al., 1997; www.seatemperature.org). In line with the findings of Tomanek, HSP70 remained low in gill tissue of *P. maximus* as long as scallops were exposed to temperatures within their environmental thermal range (14 °C – 22 °C) indicating that no thermal stress was induced (W). However, when temperatures exceeded the thermal habitat range of *P. maximus* (26 °C), gills upregulated HSP70 in response to the heat stress. Still, neither lipids nor proteins were damaged indicating that the cellular homeostasis was kept balanced at any temperature (W; **see scheme 1A**). Nevertheless, oxygen consumption and filtration rates ceased from 24 °C on (C. Eymann pers. communication) clearly indicating that *P. maximus* has surpassed its thermal optimum (according to the OCLTT, see Pörtner, 2002; Pörtner et al., 2017). This is supported by the findings of Artigaud and coworkers who found that in temperate King scallops from France respiration rates decreased coincidently to an onset of anaerobiosis at 25 °C (Artigaud et al., 2014). Moreover, this group also investigated gene expression pattern and found that the expression of three HSP genes (HSP40, HSP70, and HSP90) remained low until 21 °C but that all were upregulated at 25 °C (long-term exposure; Artigaud et al., 2015). Based on their data, the authors concluded that 23 °C is the upper thermal optimum temperature for *P. maximus*. Investigations of the branchial metabolism done in an earlier study by our group showed that gills of *P. maximus* shifted to anaerobiosis at 26 °C (significant increase of acetic acid). This supports the suggestion that 26 °C reflects a critical temperature and that the thermal optimum has been surpassed (see above; Götze et al., submitted).

4.2 Thermal stress *plus* hypoxia or hypercapnia

We exposed King scallops additionally to either hypoxia or hypercapnia and found that neither exposure altered the temperature threshold for HSR as in both HSP70 was not elevated beneath 26 °C (as in W, **see scheme 1A**). Adequately, levels of ubiquitin-conjugates and the free content of the three branched chain amino acids (BRAAs) did not show another pattern than overserved in the warming exposure. BRAAs are essential and derive either from the diet or from protein catabolism (Tom and Nair, 2006; Calder, 2006). At critical temperatures where feeding is minimal accumulation of free cytosolic BRAAs can only derive from proteins and hence this may serve as marker for protein catabolism (as happened under DT, see below).

MDA was found to be significantly lower in scallops exposed to WHo (at 26 °C) and WHc (at 22 °C and 26 °C). So far, studies which investigated oxidative damage of lipids in response to climate drivers either reported about an induction of oxidative stress and hence increasing levels of damaged lipids (e.g. Woo et al., 2013; Sui et al., 2017; Liao et al., 2019) or that no such stress was induced and MDA relevels remained constant (e.g. Sussarellu et al., 2012; Matoo et al., 2013). Why levels of MDA were found to be decreased in the present study remain unclear and demand further research.

Organismic responses, metabolic changes, and survival data clearly indicated that scallops were thermally stressed at lower temperatures under WHo or WHc than under W alone. Furthermore, both exposures lowered the upper thermal tolerance. Impairments became visible as feeding rates declined earlier than under W (at 18 °C in WHo and 20 °C in WHc compared to 21 °C in W; C. Eymann pers. comm.). Simultaneously more scallops died within the environmental relevant thermal range (LC_{50} in both, WHo and WHc, at 24 °C instead of 25 °C in W). Under WHo, gills shifted to anaerobic metabolism indicated by significant accumulations of acetic acid already from 18 °C on (Götze et al., submitted). Accordingly, maintenance of cellular components even at critical temperatures is especially remarkable. However, maintenance of cellular homeostasis likely comes for the sake of exaggerated energy expenses to facilitate the energetic costly counterbalancing processes especially at high temperatures (*Q10*; Carter and Houlihan, 2001). However, the exact mechanisms remain unclear and demand further research.

4.3 Deadly Trio

Exposure of *P. maximus* to DT revealed most striking results. The accumulation of irreversible damaged proteins at 18 °C and 22 °C clearly indicated branchial protein stress which led (with a time lag) to elevated levels of free branched chained amino acids due to protein catabolism at 26 °C (**see scheme 1B**). However, it seems unreasonable that such a pronounced protein damage which occurred at 18 °C did not induce a heat shock response. We know from cell culture experiments that inhibition of the proteasome and hence, accumulation of ubiquitinated proteins does trigger HSP expression and induce thermotolerance (Meriin et al., 1998; Liao et al., 2006; Young and Heikkila, 2010). The striking absence of HSP70 upregulation observed in DT exposed scallops might have various explanations, however, all are speculative and thus demand further research. One aspect might be the huge energetic costs for maintaining protein homeostasis as all processes from protein biosynthesis over heat-shock response to degradation by the proteasome consume ATP (Carter and Houlihan et al., 2001;

Cherkasov et al., 2006; Goldberg, 2003). However, neither organismic nor metabolic findings indicate that at 18 °C scallops suffer from such a dramatically impaired energy metabolism that they cannot afford HSR at all (C. Eymann pers. comm.; Götze et al., submitted). King scallops exposed to DT were able to regulate their oxygen consumption until 20 °C where the break point was reached and oxygen consumption could not be maintained (C. Eymann pers. comm.). Furthermore, metabolic data displayed only minor alterations in energetic pathways e.g. the accumulation of glycine (can be used for glycolysis) and acetic acid (anaerobic end product; both at 18 °C). Accordingly, it seems not very likely, that energetic limitation is the only explanation for the observed lack of HSR. High levels of damaged and ubiquitinated proteins negatively affect cellular homeostasis, cause stress at the endoplasmic reticulum and potentially induce apoptosis (reviewed by Orlowski 1999; Puthalakath et al., 2007). However, a study published by Strahl and Abele in 2010, suggested that active scallops minimize cellular stress and damage by enhanced cell turnover rather than by extended cellular defense or repair. They investigated cell proliferation, apoptosis rates and antioxidant defense mechanisms in the related queen scallop *Aequipecten opercularis* and the ocean quahog, *Arctica islandica*. The authors showed that *A. opercularis*, in contrast to *A. islandica*, counterbalanced reduced antioxidant defense mechanisms (measured by activity of the superoxide dismutase) by high cell proliferation and apoptosis rates. Based on these findings, one can speculate that King scallops exposed to DT in the current study eliminated the observed protein damage at 18-22 °C by enhanced rates of cell turnover extended cellular defense or repair mechanisms. Although we have not measured apoptosis, we did observe a drastic destruction in gill tissue of scallops exposed to 26 °C and DT (**Fig. 4A and B**). Such degradation of the gills was not observed in *P. maximus* exposed to W, WHo, or WHc. The observed gill destruction therefore hints to ongoing apoptosis and furthermore, that cell proliferation was disrupted as well. Therefore, it seems mandatory to analyze apoptosis marker such as caspase-3 (Porter and Jänicke, 1999) and cell turnover to better understand the the current findings of *P. maximus* under DT.

Funding:

The study was funded by the Deutsche Forschungsgemeinschaft (Po278/16-1) and is part of the Research Unit TERSANE (FO 2332).

Acknowledgments:

We thank Anette Tillman and Timo Hirse for the analysis of water quality and concentrations of dissolved inorganic carbon. We thank Lea Philipps, Lennard Klingenforth, and Jennifer Steffen for technical assistance of laboratory work. Finally, we thank the Biological station of Toralla (ECIMAT, Spain), in particular A. Villanueva and D. Costas for support in animal supply and F. Feliz Moraleda for transportation of scallops to the AWI.

References

Abele, D., Heise, K., Pörtner, H.O., Puntarulo, S. 2002. Temperature-dependence of mitochondrial function and production of reactive oxygen species in the intertidal mud clam *Mya arenaria*. J. Exp. Biol. 13, 1831-1841.

Anestis, A., Lazou, A., Pörtner, H.-O., Michaelidis, B. 2007. Behavioural, metabolic, and molecular stress responses of marine bivalve *Mytilus galloprovincialis* during long-term acclimation at increasing ambient temperature. Am. J. Physiol. Regul. Integr. Comp. Physiol. 293, R911-R921, https://doi.org/10.1152/ajpregu.00124.2007.

Anestis, A., Pörtner, H.-O., Michaelidis, B. 2010. Anaerobic metabolic patterns related to stress responses in hypoxia exposed mussels *Mytilus galloprovincialis*. J. Exp. Mar. Biol. Ecol. 394, 123-133, https://doi.org/10.1016/j.jembe.2010.08.008.

Artigaud, S., Lacroic, C., Pichereau, V., Flye-Sainte-Marie, J., 2014. Respiratory response to combined heat and hypoxia in the marine bivalves *Pecten maximus* and *Mytilus spp.* Comp. Biochem. Physiol. Part A 175, 135-140. https://doi.org/10.1016/j.cbpa.2014.06.005.

Artigaud, S., Richard, J., Thorne, M.AS., Lavaud, R., Flye-Sainte-Marie, J., Jean, F., Peck, L.S., Clark, M.S., Pichereau, V. 2015. Deciphering the molecular adaption of the king scallop (*Pecten maximus*) to heat stress using transcriptomics and proteomics. BMC Genomics 16, 988. https://doi.org/10.1186/s12864-015-2132-x.

Braby, C.E. and Somero, G.N. 2006. Following the heart: temperature and salinity effects on heart rate in native and invasive species of blue mussels (genus *Mytilus*). J. Exp. Biol. 209, 2554-2566, https://doi.org/10.1242/jeb.02259.

Bradford, M.M. 1976. A rapid and sensitive method for the quantification of micro-gram quantities of protein utilizing the principle of protein-dye binding. Anal. Chem. 72, 248–254. https://doi.org/10.1016/0003-2697(76)90527-3.

Brokordt, K., Pérez, H., Herrera, C., Gallardo, A. 2015. Reproduction reduces HSP70 expression capacity in *Argopecten purpuratus* scallops subject to hypoxia and heat stress. Aquatic Biol. 23, 265-274. https://doi.org/10.3354/ab00626.

Brun, N.T., Bricelj, M., MacRae, T.H., Ross, N.W. 2008. Heat shock protein responses in thermally stressed bay scallops, *Argopecten irradians* and sea scallops, *Placopecten magellanicus*. J. Exp. Mar. Biol. Ecol. 358, 151–162, https://doi.org/10.1016/j.jembe.2008.02.006.

Buckley, B.A., Owen, M.E., Hofmann, G.E. 2001. Adjusting the thermostat: the threshold induction temperature for the heat-shock response in intertidal mussels (genus Mytilus) changes as a function of thermal history. J. Exp. Biol. 204, 3571-3579.

Calder, P.C. (2006). Branched-chain amino acids and immunity. J Nut 136, 288S-293S.

Carter, C.G. and Houlihan, D.F. 2001. Protein synthesis. Fish Physiol. 20, 31-75. https://doi.org/10.1016/S1546-5098(01)20003-X.

Chapple, J.P., Smerdon, G.R., Berry, R.J., Hawkins, A.J.S. (1998). Seasonal changes in stress-70 protein levels reflect thermal tolerance in the marine bivalve *Mytilus edulis* L. J. Exp. Mar. Biol. Ecol. 229, 53-68, https://doi.org/10.1016/S0022-0981(98)00040-9.

Cherkasov, A.S., Biswas, P.K., Ridings, D.M., Ringwood, A.H., Sokolova, I.S. 2006. Effects of acclimation temperature and cadmium exposure on cellular energy budgets in the marine mollusk *Crassostrea virginica:* linking cellular and mitochondrial responses. J. Exp. Biol. 209, 1274-1284. https://doi.org/10.1242/jeb.02093.

Ciechanover, A. 2005. Proteolysis: from the lysosome to ubiquitin and the proteasome. Nat. Rev. Mol. Cell. Biol. 6, 79-86, https://doi.org/10.1038/nrm1552.

Chandel, N.S., McClintock, D.S., Feliciano, C.E., Wood, T.M., Melendez, J.A., Rodriguez, A.M., Schumacker, P.T. 2000. Reactive oxygen species generated at mitochondrial complex III stabilize hypoxia-inducible factor 1α during hypoxia. J. Biol. Chem. 275, 25130-25138, https://doi.org/10.1074/jbc.M001914200.

Costello, M.J., Coll, M., Danovaro, R., Halpin, P., Ojaveer, H., Miloslavich, P. 2010. A census of marine biodiversity knowledge, resources, and future challenges. PLosOne 5, e12110, https://doi.org/10.1371/journal.pone.0012110.

David, E., Tanguy, A., Pichavant, K., Moraga, D. 2005. Response of the Pacific oyster Crassostrea gigas to hypoxia exposure under experimental conditions. FEBS J. 272, 5635-5652, https://doi.org/10.1111/j.1742-4658.2005.04960.x.

Davies, M.J. 2005. The oxidative environment and protein damage. Biochim. Biophys. Acta, 1703, 93-109, https://doi.org/10.1016/j.bbapap.2004.08.007.

Dean, J.B. 2010. Hypercapnia causes cellular oxidation and nitrosation in addition to acidosis: implications for CO_2 chemoreceptor function and dysfunction. J. Appl. Physiol. 108, 1786-1795, https://doi.org/10.1152/japplphysiol.01337.2009.

Dutton. J.M. and Hofmann, G.E. 2008. Spatial and temporal variation in distribution and protein ubiquitination for *Mytilus* congeners in the California hybrid zone. Mar. Biol. 154, 1067-1075, https://doi.org/10.1007/s00227-008-1000-5.

Dutton. J.M. and Hofmann, G.E. 2009. Biogeographic variation in *Mytilus galloprovincialis* heat shock gene expression across the eastern Pacific range. J. Exp. Mar. Biol. Ecol. 376, 37-42, https://doi.org/10.1016/j.jembe.2009.06.001.

Fabbri, E., Valbonesi, P., Franzellitti, S. 2008. HSP expression in bivalves. Inf. Syst. 5, 135-161.

Feder, M.E. and Hofmann, G.E. 1999. Heat-shock proteins, molecular chaperones, and the stress response: Evolutionary and Ecological Physiology. Annu. Rev. Physiol. 61, 243-283.

Finkel, T., and Holbrook, N.J. 2000. Oxidants, oxidative stress and the biology of ageing. Nature 408, 239-247, https://doi.org/10.1038/35041687.

Frederich, M., and Pörtner, H.-O. 2000. Oxygen limitation of thermal tolerance defined by cardiac and ventilatory performance in spider crab, *Maja squinado*. Am. J. Physiol. Regul. Integr. Comp. Physiol. 279, R1531-R1538, https://doi.org/10.1152/ajpregu.2000.279.5.R1531.

Gattuso, J.P., Magnan, A., Bille, R., Cheung, W.W.L., Howes, E.L., Joos, F., Allemand, D., Bopp, L., Cooley, S.R., Eakin, C.M., Hoegh-Guldberg, O., Kelly, R.P., Pörtner, H.O., Rogers, A.D., Baxter, J.M., Laffoley, D., Osborn, D., Rankovie, A., rochette, J., Sumaila, U.R., Treyer, S., Turley, C. 2015. Contrasting futures for ocean and society from different anthropogenic CO_2 emissions scenarios. Science 349, aac4722-1, https://doi.org/10.1126/science.aac4722.

Goldberg, A.L. and Dice, J.F. 1974. Intracellular protein degradation in mammalian and bacterial cells. Annu. Rev. Biochem. 43, 835-869, https://doi.org/10.1146/annurev.bi.43.070174.004155.

Goldberg, A.L. 2003. Protein degradation and protection against misfolded or damaged proteins. Nature 426, 895-899. https://doi.org/10.1038/nature02263.

Goncalves, P., Thompson, Raftos, D.A. 2017. Contrasting impacts of ocean acidification and warming on the molecular responses of CO_2-resilient oysters. BMC Genomics 18, 431, https://doi.org/10.1186/s12864-017-3818-z.

Hamdoun, A.M., Cheney, D.P., Cherr, G.N. 2003. Phenotypic plasticity of HSP70 and HSP70 gene expression in the Pacific oyster (*Crassostrea gigas*): Implications for thermal limits and induction of thermal tolerance. Biol Bull 205, 160-169, https://doi.org/10.2307/1543236.

Hawkins, A.J.S. 1991. Protein turnover: A functional appraisal. Funct. Ecol. 5, 222-233, https://doi.org/10.2307/2389260.

Heckathorn, S.A., Downs, C.A., Coleman, J.S. 1999. Small Heat shock proteins protect electron transport in Chloroplasts and mitochondria during stress. Amer. Zool. 39, 865-876, https://doi.org/10.1093/icb/39.6.865

Hensley, K., Robinson, K.A., Gabbita, S.P., Salsman, S., Floyd, R.A. 2000. Reactive oxygen species, cell signaling, and cell injury. Free Radic. Biol. Med. 28, 1456-1462, https://doi.org/10.1016/S0891-5849(00)00252-5.

Hertz, C. 2012. The unfolded protein response: controlling cell fate decisions under ER stress and beyond. Nat. Rev. Mol. Cell. Biol. 13, 89-102, https://doi.org/10.1038/nrm3270.

Hochachka, P. W., and G. N. Somero. 2002. Biochemical adaptation: Mechanism and process in physiological evolution. Oxford University Press, New York.

Hofmann, G.E. and Somero, G.N. 1995. Evidence for protein damage at environmental temperatures: Seasonal changes in levels of ubiquitin conjugates and HSP70 in the intertidal mussel *Mytilus trossulus*. J. Exp. Biol. 198, 1509-1518.

Hofmann, G.E. and Somero, G.N. 1996. Interspecific variation in thermal denaturation of proteins in the congeneric mussels *Mytilus trossulus* and *M. galloprovincialis*: evidence rom the heat-shock response and protein ubiquitination. Mar. Biol. 126, 65-75, https://doi.org/10.1007/BF00571378.

Hofmann, G.E. 2005. Patterns of HSP gene expression in ectothermic marine organisms on small to large biogeographical scales. Integr. Comp. Biol. 45, 247-255, https://doi.org/10.1093/icb/45.2.247.

Kassahn, K.S., Crozier, R.H., Pörtner, H.O., Caley, M.J. 2009. Animal performance and stress:resonses and tolerance limits at different levels of biological organization. Biol. Rev. 84, 277-292, https://doi.org/10.1111/j.1469-185X.2008.00073.x.

Kregel, K.C. 2002. Molecular biology of thermoregulation: heat shock proteins — modifying factors in physiological stress responses and acquired thermotolerance. J. Appl. Phsiol. 92, 2177–2186, https://doi.org/10.1152/japplphysiol.01267.2001.

Laemmli, U.K. 1970. Cleavage of structural proteins during the assembly of the head of bacteriophage T4. Nature 227, 680-685, https://doi.org/10.1038/227680a0.

Lindquist, S. 1986. The heat-shock response. Ann. Rev. Biochem. 55, 1151-1191, https://doi.org/10.1146/annurev.biochem.55.1.1151.

Lenz, M., Ahmed, Y., Canning-Clode, J., Díaz, E., Eichhorn, S., Fabritzek, A.G., Da Gama, B.A.P., Garcia, M., von Juterzenka, K., Kraufvelin, P., Machura, S., Oberschelp, L., Paiva. F., Penna, M.A., Ribeiro, F.V., Thiel, M., Wohlgemuth, D., Zamani, N.P., Wahl, M. 2018. Heat challenges can enhance population tolerance to thermal stress in mussels: a potential mechanism by which ship transport can increase species invasiveness. Biol. Invasions 20, 3107-3122, https://doi.org/10.1007/s10530-018-1762-8.

Liao, W., Li, X., Mancini, M., Chan, L. 2006. Proteasome inhibition induces differential heat shock protein response but not unfolded protein response in HepG2 cells. J. Cell. Biochem. 99, 1085-1095, https://doi.org/10.1002/jcb.20996.

Liao, H., Yang, Z., Dou, Z., Sun, F., Kou, S., Zhang, Z., Huang, X., Bao, Z. 2019. Impact of ocean acidification on the energy metabolism and antioxidant responses of the yesso scallop (*Patinopecten yessoensis*). Front. Physiol. 9, 1967, https://doi.org/10.3389/fphys.2018.01967.

Matoo, O.B., Ivanina, A.V., Ullstad, C., Beniash, E., Sokolova, I.M. 2013. Interactive effects of elevated temperature and CO_2 levels on metabolism and oxidative stress in two common marine bivalves (*Crassostrea virginica* and *Mercenaria mercenaria*). Comp. Biochem. Physiol. Part A, 545-553, http://dx.doi.org/10.1016/j.cbpa.2012.12.025.

Meriin, A.B., Gabai, V.L., Yaglom, J., Shifrin, V.I., Sherman, M.Y. 1998. Proteasome inhibitors activate stress kinases and induce HSP72. J. Biol. Chem. 273, 6373-6379, https://doi.org/10.1074/jbc.273.11.6373.

Murphy, M.P. 2009. How mitochondria produce reactive oxygen species. Biochem. J. 417, 1-13. https://doi.org/10.1042/BJ20081386.

Orlowski, R.Z. 1999. The role of the ubiquitin-proteasome pathway in apoptosis. Cell Death Differ. 6, 303-313. https://doi.org/10.1038/sj.cdd.4400505.

Padmini E. 2010. Physiological Adaptations of Stressed Fish to Polluted Environments: Role of Heat Shock Proteins. In: Whitacre D. (Eds) Reviews of Environmental Contamination and Toxicology (Continuation of Residue Reviews) 206. Springer, New York, NY.

Park, S.H., Bolender, N., Eisele, F., Kostova, Z., Takeuchi, J., Coffino, P., Wolf, D.H. 2007. The cytoplasmic Hsp70 chaperone machinery subjects misfolded and endoplasmic reticulum import-incompetent proteins to degradation via the Ubiquitin–Proteasome System. Mol. Biol. Cell. 18, 153–165, https://doi.org/10.1091/mbc.e06-04-0338.

Piano, A., Asirelli, C., Caselli, F., Fabbri, E. 2002. HSP70 expression in thermally stressed *Ostrea edulis*, a commercially important oxster in Europe. Cell Stress Chaperones 7, 250-257, https://doi.org/10.1379/1466-1268(2002)007<0250:heitso>2.0.co;2.

Piano, A., Valbonesi, P., Fabbri, E. 2004. Expression of cytoprotective proteins, heat shock protein 70 and metallothioneins, in tissues of *Ostrea edulis* exposed to heat and heavy metals. Cell Stress Chaperones 9, 134-142, https://doi.org/10.1379/483.1.

Porter, A.G., and Jänicke, R.U. 1999. Emerging roles of caspase-3 in apoptosis. Cell Death Differ. 6, 99-104. https://doi.org/10.1038/sj.cdd.4400476.

Pörtner, H.O. 2002. Climate variations and the physiological basis of temperature dependent biogeography: systemic to molecular hierarchy of thermal tolerance in animals. Comp. Biochem. Physiol. Part A: Mol. Int. Physiol. 132, 739-761, https://doi.org/10.1016/S1095-6433(02)00045-4.

Pörtner, H.O., Bock, C., & Mark, F. C. 2017. Oxygen-and capacity-limited thermal tolerance: bridging ecology and physiology. J. Exp. Biol. 220, 2685-2696, https://doi.org/10.1242/jeb.134585.

Puthalakath, H., O'Reilly, L.O., Gunn, P., Lee, L., Kelly, P.N., Huntington, N.D., Hughes, P.D., Michalak, E.M., McKimm-Breschkin, J., Motoyama, N., Gotoh, T., Akira, S., Bouillet, P., Strasser, A. 2007. ER stress triggers apoptosis by activating BH3-only protein bim. Cell 129, 1337-1349,

https://doi.org/10.1016/j.cell.2007.04.027.
Richter, K., Haslbeck, M., Buchner, J. 2010. The Heat shock response: Life on the verge of death. Mol Cell 40, 253-266, https://doi.org/10.1016/j.molcel.2010.10.006.
Roberts, D.A., Hofmann, G.E., Somero, G.N. 1997. Heat-shock protein expression in *Mytilus californianus*: Acclimatization (Seasonal and tidal-height comparisons) and acclimation effects. Biol. Bull. 192, 309-320, https://doi.org/10.2307/1542724.
Sarge, K.D., Murph, S.P., Morimoto, R.I. 1993. Activation of heat shock gene transcription by heat shock factor 1 involves oligomerization, acquisition of DNA-binding activity, and nuclear localization and can occur in the absence of stress. Mol. Cell. Biol. 13, 1392-1407, https://doi.org/10.1128/MCB.13.3.1392.
Shi, Y., Mosser, D.D., Morimoto, R.I. 1998. Molecular chaperones as HSF1-specific transcriptional repressors. Genes Dev. 12, 654-666, https://doi.org/10.1101/gad.12.5.654.
Sokołowski, A., and Bruliska, D. 2018. The effects of low seawater pH on energy storage and heat shock protein 70 expression in a bivalve *Limecola balthica*. Mar. Environ. Res. 140, 289-298, https://doi.org/10.1016/j.marenvres.2018.06.018.
Somero, G.N. 2005. Linking biogeography to physiology: Evolutionary and acclimatory adjustments of thermal limits. Front. Zool. 2, https://doi.org/10.1186/1742-9994-2-1.
Stanton, J.C., Shoemaker, K.T., Pearson, R.G., Akçakaya, H.R. 2015. Warning times for species extinctions due to climate change. Global Change Biology 21, 1066–1077, https://doi.org/10.1111/gcb.12721.
Strobel, A., Graeve, M., Pörtner, H.O., Mark, F.C. 2013. Mitochondrial acclimation capacities to ocean warming and acidification are limited in the antarctic nototheniid fish, *Notothenia rossii* and *Lepidonotothen squamifrons*. Plos One 8, e68865, https://doi.org/10.1371/journal.pone.0068865.
Sui, Y., Hu, M., Shang, Y., Wu, F., Huang, X., Dupont, S., Storch, D., Pörtner, H.-O., Li, J., lu, W., Wang, Y. 2017. Antioxidant response of the hard shelled mussel *Mytilus coruscus* exposed to reduced pH and oxygen concentration. Ecotoxicol. Environ. Saf. 137, 94–102, https://doi.org/10.1016/j.ecoenv.2016.11.023.
Sussarellu, R., Fabioux, C., Camacho Sanchez, M., Le Goïc, N., Lambert, C., Soudant, P., Moraga, D. 2011. Molecular and cellular response to short-term oxygen variations in the Pacific oyster *Crassostrea gigas.* J. Exp. Mar. Biol. Ecol. 412, 87-95. https://doi.org/10.1016/j.jembe.2011.11.007.
Thompson, E.L., O'Connor, W., Parker, L., Ross, P., Raftos, D.A. 2015. Differential proteomic response of selectively bred and wild-type Sydney rock oyster populations exposed to elevated CO_2. Mol. Ecol. 24, 1248-1262, https://doi.org/10.1111/mec.13111.
Tom, A., and Nair, S.K. (2006). Assessment of branched-chain amino acid status and potential for biomarkers. J Nut 136, 324S–330S**.**
Tomanek, L. 2008. The importance of phsiological limits in determining biogeographica range shifts due to global climate change: The heat-shock response. Physiol. Biochem. Zool. – Ecol. Evol. App. 72, 709-717**,** https://doi.org/10.1086/590163.
Tomanek, L., Zuzow, M.J., Ivanina, A.V., Beniash, E., Sokolova, I.M. 2011. Proteomic response to elevated P_{CO2} level in eastern oysters, *Crassostrea virginica*: Evidence for oxidative stress. J. Exp. Biol. 214, 1836-1844, https://doi.org/10.1242/jeb.055475.
Tu, C., Chen, Z.Q., Harper, D.A.T. 2016. Permian-Triassic evolution of the Bivalvia: Extinction-recovery patterns linked to ecologic and taxonomic selectivity. Palaeogeogr. Palaeoclimatol. Palaeoecol. 459, 53-62.
Uchiyama, M., and Mihara, M. 1978. Determination of Malondialdehyde Precursor in tissues by thiobarbituric acid test. Anal. Biochem. 86, 271-278, https://doi.org/10.1016/0003-2697(78)90342-1.
Valles-Regino, R., Tate, R., Kelaher, B., Savins, D., Dowell, A., Benkendorff, K. 2015. Ocean warming and CO_2-induced acidification impact the lipid content of a marine predatory gastropod. Mar Drugs 13, 6019-6037, https://doi.org/10.3390/md13106019.
Wang, Q., Cao, R., Ning, X., You, L., Mu, C., Wang, C., Wei, L., Cong, M., Wu, H., Zhao, J. 2016. Effect of ocean acidifiction on immune respomses of the Pacific oyster *Crassostrea gigas*. Fish. Shellfish. Immun. 49, 24-33. https://doi.org/10.1016/j.fsi.2015.12.025.
Woo, S., Denis, V., Won, H., Shin, K., Lee, G., Lee, T.K., Yum, S., 2013. Expressions of oxidative stress-related genes and antioxidant enzyme activities in *Mytilus galloprovincialis* (Bivalvia, Mollusca) exposed to hypoxia. Zool. Stud. 52, 1-8. https://doi.org/10.1186/1810-522X-52-15.
Xing, Q., Li, Y., Guo, H., Yu, Q., Huang, X., Wang, S., Hu, X., Zhang, L., Bao, Z. 2016. Cardiac performance: a thermal tolerance indicator in scallops. Mar. Biol. 163, 244, https://doi.org/10.1007/s00227-016-3021-9.
Young, J.T.F. and Heikkila, J.J. 2010. Proteasome inhibition induces hsp30 and hsp70 gene expression as well as the acquisition of thermotolerance in Xenopus laevis A6 cells. Cell Stress Chaperones 15, 323–334. https://doi.org/10.1007/s12192-009-0147-4.

Fig 1

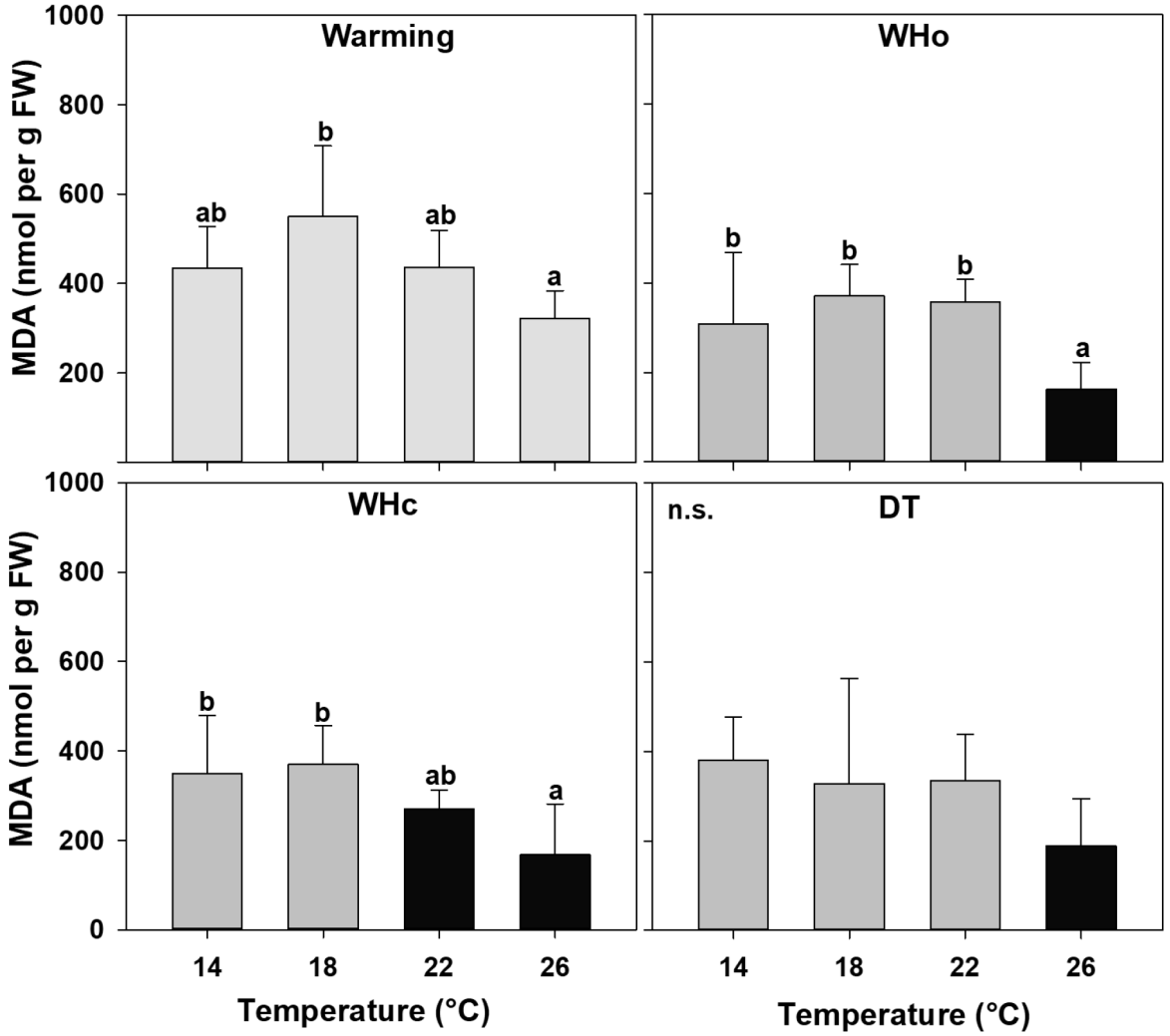

Fig 1: Malondialdehyde (MDA) concentrations in gill tissue of *P. maximus* exposed to Warming, WHo, WHc, and DT sampled at 14 °C, 18 °C, 22 °C, and 26 °C (n = 4 - 6). Data show mean concentrations in nmol per g fresh weight (FW) ± SD. Letters indicate significant differences within one exposure group ($p < 0.05$). Black bars indicate that the respective value was significantly different to the value measured at this temperature in the warming exposure.

Fig 2

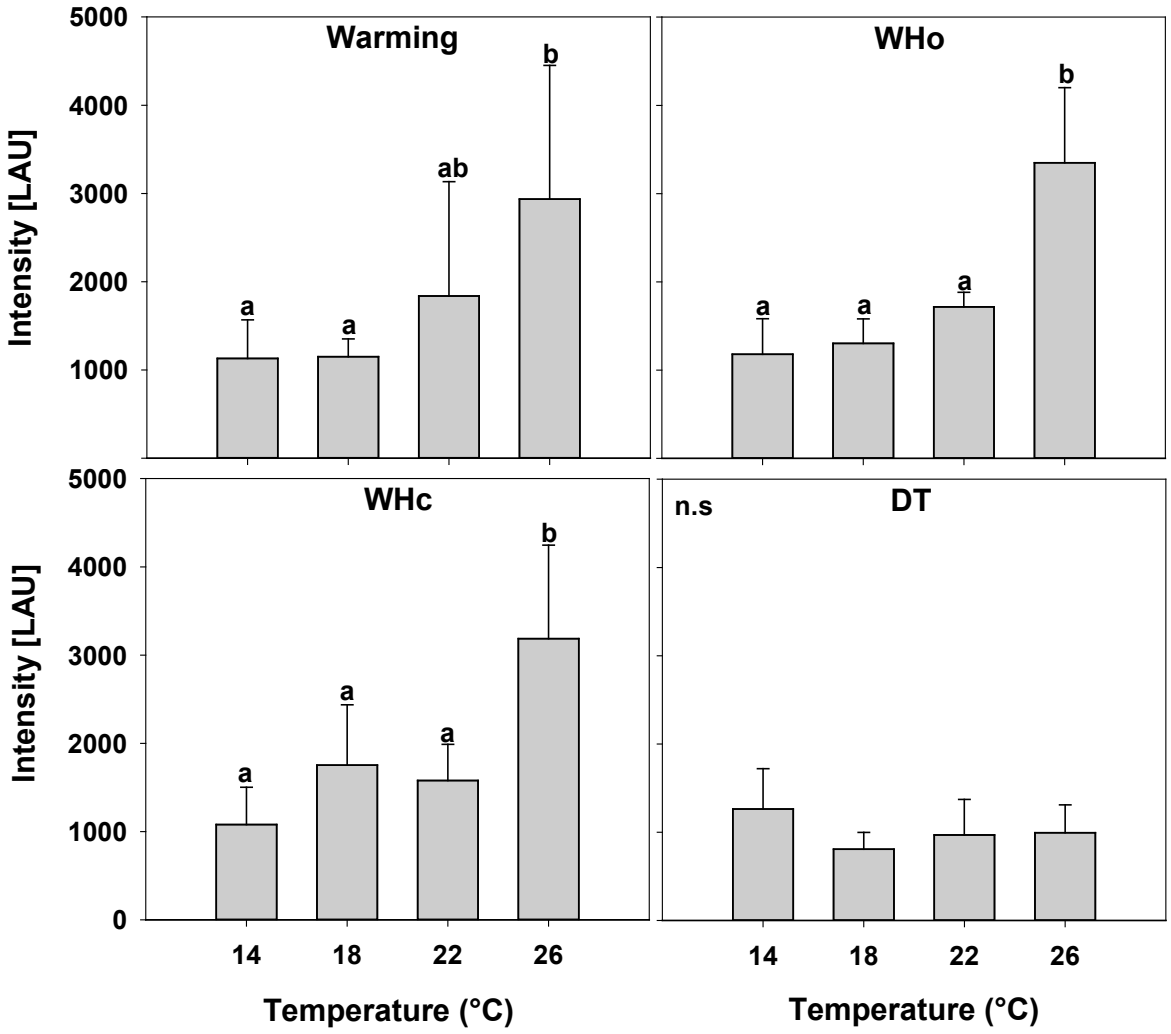

Fig 2: HSP70 concentrations in gill tissue of *P. maximus* exposed to Warming, WHo, WHc, and DT sampled at 14 °C, 18 °C, 22 °C, and 26 °C (n = 4 - 7). Data show mean and normalized concentrations expressed in luminescence arbitrary units (LAU) ± SD and letters indicate significant differences within one exposure group ($p < 0.05$).

Fig 3

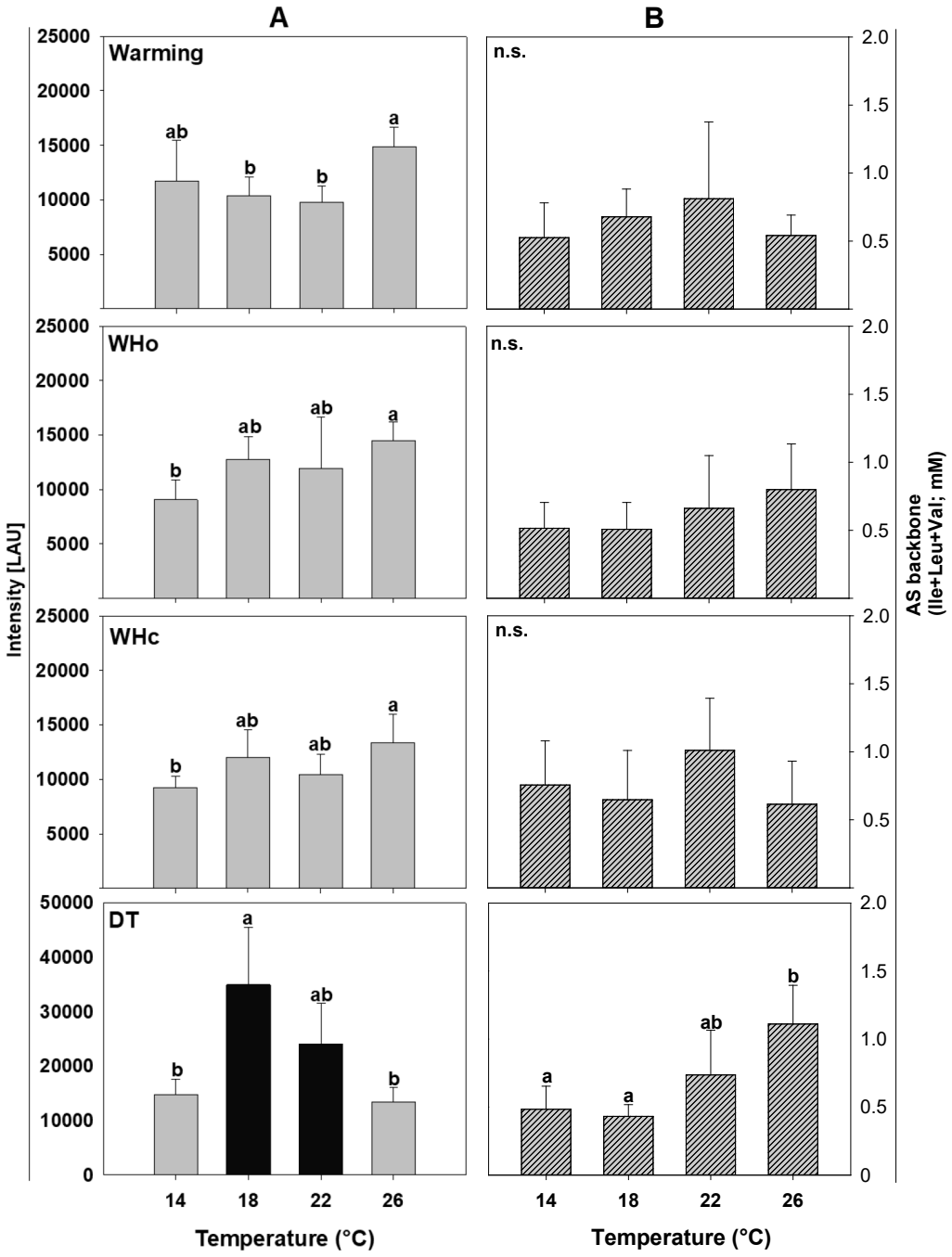

Fig 3 Panel A: Mean levels of ubiquitin-conjugates in gill tissue of *P. maximus* exposed to Warming, WHo, WHc, and DT sampled at 14 °C, 18 °C, 22 °C, and 26 °C (n = 4 - 7). Data show mean and normalized concentrations expressed in luminescence arbitrary units (LAU) ± SD and letters indicate significant differences within one exposure group ($p < 0.05$). Black bars indicate that the respective value was significantly different to the value measured at this temperature in the warming exposure. **Panel B:** Mean levels of branched chain amino acids in gill tissue of *P. maximus* (sum of valine, leucine and isoleucine) in mM. Letters indicate significant differences within one exposure group ($p < 0.05$)

Fig. 4

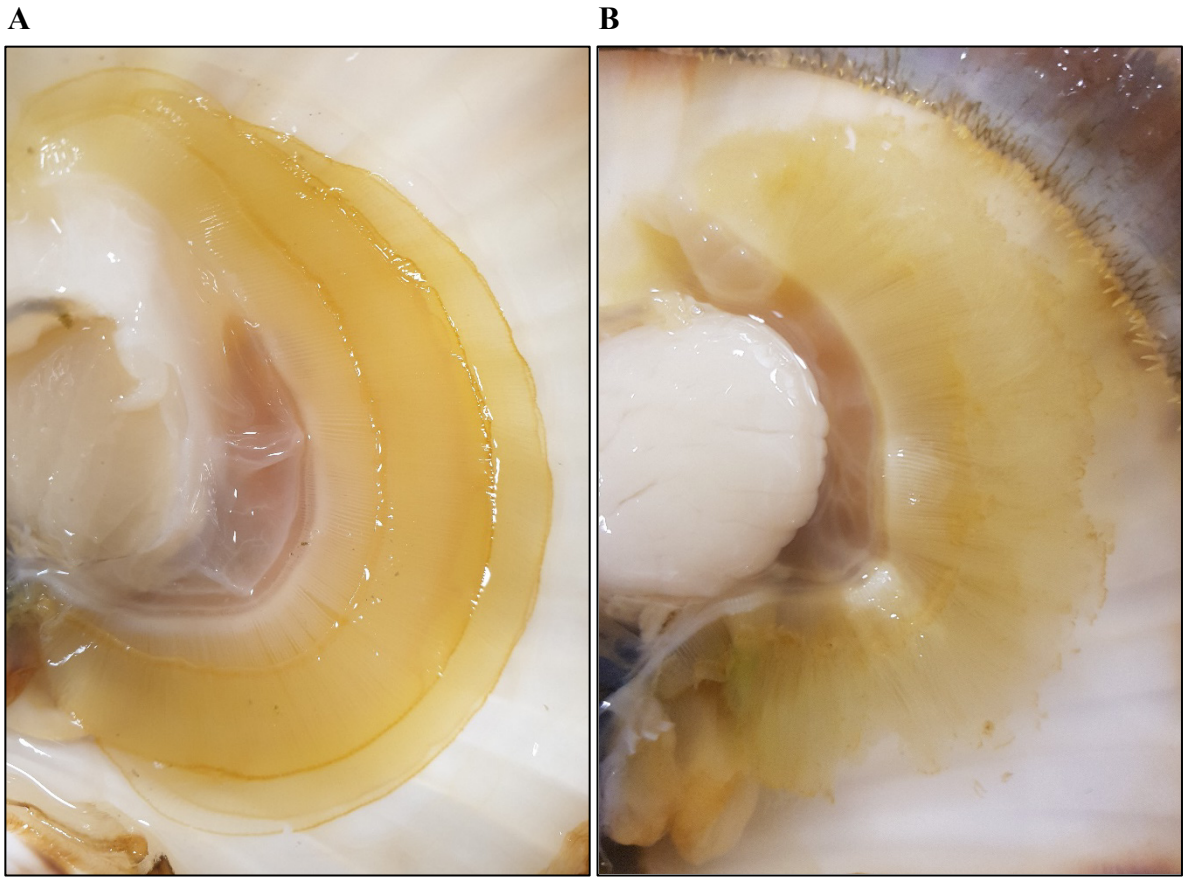

Fig 4 Image of gills of *P. maximus* taken during sampling. **A:** Gills from control scallops maintained at 14 °C under warming. **B:** Gills of *P. maximus* exposed to 26 °C and DT.

Scheme 1

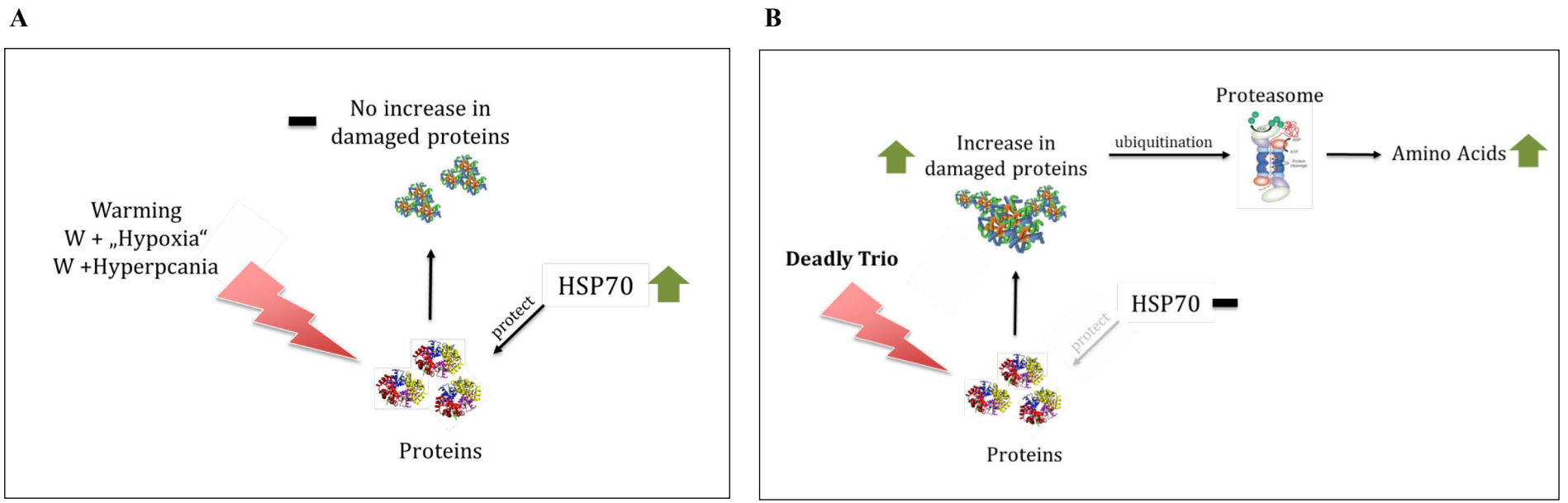

Scheme 1 Simplified illustration how the investigated measures interplay in response to environmental stresses. **A)** Single stresses (warming, warming plus hypoxia, warming plus hypercapnia) induced a sufficient upregulation of HSP70 as protective measure. Consequently, neither stressor induce protein damage. **B)** Under the Deadly Trio scallops failed to induce HSP70 (cause not determined yet) resulting an accumulation of damaged proteins (18-22 °C). Damaged proteins were likely eliminated by proteasomal degradation leading to increasing cytosolic branched chain amino-acids at 26 °C.

DISCUSSION

The current thesis determines fundamental findings of the acute thermal windows, including T_{Opt}, T_P, T_C and T_D of *Ostrea edulis* (**publication 1**) and for *Pecten maximus* (**manuscript 2, 3**). Thermal windows indicated optimal aerobic performances of both species during summer-time in Spain (18°C to 22°C). Intertidal oysters tolerated an exceptionally wide range beyond their thermal optimum while subtidal scallops did so only for few degrees. Consecutive investigations focused on in-depth analyses of metabolic pathways, which were affected by the stressors using untargeted metabolic profiling by ^{1}H-NMR spectroscopy (**manuscript 2** for *P. maximus* and supplementary **S5A-C** and **ST1** for *O. edulis*). In *P. maximus*, key changes occurred immediately after exposure to WHo or DT and were associated with energy metabolism. This underlined the special susceptibility of king scallops to warming when oxygen is limited. In both exposure groups, metabolic changes indicated an early mismatch between energy demand and supply already at temperatures, which were within the optimum range of scallops exposed to warming alone. This mismatch became most severe at T_C (26°C, **DT**). Manuscript **3** focused on cell damage and heat shock protection (HSP70) to assess whether the observed imbalances in energy metabolism were associated with cellular stress. However, neither warming (**W**), warming *plus* hypoxia (**WHo**) nor warming *plus* hypercapnia (**WHc**) induced relevant damage of proteins or lipids. The heat shock response was strictly driven by temperature but not by additional stresses and was not induced below a species-specific threshold of > 22°C. King scallops exposed to DT had high loads of protein damage in their gills (18°C - 22°C), but strikingly, HSP70 was not upregulated at any temperature. Possibly, the more severe alterations in energy metabolism at 26°C reflected the enhanced demand to counterbalance for the protein damage. Altogether, the upper thermal tolerance decreased in *P. maximus* under WHo, WHc, and was lowest when scallops faced DT (LC_{50} shifted from 25°C in W to 22.5°C in DT).

Warming exposures ran during winter and during summer revealed a season (and acclimation) dependent shift of performance in *O. edulis*. The upper thermal limits remained yet the same (34°C). Winter acclimated oysters performed best at lower temperatures than summer acclimated oysters. Furthermore, winter acclimated oysters showed a two-phase accumulation of anaerobic end products (one at 26°C and the other at 34°C). Metabolic analysis and preliminary results of the biochemical analyses of summer acclimated oysters exposed to DT revealed only minor differences in the pattern of metabolites or HSP70. W and DT exposed oysters still surpassed T_c at the same temperature (34°C), but limitations in performance likely

become visible under chronic exposure to DT as data suggest more severe heat stress around 30°C - 34°C. These findings underline the huge capacity of oysters to tolerate, at least on a short term, drastic warming and combined stress exposure (see section **4.3** for further details). In addition to the experimental part of this project, a small literature-based meta-analysis compares the LC_{50} values of several oyster and scallop species across a latitudinal cline to habitat conditions (referring to temperature only). Results outline a first hint of the possible consequences for extant Ostreoida and Pectinida under past and future ocean warming scenarios (section **4.4**). The discussion concludes with a first draft scheming the differences in underpinning mechanisms of both species in response to the Deadly Trio relevant for the leading question "What drives species into extinction?"

4.1 Shaping the fundamental thermal window (Research Aim 1)

Acute thermal windows of both species were shaped by the integration of key parameters deriving from PhD projects. Data on oxygen consumption (**MO_2**), heart rate (**HR**), filtration rate (**FR**), and hemolymph oxygen content (**PO_2**) always originate from the mutual project presented in the thesis of C. Eymann. All other data presented were determined in the current thesis (e.g., levels of succinate and acetic acid as markers for the onset of anaerobiosis, and mortality). Based on all data, optimal (**T_{Opt}**), suboptimal (**T_P** and **T_C**), and lethal temperatures (**T_D**) were defined according to the OCLTT concept if possible (latest update Pörtner et al. 2017, see introduction **Fig. 1**). In the following section, each species will be first separately discussed before both species will be compared.

4.1.1 *Ostrea edulis*

Repeated warming exposures of *O. edulis* in 2017 and in 2019 revealed that acclimation to winter (12°C) and summer temperatures (18°C) shifted the performance towards higher temperatures as described by Pörtner and coworkers (2002; 2010; **Fig. 10**). Winter acclimated oysters performed best between 18°C - 24°C (**publication 1**) while *O. edulis* acclimated to summer temperatures reached their maximal performance between 22°C - 26°C (based on FR and HR, C. Eymann). Despite this flexibility in performance, upper thermal limits remained yet the same. However, winter acclimated oysters showed a two-phase accumulation of anaerobic end products with a first rise at 2°C, indicating an early transition to critical temperatures. The second rise of anaerobic end products was observed at 34°C shortly before the lethal temperature was reached. This second rise recurred in summer acclimated oysters and confirmed that 34°C represents a life-threatening border condition (**T_c**) for adult *O. edulis*

independent of acclimation temperature (**S5-C** and **ST 1**). The capacity of winter acclimated *O. edulis* to preserve temperatures past optimum and pejus for another 10°C (equalling ten days) is remarkable, and has not been reported in any other study yet. However, oysters do experience the combination of high temperatures above maximal habitat seawater temperatures in combination with anaerobiosis during low tide. Then their body temperatures may rise as high as 40°C due to solar radiation (Helmuth, 1998; Helmuth et al., 2006). Such high body temperatures imply an extreme heat stress condition endangering cellular homeostasis. Ostreoids possess extensive amounts of genes responding to environmental stress, ensuring high phenotypic plasticity for flexible cellular adjustments and protection (investigated in the genus *Crassostrea*; Hamdoun et al., 2003; Zhang et al., 2012; Zhu et al., 2016). Many of these genes encode for heat shock proteins (**HSP**) and proteins associated with apoptosis (such as an inhibitor of apoptosis proteins = **IAP**). The heat shock response (**HSR**) mediates a transient resistance to otherwise lethal heat stress (details in manuscript 3; Lindquist, 1986; Kregel, 2002; Lenz et al., 2018). Induction of heat-protective measures has been shown to positively influence upper lethal limits in the Pacific oyster, *Crassostrea gigas,* which shifted from 44°C to 46°C (Hamdoun et al., 2003). The expansion of stress genes and their protective transcription cascade likely played a central role in oyster's adaptation to the highly stressful intertidal zone.

	(2017)	(2019)
Acclimation temperature Season	12 °C Winter	18 °C Summer
Maximal feeding rate at Maximal heart rate at Maximal oxygen consumption	18 - 22 °C 30 - 32 °C -	22 – 24 °C 32 – 34 °C 34 °C
Lipid oxidation Protein damage HSP70 induction	none - -	- - 30 °C *
Initial onset of anaerobiosis 2nd rise in anaerobiosis	26 °C (Succ, Fu, Ma) 34 °C (Succ, Fu, Ma)	34 °C (Ala, Arg) none
T_{opt} T_{pej} T_{crit} LC_{50} Lethal temperature	18 – 24 °C 24 – 26 °C 26 °C 35 °C 36 °C	22 – 24 °C 24 – 34 °C 34 °C 34 °C not. det.

Fig 10 Summary of organismic and cellular parameters (gills) measured in *O.edulis* (2017 and 2019). Feeding rates, heart rates and oxygen consumption rates were determined in the thesis of C. Eymann. Rows with an (-) indicate that the respective parameter was not measured and "none" indicates that no damage was induced. *Results for HSP70 are preliminary and have to be finished (n = 3). Anaerobiosis was determined by the accumulation of either succinate (Succ), acetic acid (Ac), fumarate (Fu), and malate (Ma). Winter acclimated oysters exhibited a second rise in anaerobic end products (2nd rise). The thermal optimum (T_{Opt}), pejus range (T_P), and the critical range (T_c) were determined considering all parameters. The LC_{50} denotes the temperature when 50% of oysters died and the lethal temperature (T_D) when 100% died. The lethal temperature has not been determined in exposures run in 2019 as experiments ended at 34°C.

Based on this knowledge, the heat-inducible isoform of the heat shock protein 70 (**HSP70**) was investigated, but so far, only preliminary data for summer-acclimated oysters are available (**S4**). These data indicate that except for two oysters (one sampled at 30°C and the other at 34°C), HSP70 was not significantly upregulated but instead was even below detection levels in all other oysters. This leads to the assumption that summer-acclimated *O. edulis* were possibly not heat stressed by the applied experimental design, but a full analysis of winter and summer acclimated oysters has to be conducted before final conclusions can be drawn.

4.1.2 *Pecten maximus*

King scallops used in this study performed best at sea surface temperatures (**SST**) occurring during summer in the Galician region (16°C to 21°C May to November; Pazos et al., 1997; www.seatemperature.org; **Fig 11**). Organismic data of filtration rates (**FR**) and oxygen consumption (**MO_2**) showed that scallops fed most at 21°C while at this temperature, MO_2 was not yet fully exploited, indicating that scallops were within T_{Opt} (C. Eymann). Above 22°C, FR and MO_2 decreased, indicating that King scallops reached the thermal pejus range (**T_P**). In accordance to their subtidal and active lifestyle, *P. maximus* have low capacities to tolerate temperatures beyond their optimum even for short periods, reaching T_{Crit} at 26°C, with 28°C already being lethal.

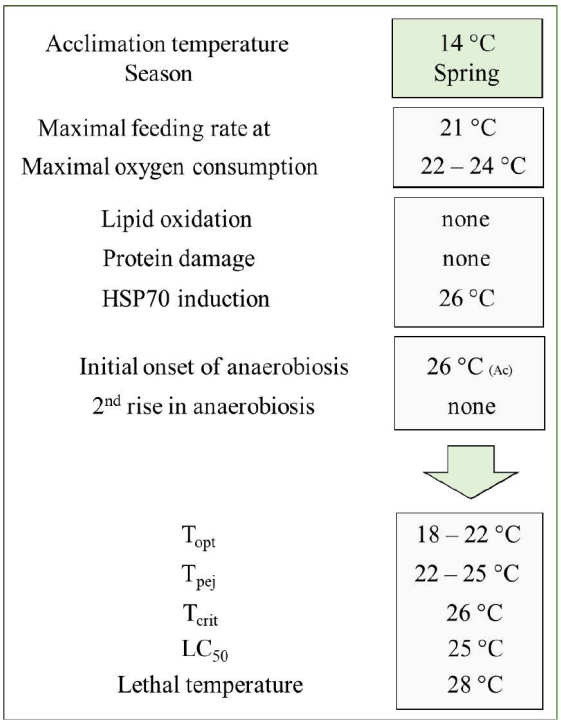

Fig 11 is a summary of organismic and cellular parameters measured in *P. maximus* (2018). Feeding rates and oxygen consumption were determined in the thesis of C. Eymann. No lipid oxidation or protein damage was found (indicated by "none", manuscript 3). HSP70 was elevated at 26°C (manuscript 3). Onset of anaerobiosis was determined by the accumulation of acetic acid (Ac). The thermal optimum (T_{Opt}), pejus range (T_P), and the critical range (T_c) were determined considering all parameters investigated. The LC_{50} denotes the temperature when 50% of scallops died and the lethal temperature (T_D) when all bivalves were dead.

This is in line with results of earlier studies using temperate *P. maximus* which showed that the thermal optimum was surpassed above 23°C (on long-term) and that this species reaches a critical temperature at 25°C (onset of anaerobiosis; Artigaud et al., 2014; 2015a; 2015b). The authors further stated that at 25°C, scallops progressively suffered from insufficient energy supply visible through decreasing condition indices (**CI**) while metabolic rates and levels of cellular stress remained elevated. Following up on these findings, in-depth analyses of metabolic pathways were performed for gill (**manuscript 2**) and phasic muscle (**S6; ST5**). Maintenance of metabolic pathways until 22°C substantiated the finding that the aerobic performance was undisturbed, and King scallops were within their thermal optimum (see above). The key metabolic change at temperatures past T_{Opt} was the accumulation of acetic acid, indicating a disruption in energy homeostasis at 26°C. *Pecten maximus* has been characterized as a moderate oxy-regulator which can better maintain respiration rates than other bivalves under declining O_2 concentrations (e.g., *Mytilus spp*; Artigaud et al., 2014). However, the increase in MO_2 in response to acute warming observed by C. Eymann, was not sufficient to maintain King scallops' hemolymph oxygen concentration (***PO*$_2$**) and led to a progressive mismatch between oxygen supply and demand (as described by the OCLTT, see section **1.2.2**). At border temperatures (in the warmth), accelerated cellular processes do not only require an extra amount of energy (***Q*10**, see introduction), but moreover, cellular processes become more prone for disorders of cell compounds (e.g., Rylander et al., 2005; Lepock, 2009). However, neither lipids nor proteins were damaged at any sample temperature, indicating that branchial homeostasis was maintained throughout the whole exposure (**manuscript 3**).

Phasic muscle was chosen as a second tissue to be investigated in *P. maximus* as it is the main tissue involved in swimming (= escape response) of scallops. As mentioned in the introduction, King scallops cannot tightly close their valves, and hence, the capacity to escape is an important indicator of performance (Wilkens, 2006; Guderley et al., 2009; Tremblay and Guderley, 2013). It was investigated whether the metabolic pattern in phasic muscle shifted in response to warming using untargeted ^{1}H-NMR spectroscopy. However, no such changes occurred and cellular pathways remained undisturbed even at 26°C shortly before residual scallops died (**S6; ST 5**). An earlier study within our research group investigated the escape response of temperate *P. maximus* exposed to warming and ocean acidification (Schalkhauser et al., 2014). This study identified a warming-dependent decrease in the mean phasic clapping forces coinciding with a prolonged recovery time in which energy was restored by anaerobic and aerobic metabolism at 20°C. Similarly, in the cold-water adapted *Placopecten magellanicus*, swimming performance

was unaffected between 5°C - 15°C, but further warming to 18°C - 19°C declined phasic contractions (Guderley et al., 2009). Accordingly, it seems likely that phasic muscle is indeed a target tissue affected by warming, but impairments do not become visible at the level of metabolites yet (see outlook).

4.2 Effects of WHo and WHc

4.2.1 *Ostrea edulis*

Single effects of WHo and WHc have been analyzed in King scallops only. Ostreoida naturally experience oxygen depletion (which can go down to anoxia) with each tidal cycle when they become emerged. Many studies investigated molecular and biochemical responses of oysters to stresses associated with the intertidal lifestyle (e.g., Le Moullac et al., 2007; Lannig et al., 2010; Goncalves et al., 2017; Stevens and Gobbler, 2018). From these studies, we learned about the exceptional tolerance to fluctuations in O_2 and CO_2 and the ability of oysters to survive even weeks of anoxia by switching to metabolic rate depression and anaerobiosis (see introduction). Regarding hypercapnia, a study of Lemasson and co-workers (2018) investigated the standard metabolic rate (**SMR**), clearance rate (**CR**) and condition index (**CI**) in adult *O. edulis* from the United Kingdom (**UK**). Oyters were exposed for 12 weeks to 1,000 ppm CO_2 at 20°C (4°C above the current maximum sea surface temperature = **SST**). Warming, but not hypercapnia, increased the SMR while neither CR nor CI were affected, leading to the overall conclusion that adult *O. edulis* are likely tolerant to moderate hypercapnia. Therefore, it seems likely that the chosen short-term exposures would not have altered the thermal tolerance of *O. edulis*. This conclusion is substantiated as the exposure of *O. edulis* to DT revealed only very little differences in organismic or cellular responses compared to warming (see discussion section **4.3**). Changes occurred mainly at T_c, indicating that the oysters' performance might be impaired under chronic exposure (see outline). Mechanisms underlying the responses of oysters to WHo and WHc will be discussed in detail in sections **4.3** and **4.4.**

4.2.2 *Pecten maximus*

WHo and WHc both shifted the thermal optimum and the upper thermal tolerance of *P. maximus* towards lower temperatures (**Fig. 12**) than under warming alone (**Fig. 11**). During WHo this became visible in higher rates of mortality (see **manuscript 2**) as 13 out of 17 scallops died at 24°C. Hemolymph PO_2 accounted for 7.2 ± 1.6 kPa at 14°C and scallops maintained this value until 18°C. Thereafter, O_2 saturation decreased to 4.1 ± 1.1 kPa (C. Eymann). As

outlined in the introduction, water-breathing organisms have to invest more effort to warrant sufficient O_2 supply to tissues, especially in the warmth (Verberk et al., 2011 and 2015) and this effort is aggravated under lowered oxygen tensions. WHo caused hypoxemia in response to few degrees of warming as indicated by the decrease in PO_2 in parallel to the early onset of branchial anaerobiosis and mobilization of lipid energy reserves via ß-oxidation, which occurred in both, phasic muscle and gill tissue (**ST5** for phasic muscle and **manuscript 2** for gills). *Pecten maximus* did not encounter metabolic depression, but instead, the induction of HSP70 at 26°C indicated that scallops sustained the rate of cellular metabolism.

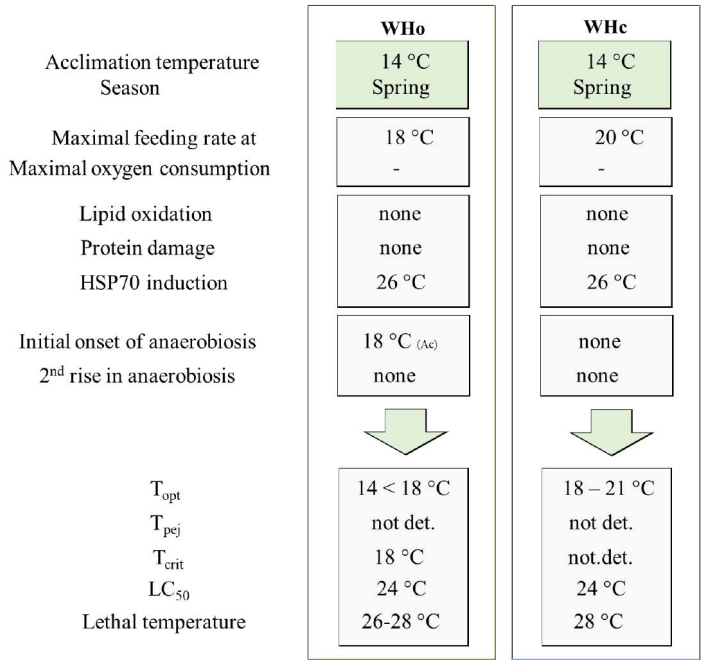

Fig 12 Summary of organismic and cellular parameters measured in *P. maximus* exposed to WHc (left) and WHc (right). Feeding rates and oxygen consumption were determined in the thesis of C. Eymann. Rows with an (-) indicate that the respective parameter was not measured and "none" indicates that no damage was induced (lipid oxidation and protein damage). Onset of anaerobiosis was determined by the accumulation of acetic acid (Ac).
Only the thermal optimum (T_{Opt}) and the critical range (T_c) could be determined for WHo exposed scallops, and for WHc exposed scallops only T_{Opt} could be determined. The LC_{50} denotes the temperature when 50% of scallops died and the lethal temperature (T_D) when all bivalves were dead.

Similar observations were made for *Aequipecten opercularis* and *Argopecten irradians* which both sustained cellular processes such as e.g., the translation of the Na^+/K^+-ATP-ase or the protein turnover in response to hypoxia (Strahl and Abele, 2010; Ivanina et al., 2016). Accordingly, under WHo the early onset of hypoxemia narrowed the thermal performance and caused high mortality at 24°C as accelerated cellular processes and maintenance of homeostasis led to an energetic crisis. This energetic crisis is probably exacerbated (compared to W) as the early onset of anaerobiosis gains only between two to six moles ATP per mole glucose instead of the up to 36 moles of ATP per mole glucose gained via oxidative phosphorylation (De Zwaan and Wijsman, 1976; Sokolova et al., 2012).

P. maximus was least affected by WHc indicated by the unaffected phasic muscle metabolism (**S6** and **ST5**), minor changes in branchial metabolism, and the overall maintenance of branchial

homeostasis (**manuscript 2 and 3**). This is in line with the few studies available that investigated hypercapnic stress in *P. maximus* (Burton-Sanders et al., 2013; Schalkhauser et al., 2014). The study released by Schalkhauser and co-workers investigated the escape performance of adult, temperate *P. maximus* under WHc (50 days, 1120 µatm at either 10°C or 20°C; 2014). They found no impact on escape performance or on metabolic rates. Interestingly, temperate King scallops were more successful in maintaining their extra-cellular pH (drop accounted to ~ 0.15 pH units) compared to cold-adapted *P. maximus* (drop accounted to ~ 0.25 pH units; Schalkhauser et al., 2013 and 2014). The higher capacities of temperate King scallops to regulate their acid-base homeostasis defend them better against hypercapnia than cold-adapted ones (see introduction). The other study which investigated *P. maximus* under hypercapnia stated that they did not find any impacts on feeding, breathing, cellular turnover, or CI after exposure to 1,140 µatm CO_2 for three months (Burton-Sanders et al., 2013). The few branchial changes in metabolites detected in the current study in response to WHc were observed past T_{Opt} and indicated changes related to cell membranes and/or cell membrane integrity (O-phosphocholine, see **manuscript 2**). Cell membrane changes in response to hypercapnia could be associated with acid-base regulatory processes (see above and introduction). However, this explanation is rather speculative as neither pH_E nor pH_I was determined and hence more research is needed to understand underlying mechanisms. Altogether, these findings lead to the assumption that *P. maximus* is more sensitive towards oxygen depletion than to hypercapnia.

4.3 Effects of the Deadly Trio

The evaluation of multiple environmental stressors such as the "Deadly Trio" yields a more realistic environmental picture than investigating single stressors. As outlined in the introduction, marine habitats are mainly affected by interactions of temperature, hypoxia and hypercapnia. Their convergence potentially amplifies (or attenuates) effects single stressors would have and further modulate the thermal window of species (see introduction; e.g., Pörtner, 2010; Tripp et al., 2017; 2019).

4.3.1 *Ostrea edulis*

Ostreoids adapted to rhythmic tidal cycles and endured combined stresses during low tides frequently. Especially, temperate intertidal bivalves may experience drastic changes, for example, in body temperature, salinity, oxygen content or carbon dioxide (see above, e.g., Helmuth et al., 2006). Accordingly, it is not surprising that short-term exposure to DT did not

alter the thermal window or the aerobic performance of *O. edulis* (**Fig. 13**). In DT exposed oysters, the hemolymph oxygen content ($\mathbf{P}\boldsymbol{O_2}$) was significantly lower than in W-exposed oysters (at 18°C and 22°C) reflecting their oxyconforming behavior (see introduction). Interestingly, *O. edulis* did not switch to metabolic rate depression in avoidance as one could have expected, but instead, oysters compensated the drop in PO_2 by higher rates of heart beats (significant increase between 24°C to 32°C) and stayed active for longer durations (indicated by respiratory time activity, **RTA,** C. Eymann). Neither feeding rates nor condition indices (the latter see in **S3**) differed between DT and W exposed oysters, and both organismic adjustments were sufficient to maintain aerobic performance under DT. Metabolic pattern differed only slightly between both exposure groups and, in most cases, only at T_c, indicating that DT exposed oysters experienced more severe heat stress when temperatures became critical (34°C; **S5A-C** and **ST1**). This is supported by preliminary data of HSP70 as the expression of this protein seemed higher in DT exposed oysters compared to W exposed oysters when temperatures reached 30°C (**S4).** Accordingly, it seems that the current experimental design was still too short to determine turning points in the organismic performance, but cellular data indicate that the tolerance of oysters to DT is time-limited, and chronic exposure to DT likely narrows the thermal window (see further discussion in section 4.4.3).

4.3.2 *Pecten maximus*

King scallops progressively suffered from organismic, cellular and metabolic impairments, which accounted for higher rates of mortality (**Fig. 13**). Similar to scallops exposed to W, DT-exposed scallops survived up to 28°C, indicating that such short-term exposure did not yet decrease maximal upper thermal limits ($\mathbf{T_D}$). However, the clear decrease in performance under acute experimental conditions suggests that King scallops likely would not survive chronic exposure to DT at temperatures close to 22.5°C (or higher). The patterns of branchial metabolites and affected pathways in response to DT were similar to those patterns found under WHo, but displayed more severe changes at critical temperatures (26°C, **manuscript 2).** Hemolymph PO_2 decreased under DT similar as under WHo (7.3 ± 1.8 kPa at 14°C to 4.1 ± 1.2 kPa at 26°C, C. Eymann) indicating that *P. maximus*, as discussed for WHo, became hypoxemic already with few degrees of warming (see section **4.2**). It cannot be stated, whether the observed protein damage between 18°C to 22°C is a consequence of hypoxemia, or whether it occurred due to yet unknown causes. For sure, such disturbances in the cellular homeostasis added to the observed pronounced alterations in mitochondrial energy metabolism, decreasing the aerobic scope of performance further. Strikingly, pronounced protein damage did not induce HSP70

expression, although ubiquitin-conjugates are known triggers of the HSR (Meriin et al., 1998; Liao et al., 2006; Young and Heikkila, 2010). As discussed in depth in manuscript three the lacking HSP response could be due to different reasons. Possibly, active scallops have distinct mechanisms to maintain cellular homeostasis. Investigations of *Aquipecten opercularis* give rise to the suggestion that scallops maintain homeostasis by apoptosis and cell proliferation rather than by extended cellular defense or repair (Strahl and Abele, 2010).

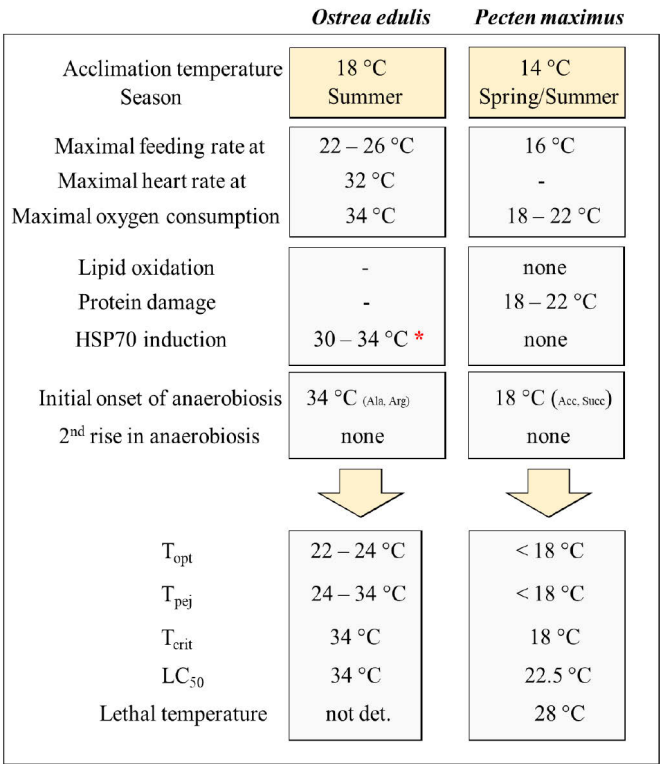

Fig 13 Summary of organismic and cellular parameters measured in *O. edulis* (left) and *P. maximus* (right) exposed to DT. Feeding rates, heart rates and oxygen consumption rates were determined in the thesis of C. Eymann. Rows with an (-) indicate that the respective parameter was not measured and "none" indicates that no damage was induced. *Results for HSP70 measured in *O. edulis* are preliminary and have to be finished (n = 3). Anaerobiosis was determined by accumulation of alanine (Ala), arginine (Arg), acetic acid (Ac), or succinate (Succ).
The thermal optimum (T_{Opt}), pejus range (T_P), and the critical range (T_c) were determined. In case of scallops, T_{Opt} and T_P can only be estimated due to missing data. The LC_{50} denotes the temperature when 50% of bivalves died and the lethal temperature (T_D) when all bivalves were dead.

Artigaud and coworkers also reported that in *P. maximus* exposed for 24 hours to severe hypoxia, the TANK binding kinase 1 (which is an anti-apoptotic acting protein) was downregulated, indicating ongoing apoptosis (see 4.3; Artigaud et al., 2015b). There's a possibility of apoptosis being induced by insufficient cellular protection (as a failure of HSR) and hence cellular damage. The lacking HSP70 response is remarkable as pectinids have, similar to oysters, expanded regions in their DNA encoding for stress and immune response genes suggesting well established cellular stress response mechanisms (Wang et al., 2017). Accordingly, more research is needed to understand the missing HSR response by investigating other HSPs (such as e.g., HSP40 or HSP90) or, for example, the heat-shock transcription factor-1 (HSF-1; see introduction manuscript two or, e.g., Sarge et al., 1993). It would be beneficial

to further investigate apoptosis and to learn whether observed patterns are due to a "strategy" or are the consequences of failure in cellular protection (see outlook).

4.4 Bridging present findings to past and future climate events

What can we learn from past mass extinctions for present and predicted marine ecosystem changes and how can modern ecophysiology help to better understand fossil extinction pattern of past crises? These were the driving question associated to the interdisciplinary RU "TERSANE" and "BIV-TRS". Accordingly, the subsequent section starts to bridge findings obtained during "BIV-TRS" to the PT-ME to approach this question.

4.4.1 Thermal tolerance of Ostreida and Pectinida

As discussed above (see section **4.1**), *O. edulis* and *P. maximus* have distinct (acute) thermal windows associated with their lifestyle and habitat. European oysters tolerated higher temperatures (lethal temperature reached at 36°C) as King scallops (lethal temperature reached at 28°C). This is in line with several earlier studies which already supported the perception that organisms living higher on the shore (as oysters do) are more tolerant to high temperatures than organisms living lower on the shore or living submerged (as scallops do; e.g., Southward, 1958; Kennedy and Mihurski, 1971; Vernberg and Vernberg, 1972; Davenport and Davenport, 2005). To better understand the fate of taxonomic orders instead of single species only, a small meta-analysis based on literature was carried out. In total five adult scallop species (all subtidal) and six adult oyster species (all intertidal, with two different population of *O. edulis*) were compared using the acute half-maximal lethal temperature (LC_{50}) as an indicator for lethal limits (**Fig. 14 A, B; supplementary Tab2;** Stillmann, 2002; Angilletta, 2009). In *P. maximus* and *O. edulis,* acute LC_{50} values correlated to critical temperatures ($\mathbf{T_c}$). However, LC_{50} values may shift depending on the experimental design (duration of exposure, direct *vs*. stepwise temperature increase, time of the season). The acute LC_{50} determined in a species hence lies either at the border or outside the range of aerobic performance where survival is strictly time-limited (see Pörtner et al., 2017). The upper thermal limits of the realized thermal niche, which supports long-term survival, will be several degrees below the acute LC_{50}. Nevertheless, the results give an impression of the exceptional tolerance of (emerged) oysters to temperatures above environmental sea surface temperatures (**SST**). Oysters reached LC_{50} on average at temperatures of 41.1°C ± 4.8°C. The LC_{50} determined in scallops was significantly lower, with 28.3°C ± 4.3°C ($P < 0.001$, **Fig. 14A**). An even more interesting picture is obtained for both

taxa when for these species, the maximal habitat temperature is further taken into account (**Fig. 14B**). The margin between maximal habitat temperature (when submerged) and the LC_{50} may serve as an approximation for a species short-term capacity to endure unfavorable conditions in its habitat. It becomes apparent that oysters can tolerate bigger margins beyond maximal habitat temperatures (more than 10°C) before surpassing to a critical temperature compared to scallops (below 10°C). These margins may reflect the adaptation of oysters to the high body temperatures they experience during low tide (see **4.1.1**.) and which subtidal pectinids likely never encounter in their habitat.

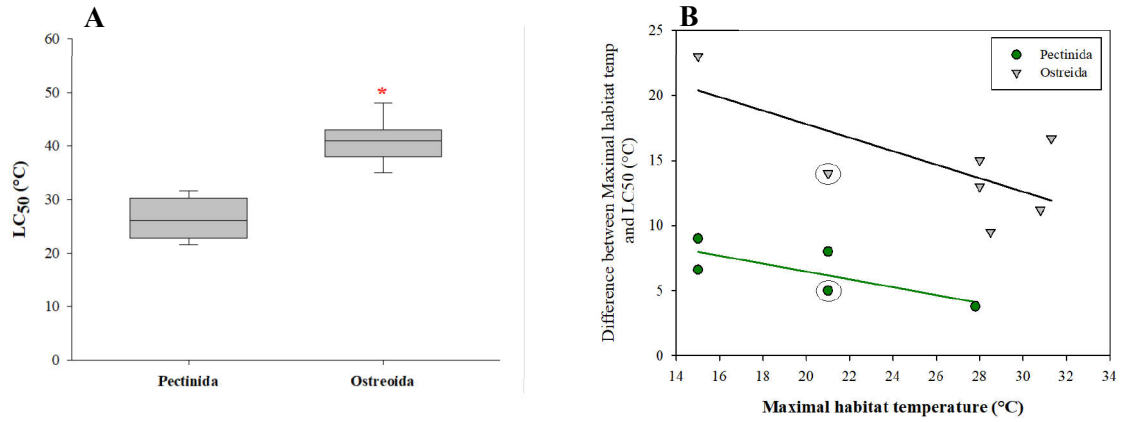

Fig 14 Comparison of LC_{50} values of five scallop species and six oyster species (full list of species can be found in **ST7**, data include two populations of *O. edulis*). **A** Mean $LC_{50} \pm$ SD with oysters being significantly different from scallops indicated by a red asterisk ($P < 0.001$). **B** Margin between maximal habitat temperature (when submerged) and LC_{50} of oysters (black triangle) and scallops (green circles) plotted against the maximal habitat temperature of the respective species. Circles indicate species used in the current thesis.

4.4.2 Projections how extant bivalves cope with current and future waming

Near future climate projections predict a rise in SST by up to 4°C by the end of the century (RCP 8.5 IPCC; Hoegh-Guldberg et al., 2014). Estimates of the PT-ME anticipate that marine ecosystems had to face a rise in SST to ~ 36° at the boundary, possibly even exceeding 40°C (Sun et al., 2012). Global warming during the PT-ME is thought to have happened over ~ 800 thousand years. As part of the meta-analysis, LC_{50} values of the above-mentioned scallops and oysters were plotted according to their latitude of origin (depicted in both **Fig 15A, B**). As stated above, under today's temperature regime oysters have a high margin between the LC_{50} and maximal SST, in line with their geographical origin. Under a "business as usual behavior" (RCP 8.5), a four-degree increase of maximal SST will not encounter critical temperatures. Furthermore, it seems likely, that oysters will be able to acclimate to this proposed rise in SST

by shifting their performance towards higher temperatures as observed in the current study and described in the literature (see section 4.1.1 and, e.g., Pörtner, 2010).

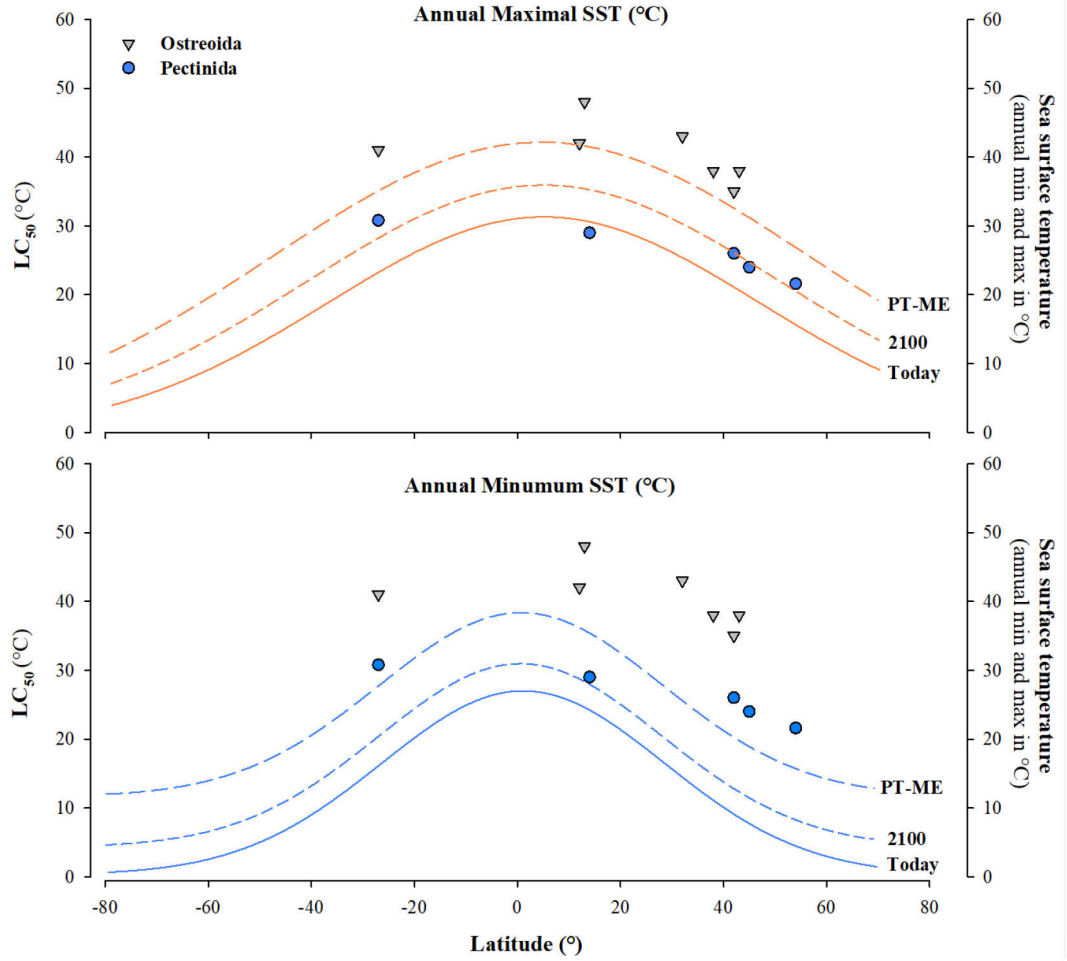

Fig 15 LC_{50} values from six oyster species and five scallop species depending on their latitudinal origin. The same species are shown in **A** and **B**. Furthermore, in **A** the extrapolated curves for the annual maximum sea surface temperatures (SST, °C), the anticipated SST for the year 2100 (+ 4°C, RCP 8.5 IPCC), and a warming scenario of *plus* 11°C as it could have happened during the PT-ME are shown. Curves derive from SSTs measured at 38 locations across the world (2019, www.seatemperature.org)**.**
B shows for the same locations as in A the annual sea surface minimum temperatures, again for 2019, 2100, and the PT-ME. All extrapolations were done using a Gaussian curve with r^2=0.94 for min SST and r^2=0.86 for max SST. Full table of locations and temperatures used are shown in **ST6**). The figure does not consider the effect of additional stressors.

Conditions that mimic warming during the PT-ME (+ 11°C) would challenge extant oysters mostly during summer as temperatures then get close to the acute LC_{50} values. In this scenario, oysters' performance and abundance would likely decrease, but due to their anticipated high

capacity for passive endurance (see below), one can hypothesize that at least the fittest oyster species would outlive other more sensitive taxa (such as scallops).

Already today, (during summer) subtidal scallops live closer to their upper thermal limits (**Fig. 14** and **Fig. 15**). An anticipated rise of 4°C by the end of the century will approach upper thermal limits as LC_{50} values of all scallop species are already close to maximal summer SST. It remains unclear whether scallops will have the capacity to shift their upper thermal tolerances or whether populations may move towards colder areas as hypothesized for other taxa (see introduction; e.g., Koenigstein et al. 2016). The latter is more likely the case, especially in areas where oxygen becomes limited. Our results indicate that even a few degrees of warming, in combination with a mild reduction of oxygen, are already sufficient to impair the energy homeostasis of gills. Accordingly, it is questionable how successful, for example, temperate scallops as *P. maximus* can adapt to the anticipated rise of 4°C by 2100. This is in line with long-term exposures run by Artigaud and co-workers who also stated that their proxies indicate that a projected SST increase of less than 4°C until the end of the century might push *P. maximus* beyond its thermal limits (Artigaud et al., 2015a,b). Sea surface temperatures mimicking warming during the PT-ME would be close or even above critical temperatures throughout the year with worst conditions for scallops in tropical areas. Accordingly, at least modern pectinid species would be at the edge of extinction if they are not capable to relevantly shift their thermal performance. Upper thermal limits of extant oysters and scallops subjected to warming as anticipated for the PT-ME seem to reflect the fate of ancient scallops and oysters. From fossil records, we learned that Pectinida, together with Myalinida, and Pholadomyida form those groups with higher extinction rates among bivalves, while ancient Ostreoida together with Trigoniida and Mytilida form those groups with lower extinction rates (Tu et al., 2016).

4.4.3 What drives species into extinction?

In order to understand the pattern of past marine mass extinctions and to project the fate of extant species under future climate challenges, it becomes crucial to understand the complex physiological mechanisms responding to temperature-related stresses. Paleontological research reconstructs environmental changes, which may explain the extinction pattern of ancient species by analyzing geological proxies (e.g., Kasting et al., 2006; Clarkson et al., 2015; Veizer and Prokoph, 2015). In one study, the occurrence of Ostreoida and Pectinida through geological history was compared (based on data from the Palaeobiology Database;

https://palaeobiodb.org/#/; Guo et al., 2018). The authors suggested that evolution favored oysters and other bivalves being more tolerant of warming and low oxygen concentrations (anoxia). Research on extant bivalve species, including BIV-TRS further supports the assumption that especially mechanisms facilitating the tolerance to hypoxia might have been decisive during past ME and will be decisive during future environmental crises. Mirroring fossil records of the PT-ME (see above), *P. maximus* the representative member of the Pectinida investigated during BIV-TRS was more severely affected by DT than *O. edulis* the representative member of the Ostreoida. Based on all findings, observations and literature knowledge, conceptual models were developed for each species to approach underlying mechanisms that possibly shape species survival under DT (**Fig. 16** for *O. edulis* and **Fig. 17** for *P. maximus*).

The responses of both species to short-term exposure of DT indicated different modes of action likely related to hypoxia-tolerance. One of the clear differences between the two species was that PO_2 decreased in both species under DT but *O. edulis* was able to counterbalance and to maintain its performance while *P. maximus* was not. Sessile European oysters passively endure unfavorable environmental changes as a result of adaption to the tidal rhythm where they encounter hypoxic conditions while being shut close during low-tides (see discussion above, Grieshaber et al., 1994; Michaelidis et al., 2005). While being emerged metabolic depression prolongs the time of survival. Interestingly, submerged oysters exposed to DT did not switch to metabolic depression, but instead, increased cardiac and respiratory circulation to cover their energy demand. Under oxygenated conditions (as applied in the present experiments), the high capacities of oysters to adjust their metabolic rates (ATP-generating and ATP-consuming processes) enable them to keep ATP-demand and supply balanced and to maintain aerobic metabolism which is superior to encountering metabolic rate depression. The described high genetic and phenotypic plasticity likely supports endurance (see section 4.1.1; Hedgecock et al. 2005; Zhang et al., 2012; Zhu et al., 2016). However, protective underlying mechanisms are still faint and only underline how tolerant *O. edulis* are to changes in environmental conditions (see also section **4.3.1**). Therefore, it is mandatory to continue investigating mechanisms emerging under chronic exposure (see outlook). Subtidal King scallops have to be alert and active to defend themselves against predators by escaping and hence evolved a different survival strategy (**Fig. 17**). Fast escape reactions require active metabolism and sufficient energy supply. This lifestyle does not permit metabolic depression to the extent Ostreoids can do as a decrease of the standard metabolic rate would not support fast escape reactions. Optimal

performance hence relies on higher aerobic energy provision (compared to, e.g., oysters) to keep cellular homeostasis and cell turnover balanced.

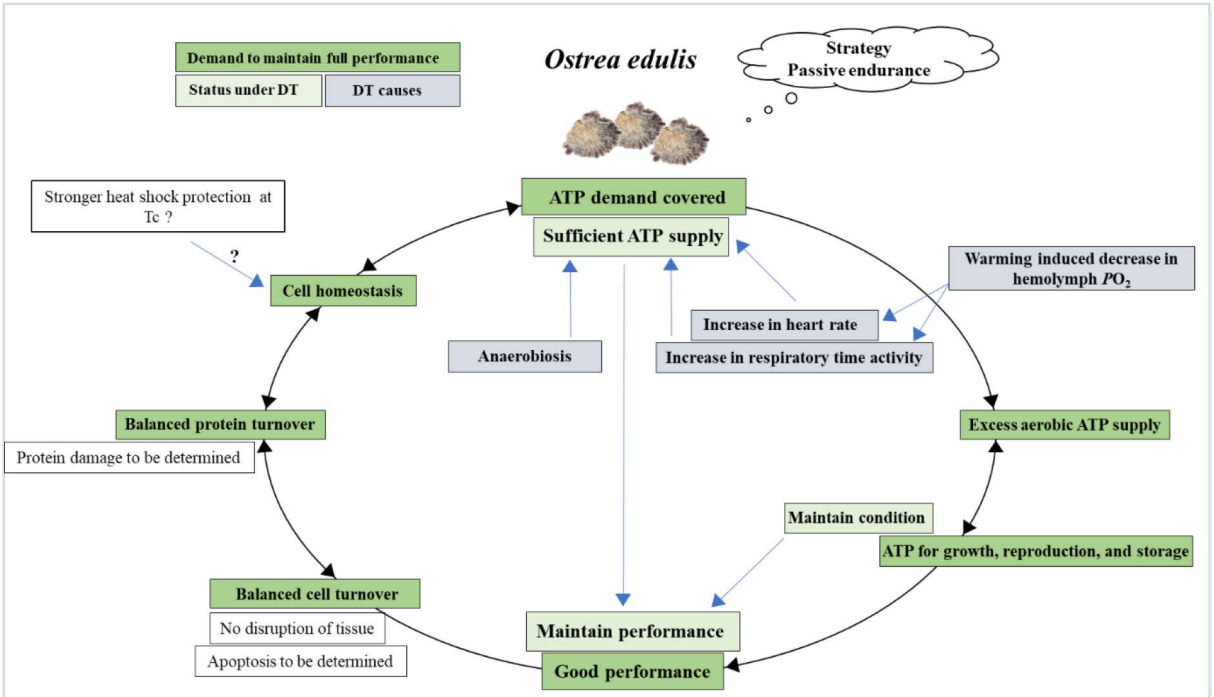

Fig 16 Simplified conceptual scheme of *Ostrea edulis* exposed to short-term exposure of the Deadly Trio (DT), integrating experimental findings and literature knowledge. Oyster passively endure unfavorable environmental conditions. The sessile (inactive) lifestyle does not require high metabolic rates. Furthermore, due to the adaptation to the intertidal, oysters have high capacities to adjust ATP-demand and ATP-supply accordingly (literature). For long-term survival, organismic and cellular demands have to be covered. Organismic demand which allows full performance is shown in dark green boxes along the orbital (see Pörtner, 2010). Excess aerobic energy supply allows growth, reproduction, or energy storage. Short-term exposure to DT caused an immediate warming-induced decrease in the hemolymph oxygen concentration (PO_2), which was counterbalanced by organismic adjustments indicated by increasing heart rates and longer durations of respiratory activity (grey boxes, HR and RTA, C. Eymann). These adjustments were sufficient to match the energetic demand indicated by unaffected performance and metabolic pathways (status under DT is shown in light green boxes). The thermal window was not narrowed under the chosen stress exposure. At the critical temperature (T_c) gills accumulated higher levels of anaerobic products (see **4.3.1**). This indicates that under chronic exposure to DT energy homeostasis might be impaired. No data are available for protein damage yet. Preliminary data for HSP70 indicate a possibly stronger induction at temperatures close to T_c. Open questions to be investigated should include a.o. the status of protein homeostasis and how *O. edulis* will respond under chronic exposure to DT at temperatures beyond T_{Opt} (see outlook for more details).

Indeed, changes in metabolites and cellular impairments became visible under short-term exposure to DT, finally decreasing the performance (see **manuscript 2** and **3**, and discussion sections **4.3.2**) and confirming lower capacities of scallops to adjust metabolic rates.

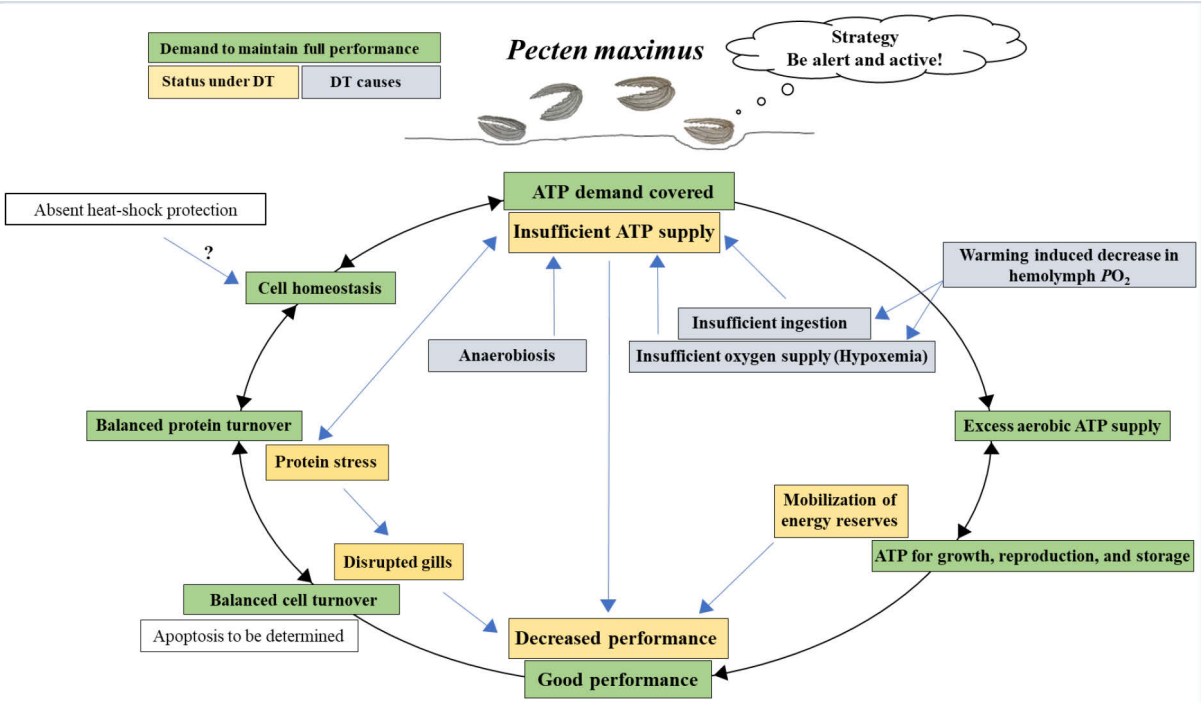

Fig 17 Simplified conceptual scheme integrating experimentally derived findings and literature knowledge to frame underlying mechanisms involved in *Pecten maximus* challenged to short-term exposure of the Deadly Trio (DT). Scallops have a more active life style as they can react and escape, e.g., under predation. The mobile life style does require higher metabolic rates than the sessile lifestyle of oysters. For long-term survival, organismic and cellular demands have to be fulfilled. Organismic demand which allows full performance is shown in dark green boxes along the orbital (see Pörtner, 2010). Short-term exposure to DT caused an immediate warm-induced decrease in the hemolymph oxygen concentration (PO_2), which could not sufficiently be counterbalanced by organismic adjustments measured by early breakpoint temperatures in heart rates and filtration rates (grey boxes, C. Eymann). Hypoxemia affected energy supply and did no longer meet the energy demand (status under DT is shown in yellow boxes). An early onset of anaerobiosis and accumulation of metabolites involved in lipid mobilization was observed to compensate for the decrease in aerobic energy gain. Furthermore, protein damage occurred and at 26°C gills were disrupted (yellow boxes). Altogether impaired processes contributed to a decreased performance narrowing the acute thermal window. It seems likely that under chronic exposure to the Deadly trio *P. maximus* might not be able to sustain long-term (see outlook). Further open questions to be investigated will include what caused the lacking heat-shock protection, and whether this accounted to the observed protein damage.

Possibly, the high metabolic rates and lower capacities to decrease standard metabolic rate also selected for the proposed better capacity of king scallops to maintain PO_2 under declining oxygen concentrations (Artigaud et al., 2014) and the observed higher capacities for acid-base regulation in temperate King scallops (Schalkhausser et al., 2013 and 2014). However, it seems that once hypoxemia is induced, *P. maximus* only have limited capacities to maintain performance. The effect of oxygen reduction is further intensified as it's more difficult for larger species to maintain oxygen supply and demand balanced, especially at suboptimal temperatures as they have an unfavorable surface to volume ratio (Chapelle and Peck, 1999;

Pauly, 2010). Due to this, individuals can grow larger at colder temperatures than at warmer temperatures; a phenomenon called the "temperature-size rule" (**TSR**; Angilletta et al., 2004; Forster et al., 2012). Fossil records prove that past MEs selected for smaller organisms indicating the operation of the TSR (Lilliput effect", Twitchett, 2007; Piazza et al. 2019). Accordingly, it can be assumed that under rapid climate change now and during past crises, especially the combination of warming and hypoxia affected large and active Pectinida negatively while the smaller and inactive Ostreoida were less affected.

4.5 Outlook

The current thesis comprises fundamental and new insights into biochemical and molecular mechanisms identified in two bivalve model organisms in response to acute TRS as a baseline for future research. As the first step for future research analyses of HSP70 and ubiquitin-conjugates in gills of warm-acclimated *O. edulis* (2019) will have to be finished and findings implemented into the draft of manuscript 4. Furthermore, disrupted gills of *P. maximus* found under DT (26°C) indicate an involvement of apoptotic processes. It would be beneficial to verify apoptosis in order to better understand underlying mechanisms. For this purpose, the status of pro-apoptotic and anti-apoptotic regulator proteins such as caspase-3 or p53 can be determined.

For a better understanding of past and future crises, it is crucial to consider the long time-scales during which changes occur. The speed of change becomes dangerous when it exceeds the speed of the adaption of a species. Accordingly, based on the findings gained during TERSANE, subsequent research scheduled for the upcoming TERSANE II period will focus on the passive tolerance capacity of O. *edulis* and *P. maximus* to acclimate during long-term exposures to temperatures past T_p (described by Pörtner, 2010). Acclimation of protective cellular mechanisms (such as HSR), which protect cells against damage (e.g., lipids, proteins, or DNA) or metabolic stress (e.g., stress at the endoplasmic reticulum or cause mitochondrial proton leakage) can shift heat tolerance limits in time and stress-dependent manner. Accordingly, understanding mechanisms involved in successful cellular acclimation enabling long term survival will better help to understand the fate of past and extant species during climate crises.

SUPPLEMENTARY

SUPPLEMENTARY

S1

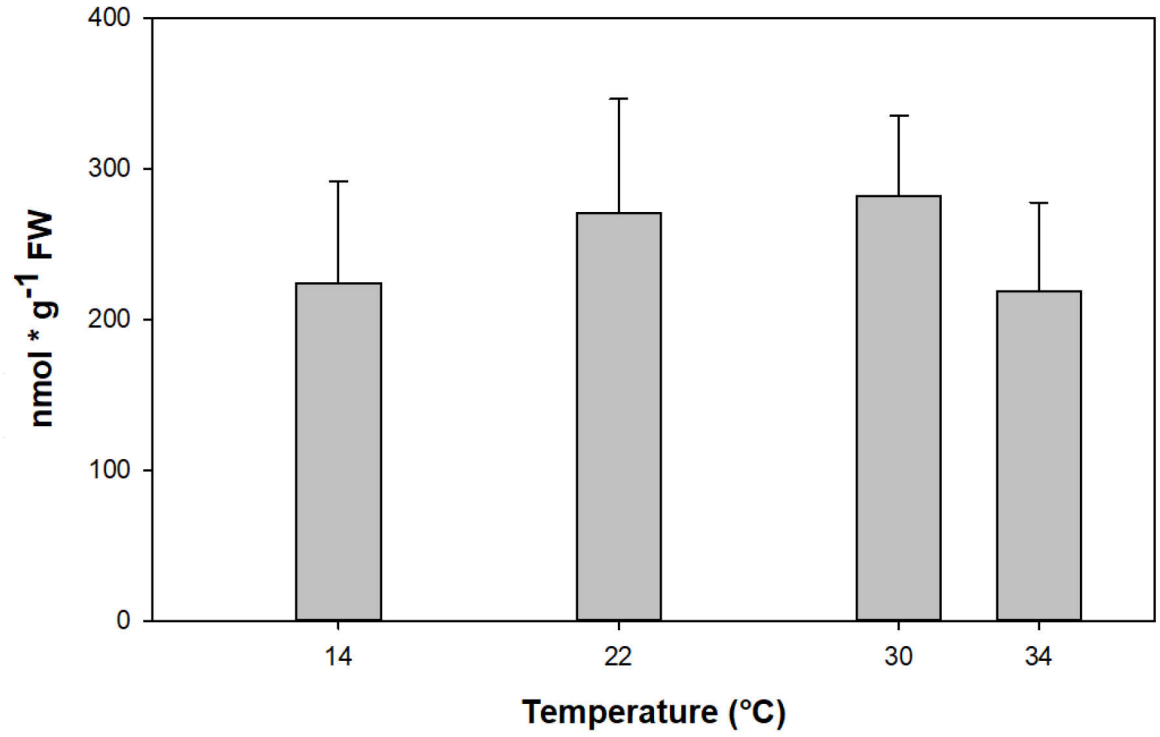

S1 Levels of Malondialdehyde (MDA) in gill tissue of *O. edulis* exposed to warming (2017) determined at 14, 22, 30, and 34 °C. Samples were measured as described in section 2.3.2. Shown are the mean concentrations ± SD in nmol ˙ g fresh weight (FW) with n=6. Statistical analysis by 1Way-ANOVA did not reveal any significant differences between temperatures ($p = 0.249$).

S2

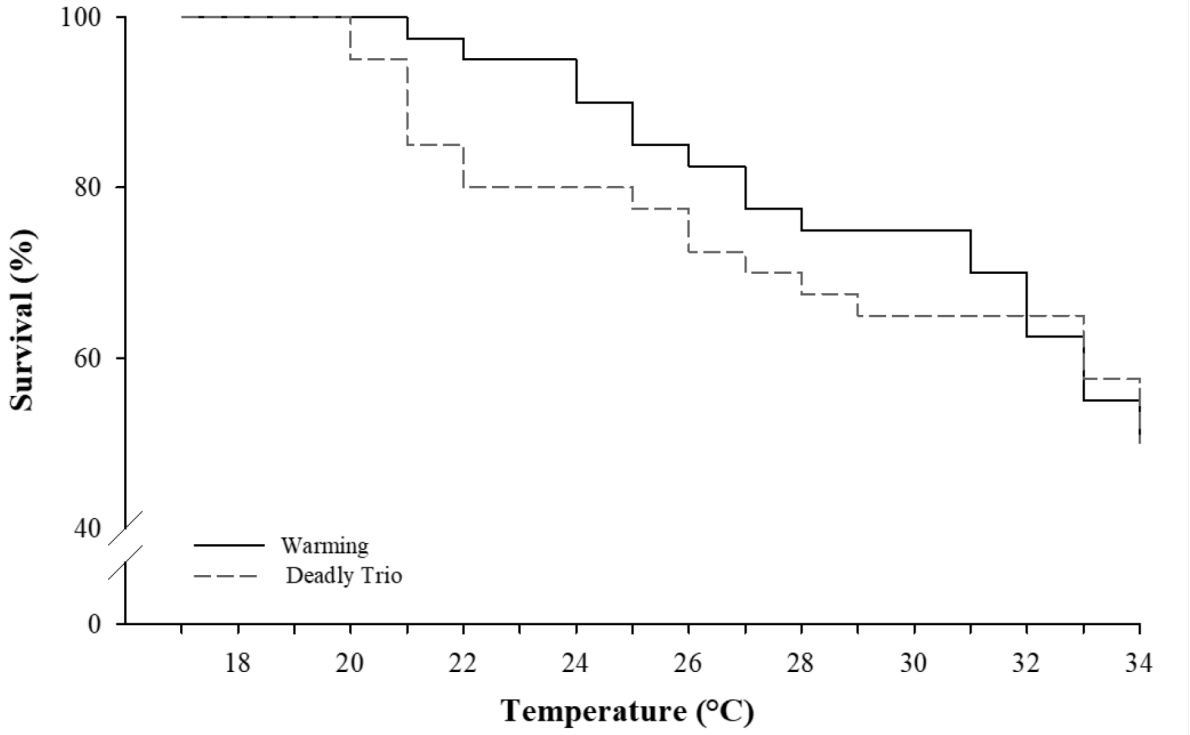

S2 Survival of *O. edulis* exposed to warming (black) and Deadly Trio (warming *plus* Hypoxia *plus* Hypercapnia, grey). The percentage of surviving scallops is shown for every 2 °C temperature increase. N at start = 20 oysters per group.In both groups 50 % of oysters died at 34 °C (LC_{50}).

S3

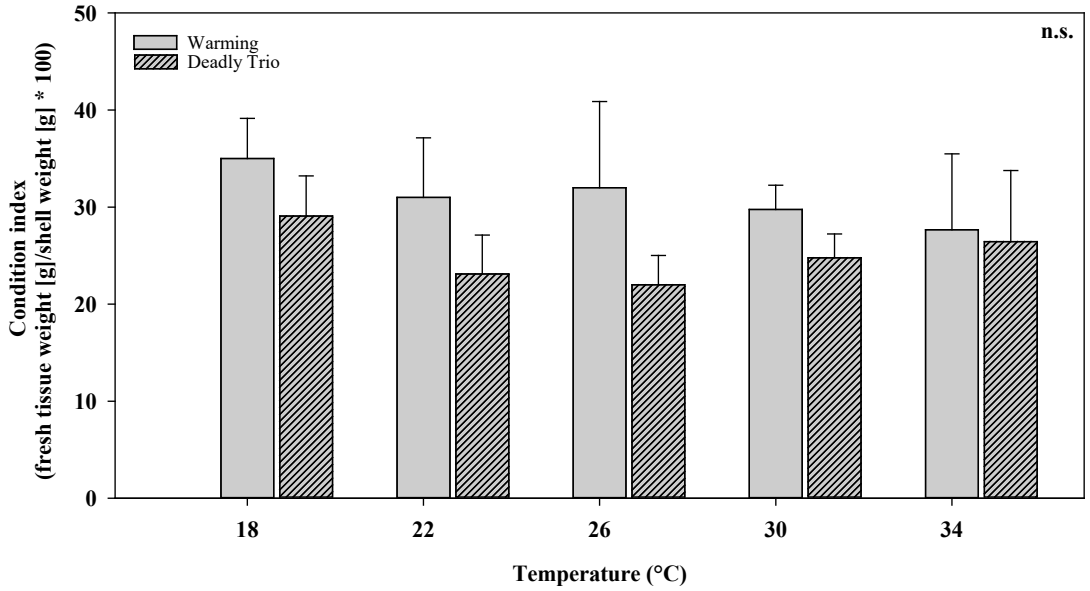

S3 Condition indices (CI) of *O. edulis* exposed to warming (grey) and Deadly Trio (striated) sampled at 18, 22, 26, 30, and 34 °C. CI was calculated as fresh weight of the soft tissue (g) divided by the dried shell weight (g) times 100. Shown are the mean CI ± SD (n = 4-6). Statistical analysis by 2way-ANOVA did not reveal an effect of temperature ($p = 0.111$) or exposure group ($p = 0.511$). No significant differences between groups were detected ($p = 0.359$).

S4

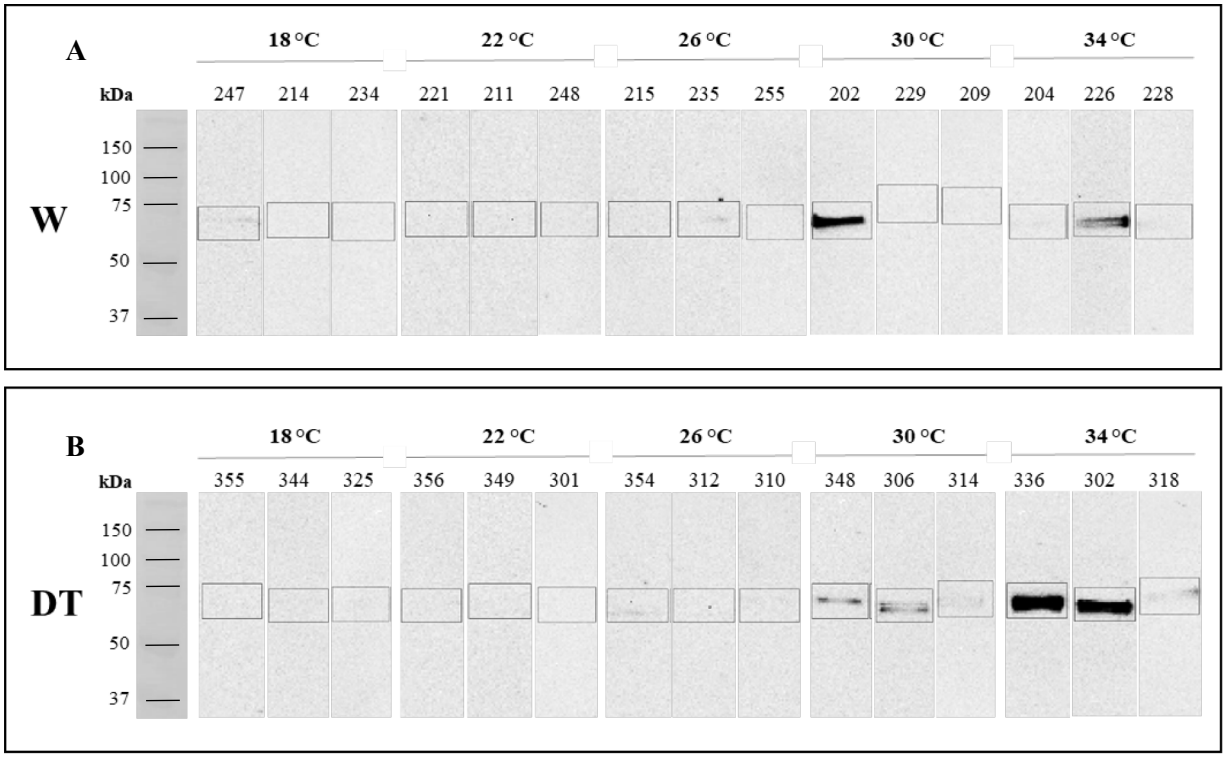

S3 Branchial levels of HSP70 determined in *O. edulis* exposed to warming (A) and Deadly Trio (B) acclimated at 18 °C (2019). Always three oysters were sampled at 18, 22, 26, 30, and 34 °C were analyzed for HSP70 as described in section 2.2.3. Primary antibody was used at 1:5000 dilution and exposure lasted 10 min. The number above each lane indicates the identity of each oyster. On the left hand side the molecular weight marker is shown with its respective kDa size (37 - 150 kDa area shown) range aside. As the marker is not clearly visible in the image black lines indicate its location. Boxes indicate the area around 70 kDa highlighting where the HSP70 isoform should occur. No signal indicates that HSP70 levels were below baseline.

S5-A

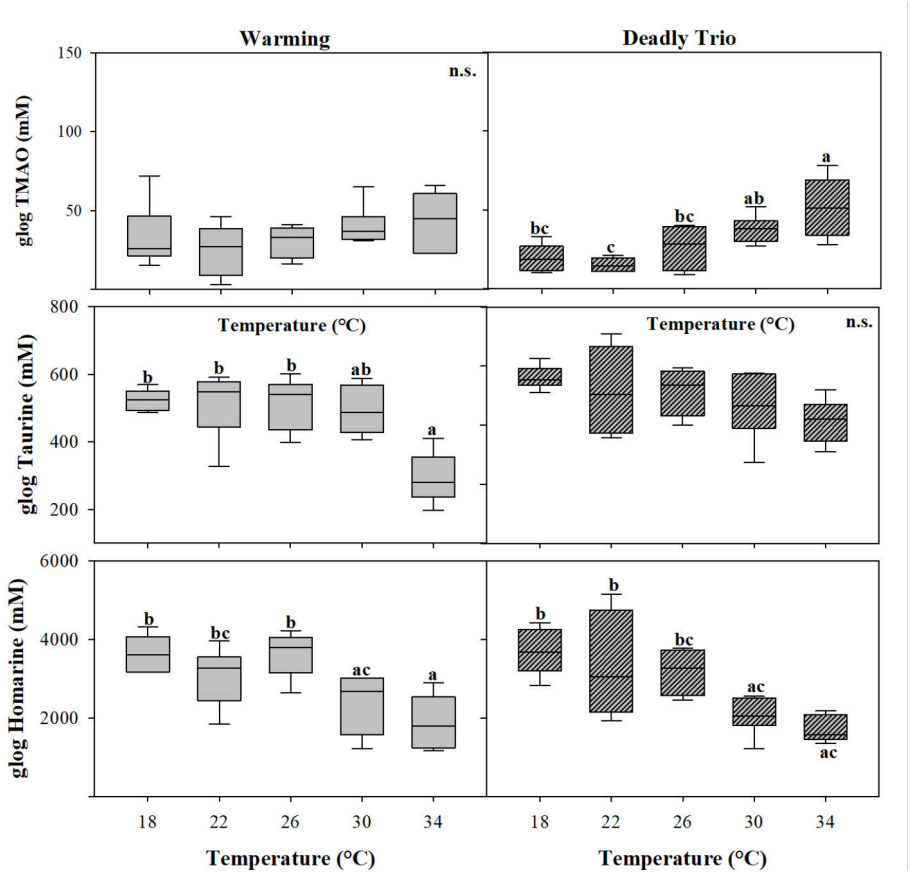
Warming
Deadly Trio
glog TMAO (mM)
glog Taurine (mM)
glog Homarine (mM)
Temperature (°C)
n.s.
18
22
26
30
34

S5 B

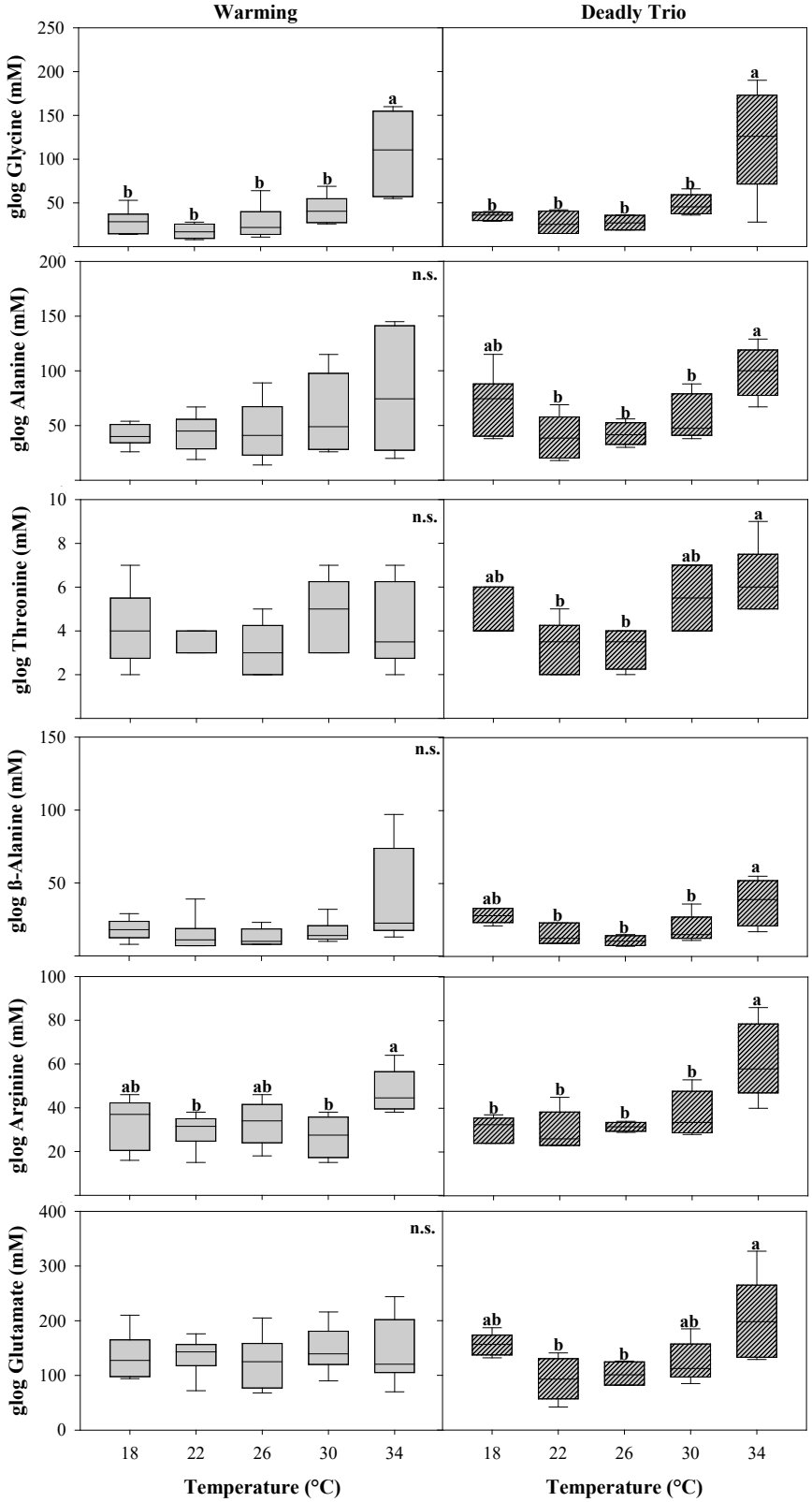
Warming
Deadly Trio
glog Glycine (mM)
glog Alanine (mM)
glog Threonine (mM)
glog ß-Alanine (mM)
glog Arginine (mM)
glog Glutamate (mM)
n.s.
Temperature (°C)
Temperature (°C)

S5 C

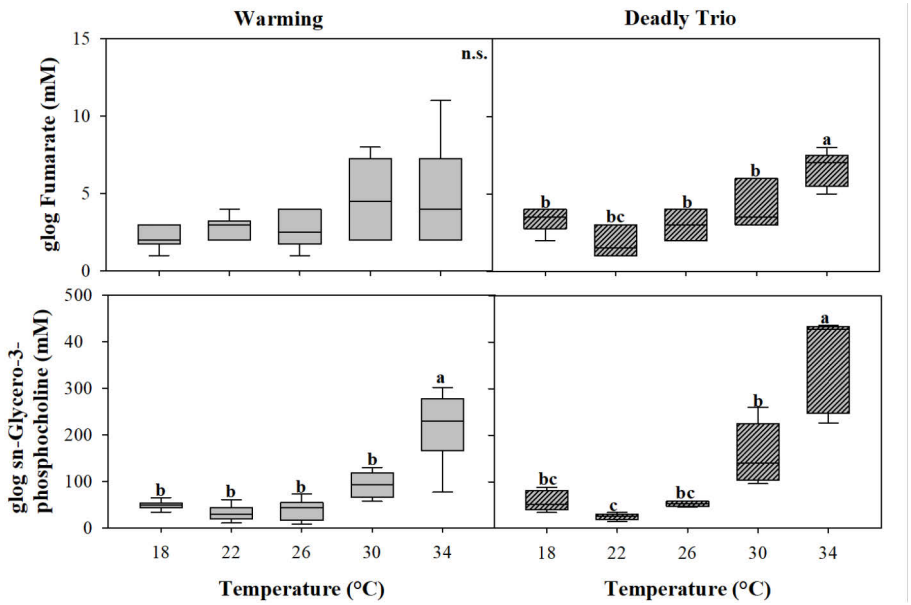

S3A-C Metabolite levels in gill tissue of summer acclimated *Ostrea edulis* run and sampled 2019 at 18, 22, 26, 30, and 34 °C. On the left oysters exposed to warming and on the right oysters were exposed to DT. Data show mean, normalized and glog transformed concentrations (mM) ± SD analyzed by 1-way ANOVA, followed by a Post-Hoc test. Significant differences between data are indicated by different letters ($P<0.05$). Data are shown as box plots, n = 4-6.

A The panel shows significant changing metabolites belonging to the class of osmolytes, in detail tri-methyl-amine-oxide (TMAO), taurine, and homarine.
B This panel shows significant changing metabolites belonging to the class of amino acids, in detail glycine, alanine, ß-alanine, threonine, arginine and glutamate.
C This panel shows significant changing fumarate (marker for anaerobiosis) and sn-glycero-3-phophocholine.

S6

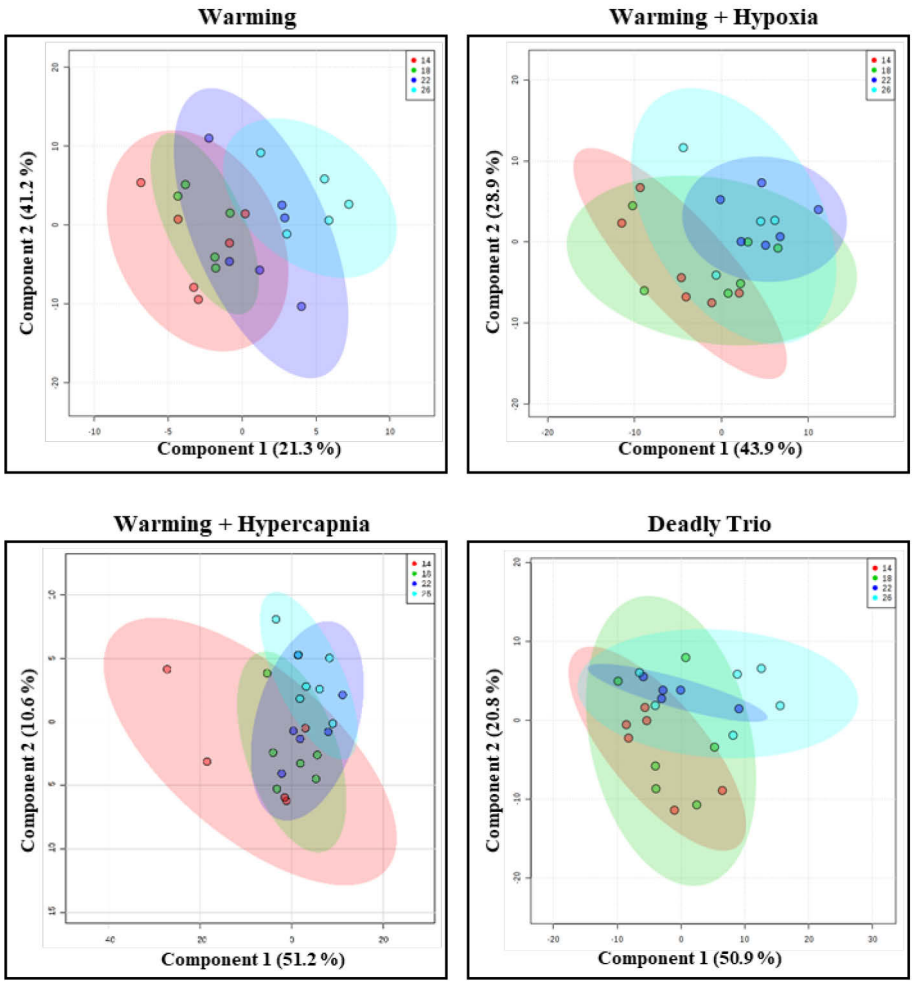

S6 Impact of the different sampling temperatures on the phasic muscle metabolic profile of *P. maximus*. Score Plots show the PLS-DA model of assigned phasic muscle tissue metabolites sampled at 14 °C (red), 18 °C (green), 22 °C (dark blue), and 26 °C (light blue) in the respective exposures. Ellipses correspond to a confidence interval of 95%. The two components accounting for the highest variance are illustrated and the distance of the samples reflect the dissimilarity in metabolite patterns.

S7

S7 Assigned phasic muscle metabolites to proposed metabolic pathways of *P. maximus* exposed to acute warming. No identified metabolites were altered with warming up to 26 °C.

S8

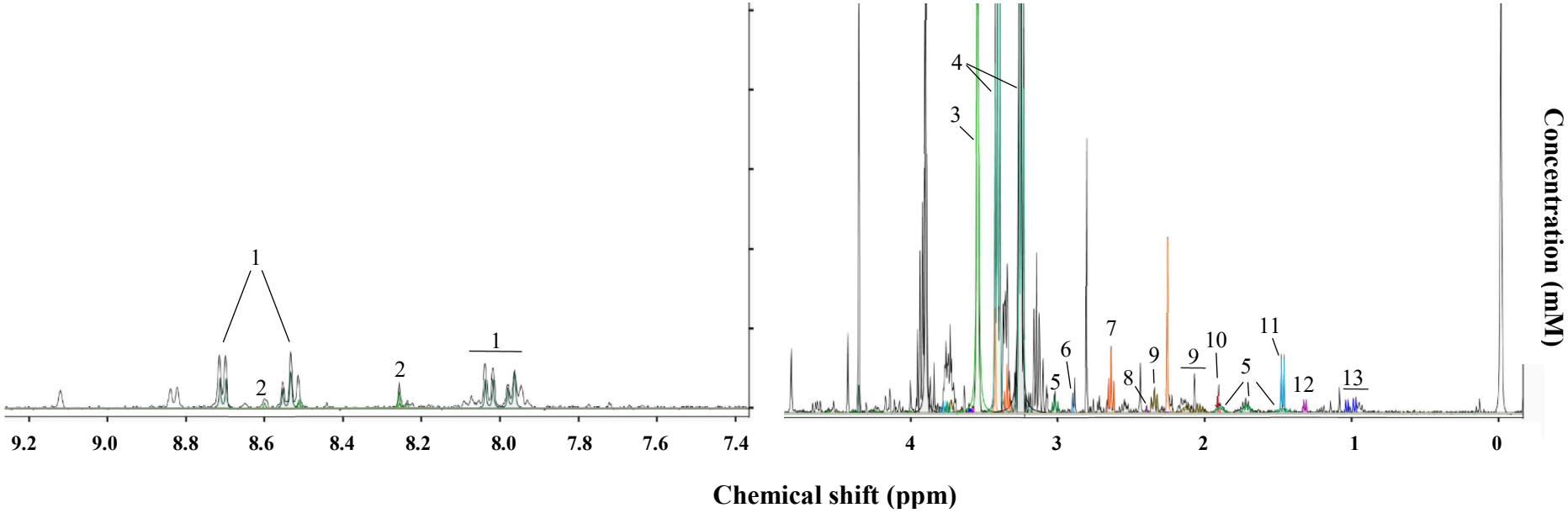

S8 Exemplary gill tissue spectra of *P. maximus* illustrating a selection of assigned metabolites including the chemical shift (ppm). (1) homarine, (2) adenylates, (3) glycine, (4) taurine, (5) lysine, (6) dimethylglycine, (7) hypotaurine, (8) succinate, (9) glutamate, (10) acetic acid, (11) alanine, (12) threonine, and (13) valine

ST 1

Results of one-way ANOVA for significant changes in gill metabolite levels of *O. edulis* (2019) tested against temperature within one exposure. Shown is the compound, the f-value, p-value, and the resulted Tukey Post-Hoc test.

Warming

Compound	F-value	p-value	Tukey
sn-Glycero-3-phosphocholine	23.17	< 0.001	18-30 < 34
Glycine	11.41	< 0.001	18-30 < 34
Taurine	10.78	< 0.001	18, 22, 26 > 34
Homarine	6.85	< 0.001	18, 26 > 34

Deadly Trio

Compound	F-value	p-value	Tukey
sn-Glycero-3-phosphocholine	30.97	< 0.001	18-30 < 34; 22 < 30
Fumarate	13.06	< 0.001	18-30 < 34; 22 < 30
Glycine	11.04	< 0.001	18-30 < 34
Arginine	8.84	< 0.001	18-30 < 34
Homarine	6.83	< 0.001	18, 22 > 30; 34
Trimethylamine N-oxide	6.67	< 0.001	18-26 < 34; 22 < 30
ß-Alanine	6.56	< 0.001	22, 26, 30 < 34
Threonine	6.45	0.004	22, 26 < 34
Glutamate	4.87	0.006	22, 26 < 34
Alanine	5.97	0.002	22, 26, 30 < 34

ST 2

Assigned metabolites in gill tissue of *O.edulis* with main chemical shift signals used for identification. Metabolites are sorted to osmolytic function, class of amino acids, intermediates of Krebs cycle, or others.

	Metabolite	Chemical shift
Osmolytes		
	Taurine	3.3, 3.4
	Betaine	3.3, 3.9
	Trimethyl-N-Oxide (TMAO)	3.3
	Homarine	4.4, 8.0, 8.6, 8.7
	Hypotaurine	2.6, 3.3
Amino Acids		
	Glutamate	2.0, 2.1, 2.3, 2.4, 3.7
	Glutamine	2.1, 2.2, 2.4, 2.5, 3.8, 6.9, 7.6
	Glycine	3.5
	Alanine	1.5, 3.8
	ß-Alanine	2.5, 3.2
	Isoleucine	0.9, 1.0,1.2, 1.5, 2.0, 3.7
	Valine	1.0, 2.3, 3.6
	Aspartate	2.7, 2.8, 3.9
	Lysine	1.4, 1.5, 1.7, 1.9, 3.0, 3.8
	Leucine	0.9, 1.0, 1.7, 3.7
	Arginine	1.6, 1.7, 1.9, 3.3, 3.8, 6.7, 7.2
	Homocysteine	2.1, 2.2, 2.6, 2.7, 3.8
Krebs Cycle Intermediates		
	Succinate	2.4
	Fumarate	6.5
	Malate	2.4, 2.7, 4.3
	Acetate	1.9
Others		
	Tri-phosphates (ADP)	4.3, 4.4, 6.1, 8.3, 8.5
	Choline	3.2, 3.5, 4.1
	O-Phosphocholine	3.2, 3.6, 4.2
	Sn-Glycero-3-phosphocholine	3.2, 3.6, 3.7, 3.9, 4.3
	UDP-Glucose	3.8, 6.0, 7.9
	4-Aminobutyrate	1.9, 2.3, 3.0

ST3

Assigned metabolites in gills of *P.maximus* with main chemical shift signals used for identification. Metabolites are sorted to osmolytic function, class of amino acids, intermediates of Krebs cycle, or others.

Gill	**Metabolite**	**Chemical shift**
Osmolytes		
	Taurine	3.3, 3.4
	Betaine	3.3, 3.9
	Trimethyl-N-Oxide (TMAO)	3.3
	Homarine	4.4, 8.0, 8.6, 8.7
	Hypotaurine	2.6, 3.3
Amino Acids		
	Glutamate	2.0, 2.1, 2.3, 2.4, 3.7
	Glutamine	2.1, 2.2, 2.4, 2.5, 3.8, 6.9, 7.6
	Glycine	3.5
	Alanine	1.5, 3.8
	ß-Alanine	2.5, 3.2
	Isoleucine	0.9, 1.0,1.2, 1.5, 2.0, 3.7
	Valine	1.0, 2.3, 3.6
	Aspartate	2.7, 2.8, 3.9
	Lysine	1.4, 1.5, 1.7, 1.9, 3.0, 3.8
	Leucine	0.9, 1.0, 1.7, 3.7
	Arginine	1.6, 1.7, 1.9, 3.3, 3.8, 6.7, 7.2
	Homocysteine	2.1, 2.2, 2.6, 2.7, 3.8
	Sarcosine	2.7, 3.6
	Threonine	1.3, 3.6, 4.3
	NN Dimethylglycine	2.9, 3.7
Krebs Cycle Intermediates		
	Succinate	2.4
	Acetate	1.9
Others		
	UDP-glucose	3.5, 3.8, 3.9, 4.2, 4.3, 4.4, 5.6, 6.0, 7.9
	sn-Glycero-3-phosphocholine	3.2, 3.6, 3.7, 3.9, 4.3
	Choline	3.2, 3.5, 4.0
	O-Phosphocholine	3.2, 3.6, 4.2
	Trimethylamine	2.9
	Dimethylamine	2.7
	Acetoacetate	2.3, 3.4
	Dimethy sulfone	3.1
	Trigonelline	4.4, 8.1, 8.8, 9.1
	Adenosinmonophosphat	4.0, 4.3, 4.5, 4.8, 6.1, 8.2, 8.6
	Adenosindiphosphat	4.2, 4.6, 4.7, 6.1, 8.2, 8.5
	Adenosintriphosphat	4.2, 4.3, 4.4, 4.6, 4.7, 6.1, 8.2, 8.5

ST4

Assigned metabolites in phasic muscle of *P.maximus* with main chemical shift signals used for identification. Metabolites are sorted to osmolytic function, class of amino acids, intermediates of Krebs cycle, or others.

Phasic muscle	**Metabolite**	**Chemical shift**
Osmolytes		
	Taurine	3.2, 3.4
	Betaine	3.3, 3.9
	Trimethyl-N-Oxide (TMAO)	3.3
	Homarine	4.4, 8.0, 8.6, 8.7
	Hypotaurine	2.6, 3.3
Amino Acids		
	Glutamate	2.0, 2.1, 2.3, 2.4, 3.8
	Glycine	3.5
	Alanine	1.5, 3.8
	Isoleucine	0.9, 1.0,1.2, 1.5, 2.0, 3.7
	Valine	1.0, 2.3, 3.6
	Aspartate	2.7, 2.8, 3.9
	Leucine	0.9, 1.0, 1.7, 3.7
	Arginine	1.6, 1.7, 1.9, 3.2, 3.8, 6.7, 7.2
	Sarcosine	2.7, 3.6
	Threonine	1.3, 3.6, 4.2
	NN Dimethylglycine	2.9, 3.7
Krebs Cycle Intermediates		
	Succinate	2.4
	Malonate	3.1
Others		
	UDP-glucose	3.8, 6.0, 7.9
	sn-Glycero-3-phosphocholine	3.2, 3.6, 3.7, 3.9, 4.3
	Choline	3.2, 3.5, 4.1
	O-Phosphocholine	3.2, 3.6, 4.2
	Trimethylamine	2.9
	Dimethylamine	2.7
	Dimethylglycine	2.9, 3.7
	Trigonelline	4.4, 8.1, 8.8, 9.1
	Lactate	1.3, 4.1
	Carnitine	2.4, 2.5, 3.2, 3.4, 4.6
	O-Acetylcarnitine	2.1, 2.5, 2.6, 3.2, 3.9, 5,6
	Adenosinmonophosphat	4.0, 4.3, 4.5, 4.8, 6.1, 8.2, 8.6
	Adenosindiphosphat	4.2, 4.6, 4.7, 6.1, 8.2, 8.5
	Adenosintriphosphat	4.2, 4.3, 4.4, 4.6, 4.7, 6.1, 8.2, 8.5
	Creatine	3.0, 3.9

ST5

Results of one-way ANOVA for significant changes in phasic muscle metabolites of *P. maximus* tested against a) temperature and b) exposure. Shown is the compound, the f-value, p-value, [-LOG10(p)], and the resulted Fisher' LSD.

Warming

Compound	F-value	p.value	[-LOG10(p)]	Fisher's LSD
no significant changes				

Hypoxia

Compound	F-value	p.value	[-LOG10(p)]	Fisher's LSD
Valine	12,0	1,5E-04	3,8	14 - 18; 14 - 22; 14 - 26; 18 - 22; 22 - 26
Threonine	11,4	2,0E-04	3,7	14 - 18; 14 - 22; 14 - 26; 18 - 22
Betaine	8,3	1,1E-03	3,0	14 - 18; 14 - 22; 18 - 26; 22 - 26
O-Acetylcarnidine	7,0	2,5E-03	2,6	14 - 18; 14 - 22; 22 - 26
Leucine	6,9	2,8E-03	2,5	14 -18; 14 - 22; 14 - 26; 18 - 22
Isoleucine	5,8	5,9E-03	2,2	14 - 18; 14 - 22

Hypercapnia

Compound	F-value	p.value	[-LOG10(p)]	Fisher's LSD
no significant changes				

Deadly Trio

Compound	F-value	p.value	[-LOG10(p)]	Fisher's LSD
Threonine	17,5	1,1E-05	5,0	14 - 22; 14 - 26; 18 - 22; 18 - 26
Valine	8,9	6,8E-04	3,2	14 - 22; 14 - 26; 18 - 22; 18 - 26
Leucine	5,9	5,1E-03	2,3	14 - 22; 14 - 26; 18 - 22; 18 - 26

14 °C

Compound	F-value	p.value	[-LOG10(p)]	Fisher's LSD
Hypotaurine	31,5	1,4E-07	6,9	W - HO; W - HC; HO - DT; HC - DT

18°C

Compound	F-value	p.value	[-LOG10(p)]	Fisher's LSD
Hypotaurine	10,2	3,2E-04	3,5	W - HO; HO - HC; HO - DT

22°C

Compound	F-value	p.value	[-LOG10(p)]	Fisher's LSD
Hypotaurine	24,4	1,0E-06	6,0	W - HO; W - HC; HO - DT; HC - DT
Aspartate	5,7	5,7E-03	2,2	W - HO; HO - HC; HO - DT
NN-Dimethylglycine	5,6	6,3E-03	2,2	W - HO; W- DT; HO - HC; HC - DT
Homarine	5,3	7,7E-03	2,1	W - HO; HO - HC; HC - DT

26°C

Compound	F-value	p.value	[-LOG10(p)]	Fisher's LSD
Hypotaurine	68,3	5,0E-10	9,3	W - HO; W - HC; HO - DT; HC - DT
TMAO	6,4	3,7E-03	2,4	W - DT; HC - DT
Glycine	6,0	5,2E-03	2,3	W - DT; HO - DT; HC - DT

ST6

Locations with geographical coordinates used for extrapolated annual minimum and maximum SST (°C) curves shown in Fig. **15 A-B.**

Location	Longitude °	Latitude °	min SST (°C)	max SST (°C)
Fleedwood, GB	54	-3	8,0	15,0
Guaratuba, Brazil	-26	-48	15,6	27,8
Saint John, Canada	45	-66	3,0	15,0
Vigo, Spain	42	-8	11,0	21,0
Caloundra, Australia	-27	153	17,0	28,0
Hofn, Iceland	64	-15	4,1	11,4
Cayenne, French Guiana	5	-52	26,1	30,3
Fukuoka, Japan	33	130	18,0	28,0
Bari, Italy	41	17	8,3	28,5
Manzanillo, Mexico	19	-104	23,1	30,9
Scheveningen, Netherlands	52	4	4,3	19,5
Manta, Equador	-1	-81	23,6	28,7
Venice, Italy	45	12	7,0	28,1
Ko Si Chang, Thailand	13	130	25,7	31,3
Chennai, India	13	80	25,3	30,8
Rio Gallegos, Argentina	52	68	4,3	12,9
Arraial do Cabo, Brazil	-23	-42	19,3	27,6
Havanna, Kuba	23	-82	22,9	31,5
Uummannaq, Greenland	71	52	-2,2	7,6
Nome, Alaska	64	165	-3,1	13,8
Pevek, Russia	70	170	-3,2	3,1
Manado, Indonesia	1,5	125	27,6	30,5
Helgoland, Germany	54	8	1,9	20,5
Makassar, Indonesia	5	119	26,2	30,9
Antsiranana, Madagascar	12	49	24,2	27,9
La Serena, Chile	-30	72	11,8	19,1
Tromso, Norway	69	19	3,0	13,2
Sao Luis, Brazil	-2	-44	26,6	28,1
Siridao, India	15	74	26,2	31,1
Luanda, Angola	-9	13	19,3	29,9
Ancud, Chile	42	74	9,5	16,4
Tak Bai, Thailand	6	102	26,2	31,3
Cape Town, South Africa	-34	18	14,1	20,8
Stanley, Falkland Islands	-52	-58	3,8	10,9
Punta Arenas, Chile	-53	-71	5,2	10,8
Marambio Base, Antarctica	-64	-56	0,0	0,0
MCMurdo, Antarctica	-78	167	0,0	0,0

ST7

List of ostreoids and pectinids which were used in the meta-analysis (section 4.4). Shown are the species, their site of collection including the geographical latitude (°) and longitude (°), minimum and maximum habitat sea surface temperatures (°C), acclimation temperature (°C) and duration of experimental exposure (h), the determined LC_{50} (°C), and the source of the study.

Species	Order	Site of Collecction	Latitude °	Longitude °	Habitat min (°C)	Habitat max (°C)	Accl temp (°C)	Exposure (h)	LC_{50} (°C)	Source
Argopecten purpuratus	Pectinida	Bay of Indipencia, Peru	14	-76	16	21	19	24	29,0	Urban (1994). *Mar Ecol Prog Ser* **107**, 139-145
Aequipecten opercularis		Isle of Man, GB	54	-4	8	15	15	48	21,6	Paul (1980). *J Exp Mar Biol Ecol* **46,** 41-50
Nodipecten nodosus		Porto Belo, Santa Catarina State	-27	-48	15,6	27,8	27	24	31,6	Rupp and Parson (2004). *J Exp Mar Biol Ecol* **309,** 173-198
Placopecten magellanicus		Mascarene, Passamaquoddy Bay	45	-67	3	15	15,5	48	24	Dickie (1958). *J Fish Res Board Can* **15,** 1189-1211
Pecten maximus		Vigo, Spain	42	-8	11	21	14	Ramp	26	This study
Ostrea conchaphila	Ostreoida	Tomales Bay, California	38	-122	8,3	15	12-15	1	38	Brown et al. (2004). *J Shell Res* **2**, 135-141
Crassostrea commercialis		Moreton Island, Queensland Coast	-27	153	17	28	23	24	41	Potter and Hill (1982). *Aquaculture* **29**, 101-108
Crassostrea sikamea		Goshonoura, Kumamoto, Japan	32	130	18	28	10	1	43	Nagata et al. (2017). *Fish Sci* **83**, 273-281
Ostrea edulis		Vigo Estuary (Spain)	42	-8	11	21	14	Ramp	35	This study
Ostrea edulis		North Adriatic Sea coast (Italy)	43	15	8,3	28,5	15	1	38	Piano et al. (2002). *Cell Stress Chaperones* **7**, 250-257
Isognomon nucleus		Sichang Island, Gulf of Thailand	13	130	25,7	31,3	26	Ramp	48	Giomi et al. (2016). *J Exp Biol* **219**, 686-694
Crassostrea madrasensis		Madras, East Coast of India	12	80	25,3	30,8	30	2	42	Rajagopal et al. (2005). *Water Res* **39**, 4335-4342

REFERENCES

Abele, D., Heise, K., Pörtner, H.O., Puntarulo, S. (2002). Temperature-dependence of mitochondrial function and production of reactive oxygen species in the intertidal mud clam *Mya arenaria*. *Journal of Experimental Biology* **205**, 1831-1841.

Abele, D., Kruppe, M., Philipp, E.E.R., Brey, T. (2010). Mantle cavity water oxygen partial pressure ($P\underline{O_2}$) in marine molluscs aligns with lifestyle. *Canadian Journal of Fisheries and Aquatic Sciences* **67**, 977-986.

Angilletta, M.J., Steury, T.D., Sears, M.W. (2004). Temperature, growth rate, and body size in ectotherms: Fitting pieces of a life-history puzzle. *Integrative and comparative Biology* **44**, 498-509.

Angilletta, M.J. (2009). Thermal Adaption : A theoretical and empirical synthesis. *Oxford: Oxford University Press.*

Artigaud, S., Lacroix, C., Pichereau, V., Flye-Sainte-Marie, J. (2014). Respiratory response to combined heat and hypoxia in the marine bivalves *Pecten maximus* and *Mytilus spp. Comparative Biochemistry and Physiology A - Molecular and Integrative Physiology* **175**, 135-140.

Artigaud, S., Richard, J., Thorne, M.A.S., Lavaud, R., Flye-Sainte-Marie, J., Jean, F., Peck, L.S., Clark, M.S., Pichereau, V. (2015a). Deciphering the molecular adaption of the king scallop (*Pecten maximus*) to heat stress using transcriptomics and proteomics. BMC Genomics, 16, 988.

Artigaud, S., Lacroix, C.C.L., Richard, J.J.R., Flye-Sainte-Marie, J., Bargelloni, L.L.B., Pichereau, V. (2015b). Proteomic responses to hypoxia at different temperatures in the great scallop (*Pecten maximus*). PeerJ, 3:e871 https://doi.org/10.7717/peerj.871.

Asmus, R.M., and Asmus, H. (1991). Mussel beds_ limiting or promoting phytoplankton? *Journal of Experimental Marine Biology and Ecology* **148(2)**, 215-232.

Bambach, R.K, Knoll, A.H., Wang, S.C. (2004). Origination, extinction, and mass depletions of marine diversity. *Paleobiology* **30(4)** 522–542.

Beck, M.W., Brumbaugh, R.D., Airoldi, L., Carranza, A., Coen, L.D., Crawford, C., Defeo, O., Edgar, G.J., Hancock, B., Kay, M.C., Lenihan, H.S., Luckenbach, M.W., Toropova, C.L., Zhang, G., Guo, X. (2011). Oyster Reefs at Risk and Recommendations for Conservation, Restoration, and Management. *BioScience* **61(2)** 107–116.

Benson, B.B., and Krause, D. (1984). The concentration and isotopic fractionation of oxygen dissolved in freshwater and seawater in equilibrium with the atmosphere. *Limnology and Oceanography* **29(3)**, 620-632.

Benton, M.J., and Twitchett, R.J. (2003). How to kill (almost) all life: the end-Permian extinction event. *Trends in Ecology & Evolution* **18(7)**, 358-365.

Beukema, J.J., Dekker, R., Jansen, J.M. (2009). Some like it cold: populations of the tellinid bivalve *Macoma balthica* (L.) suffer in various ways from a warming climate. *Marine Ecology Progress Series* **384**, 135-145.

Bijma, J., Pörtner, H.O., Yesson, C., Rogers, A.D. (2013). Climate change and the oceans – What does the future hold? *Marine Pollution Bulletin* **74(2)**, 495-505.

Braby, C.E. and Somero, G.N. (2006). Following the heart: temperature and salinity effects on heart rate in native and invasive species of blue mussels (genus Mytilus*). The Journal of Experimental Biology* **209**, 2554-2566.

Bradford, M.M. (1976). A rapid and sensitive method for the quantitation of micro-gram quantities of protein utilizing the principle of protein-dye binding. *Analytical Chemistry* **72**, 248–254.

Brand, A.R. (2006). The European scallop fisheries for *Pecten maximus*, *Aequipecten opercularis* and *Mimachlamys varia*. In: Scallops: Ecology and Aquaculture, Vol. 35, Editors: S.E. Shumway and G.J. Parson.

Breitburg, D., Levin, L.A., Oschlies, A., Grégoire, M., Chavez, F.P., Conley, D.J., Garçon, V., Gilbert, D., Gutiérrez, D., Isensee, K., Jacinto, G.S., Limburg, K.E., Montes, I., Naqvi, S.W.A., Pitcher, G.C., Rabalais, N.N. Roman, M.R., Rose, K.A., Seibel, B.A., Telszewski, M., Yasuhara, M., Zhang, J. (2018). Declining oxygen in the global ocean and coastal waters. *Science* 359(6371), DOI: 10.1126/science.aam7240

Brinkhoff, W., Stöckmann, K., Grieshaber, M. (1983). Natural occurrence of anaerobiosis in molluscs from intertidal habitats. *Oecologia* **57**:151 155.

Byrne, M., and Przeslawski, R. (2013). Multistressor impacts of warming and acidification of the ocean on marine invertebrates' life history. *Integrative and Comparative Biology* **53(4)**, 582-596.

Burgess, S.D., Muirhead, J.D., Bowring, S.A. (2017). Initial pulse of Siberian Traps sills as the trigger of the end-Permian mass extinction. *Nature communications* **8(164)**.

Burton Sanders, M., Bean, T.P., Hutchinon, T.H., Le Quesne, W.J.F. (2013). Juvenile king scallop, *Pecten maximus*, is potentially tolerant to low levels of ocean acidification when food is unrestricted. *PLoS ONE* **8(9)**, e74118.

Burrows, M.T., Schoeman, D.S., Buckley, L.B., Moore, P., Poloczanska, E.S., Brander, K.M., Brown, C., Bruno, J.F., Duarte, C.M., Halpern, B.S., Holding, J., Kappel, C.V., Kiessling, W., O'Connor, M.I., Pandolfi, J.M., Parmesan, C., Schwing, F.B., Sydeman, W.J., Richardson, A.J. (2011). The pace of shifting climate in marine and terrestrial ecosystems. *Science* **334**, 652-655.

Calder, P.C. (2006). Branched-chain amino acids and immunity. *Journal of Nutrition* **136**, 288S-293S.

Calosi, P., De Witt, P., Thor, P., Dupont, S. (2016). Will life find a way? Evolution of marine species under global change. *Evolutionary Applications* **9**, 1035-1042.

Cappello, T., Gianetto, A., Parrino, V., Maisano, M., Oliva, S., De Marco, G., Guerriero, G., Mauceri, A., Fasulo, S. (2018). Baseline levels of metabolites in different tissues of mussel *Mytilus galloprovincialis* (Bivalvia: Mytilidae). *Comparative Biochemistry and Physiology – Part D* **26**, 32-39.

Carter, C.G., and Houlihan, D.F. (2001). Protein synthesis. *Fish Physiology* **20**, 31-75.

Cattaneo-Vietti, R. (2018). Structural changes in Mediterranean marine communities: lessons from the Ligurian Sea. *Rendiconti Lincei. Scienze Fisiche e Naturali*, https://doi.org/10.1007/s12210-018-0670-2.

Chapelle, G. and Peck, L. S. (1999). Polar gigantism dictated by oxygen availability. *Nature* **399**, 114-115.

Cherkasov, A.S., Biswas, P.K., Ridings, D.M., Ringwood, A.H., Sokolova, I.S. (2006). Effects of acclimation temperature and cadmium exposure on cellular energy budgets in the marine mollusk *Crassostrea virginica*: linking cellular and mitochondrial responses. *Journal of Experimental Biology* **209**, 1274-1284

Clark, M.S., Husmann, G., Thorne, M.A.S., Burns, G., Truebano, M., Peck, L.S., Abele, D., Philipp, E.E.R. (2013). Hypoxia impacts large adults first: consequences in a warming world. *Global Change Biology* **19**, 2251-2263.

Clark, M.S., Sommer, U., Sihra, J.K., Thorne, M.S., Morley, S.A., King, M., Viant, M.R., Peck, L.S. (2016). Biodiversity in marine invertebrate responses to acute warming revealed by a comparative multi-omics approach. Global Change Biology, doi: 10.1111/gcb.1335

Clarkson, M.O., Kasemann, S.A., Wood, R.A., Lenton, T.M., Daines, S.J., Richoz, S., Ohnemueller, F., Meixner, A., Poulton, W., Tipper, T. (2015). Ocean acidification and the Permo-Triassic mass extinction. *Science* **348(6231)**, 229-232.

Culloty, S.C., and Mulcahy, M.F. (2007). *Bonamia ostreae* in the Native Oyster *Ostrea edulis*. *Marine Environment and Health Series* **29**, Marine Institute 2007.

Dame, R.F. (2016). Ecology of marine bivalves. An ecosystem approach. CRC Press, New York.

Davenport, J., and Davenport, J.L. (2005). Effects of shore height, wave exposure and geographical distance on thermal niche width of intertidal fauna. *Marine Ecology Progress Series* **292**, 41-50.

Da Silva, P.M., Fuentes, J., Villalba, A. (2005). Growth, mortality and disease susceptibility of oyster *Ostrea edulis* families obtained from brood stocks of different geographical origins, through on-growing in the Rıa de Arousa (Galicia, NW Spain). *Marine Biology* **147**, 965–977.

De Zwaan, A., and Wijsman, T.C.M. (1976). Anaerobic metabolism in bivalvia (Mollusca) – Characteristics of anaerobic metabolism. *Comparative Biochemistry and Physiology* **54B**, 313-324.

Diaz, R.J., and Rosenberg, R. (2008). Spreading Dead Zones and consequences for marine ecosystems. *Science* **321(5891)**, 926-929.

Dickson, A.G. (1990). Standard potential of the (AgCl(s)+1/2H2(g) = Ag(s)+HCl(aq))cell and the dissociation constant of bisulfate ion in synthetic sea water from 273.15 to 318.15K. *Journal of Chemical Thermodynamics* **22**, 113–127.

Doney S.C., Fabry V.J., Feely R.A., Kleypas J.A. (2009). Ocean acidification: The other CO2 problem. *Annual Review of Marine Science* **1**, 169-192.

Forster, J., Hirst, A.G., Atkinson, D. (2012). Warming-induced reductions in body size are greater in aquatic than terrestrial species. *Proceedings of the National Academy of Sciences of the United States of America* **109**, 19310-19314.

Foster, W.J., Lehrmann, D.J., Yu, M., Martindale, R.C. (2019). Facies selectivity of benthic invertebrates in a Permian/Triassic boundary microbialite succession: Implications for the "microbialite refuge" hypothesis. *Gebiology* **17(5)**, 523-535.

Fraiser, M.L., Bottjer, D.J. (2007). When bivalves took over the world. *Palaeobiology* **33(3)**, 397-413.

Frederich, M., and Pörtner, H.O. (2000). Oxygen limitation of thermal tolerance defined by cardiac and ventilatory performance in spider crab, *Maja squinado*. *American Journal of Physiology-Regulatory, Integrative and Comparative Physiology* **279(5)**, R1531-R1538.

Gattuso, J.P., Magnan, A., Bille, R., Cheung, W.W.L., Howes, E.L., Joos, F., Allemand, D., Bopp, L., Cooley, S.R., Eakin, C.M., Hoegh-Guldberg, O., Kelly, R.P., Pörtner, H.O., Rogers, A.D., Baxter, J.M., Laffoley, D., Osborn, D., Rankovie, A., rochette, J., Sumaila, U.R., Treyer, S., Turley, C. (2015). Contrasting futures for ocean and society from different anthropogenic CO_2 emissions scenarios. *Science* **349**, aac4722-1

Goldberg, A.L. (2003). Protein degradation and protection against misfolded or damaged proteins. *Nature* **426**, 895-899.

Goncalves, P., Thompson, E.L., Raftos, D.A. (2017). Contrasting impacts of ocean acidification and warming on the molecular responses of CO_2-resilient oysters. *BMC Genomics* **18**, article 431.

Grant, P.R., Grant, B.R., Huey, R.., Johnson, M.T.J., Knoll, A.H., Schmitt, J. (2017). Evolution caused by extreme events. *Philosophical Transactions B* **372**(1723), https://doi.org/10.1098/rstb.2016.0146

Grieshaber, M. (1978). Breakdown and formation of high-energy phosphates and octopine in the adductor muscle of scallops, *Clamys opercularis* (L.) during escape swimming and recovery. *Journal of Comparative Physiology – Part B* **126**, 269-276.

Grieshaber, K.K., and Gäde, G. (1977). Energy supply and the formation of octopine in the adductor muscle of the scallop, *Pecten jacobaeus* (Lamarck). *Comparative Biochemistry and Physiology Part B: Comparative Biochemistry* **58(3)**, 249-252.

Grieshaber M.K., Kreutzer U., Pörtner H.O. (1988). Critical PO_2 of Euryoxic Animals. In: Acker H. (eds) Oxygen Sensing in Tissues. Springer, Berlin, Heidelberg.

Grieshaber, M.K., Hardewig, I., Kreutzer, U., Pörtner, H.O. (1994). Physiological and metabolic responses to hypoxia in invertebrates. *Reviews of Physiology, Biochemistry and Pharmacology* **125**, 43-147.

Guderley, H., Labbé-Giguere, S., Janssoone, X., Bourgeois, M., Pérez, H.M., Tremblay, I. (2009). Thermal sensitivity of escape response performance by the scallop *Placopecten magellanicus*: Impact of environmental history. *Journal of Experimental Marine Biology and Ecology* **377**, 113-119.

Guderley, H., and Pörtner, H.O. (2010). Metabolic power budgeting and adaptive strategies in zoology: examples from scallops and fish. *Canadian Journal of Zoology* **88**, 753-763.

Guinotte, J.M., Fabry, V.J. (2008). Ocean acidification and its potential effects on marine ecosystems. *Annals of the New York Academy of Sciences* **1134(1)**, 320–342.

Gutiérrez, J.L., Jones, C.G., Strayer, D.L., Iribarne, O.O. (2003). Mollusks as ecosystem engineers: the role of shell production in aquatic habitats. *Oikos* **101**, 79-90.

Guo, X., Li, C., Wang, H., Xu, Z. (2018). Diversity and evolution of oysters. *Journal of Shellfish Research* **37(4)**, 755-771.

Hamdoun, A.M., Cheney, D.P., Cherr, G.N. (2003). Phenotypic plasticity of HSP70, and HSP70 gene expression in the Pacific oyster (*Crassostrea gigas*): Implications for thermal limits and induction of thermal tolerance. *Biological Bulletin* **205**, 160-169.

Hautmann, M. (2010). The first scallop. *Paläontologische Zeitschrift* **84**, 317-322.

Hedgecock, D., Gaffney, P., Goulletquer, X., Guo, K.R., Warr, G. (2005). The case for sequencing the Pacific oyster genome. *Journal of Shellfish Research* **24**, 429-441.

Helmuth, B.S.T. (1998). Intertidal mussel microclimates: Predicting the body temperature of a sessile invertebrate. *Ecological Monographs* **68**, 51–74.

Helmuth, B.S.T., Broitman, B.R., Blanchette, C.A., Gilman, S., Halpin, P., Harley, C.D.G., O' Donell, M.O.J., Hofmann, G.E., Menge, B., Strickland, D. (2006). Mosaic patterns of thermal stress in the rocky intertidal zone: Implications for climate change. *Ecological Monographs* **76**, 461–479.

Heise, K., Puntarulo, S., Nikinmaa, M., Abele, D., Pörtner, H.O. (2006). Oxidative stress during stressful heat exposure and recovery in the North Sea eelpout *Zoarces viviparus* L. *The Journal of Experimental Biology* **209**, 353-363

Heisler N. (1988). Acid-Base Regulation. In: Shuttleworth T.J. (Eds) Physiology of Elasmobranch Fishes. Springer, Berlin, Heidelberg

Hertz, C. (2012). The unfolded protein response: controlling cell fate decisions under ER stress and beyond. *Nature Reviews Molecular Cell Biology* **13(2)**, 89-102.

Hochachka, P. W., and G. N. Somero. (2002). Biochemical adaptation: Mechanism and process in physiological evolution. Oxford University Press, New York.

Hoegh-Guldberg, O., and Bruno, J.F. (2010). The impact of climate change on the world's marine ecosystems. *Science* **328(5985)**, 1523-1528.

Hoegh-Guldberg, O., Cai, R., Poloczanska, E. S., Brewer, P. G., Sundby, S., Hilmi, K., et al. (2014). The Ocean. In Climate Change 2014: Impacts, Adaptation, and Vulnerability Part A: Global and Sectoral Aspects Contribution of Working Group II to the Fifth Assessment Report of the Intergovernmental Panel of Climate Change, eds. C. B. Field, V. R. Barros, D. J. Dokken, K. J. Mach, M. D. Mastrandrea, T. E. Bilir, et al. (Cambridge; New York, NY: Cambridge University Press), 1655–1731.

Ivanina, A.V., Nesmelova, I., Leamy, L., Sokolov, E.P., Sokolova, I.M. (2016). Intermittent hypoxia leads to functional reorganization and affects cellular bioenergetics in marine molluscs. *Journal of Experimental Biology* **219**, 1659-1674.

Joachimski, M.M., Lai, X., Shen, S., Jiang, H., Luo, G., Chen, B., Chen, J., Sun, Y. (2012). Climate warming in the latest Permian and the Permian–Triassic mass extinction. *Geology* **40(3)**, 195-198.

Kassahn, K.S., Vrozier, R.H., Pörtner, H.O., Caley, M.J. (2009). Animal performance and stress: responses and tolerance limits at different levels of biological organization. *Biological Reviews* **84(2)**, 277-292.

Kasting, J.F., Howard, M.T., Wallmann, K., Veizer, J., Shields, G., Jaffrés, J. (2006). Paleoclimates, ocean depth, and the oxygen isotopic composition of seawater. *Earth and Planetary Science Letters* 252, 82-93.

Keeling, R.F., Körtzinger, A., Gruber, N. (2010). Ocean deoxygenation in a warming world. *Annual Review of Marine Science* **2**, 199-229.

Kennedy, V.S., and Mihurski, J.A. (1971). Upper thermal tolerances of some estuarine bivalves. *Chesapeake Science* **12(4)**, 193-204.

Knoll, A.H., Bambach, R.K., Canfeld, D.E., Grotzinger, J.P. (1996). Comparative Earth history and late Permian mass extinction. *Science* **273(5274)**, 452-457.

Knoll, A.H., Bambach, R.K., Payne, J.L., Pruss, S., Fischer, W.W. (2007). Paleophysiology and end-Permian mass extinction. *Earth and Planetary Science Letters* **256**, 295–313.

Koenigstein, S., Mark, F.C., Gößling-Reisemann S., Reuter, H., Poertner, H.-O. (2016). Modelling climate change impacts on marine fish populations: process-based integration of ocean warming, acidification and other environmental drivers. *Fish and Fisheries* **17**, 972-1004.

Kreeger, D.A., Gatenby, C.M., Bergstrom, P.W. (2018). Restoration potential of several native species of bivalve molluscs for water quality improvement in mid-Atlantic watersheds. *Journal of Shellfish Research* **37(5)**, 1121-1157.

Kregel, K.C. (2002). Heat shock proteins: modifying factors in physiological stress responses and acquired thermotolerance. *Journal of Applied Physiology* **92**, 2177-2186.

Kroeker, K.J., Kordas, R.L., Crim, R.N., Singh, G.G. (2010). Meta-analysis reveals negative yet variable effects of ocean acidification on marine organisms. *Ecology Letters* **13**, 1419-1434.

Laemmli, U.K. (1970). Cleavage of Structural Proteins during the Assembly of the head of Bacteriophage T4. *Nature* **227**, 680-685.

Lannig, G., Eilers, S., Pörtner, H.O., Sokolova, I., Bock, C. (2010). Impact of Ocean acidification on energy metabolism of oyster, *Crassostrea gigas* – Changes in metabolic pathways and thermal response. *Marine Drug*s **8**, 2318-2339.

Larade, K., and Storey, K.B. (2002). A profile of the metabolic responses to anoxia in marine invertebrates. Cell and Molecular Responses to Stress Edited by K.B. Storey and J.M. Storey Vol. 3: Sensing, Signaling and Cell Adaptation. Elsevier Press, Amsterdam (2002), pp. 27-46

Lau, K.V., Maher, K., Altinen, D., Kelley, B.M., Kump, L.R., Lehrmann, D.J., Silva-Tamayo, J.C., Weaver, K.L., Yu, M., Payne, J.L. (2016). Marine anoxia and delayed Earth system recovery after the end-Permian extinction. *PNAS* 113, 2360–2365.

Le Moullac, G.L., Quéau, I., Le Souchu, P., Pouvreau, S., Moal, J., Le Coz, J.R., Samain, J.F. (2007). Metabolic adjustments in the oyster Crassostrea gigas according to oxygen level and temperature. *Marine Biology Research* **3(5)**, 357 – 366.

Lemasson, A.J., Hall-Spencer, J.M., Fletcher, S., Provstgaard-Morys, S., Knights, A.M. (2018). Indications of future performance of native and non-native adult oysters under acidification and warming. *Marine Environmental Research* **142**, 178-189.

Lenz, M., Ahmed, Y., Canning-Clode, J., Díaz, E., Eichhorn, S., Fabritzek, A.G., Da Gama, B.A.P., Garcia, M., von Juterzenka, K., Kraufvelin, P., Machura, S., Oberschelp, L., Paiva. F., Penna, M.A., Ribeiro, F.V., Thiel, M., Wohlgemuth, D., Zamani, N.P., Wahl, M. (2018). Heat challenges can enhance population tolerance to thermal stress in mussels: a potential mechanism by which ship transport can increase species invasiveness. *Biological Invasions* **20**, 3107-3122.

Lepock, J.R. (2009). Cellular effects of hyperthermia: relevance to the minimum dose for thermal damage. *International Journal of Hyperthermia* **19**, 252-266.

Lesser, M.P. (2006). Oxidative stress in marine environments: biochemistry and physiological ecology. *Annual Review of Physiology* **68**, 253-278.

Lewis, E., Wallace, D.W.R. (1998). Program Developed for CO2System Calcula-tions. ORNL/CDIAC-105. Carbon Dioxide Information Analysis Center, Oak RidgeNational Laboratory, U.S. Department of Energy, Oak Ridge, Tennessee.

Liao, W., Li, X., Mancini, M., Chan, L. (2006). Proteasome inhibition induces differential heat shock protein response but not unfolded protein response in HepG2 cells. Journal of Cellular Biochemistry **99**, 1085-1095.

Lindquist, S. (1986). The heat-shock response. *Annual Reviews in Biochemistry* **55**, 1151-1591.

Meriin, A.B., Gabai, V.L., Yaglom, J., Shifrin, V.I., Sherman, M.Y. (1998). Proteasome inhibitors activate stress kinases and induce HSP72. *Journal of Biological Chemistry* **273(11)**, 6373-6379.

Melzner, F., Gutowska, M., Hu, M.Y-A., Stumpp, M. (2009). Acid-base regulatory capacity and associated proton extrusion mechanisms in marine invertebrates: An overview. *Comparative Biochemistry and Physiology A - Molecular and Integrative Physiology* **153(2)**, DOI 10.1016/j.cbpa.2009.04.056.

Metzger, R., Sartoris, F.J., Langenbuch, M., Pörtner, H.O. (2007). Influence of elevated CO_2 concentrations on thermal tolerance of the edible crab *Cancer pagurus. Journal of Thermal Biology* **32,** 144-151.

Michaelidis, B., Haas, D., Grieshaber, M.K. (2005). Extracellular and intracellular acid-base Status with regard to the energy metabolism in the oyster *Crassostrea gigas* during exposure to air. *Physiological and Biochemical Zoology: Ecological and Evolutionary Approaches* **78(3)**, R911–R921.

Millero, F.J., DiTrolio, B.R. (2010). Use of thermodynamics in examining the effects of ocean acidification. *Elements* **6**, 299–303.

Müller, M., Mentel, M., van Hellemond, J.J., Henze, K., Woehle, C., Gould, S.B., Yu, R.-Y., van der Giezen, M., Tielens, A.G.M., Martin, W.F. (2012). Biochemistry and Evolution of Anaerobic Energy Metabolism in Eukaryotes. *Microbiology and Molecular Biology Reviews* **76(2)**, 444–495.

Nakazawa, K., and Newell, D.N. (1968). Permian Bivalves of Japan. *Memoirs of the Faculty of Science, Kyoto University. Series of Geology and Mineralogy* **35(1)**, 1-108.

Pandolfi, J.M., Connolly, S.R., Marschall, D.J., Cohen, A.L. (2011). Projecting coral reef futures under global warming and ocean acidification. *Science* **333(6041)**, 418-422.

Orr, J.C., Fabry, V.J., Aumont, O., Bopp, L., Doney, S.C., Feely, R.A., Gnanadesikan, A., Gruber, N., Ishida, A., Joos, F., Key, R.M., Lindsay, K., Maier-Reimer, E., Mataer, R., Monfray, P., Mouchet, A., Najjar, R.G., Plattner, G.K., Rodgers, K.B., Sabine, C.L., Sarmiento, J.L., Schlitzer, R., Slater, R.D., Totterdell, I.J., Weirig, M.F., Yamanaka, Y., Yool, A. (2005). Anthropogenic ocean acidification over the twenty-first century and its impact on calcifying organisms. *Nature* **437**, 681-686.

Parker, L.M., Ross, P., O'Connor, W.A., Pörtner, H.O., Scanes, E., Wright, J.M. (2013). Predicting the response of molluscs to the impact of ocean acidification. *Biology* **2**, 651-692.

Pauly, D. (2010). Gasping Fish and Panting Squids: Oxygen, Temperature and the growth of water-breathing animals. International Ecology Institute, Oldendorf/Luhe.

Pazos, A.J., Román, G., Acosta, C.P., Abad, M., Sánchez, J.L. (1997). Seasonal changes in condition and biochemical composition of the scallop *Pecten maximus* L. from suspended culture in the Ria de Arousa (Galicia, N.W. Spain) in relation to environmental conditions. *Journal of Experimental Marine Biology and Ecology* **211**, 169-193.

Penn, J.L., Deutsch, C., Payne, J.L. Sperling, E.A. (2018). Temperature-dependent hypoxia explains biogeography and severity of end-Permian marine mass extinction. *Science* **362** (6419), Doi: 10.1126/science.aat1327.

Perry, A.L., Low, P.J., Ellis, J., Reynolds, J.D. (2005). Climate Change and distribution shifts in marine fishes. *Science* **308**, 1912-1915.

Piazza, V., Duarte, L.V., Renaudie, J., Aberhan, A. (2019). Reductions in body size of benthic macroinvertebrates as a precursor of the early Toarcian (Early Jurassic) extinction event in the Lusitanian Basin, Portugal. *Paleobiology* **45**, 296-316.

Ros, S., and Echevarría, J. (2011). Bivalves and evolutionary resilience: old skills and new strategies to recover from the P/T and T/J extinction events. *Historical Biology* **23(4)**, 411-429.

Runnegar, B., and Pojeta, J. (1974). Molluscan Phylogeny: The Palaentological Viewpoint. *Science* **186**, 311-317.

Pörtner, H.O. and Grieshaber, M.K. (1993). Critical PO_2(s) in oxyconforming and oxyregulating animals: gas exchange, metabolic rate and the mode of energy production. In The Vertebrate Gas Transport Cascade: Adaptations to Environment and Mode of Life (ed. J.E.P.W. Bicudo), pp. 330-357. Boca Raton FL, USA: CRC, Press Inc.

Pörtner, H.O., Hardewig, I., Peck, L.S. (1999). Mitochondrial function and critical temperature in the Antarctic bivalve, *Laternula elliptica. Comparative Biochemistry and Physiology Part A* **124***, 179–189.*

Pörtner, H.O., and Bock, C. (2000). A contribution of acid-base regulation to metabolic depression in marine ectotherms. Life in the cold /Eleventh International Hibernation Symposium. Gerhard Heldmaier ... (eds.); Berlin [u.a.]: Springer, ISBN: 3-540-67410-1.

Pörtner, H.O. (2001). Climate change and temperature-dependent biogeography: oxygen limitation of thermal tolerance in animals. *Naturwissenschaften* **88**, 137-146.

Pörtner, H.O. (2002). Climate variations and the physiological basis of temperature dependent biogeography: systemic to molecular hierarchy of thermal tolerance in animals. *Comparative Biochemistry and Physiology Part A: Molecular & Integrative Physiology* **132(4)**, 739-761.

Pörtner, H.O., Langenbuch, M., Reipschläger, A. (2004). Biological impact of elevated ocean CO2 concentrations: Lessons from animal physiology and earth history. *Journal of Oceanography* **60**, 705-718.

Pörtner, H.O. (2008). Ecosystem effects of ocean acidification in times of ocean warming: a physiologist's view. *MEPS* **373**, 203-217.

Pörtner, H.O., and Farrell, A.P. (2008). Physiology and Climate Change. *Science* **322**, 690-602.

Pörtner, H.O. (2010). Oxygen- and capacity-limitation of thermal tolerance: a matrix for integrating climate-related stressor effects in marine ecosystems. *The Journal of Experimental Biology* **213**, 881-893.

Pörtner, H.O., Bock, C., & Mark, F. C. (2017). Oxygen-and capacity-limited thermal tolerance: bridging ecology and physiology. *Journal of Experimental Biology* **220(15)**, 2685-2696.

Purohit P.V., Rocke, D.M., Viant, M.R., Woodruff, D.L. (2004). Discrimination models using variance-stabilizing transformation of metabolomic NMR data. *Omics* **8**, 118-130.

Reipschläger, A., and Pörtner, H.O. (1996). Metabolic depression during environmental stress: The role of extracellular *versus* intracellular pH in *Sipunculus nudus*. *The Journal of Experimental Biology* **199**, 1801-1807.

Richter, K., Haslbeck, M., Buchner, J. (2010). The Heat shock response: Life on the verge of death. *Molecular Cell* 40, 253-266

Riebesell, U., Fabry V.J., Hansson, L., and Gattuso J.-P. (2010). (Eds.). Guide to best practices for ocean acidification research and data reporting, pp. 243-258. Luxembourg: Publications Office of the European Union.

Rhein M, Rintoul SR, Aoki S, et al (2013). Observations: Ocean. In Stocker TF, Qin D, Plattner G-K, Tignor M, Allen SK, Boschung J, Nauels A, Xia Y, Bex V, Midgley PM (eds.) Climate Change 2013: The Physical

Science Basis. Contribution of Working Group I to the Fifth Assessment Report of the Intergovernmental Panel on Climate Change. Cambridge, GB. Cambridge University Press, pp. 255-316.

Ries, J.B., Cohen, A.L., McCorkle, D.C. (2009). Marine calcifiers exhibit mixed responses to CO2-induced ocean acidification. *Geology* **37(12)**, 1131–1134.

Ros, S., and Echevarría, J. (2011). Bivalves and evolutionary resilience: old skills and new strategies to recover from the P/T and T/J extinction events. *Historical Biology* **23**, 411–429.

Rylander, M. N., Feng, Y., Bass, J., Diller, K.R. (2005). Thermally induced injury and heat shock protein expression in cells and tissues. *Annals of the New York Academy of Sciences* **1066**, 222-242.

Sabine, C.L., Feely, R.A., Gruber, N., Key, R.M., Lee, K., Bullister, J.L, Wanninkhof, R., Wong, C.S., Wallace, D.R., Tilbrook, B., Millero, F.J., Peng, T.-H., Kozyr, A., Ono, T., Rios, A.F. (2004). The oceanic sink for anthropogenic CO_2. *Science* 305, 367-371.

Sarge, K.D., Murph, S.P., Morimoto, R.I. (1993). Activation of heat shock gene transcription by heat shock factor 1 involves oligomerization, acquisition of DNA-binding activity, and nuclear localization and can occur in the absence of stress. *Molecular and Cellular Biology* **13**, 1392-1407.

Seaman, M.N.L. (1991). Survival and aspects of metabolism in oysters*, Crassostrea gigas*, during and after prolonged air storage.

Schalkhausser, B., Bock, C., Stemmer, K., Brey, T., Pörtner, H.O., Lannig, G. (2013). Impact of ocean acidification on escape performance of the king scallop; Pecten maximus, from Norway. *Marine Biology* **160**, 1995-2006.

Schalkhausser, B., Bock, C., Pörtner, H.-O., Lannig, G. (2014). Escape performance of temperate king scallop, Pecten maximus under ocean warming and acidification. *Marine Biology* **161**, 2819-2829.

Sepkoski, J.J. (1981). A factor analytic description of the Phanerozoic marine fossil record. *Palaeobiology* **7**, 36-53.

Smith, C., Papadopoulou, N., Sevastou, K., Franco, A., Teixeira, H., Piroddi, C., Katsanevakis, S., Fürhaupter, K., Beauchard, O., Cochrane, S., Ramsvatn, S., Feral, J.-P., Chenuil, A., David, R., Kiriakopoulou, N., Zaiko, A., Moncheva, S., Stefanova, K., Churilova, T., Kryvenko, O. (2014). Report on identification of keystone species and processes across regional seas. Deliverable 6.1, DEVOTES Project. 105 pp + 1 Annex.

Sokolova, I.M., Frederich, M., Bagwe, R., Lannig, G., Sukhotin, A.A. (2012). Energy homeostasis as an integrative tool for assessing limits of environmental stress tolerance in aquatic invertebrates. *Marine Environmental Research* **79**, 1-15.

Somero, G.N. (2005). Linking biogeography to physiology: Evolutionary and acclimatory adjustments of thermal limits. *Frontiers in Zoology* **2(1),** doi:10.1186/1742-9994-2-1.

Song, H., Wignall, P.B., Tong, J., Yin, H. (2013). Two pulses of extinction during the Permian–Triassic crisis. *Nature Geoscience* **6**, 52-56.

Southward, A.J. (1958). A not on the temperature tolerances of some intertidal animals in relation to environmental temperatures and geographical distribution. *Jpurnal of the Marine Biological Association of th United Kingdom* 37, 49-66.

Stanley, S.M. (2016). Estimates of the magnitudes of major marine mass extinctions in earth history. Proceeedings of the National Academy of Sciences of the United States of America **113**, E6325-E6334.

Stevens, A.M., and Gobler, C.J. (2018). Interactive effects of acidification, hypoxia, and thermal stress on growth, respiration, and survival of four North Atlantic bivalves. *Marine Ecology Progress Series* **606**, 143-161.

Stickle, W.B., Kapper, M.A., Liu, L.L., Gnaiger, E., Wang, S.Y. (1989). Metabolic adaptions of several species of crustaceans and molluscs to hypoxia: tolerance and microcalorimetric studies. *The Biologcial Bulletin* **177**, 303-312.

Stillmann, J.H. (2002). Causes and consequences of thermal tolerance limits in rocky intertidal porcelain crabs genus *Petrolisthes*. *Integrative and Comparative Biology* **42**, 790-796.

Stoll, M.H.C., Bakker, K., Nobbe, G.H., Haesel, R.R. (2001). Continuous-Flow Analysis of Dissolved Inorganic Carbon Content in Seawater. *Analytical Chemistry* **73(17)**, 4111–4116.

Storey, K.B., and Storey, J.M. (1990). Metabolic rate depression and biochemical adaption in anaerobiosis, hibernation and estivation. *The Quarterly Review of Biology* **65(2)**, 145-174.

Storey, K.B., and Storey, J.M. (2007). Tribute to P.L. Lutz: Putting life on "pause" – molecular regulation of hypometabolism. *The Journal of Experimental Biology* **210**, 1700-1714.

Strahl, J., and Abele, D. (2010). Cell turnover in tissues of the long-lived ocean quahog *Actica islandica*

Sun, Y., Joachimski, M.M., Wignall, P.B., Yan, C., Chen, Y., Jiang, H., Wang, L., Lai, X. (2012). Lethally hot temperatures during the early triassic greenhouse. *Science* **338(6105)**, 366-370.

Thomsen, J., Haynert, K., Wegner, K.M., Melzner, F. (2015). Impact of seawater carbonate chemistry on the calcification of marine bivalves. *Biogeosciences* **12**, 4209-4220.

Tikunov, A.P., Johnson, C.B., Lee, H., Stoskopf, M.K., Macdonald, J.M. (2010). Metabolic investigations of american oysters using ^{1}H-NMR spectroscopy. *Marine Drugs* **8**, 2578-2596.

Tikunov, A.P., Stoskopf, M.K., Macdonald, J.M. (2014). Fluxomics of the Eastern Oyster for environmental stress studies. *Metabolomics* **4**, 53-70.

Tom, A., and Nair, S.K. (2006). Assessment of branched-chain amino acid status and potential for biomarkers. *The Journal of Nutrition* **136**, 324S–330S**.**

Tomanek, L. (2008). The importance of phsiological limits in determining biogeographica range shifts due to global climate change: The heat-shock response. *Physiological and Biochemical Zoology Ecological and Evolutionary Approaches* **72**, 709-717.

Tomanek, L., Zuzow, M.J., Ivanina, A.V., Beniash, E., Sokolova, I.M. (2011). Proteomic response to elevated PCO_2 level in eastern oysters, Crassostrea virginica,: Evidence for oxidative stress. *Journal of Experimental Biology* **214**, 1836-1844.

Tremblay, I., and Guderley, H.E. (2013). Scallops show that muscle metabolic capacities reflect locomotor style and morphology. *Physiological and Biochemical Zoology* **87(2)**, 231–244.

Tripp-Valdez, M.A., Bock, C., Lucassen, M., Lluch-Cota, S.E., Sicard, M. T., Lannig, G., and Pörtner, H.O. (2017). Metabolic response and thermal tolerance of green abalone juveniles (Haliotis fulgens: Gastropoda) under acute hypoxia and hypercapnia. *Journal of Experimental Marine Ecology* **497**, 11-18.

Tripp-Valdez, M.A., Bock, C., Lannig, G., Koschnick, N, Pörtner, H.O., Lucassen, M. (2019). Assessment of muscular energy metabolism and heat shock response of the green abalone *Haliotis fulgens* (Gastropoda: Philipi) at extreme temperatures combined with acute hypoxia and hypercapnia. *Comparative Biochemistry and Physiology Part B: Biochemistry and Molecular Biology* **227**, 1-11.

Tu, C., Chen, Z.Q., Harper, D.A.T. (2016). Permian-Triassic evolution of the Bivalvia: Extinction-recovery patterns linked to ecologic and taxonomic selectivity. *Palaeography, Palaeoclimtology, Palaeoecology* **459**, 53-62.

Twitchett, R.J. (2007). The Lillyput effect in the aftermath of the end-Permian extinction event. *Palaeogeography, Palaeoclimatology, Palaeoecology* **252,** 132–144.

Uchiyama, M., and Mihara, M. (1978). Determination of Malondialdehyde Precursor in tissues by thiobarbituric acid test. *Analytical Biochemistry* **86**, 271-278.

Uppström, L.R. (1974). Boron/chlorinity ratio of deep-sea water from the Pacific Ocean. D*eep-Sea Research* **21**, 161–162.

Veizer, J., and Prokoph, A. (2015). Temperatures and oxygen isotopic composition of Phanerozoic oceans. *Earth-Science Reviews* **146**, 92-104.

Verberk, W.C.E.P., and Bilton, D.T. (2011). Can oxygen set thermal limits in an insect and drive gigantism? *PLoS One* **6**, e22610.

Verberk, W.C.E.P., Bartolini, F., Marshall, D.J., Pörtner, H.O., Terblanche, J.S., White, C.R., Giomi, F. (2015). Can respiratory physiology predict thermal niches? *Annals of the New York Academy of Sciences* **1365**, 73-88.

Vernberg, W.B., and Vernberg, F.J. (1972). Environmental physiology of marine animals. Springer Verlag, New York.

Waller, T.R. (2006). Phylogeny of families in the Pectinoidea (Mollusca:Bivalvia): importance of the fossil record. *Zoological Journal of the Linnean Society* **148**, 313-342.

Walsh, P., McDonald, D., Booth, C. (1984). Acid-base balance in the sea mussel, *Mytilus edulis* II. Effects of hypxia and air-exposure on intracellular acid base status. Marine Biology Letters **5**, 359-369.

Waters, J.F., and Millero, F.J. (2013). The free proton concentration scale for seawater pH. *Marine Chemistry* **149**, 8-22.

Weidlich, O., Kiessling, W., Flügel, E. (2003). Permian-Triassic boundary interval as a model for forcing marine ecosystem collapse by long-term atmospheric oxygen drop. *Geology* **31**, 961- 964.

Wignall PB and Twitchett RJ (1996). Oceanic anoxia and the end Permian mass extinction. *Science* **272**,1155-1158. DOI:10.1126/science.272.5265.1155.

Wilkens, L.A. (2006). Neurobiology and behaviour of the scallop. In: Shumway SE, Parson GJ (eds) *Scallops: biology, ecology and aquaculture*, 1st edn. Elsevier, Amsterdam, 317–356.

Wittmann, A.C. and Pörtner, H.O. (2013). Sensitivities of extant animal taxa to ocean acidification. *Nature Climate Change* **3**, 995-1001.

Xia, J., and Wishart, D.S. (2010). MetPA: a web based metabolomics tool for pathway analysis and visualization. *Bioinformatics* **26**, 2342-2344.

Xia, J., and Wishart, D.S. (2016). Using MetaboAnalyst 3.0 for Comprehensive Metabolomics Data Analysis. *Current Protocols in Bioinformatics* **55**, 14.10.1-14.10.91

Xing, Q., Li, Y., Guo, H., Yu, Q., Huang, X., Wang, S., Hu, X., Zhang, L., Bao, Z. (2016). Cardiac performance: a thermal tolerance indicator in scallops. *Marine Biology* **163(12)**, 244.

Young, J.T.F., and Heikkila, J.J. (2010). Proteasome inhibition induces hsp30 and hsp70 gene expression as well as the acquisition of thermotolerance in *Xenopus laevis* A6 cells. *Cell Stress and Chaperones* **15**, 323–334.

Zhang, Z., and Zhang, Q. (2012). Molecular cloning, characterization and expression of heat shock protein 70 gene from the oyster *Crassostrea hongkongensis* responding to thermal stress and exposure of Cu2+ and malachite green. *Gene* **497**, 172-180.

Zhu, Q., Zhang, L., Li, L., Que, H., Zhang, G. (2016). Expression characterization of stress genes under high and low temperature stresses in the Pacific oyster, *Crassostrea gigas*. *Marine Biotechnology* **18**, 176-188.

ACKNOWLEGDEMENTS

First, I want to express my sincere gratitude to **Prof. Dr. Hans-Otto Pörtner** who gave me the opportunity to contribute to TERSANE and this challenging project. Furthermore, I want to thank him for all the great and helpful discussions about the project and obtained data.

Special thanks goes to **Dr. Gisela Lannig** and **Dr. Christian Bock** for all their advices, guidance, and many, many discussions throughout the last three and a half years. Thanks for always having a sympathetic ear when (again) something went ultimately wrong in the TK-rooms or with the HTK. Thanks Christian for introducing me into the world of NMR spectroscopy.

I thank **Charlotte Eymann** for being my mutual project-mate and for getting through this together. Thanks for a lot of fun in the lab and discussions about the project. Guess you are the next ☺

Another thanks goes to our (other) thesis committee members – **Prof. Dr. Inna Sokolova**, **Dr. Martin Aberhan**, **Prof. Dr. Andrew Knoll**, and **Prof. Dr. Helga Guderley**. Thanks for your valuable advices during our meetings. Thanks **Martin** for discussions about "Palaeobiology" and evolution of bivalves and fossil records. **Dr. Carl Reddin** for the help and advice with the super-duper meta-analysis table. Thank you **Inna** for advices about biochemical pathways and for being willing to be a referee of this thesis. Thanks to **Dr. Reinhard Saborowski** for introducing me to the path of Science and being a mentor for so many years. Furthermore, I want to thank **Dr. Tina Loebl** and **Maja Lindken** for proof-reading**.**

As lab work and animal maintenance cannot be performed, alone I want to express my gratitude to all technicians of the group "Integrative Ecophysiology" – especially **Anette Tillmann**, **Isabell Ketelsen**, **Freddy Veliz Moraleda**, and **Nils Koschnick** for help, advice and guidance in the laboratory equipment, and bivalve acquisition and maintenance. In line I want to thank **Timo Hirse** for apportion of lab-trainees and **Rebecca Gorniak**, **Lea Phillipps**, **Lennard Klingenforth, and Carolin Tscheschlok** for their help during exposures, helping with animal maintenance and lab work.

Thanks to all other PhD students for your friendship, coffee breaks, glühwein and burgers ☺ **Nina Paul** and **Nina Krebs** - Keep going ☺. Moreover, I am grateful for my social network and all my friends and family who were always there, motivating and calming me down when I thought I could not manage it anymore.